ADVANCES IN PHYSICS

A QUARTERLY SUPPLEMENT of the PHILOSOPHICAL MAGAZINE

VOLUME 9 OCTOBER 1960 NUMBER 36

PRICE per part 20*s.*
PRICE per annum £3 15*s.* 0*d.* post free

PRINTED AND PUBLISHED BY TAYLOR & FRANCIS LTD
RED LION COURT, FLEET ST., LONDON E.C.4

Contents of June, 1960

CONTENTS

Extinction in X-ray Crystallography

By S. Chandrasekhar

Davy Faraday Research Laboratory,
The Royal Institution, 21 Albemarle Street, London, W.1

CONTENTS

§ 1. Introduction

Very soon after the discovery of x-ray diffraction in crystals it was realized that the intensity of an x-ray reflection is influenced greatly by the degree of perfection of the crystal. According to the dynamical theory of diffraction in perfect crystals (Darwin 1914, Ewald 1917), the integrated reflection from the face of a large crystal is given by

$$\rho = \frac{8}{3\pi}\frac{Ne^2\lambda^2}{mc^2}|F|\frac{1+|\cos 2\theta|}{2\sin 2\theta} \quad . \quad . \quad . \quad . \quad . \quad . \quad (1)$$

when the incident x-rays are unpolarized and the absorption small†. Although in isolated instances there was quantitative agreement between experiment and theory, in the vast majority of cases the observed intensities far exceeded the values calculated on the basis of (1). Furthermore, the theory predicted that the angular range of reflection should be a few seconds of arc, whereas in most real crystals the angular range was found to be of the order of a few minutes of arc.

† In this formula, the reflecting planes are taken to be parallel to the crystal face ; N is the number of unit cells per unit volume, F the structure factor corrected for thermal vibration, θ the Bragg angle, e, m the electronic charge and mass, c the velocity of light and λ the wavelength.

These discrepancies were noticed by Darwin as early as 1914. From measurements of the intensity of reflection of white radiation from rock salt made by Moseley and himself, he concluded that this crystal could not be perfect. But the distinction between the perfect and the imperfect crystal was not fully understood till very much later. In 1922, Darwin put forward the first theoretical model of the 'mosaic crystal'†. With the introduction of this concept the difficulties were soon resolved and all the experimental facts could be explained in a rigorous manner.

An ideally imperfect or mosaic crystal is supposed to be built up of a large number of blocks which are slightly disorientated with respect to each other. Each block is in itself perfect but so small that its integrated reflection is proportional to its volume Δv and is given by

where

$$\left.\begin{aligned} &\rho = Q\Delta v, \\ &Q = N^2\lambda^3\left(\frac{e^2}{mc^2}\right)^2 |F|^2 \frac{1+\cos^2 2\theta}{2\sin 2\theta} \end{aligned}\right\} \quad . \quad . \quad . \quad . \quad . \quad (2)$$

for unpolarized x-rays (see, for instance, W. L. Bragg 1949, p. 335). The reflections from the different blocks are taken to be optically independent, and therefore the total intensity reflected by the crystal is simply the sum of the intensities reflected by the individual blocks. However, it must be remembered that the contributions of the deeper blocks will be lessened on account of the normal linear absorption, for both the incident and diffracted beams would then have to travel a greater path in the crystal than they would have to for blocks lying at the surface. In addition, there will be an impoverishment of the primary beam when it passes through the crystal because of the fact that the energy is being constantly reflected away. But in an ideally imperfect crystal, the blocks are assumed to be of such small dimensions and so widely distributed in angle that the energy lost by reflection is negligible as compared with that lost by absorption. In such a case, it can be shown that for a symmetrical reflection from the face of a thick crystal

$$\rho = Q/2\mu \quad . \quad . \quad . \quad . \quad . \quad . \quad . \quad . \quad . \quad (3)‡$$

where μ is the linear absorption coefficient for the wavelength λ (see W. L. Bragg, *loc. cit.*). The angular range of reflection from a mosaic crystal will be very large, being governed by the amount of disorientation of the constituent blocks.

Formulae (1) and (3) are very different. The integrated reflection from the mosaic crystal is proportional to the square of the number of unit cells

† The term 'mosaic crystal' was first introduced by P. P. Ewald.

‡ In this formula and in (1), $\rho = E\omega/I$, where E is the energy reflected by the crystal when it rotates with uniform angular velocity ω about an axis parallel to the crystal planes, and I is the total energy incident on the crystal in unit time. In (2), $\rho = E\omega/I_0$, where I_0 is the energy incident per unit area per unit time.

per unit volume and to the square of the structure factor; that for a perfect crystal is proportional to the first powers of these quantities. For a strong reflection, ρ calculated on the basis of (3) may be as much as 30 or 40 times that calculated on the basis of (1) (see table 2).

The ideally perfect and the ideally imperfect crystals represent the two limiting types. A real crystal will as a rule lie somewhere between these two extremes and will exhibit what is called primary and secondary extinction. The first evidence of the existence of extinction came in 1914 from experiments of W. H. Bragg, who noticed that the integrated reflections for the strong spectra from some small pieces of diamond were not proportional to the volume as they should have been according to (2). He then made the interesting observation that diamond exhibits abnormal absorption for X-rays passing through it at the reflecting angle. W. L. Bragg *et al.* (1921, 1922) found a similar effect in rock salt, and demonstrated experimentally that the increase in absorption is proportional to the intensity of the spectrum. In 1922, Darwin examined the problem in detail and showed clearly that two distinct phenomena are operative in any real crystal, namely, primary and secondary extinction, both of which tend to reduce the intensity of the reflection. He developed formulae by means of which the magnitude of these effects could be estimated. In a later paper, W. L. Bragg *et al.* (1926) reviewed the various formulae and discussed their applicability to different types of crystals, and it is to this paper that we owe an elucidation of the principles governing the reflection of X-rays from real crystals. Darwin's choice of the imperfect crystal model has proved to be fortunate, for there is ample evidence to-day to show that his ideas correspond closely to physical reality.

§ 2. Primary Extinction

When a beam of X-rays falls on a perfect crystal at the reflecting angle, the wave reflected by each crystal plane suffers a phase difference of $\pi/2$ with respect to the incident wave†. Twice reflected waves, which travel exactly in the direction of the primary beam, will have a phase difference of π relative to it and consequently will diminish its amplitude. So the intensity of the primary beam will fall off rapidly with increasing depth as though the crystal had a large absorption coefficient even if the true absorption were negligible, and the reflection will take place effectively from the 'skin' of the crystal. Moreover, thrice reflected waves, being opposite in phase with once reflected waves, will conspire to reduce the intensity of the reflected beam. Thus at every point in the crystal there is a dynamical interaction between the incident and diffracted wave-fields. The screening of the lower layers of the crystal at the reflecting angle and the simultaneous diminution in the integrated reflection brought about by this kind of inter-

† This can be proved by an ordinary Fresnel construction. The wave scattered by each atom is opposite in phase to the incident wave, but the Fresnel addition of the wavelets from a plane sheet of atoms introduces a phase change of $\pi/2$.

action is known as primary extinction. At first sight it would seem that we have a paradoxical result in that both the transmitted and reflected beams decrease in intensity. The dynamical equations show that the energy is in fact diverted into the reflected beam, but at the same time the angular range of reflection becomes so exceedingly small that there is a resultant decrease in the *integrated* reflection.

Now consider an imperfect crystal like the mosaic we described earlier but with each perfect block sufficiently thick to show primary extinction. Under such circumstances the integrated reflection from a single block will not be given by (2). Darwin (1922) investigated the symmetrical reflection from the face of a perfect plate having p planes, and found that the contribution to the integrated reflection from a volume Δv is $Q'\Delta v$, where

$$Q' = \frac{Q \tanh pq}{pq}, \qquad \ldots\ldots\ldots \quad (4)$$

q being the amplitude reflected by a single crystal plane when a plane wave of unit amplitude falls on it. Neglecting polarization

$$|q| = \frac{2Ne^2d^2}{mc^2}|F|,$$

d being the spacing of the planes. Therefore to correct for primary extinction, Q in (3) has to be replaced by Q'.

Equation (4) in its present form does not bring out the polarization factor explicitly. Hence we shall rewrite it as follows: if ρ' and ρ are the integrated reflections for unpolarized X-rays with and without extinction respectively, then

$$\frac{\rho'}{\rho} = \frac{Q'}{Q} = \frac{\tanh A_0 + |\cos 2\theta| \tanh |A_0 \cos 2\theta|}{A_0(1+\cos^2 2\theta)} \qquad \ldots \quad (5)$$

where

$$A_0 = \frac{Ne^2\lambda}{mc^2} \cdot \frac{t_0}{\gamma_0} \cdot |F|,$$

t_0 being the thickness of the perfect plate, γ_0 the direction cosine of the incident (or reflected) beam relative to the normal to the crystal plate (see Zachariasen 1945, p. 169).

For a symmetrical reflection through a plate, the correction is (Waller 1926)

$$\frac{\rho'}{\rho} = \frac{\sum_{n=0}^{\infty} J_{2n+1}(2A_0) + |\cos 2\theta| \sum_{n=0}^{\infty} J_{2n+1}(|2A_0 \cos 2\theta|)}{A_0(1+\cos^2 2\theta)}. \qquad \ldots \quad (6)$$

When $A_0 \ll 1$, $\rho' = \rho$, i.e. primary extinction is negligible. This condition is satisfied either when t_0, the thickness of the perfect block, is very small, or when the structure factor $|F|$ is very small. For a given crystal, primary extinction is greatest for the strongest spectra. To illustrate this point, we reproduce here some calculations of $\tanh pq/pq$ for a few reflections from perfect plates of rock salt and diamond of different thicknesses given by Lonsdale (1947 a).

Both Darwin and Waller derived their expressions for a thin plate of infinite extent. In other words, the correction for primary extinction has been introduced for a crystal consisting of parallel-sided slabs. Crystals of this structure do not, in fact, exist. A real mosaic consists of small disorientated blocks. However, it is possible that so long as the individual blocks are not so small that the widths of the diffraction maxima produced by them becomes appreciable in comparison with the angular disorientations of the blocks themselves, the formulae of Darwin and Waller might apply reasonably well.

Table 1. Primary Extinction

Rock Salt

hkl	*d* (Å)	$q \times 10^4$	tanh *pq*/*pq*		
			$t_0 = 10^{-3}$ cm	$t_0 = 10^{-4}$ cm	$t_0 = 10^{-5}$ cm
200	2·814	2·05	0·14	0·85	1·00
400	1·407	$0{\cdot}30_7$	0·46	0·98	1·00
600	0·938	$0{\cdot}08_1$	0·81	1·00	1·00
800	0·703	$0{\cdot}02_6$	0·90	1·00	1·00
10, 0, 0	0·563	$0{\cdot}00_9$	0·99	1·00	1·00

Diamond

hkl	$q \times 10^5$	tanh *pq*/*pq*	
		$t_0 = 10^{-3}$ cm	$t_0 = 10^{-4}$ cm
111	9·84	0·21	0·93
220	2·85	0·45	$0{\cdot}98_2$
113	1·22	0·71	$0{\cdot}99_5$
004	1·09	0·68	$0{\cdot}99_4$
331	0·65	0·83	$0{\cdot}99_8$

A formula for spherical crystals is, perhaps, a better approximation to reality. Ekstein (1951) has treated this problem for the case of neutron scattering by a perfect crystalline sphere which has small but not negligible primary extinction. His expression, when altered to suit the x-ray case, is

$$\frac{I'_{\mathrm{p}}}{I_{\mathrm{p}}} = 1 - \frac{7}{16} N^2 t_0^2 \lambda^2 \left(\frac{e^2}{mc^2}\right)^2 |F|^2 \frac{1+\cos^4 2\theta}{1+\cos^2 2\theta} \quad . \ . \ . \quad (7)$$

for unpolarized x-rays, where I'_p and I_p are the peak intensities of reflection with and without extinction respectively, and t_0 in this case, is the diameter of the sphere. The applicability of this formula to integrated intensities is, however, uncertain.

§ 3. Secondary Extinction

When x-rays fall on an imperfect crystal, the primary beam in the Bragg direction becomes progressively weaker on penetrating it, partly due to the normal linear absorption coefficient, and partly due to the fact that the beam is being constantly reflected away. Now consider a block in the reflecting position. The intensity of the radiation reaching it is reduced by the reflection from the parallel blocks through which the beam has passed; the intensity of the reflected beam also suffers diminution in its outward path in a similar manner. The effect of this is to increase the normal absorption of the crystal. This enhancement of the absorption at the reflecting angle is called secondary extinction. One can see in a simple way that secondary extinction will be dependent on the degree of parallelism of the blocks and on the intensity of the reflection. In an ideally imperfect crystal, the blocks are so small and their disorientation so large that the amount of energy lost by reflection is negligible as compared with that lost by absorption.

The problem of estimating this effect appears at first to be somewhat similar to the case of multiple reflections and primary extinction in a perfect crystal, but it is in fact quite different. In a perfect crystal, there is complete coherence between the primary and reflected waves and the resultant effect is obtained by summing the amplitudes of the waves. In an imperfect crystal the different blocks are optically independent and the resultant effect is obtained by summing the intensities. Darwin, in the paper already referred to, showed that when secondary extinction is present, the absorption coefficient has to be replaced by the quantity μ', where

$$\mu' = \mu + gQ - g'Q^2 + \ldots .$$

Terms involving squares and higher powers of Q are probably negligible in most real crystals. Hence, for a symmetrical reflection from the incident side of a thick crystal having secondary extinction

$$\rho' = \frac{Q}{2(\mu + gQ)} . \quad . \quad . \quad . \quad . \quad . \quad . \quad . \quad . \quad (8)$$

To bring out the polarization factor explicitly in the above formula, the procedure is to take the mean of the integrated reflections for the electric vector polarized perpendicular and parallel respectively to the plane of incidence, the two components being incoherent in unpolarized radiation. Equation (8) then becomes

$$\rho' = \tfrac{1}{2}\left[\frac{Q_\perp}{2(\mu + gQ_\perp)} + \frac{Q_\parallel}{2(\mu + gQ_\parallel)}\right] \quad . \quad . \quad . \quad . \quad . \quad (9)$$

where

$$Q_\perp = N^2\lambda^3\left(\frac{e^2}{mc^2}\right)^2 \frac{|F|^2}{\sin 2\theta}$$

and

$$Q_\parallel = Q_\perp \cos^2 2\theta.$$

g is called the secondary extinction coefficient. An exact description of

the disorientation of the blocks will be extremely difficult, but for convenience, the distribution function may be taken to be of the type $W(\Delta)$, where Δ is the magnitude of the angular deviation from the mean. If W is an error function,

$$W(\Delta) = \frac{1}{\eta\sqrt{(2\pi)}} \exp(-\Delta^2/2\eta^2)$$

where η is the standard deviation. It can then be shown that (see Zachariasen, *loc. cit.*, p. 168)

$$g = 1/2\eta\sqrt{\pi}.$$

As an example, if we take $\eta = 1{\cdot}1 \times 10^{-3}$ (4′ or arc), $g = 260$.

Since gQ is proportional to $|F|^2$, secondary extinction, like primary extinction, is greatest for the strongest spectra. This will be appreciated from the data on a single crystal of aluminium due to James *et al.* (1929).

Table 2. Secondary Extinction. Integrated Reflections from Aluminium

$\lambda = 0{\cdot}71$ Å. $\mu = 14{\cdot}35$

hkl	$\rho \times 10^6$ (absolute)			
	Observed	Calculated		
		Perfect	Ideal mosaic	Imperfect crystal $g = 300$
111	580	19·6	818	547
200	436	16·2	619	450
222	144	6·3	158	144
400	86	4·47	91	86
333	26·2	2·19	28·3	27·8
600	12·2	1·31	12·0	11·9
444	4·95	0·76	5·14	5·13
800	2·10	0·40	2·09	2·09
555	1·43	0·37	1·39	1·39

The agreement between the observed intensities and the values calculated on the assumption that there is only secondary extinction indicates that primary extinction is small if not absent in this crystal.

In general, we may expect both primary and secondary extinction to be present in a crystal. In such a case, Q in (8) and (9) has to be replaced by Q', where Q'/Q is defined by (5), (6) or (7).

§ 4. Theoretical Dependence of Extinction on Wavelength

Equations (5) and (6) for primary extinction are functions of the quantity

$$A_0 = \frac{Ne^2\lambda}{mc^2} \cdot \frac{t_0}{\gamma_0} \cdot |F|.$$

For a symmetrical reflection from a crystal face, $\gamma_0 = \sin\theta$, and since $\lambda/\sin\theta = 2d$, A_0 in (5) becomes independent of λ (assuming, of course, that F is independent of λ, i.e. that dispersion effects are small). Thus, by Darwin's theory, primary extinction is independent of wavelength. The polarization factor in (5) varies with wavelength, and has the effect of increasing the extinction slightly with decrease of wavelength; but, for the range of wavelengths usually employed, this increase is so small that we shall neglect it in the present discussion.

For a symmetrical reflection through a plate, $\gamma_0 = \cos\theta$; hence, A_0 in (6) involves λ. Therefore, according to Waller's theory, primary extinction decreases with decrease of wavelength.

By Ekstein's theory also primary extinction decreases with decrease of wavelength.

The theories do not agree on this point, and the exact dependence on wavelength of primary extinction in real crystals can be decided only by further investigation (see § 7).

The theory is, however, quite straightforward for secondary extinction. gQ in (9) is proportional to $\lambda^3/\sin 2\theta$ but μ itself varies approximately as λ^3. Hence the ratio of secondary extinction to absorption increases with decrease of wavelength.

§ 5. Experimental Studies of Extinction—General Survey

We shall now outline some of the information on crystal perfection obtained from measurements of absolute integrated intensities of x-ray reflections.

Experiments have established that highly perfect crystals which reflect x-rays exactly as required by the dynamical theory of diffraction in ideal crystals do exist. Notable examples are some specimens of diamond (W. H. Bragg 1921), calcite (W. H. Bragg 1915, Allison 1932, Parratt 1932) and rock salt (Renninger 1934). Such crystals are, however, extremely rare. Most real crystals approximate more closely to the mosaic than to the perfect type as far as their properties of reflecting x-rays are concerned. As a rule they exhibit both primary and secondary extinction, though some have been found to show only the latter. There have been very few attempts at making a direct determination of extinction by a method which does not require a knowledge of the structure of the crystal. In most cases, the extinction has been estimated by trying to account for the discrepancy between the observed intensities and the intensities calculated from the known structure on the basis of the mosaic formula. Extinction effects have also been studied with the object of determining block size in annealed material. For instance, it is found that strong low-angle lines in x-ray

photographs of metal powders are weaker for annealed material than for cold worked material (Lang 1953, Williamson and Smallman 1955). However, estimates of block size and degree of perfection are difficult and necessarily inaccurate, since the presence of dislocations and strains will reduce the extinction by an amount which is by no means easy to calculate. In theoretical work, the block model of the mosaic was chosen for mathematical convenience. Such a structure is often only approximately realized in actual crystals. Imperfections can be caused by warping, clusters of vacancies, stacking faults, variation of lattice parameters, impurities and many other reasons. Anything that prevents an exact regularity of arrangement from persisting over more than a few thousand atomic planes will result in the crystal reflecting x-rays like a mosaic. Taking these factors into consideration, it is indeed remarkable that even a few highly perfect crystals of the size of a few millimetres or more have actually been found in nature.

The intensity of an x-ray reflection is extremely sensitive to surface treatment. Rubbing, grinding and mechanical polishing may increase the intensity of reflection by several times and can change a perfect crystal into an ideally imperfect surface (Renninger, *loc. cit.*, Sakisaka 1930, Evans *et al.* 1948, Gay *et al.* 1952). Both the average size of the blocks (primary extinction) and their relative orientation (secondary extinction) will be altered by surface treatment. An important point which emerges from studies of this type is that the state of the surface of the crystal will almost certainly not be representative of its interior.

Thermal treatment also influences the intensity of a reflection very greatly. James (1925) found that the intensities of the low-order spectra of rock salt were decreased permanently when the crystals were heated for some time at about 600°C. The decrease could be explained as due to primary extinction caused by recrystallization of the mosaic at high temperature. That this explanation was true was confirmed by the fact that the decrease in intensity was greater for the stronger spectra. A similar effect has been detected in annealed metal powders. Dipping certain organic crystals in liquid air, on the contrary, increases the intensity of the reflection considerably. The sudden fall of temperature causes a type of shock, destroying the perfection of the crystal and breaking it up into a mosaic (Lonsdale 1947 b, 1948).

In view of the variety of factors which affect the intensity of an x-ray reflection, the problem of assessing crystal perfection is a very complex one. In the present report we are interested in the phenomenon of extinction mainly from the point of view of crystal structure analysis. Therefore, we shall not deal with the texture of crystals in detail, but reference may be made to a review article by Hirsch (1956) for a thorough discussion of the different aspects of this subject. We shall consider only a few experiments which have attempted to correct for extinction in the course of the determination of the electron density distribution in crystals, and a few others which throw light on the degree of perfection of large single crystals.

§ 6. Determination of Secondary Extinction

The first experiment for making an actual estimate of extinction was by W. L. Bragg *et al.* (*loc. cit.*). They measured the absolute integrated reflections from rock salt with the object of determining the scattering factors of Na and Cl experimentally. When they plotted f_{Na} and f_{Cl} against $\sin\theta$, they found that for small angles the curves for both Na and Cl were about 20% lower than the expected values of 10 and 18 respectively (assuming that both the atoms are ionized in the crystal). Realizing that this discrepancy was due to the enhanced absorption of the crystal at the reflecting angle, they proceeded to determine the effective absorption directly. In order to do this, they measured the integrated intensities from a number of plates of different thicknesses cut from the same crystal of rock salt so that the reflecting planes were normal to the faces. The integrated reflection in the presence of extinction in such a case is given by

$$\rho' = Q'\,T\sec\theta\exp\left[-(\mu+gQ')\,T\sec\theta\right],$$

where T is the thickness of the plate. Therefore,

$$\log\left(\rho'/T\sec\theta\right) = -(\mu+gQ')\,T\sec\theta + \text{const.}$$

For any reflection, the plot of $\log(\rho'/T\sec\theta)$ against T should be a straight line, the slope of which is proportional to $(\mu+gQ')$. Table 3 gives the values of gQ' obtained by them for a particular specimen of rock salt.

Table 3. Secondary Extinction in Rock Salt

Rh K_α radiation. $\mu = 10{\cdot}70$

hkl	Effective absorption coefficient $(\mu+gQ')$	Secondary extinction gQ'	Integrated reflection ρ' (arbitrary units)
200	16·30	5·6	100
220	13·60	2·9	50·5
400	12·66	1·96	19·9
600	10·72	0·02	4·9

The approximate proportionality between gQ' and ρ' (within experimental limits) is a proof of the essential correctness of their theoretical deductions. It was gratifying to find that when the measured scattering factors were corrected for extinction, they tended much more towards the expected values.

This method makes it possible to correct for secondary extinction (gQ'), but not for primary extinction (Q'/Q). When the crystal exhibits appreciable primary extinction as well, the method may prove to be unsatisfactory even for determining the secondary coefficient, as was found by Bragg

and West (1928) with topaz. The plot of log $(\rho'/T\sec\theta)$ versus T did not give a straight line and it was not possible to judge the slope accurately. The explanation for this is that when the crystal, which is fairly perfect, is ground, the surface layers are rendered imperfect while the interior still remains undisturbed. Thus the thinner the plate the greater the fraction of its volume which is likely to show only secondary extinction, and since the property of the plate as a whole varies from one value of T to another, the experimental points will not lie on a straight line.

In practice it may not always be possible to obtain good plates of crystal. James and Firth (1927) suggested another method which will give the secondary extinction coefficient by direct measurement without any need to destroy the crystal by grinding it. The absolute integrated reflections are measured for two wavelengths λ_1 and λ_2. If dispersion is negligible for these two wavelengths, Q_1/Q_2 is a known quantity. The ratio Q_1/Q_2 and the two relations

$$\rho_1' = Q_1/2(\mu_1 + gQ_1) \quad \text{and} \quad \rho_2' = Q_2/2(\mu_2 + gQ_2)$$

give three equations from which Q_1, Q_2 and g may be solved. James and Firth used rhodium and molybdenum radiations to measure the secondary extinction in rock salt and got good agreement with the previous method.

§ 7. Determination of Primary Extinction

Recently Weiss and De Marco (1958) have developed a method of correcting for primary extinction. The aim of their investigation was to measure the atomic scattering factors of Cu, Ni, Co, Fe and Cr in order to determine their outer electron configurations in the solid state. The free atom configurations in all these metals consist of an 'argon core' plus electrons in the 3d and 4s states. They assumed that the 'argon core' is essentially unchanged in the solid, and therefore their procedure was to measure the absolute scattering factors and to subtract the contribution of the 'argon core' as calculated by self-consistent field techniques for the free atom.

They obtained absolute intensity data by measuring the symmetrical reflection from the face of a thick crystal. In passing, it may be remarked that this is the most convenient way of measuring absolute intensities of reflections, the integrated reflection without extinction being given by $Q/2\mu$, provided the surface of the crystal is perfectly flat and exactly parallel to the reflecting planes. Non-parallelism can be corrected for by reversing the incident and diffracted beams and averaging the two integrated reflections (W. H. Bragg 1914). The effect of deviations from flatness is, however, extremely difficult to calculate. Weiss and De Marco overcame that by polishing the crystal surface to a mirror finish with fine diamond dust.

From the reflection curve, they estimated the angular disorientations of the blocks in the mosaic to be of the order of $\frac{1}{2}°$ and concluded that secondary

extinction was negligible. To correct for primary extinction, they assumed a first order correction term of the type

$$\frac{|F'|^2}{|F|^2} = 1 - P^2 K\lambda^2 \qquad \ldots\ldots\ldots \quad (10)$$

where $|F'|$ is the observed structure factor without correcting for extinction, $|F|$ is the true structure factor, P is a constant which depends on the size and shape of the blocks and on $|F|$, and K is the polarization factor. This expression is similar to Ekstein's correction for primary extinction (eqn. (7)) and has the same dependence on wavelength. If the incident beam has been monochromatized by reflection from a *mosaic* crystal

$$K = \frac{1 + \cos^2 2\alpha \cos^4 2\theta}{1 + \cos^2 2\alpha \cos^2 2\theta}$$

where α is the Bragg angle of the monochromator reflection (Lang 1953).

Now if the absolute integrated intensity for a particular reflection is measured for a few wavelengths chosen so that dispersion effects are small, a plot of $|F'|^2$ versus $K\lambda^2$ will give a straight line, since $|F|^2$ and P^2 may be treated as constants. This line when extrapolated to $K\lambda^2 = 0$ will give the true value of $|F|^2$ for the reflection. Weiss and De Marco used three wavelengths (0·49 Å, 0·709 Å and 0·91 Å) monochromatized by the 200 reflection from NaCl. The plot of $|F'|^2$ versus $K\lambda^2$ was in fact a straight line, supporting their hypothesis that the primary extinction was not very large.

If these results are confirmed and proved to be generally true, it would mean that even though Ekstein's correction for peak intensities may not be directly applicable to integrated intensities, the essential form of his expression is valid as far as the dependence of primary extinction on wavelength is concerned. It might be recalled that Darwin's correction for primary extinction is independent of wavelength, and Waller's correction varies with wavelength in approximately the same manner as Ekstein's correction.

The straightness of the line connecting $|F'|^2$ versus $K\lambda^2$ also indicates that secondary extinction was not operative in the crystal. If secondary extinction is also present, the method turns out to be unsatisfactory, as will be evident from the following consideration. If ρ' is the integrated reflection from a crystal face in the presence of secondary extinction,

$$\frac{\rho'}{\rho} = \frac{|F'|^2}{|F|^2} = \frac{\mu}{(\mu + gQ)}.$$

Neglecting the polarization factor,

$$Q \propto \frac{\lambda^3}{\sin 2\theta} |F|^2 \propto \lambda^2 |F|^2$$

for small values of θ. Therefore

$$\frac{|F'|^2}{|F|^2} = 1 - \frac{S^2 K\lambda^2}{\mu}$$

to a first approximation, where S = constant $\times |F|$, and K is the polarization

factor. The plot of $|F'|^2$ versus $K\lambda^2$ will no longer be a straight line since μ itself varies rapidly with wavelength (Authier and Warren 1956). Thus, when there is an unknown proportion of primary and secondary extinction existing simultaneously,

$$\frac{|F'|^2}{|F|^2} = 1 - \left(P^2 + \frac{S^2}{\mu}\right) K\lambda^2,$$

and the extrapolation to $K\lambda^2 = 0$ becomes difficult.

Weiss and De Marco obtained unexpected values for the number of 3d electrons in some of the crystals they examined. (The radial distributions of the 4s electrons in these metals are such that their scattering factors are negligible even for the lowest Bragg angles.) Their results have been the subject of subsequent discussion (Hume-Rothery *et al.* 1958, Batterman 1959, Weiss and De Marco 1959, Freeman and Weiss 1959).

§ 8. Divergent Beam X-ray Photography

A direct way of qualitatively demonstrating primary and secondary extinction in crystals is by the use of divergent beam x-ray photography developed by Lonsdale (1947 b). A thin crystal plate is placed in contact with a divergent source of x-rays and the transmission picture is recorded on a film placed at some distance. On such photographs, under appropriate experimental conditions, there is a grey background on which are white (deficiency) lines marking those directions in which *differential* absorption has occurred. Lonsdale found that no patterns are recorded either when the crystal is too nearly perfect (primary extinction) or when it is too completely imperfect. When the crystal is perfect, the actual amount of radiation removed from the primary beam is so small that no absorption lines are visible, though if they do appear occasionally they are sharp, as is to be expected. When the crystal is highly imperfect and the range of reflection exceedingly large, there is no noticeable difference in absorption in the reflecting region and consequently no lines show up. It is only with crystals of the more usual degree of imperfection that good patterns are obtained. A noteworthy fact which Lonsdale discovered is that many organic crystals, which are generally so brittle and soft that one would expect them to be mosaic in character, show appreciable primary extinction, a point of great importance in crystal analysis. At first it was difficult to decide whether the absence of patterns with such crystals was due to perfection or a high degree of imperfection. But when the crystals were subjected to a thermal shock by immersion in liquid air for a few seconds, the white lines appeared very clearly in the photographs. This treatment destroyed the perfection of the crystal and broke it up into a mosaic.

This technique provides a quick method of distinguishing between primary and secondary extinction without resort to accurate determinations of absolute integrated intensities and half-widths of x-ray diffraction maxima from crystals.

§ 9. Bragg Reflection of Polarized X-rays

The influence of crystal imperfection on the reflection of polarized x-rays has been investigated by Ramaseshan and Ramachandran (1953, 1954). They showed experimentally for the first time that the polarization characteristic of a reflection depends on the degree of perfection of the crystal.

When the incident x-rays are unpolarized, the integrated reflections from a mosaic and a non-absorbing perfect crystal are respectively given by

$$\rho_{\mathrm{M}} = \frac{1}{2\mu} N^2\lambda^3 \left(\frac{e^2}{mc^2}\right)^2 |F|^2 \frac{1+\cos^2 2\theta}{2\sin 2\theta} = R_{\mathrm{M}}\left(\frac{1+\cos^2 2\theta}{2}\right),$$

$$\rho_{\mathrm{P}} = \frac{8}{3\pi} N\lambda^2 \frac{e^2}{mc^2} |F| \frac{1+|\cos 2\theta|}{2\sin 2\theta} = R_{\mathrm{P}}\left(\frac{1+|\cos 2\theta|}{2}\right).$$

If the incident x-rays are polarized with the electric vector making an angle ϕ with respect to the plane of incidence,

$$\rho_{\mathrm{M}\phi} = R_{\mathrm{M}}(\sin^2\phi + \cos^2\phi\cos^2 2\theta),$$

$$\rho_{\mathrm{P}\phi} = R_{\mathrm{P}}(\sin^2\phi + \cos^2\phi\,|\cos 2\theta|),$$

or

$$r_{\mathrm{M}}(\phi) = \rho_{\mathrm{M}\phi}/\rho_{\mathrm{M}\sigma} = \sin^2\phi + \cos^2\phi\cos^2 2\theta,$$

$$r_{\mathrm{P}}(\phi) = \rho_{\mathrm{P}\phi}/\rho_{\mathrm{P}\sigma} = \sin^2\phi + \cos^2\phi\,|\cos 2\theta|,$$

where the subscript σ refers to the case when $\phi = 90°$. Except for values $\theta = 0°$, $45°$ or $90°$, the above two equations are different. Thus the mosaic and the perfect crystal will behave differently towards polarized x-rays.

Ramaseshan and Ramachandran used copper radiation and the 440 reflection from a large KCl crystal ($2\theta \sim 88°$) to give monochromatic polarized x-rays. Perfect polarization may be obtained only if $2\theta = 90°$ (i.e. $\cos 2\theta = 0$), but with this arrangement they had less than 1% of unpolarized radiation. They measured the integrated reflections for various values of ϕ, ranging from $90°$ to $0°$, from crystals of sodium nitrate grown from a saturated solution, first using a natural face and later after grinding it. Different values of ϕ were obtained by rotating the goniometer about an axis coincident with the incident beam. They obtained the important result that the experimental points for both the natural and the ground face lay between the theoretical curves $r_{\mathrm{P}}(\phi)$ and $r_{\mathrm{M}}(\phi)$ versus ϕ for the perfect and the mosaic crystal respectively. The points for the ground face were very near the curve for the mosaic crystal, while those for the natural face were consistently higher and closer to the curve for the perfect crystal. Ramaseshan and Ramachandran suggested that the degree of perfection of the crystal may be estimated by the quantity

$$\frac{r_{\mathrm{c}}(\phi) - r_{\mathrm{M}}(\phi)}{r_{\mathrm{PA}}(\phi) - r_{\mathrm{M}}(\phi)}$$

where $r_{\mathrm{c}}(\phi)$ is the experimental value for the crystal, and $r_{\mathrm{P}A}(\phi)$ has the same significance as $r_{\mathrm{P}}(\phi)$, but with the absorption of the crystal taken into account (Hirsch and Ramachandran 1950). The ratio was found to be 63% for the natural face and 20% for the ground one.

Similar measurements have been carried out by Chandrasekaran (1959). In his experiments he used the 311 reflection of copper to monochromatize copper radiation ($2\theta = 90^\circ 12'$), thus obtaining almost perfectly polarized X-rays.

The physical significance of this empirical definition of the degree of perfection of a crystal is, however, rather ambiguous. A high degree of perfection would seem to imply that the size of the perfect blocks constituting the mosaic is large, i.e. large primary extinction, whereas, as we shall see later (§ 11), polarization measurements cannot in fact distinguish between primary and secondary extinction. Moreover, so far as the properties of reflecting X-rays are concerned, the degree of perfection of a crystal may vary a great deal from reflection to reflection. For instance, it is well known that a crystal may behave like an ideal mosaic for a very weak reflection and yet show considerable perfection (extinction) for a very strong reflection. This method of estimating the degree of perfection of a crystal is, for this reason, somewhat inconclusive.

§ 10. Extinction in Crystal Analysis

In crystal structure analysis, the specimens employed are usually very small and completely bathed in the incident X-ray beam. Even tiny crystals as a rule exhibit a small amount of extinction which reduces the intensities of the strongest reflections by about 30% or so. Some crystals show more pronounced extinction effects, but in the majority of such cases the specimens may be rendered imperfect by grinding or by thermal shock produced by immersion in liquid air. Although it is possible to reduce extinction by such treatment one can rarely be certain of having eliminated it altogether. Extinction is, in fact, a major source of error in the determination of a set of structure factors. In structure analysis, it is often found that in the final stages of refinement, the calculated structure factors (F_c) for the strongest reflections tend to be slightly greater than the corresponding observed values (F_0). It is generally assumed that this is due to extinction. The usual procedure is to replace F_0 by F_c for these reflections, or to weight the difference between them suitably, before proceeding with the refinement. Such methods, which seek to correct for extinction by a comparison of F_0 and F_c, may prove to be efficacious for obtaining the atomic coordinates (e.g. Vand 1955, Jellinek 1958), but in all of them it is taken for granted that the assumed scattering factors, which are based on the theoretical calculations for the free atom, are unaltered in the molecule or crystal. If, however, the object of the analysis is the accurate determination of the electron density distribution and the outer electron configuration in the solid state, the expedient of replacing F_0 by F_c is obviously unsatisfactory.

One of the first attempts to correct for extinction errors in small crystals was by Robinson (1933). According to theory, the form of the reflection curve from an imperfect crystal is determined by the function defining the disorientation of the blocks in the mosaic. Since the secondary extinction

coefficient (g) is dependent on this distribution function, it should be possible in principle to measure the secondary extinction directly by plotting the curve swept out by the reflected beam as the crystal is rotated, provided the distribution of the blocks is uniform throughout the volume of the crystal. The method was used by Robinson to account for secondary extinction in crystals of anthracene. However, subsequent investigations have shown that, while the width of the reflection is an indication of the degree of imperfection of the crystal, estimates of the actual amount of extinction from reflection curves are liable to be very much in error. For a crystal may consist of relatively large scale fragments which modify the whole reflection curve, but it is the texture of the individual fragments which will be responsible for extinction (see James 1954, p. 282).

Cochran (1953) has developed a technique for correcting for secondary extinction which has proved to be useful in crystal analysis. When the integrated reflections are measured from a few crystals of different radii, it is generally found that the relative intensities for the strongest reflections (after accounting for the normal absorption) are less for the larger specimens because of extinction. If, for any reflection, the proportional change in the relative intensity is plotted against crystal radius, the points lie very approximately on a straight line, the slope of which is proportional to the intensity of the reflection, being practically zero for the weak reflections. The true value of the relative intensity may be taken to be equal to that for the smallest crystal if it is sufficiently small, or more accurately by extrapolating the line to zero radius. The principle of this method, which is in fact essentially similar to that of Bragg, James and Bosanquet, may be explained in the following way. The integrated reflection without extinction from a crystal of volume V, completely bathed in the incident x-ray beam, is given by

$$\rho = AQV$$

where A is the absorption factor. We shall assume in the present discussion that the crystal is *weakly* absorbing. If we express the absorption factor as $\exp(-\mu T_{\text{eff}})$, where μ is the linear absorption coefficient for the wavelength λ, and T_{eff} the effective path traversed by the beam in the crystal, the integrated reflection in the presence of secondary extinction may be written as

$$\rho' = QV \exp[-(\mu + gQ)T_{\text{eff}}]$$

when the extinction is not large. Therefore

$$\frac{\rho'}{\rho} \approx (1 - gQT_{\text{eff}}). \quad \ldots\ldots\ldots \quad (11)$$

It is not unreasonable to suppose that T_{eff} is proportional to the radius of the crystal, and hence a plot of the proportional change in the intensity versus radius should be a straight line, provided g does not vary from specimen to specimen. This line when extrapolated to zero radius gives the corrected value of the intensity. The method, however, makes no correction for primary extinction (Q'/Q).

It may be useful at this point to discuss the wavelength dependence of primary and secondary extinction in small *weakly* absorbing crystals. Let us first consider primary extinction. Assuming that primary extinction is expressible by a formula of the Ekstein type (see § 7, eqn. (10)), we have in the absence of secondary extinction

$$\frac{|F'|^2}{|F|^2} = 1 - P^2 K\lambda^2.$$

Now if the integrated intensity for any reflection is measured for a few wavelengths chosen so that dispersion effects are small, and the different measurements are corrected for absorption and brought to the same relative scale, then a plot of $|F'|^2$ versus $K\lambda^2$ will be a straight line, which when extrapolated to $\lambda^2 = 0$ will give the true value of $|F|^2$.

If the crystal suffers from secondary extinction only, the integrated reflection is given by (11). Neglecting the polarization factor, Q is approximately proportional to $\lambda^2 |F|^2$, and hence after correcting for absorption

$$\frac{|F'|^2}{|F|^2} = 1 - S^2 T_{\text{eff}} K\lambda^2$$

where $S = \text{constant} \times |F|$. For a crystal of arbitrary shape T_{eff} itself will vary from one wavelength to another, and therefore in this case $|F'|^2$ plotted against $T_{\text{eff}} K\lambda^2$ results in a straight line which could be extrapolated to $\lambda^2 = 0$ as before.

In the general case when both primary and secondary extinction exist simultaneously,

$$\frac{|F'|^2}{|F|^2} = 1 - (P^2 + S^2 T_{\text{eff}}) K\lambda^2. \quad . \quad . \quad . \quad . \quad . \quad (11\,a)$$

Here the plot of $|F'|^2$ versus $K\lambda^2$ is not a straight line and the extrapolation to $\lambda^2 = 0$ becomes uncertain. Measurements over a variety of wavelengths may, however, be used to check whether the crystal is reflecting like an ideal mosaic. For if the observed structure factor is found to be independent of the wavelength, it means that both P and S in (11 *a*) are zero, i.e. that the reflection is not subject to extinction.

For a symmetrical reflection through a thin crystal plate of thickness T, $T_{\text{eff}} = T \sec\theta \approx T$ when θ is small. In this special case, (11 *a*) can be used to correct for both primary and secondary extinction, since T_{eff} may without sensible error be regarded as independent of λ for small values of θ. A similar method has been applied by Gatineau and Mering (1956).

§ 11. Correction for Extinction Errors by the Use of Polarized X-rays

Polarized x-rays may be used to obtain the true value of the structure factor in the presence of extinction (Chandrasekhar 1956, 1960). The principal merit of this technique is that it accounts for both primary and secondary extinction simultaneously in a crystal of any shape. We shall derive the theory for a small crystal completely bathed in the incident x-ray

beam, but the equations may be readily modified for any other type of experimental arrangement.

We shall assume in the first instance that the incident x-rays are polarized perpendicular to the plane of incidence, so that the polarization factor is taken to be unity. For a mosaic crystal of arbitrary shape and of volume completely bathed in the x-ray beam,

$$\left.\begin{aligned} &\rho = AQV \\ \text{where} \quad &Q = \left(\frac{Ne^2}{mc^2}\right)^2 \frac{\lambda^3}{\sin 2\theta} \cdot |F|^2; \end{aligned}\right\} \quad . \quad . \quad . \quad . \quad (12)$$

A is the absorption factor given by $(1/V)\int \exp(-\mu r)\,dV$, where dV is a small element of volume in the crystal, r is the total path traversed by the beam in the crystal before and after reflection from the element of volume under consideration, and μ is the linear absorption coefficient for the wave-length λ. The integral can be evaluated by numerical methods if the shape of the crystal is known.

Let ρ' be the integrated reflection in the presence of extinction. For primary extinction

$$\rho'/\rho = f(A_0),$$

where, for Darwin's correction,

$$f(A_0) = \tanh A_0/A_0,$$

and for Waller's correction,

$$f(A_0) = \sum_{n=0}^{\infty} \frac{J_{2n+1}(2A_0)}{A_0},$$

where

$$A_0 = Ne^2\lambda/mc^2 \cdot t_0/\gamma_0 \cdot |F|,$$

t_0/γ_0 being the effective thickness of the perfect blocks constituting the mosaic.

For small values of A_0,

$$\frac{\tanh A_0}{A_0} = 1 - \frac{A_0^2}{3} + \frac{2A_0^4}{15} - \ldots$$

and

$$\sum_{n=0}^{\infty} \frac{J_{2n+1}(2A_0)}{A_0} = 1 - \frac{A_0^2}{3} + \frac{A_0^4}{20} - \ldots,$$

so that, to a first approximation in both cases,

$$\frac{\rho'}{\rho} = 1 - \frac{N^2 e^4 \lambda^2 t_0^2}{3m^2c^4\gamma_0^2} \cdot |F|^2. \quad . \quad . \quad . \quad . \quad . \quad . \quad (13)$$

Substituting for ρ in (13), we find that the integrated reflection in the presence of primary extinction may be written as

$$\rho' = \alpha|F|^2 - \beta|F|^4, \quad . \quad . \quad . \quad . \quad . \quad . \quad . \quad (14)$$

where α is a known quantity, while β is unknown, since t_0/γ_0 is unknown.

Ekstein's formula for primary extinction is

$$\frac{I'_p}{I_p} = 1 - \frac{7}{16} N^2 t_0^2 \lambda^2 \left(\frac{e^2}{mc^2}\right)^2 |F|^2 \quad . \quad . \quad . \quad . \quad (15)$$

where I_p' and I_p are the peak intensities of the reflection with and without extinction respectively, and t_0 in this case refers to the diameter of the perfect crystalline sphere. The formula for the integrated intensity in Ekstein's case has not yet been worked out, but as pointed out by Lang (1953), it will probably differ from that for the peak intensity by a numerical factor in the negative term of (15) (see also § 7). So the integrated reflection can still be represented by a formula of the type (14).

If the crystal suffers from secondary extinction,

$$\rho' = Q \int \exp\left[-(\mu + gQ)r\right] dV$$

$$= Q \int \exp(-\mu r)\, dV - gQ^2 \int r \exp(-\mu r)\, dV \quad . \quad . \quad . \quad (16)$$

to a first approximation, where g is the secondary extinction coefficient. Again, since $Q \propto |F|^2$, (16) may be expressed in the same form as (14), where, as before, α is known and β is unknown, since g is unknown.

When both primary and secondary extinction exist simultaneously, Q in (16) has to be replaced by Q', where

$$Q' = Q\left(1 - \frac{{A_0}^2}{3}\right).$$

It may easily be verified that, to a first approximation, the integrated reflection will then be given by

$$\rho' = \alpha |F|^2 - (\beta_{\text{prim}} + \beta_{\text{sec}}) |F|^4.$$

We thus arrive at the interesting result that whatever be the type of extinction present, the integrated reflection for normal polarization may be written as

$$\rho_\perp' = \alpha |F|^2 - \beta |F|^4 \quad . \quad . \quad . \quad . \quad . \quad . \quad . \quad (17)$$

when the extinction is not large†. If, on the other hand, the incident x-ray beam is polarized parallel to the plane of incidence, the integrated reflection is obtained simply by replacing $|F|$ by $|F \cos 2\theta|$, since all other factors remain unchanged, and we have

$$\rho_\parallel' = \alpha |F|^2 \cos^2 2\theta - \beta |F|^4 \cos^4 2\theta. \quad . \quad . \quad . \quad . \quad . \quad (18)$$

Eliminating β from (17) and (18), we get

$$|F|^2 = \frac{\rho_\parallel' - \rho_\perp' \cos^4 2\theta}{\alpha(\cos^2 2\theta - \cos^4 2\theta)}. \quad . \quad . \quad . \quad . \quad . \quad (19)$$

A measurement of the integrated reflections for x-rays polarized perpendicular and parallel to the plane of incidence should, therefore, enable one to eliminate extinction effects.

† The same type of expression is also valid for the integrated reflection from a crystal completely bathed in a neutron beam, when the extinction (primary or secondary) is not large. The only difference in this case is that μ may be taken to be nearly equal to zero, since the linear absorption coefficient for neutrons is almost negligible as compared with that for x-rays. Extinction effects may be eliminated by the use of polarized neutrons to obtain accurate magnetic scattering factors (Chandrasekhar and Weiss 1957).

It is interesting to consider the problem from a slightly different standpoint. If the incident x-rays are polarized with the electric vector making an angle ϕ with respect to the plane of incidence, then for an ideally mosaic crystal

$$\rho_\phi/\rho_\perp = \sin^2\phi + \cos^2\phi\cos^2 2\theta \quad . \quad . \quad . \quad . \quad . \quad (20)$$

(see § 9), while for an imperfect crystal exhibiting extinction, we have from (17) and (18)

$$\rho_\phi'/\rho_\perp' = \frac{\alpha|F|^2(\sin^2\phi + \cos^2\phi\cos^2 2\theta) - \beta|F|^4(\sin^2\phi + \cos^2\phi\cos^4 2\theta)}{\alpha|F|^2 - \beta|F|^4} . \quad . \quad . \quad . \quad (21)$$

Fig. 1

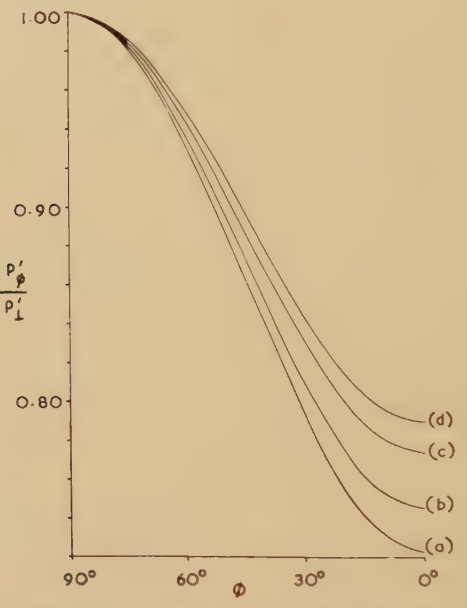

$\rho_\phi'/\rho_\perp'$ versus ϕ for the 200 reflection of rock salt ($2\theta = 31^\circ 48'$); (*a*) no extinction, (*b*) 10% extinction, (*c*) 20% extinction, (*d*) 25% extinction.

Except for $2\theta = 0^\circ$, 90° and 180°, the above two equations are different. The variation of $\rho_\phi'/\rho_\perp'$ with ϕ is shown in figs. 1 and 2 for the 200 and 220 reflections of rock salt for $\lambda = 1{\cdot}5418$ Å (weighted mean of CuK_{α_1} and CuK_{α_2}). The percentage of extinction in these curves is defined in terms of the reduction in intensity due to extinction for *normal* polarization; for example, the curve for 10% extinction is obtained by putting $\beta|F|^4 = 0{\cdot}1\,\alpha|F|^2$ in (21). These curves provide an alternative method of estimating extinction which involves the measurement of the variation of the integrated reflection with angle of polarization. Although (19) provides a straightforward method of eliminating extinction, and is theoretically simpler, the latter approach is superior from the point of view of experiment, since it requires the fitting of a theoretical curve through a number of observed points.

The principle of the method may be stated physically as follows. Extinction, whether it is primary or secondary, is greater for the stronger reflections. By the technique of varying the angle of polarization of the incident beam, we are altering the effective structure factor, and consequently the extinction, by a known quantity. This enables the extinction to be directly estimated. The method will obviously be more sensitive the greater the value of θ, as can be seen from figs. 1 and 2. For the 200 reflection of rock salt, the presence of 25% extinction causes an increase in $\rho_{\parallel}'/\rho_{\perp}'$ of about 10% (of the mosaic value), whereas for the 220 reflection the increase is nearly 15%. For this reason, the method will prove to be

Fig. 2

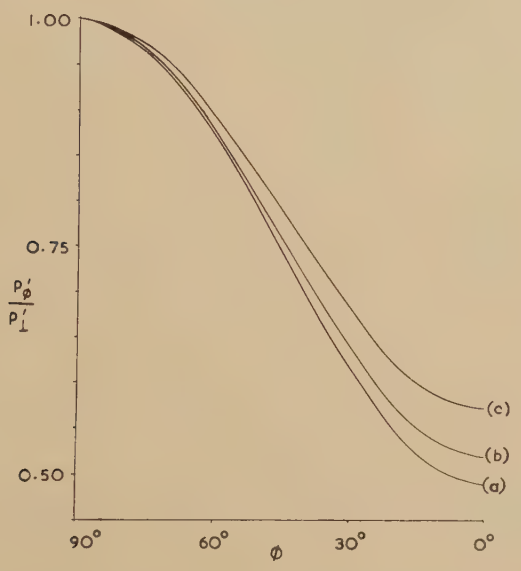

$\rho_{\phi}'/\rho_{\perp}'$ versus ϕ for the 220 reflection of rock salt ($2\theta = 45° 34'$); (*a*) no extinction, (*b*) 10% extinction, (*c*) 25% extinction.

unsatisfactory for small values of θ, say $\theta < 10°$, the exact limit of applicability depending on the accuracy of the intensity determinations. (For a detailed discussion of this point, see Chandrasekhar 1960).

The 311 reflection of diamond ($2\theta \sim 91° 30'$ for copper radiation) was used to obtain polarized x-rays. Intensity measurements were made with a Geiger counter diffractometer designed for three-dimensional x-ray work. The arcs with the crystal under investigation were mounted on a vertical circle, the axis of which was collinear with the polarized beam, so that the plane of incidence could be rotated through any desired angle. It was realized at the outset that, as the experiment consisted of an accurate study of the variation of the integrated reflection with angle of polarization, the non-uniformity of the divergence of the diamond reflected

beam might be a possible source of error in the measurements. The following procedure was adopted to check whether any correction was necessary. For an ideally perfect crystal with negligible absorption

$$\rho_\phi/\rho_\perp = \sin^2\phi + \cos^2\phi|\cos 2\theta| \quad . \quad . \quad . \quad . \quad . \quad (22)$$

When $2\theta = 90°$, (20), (21) and (22) become identical, and thus, irrespective of the state of perfection of the crystal,

$$\rho_\phi/\rho_\perp = \sin^2\phi.$$

Any departure from the $\sin^2\phi$ variation could only be due to the non-uniformity of the divergence and (or) the lack of perfection of polarization of the incident beam. The 311 reflection from a small specimen of diamond (less than 1 mm diameter) was used for the measurement. It was found that the integrated reflection exhibited the expected variation with ϕ within the limits of experimental error. This was indeed a repetition of the early polarization experiments of Barkla, Compton and others which proved that x-rays consist of electromagnetic waves (see Compton and Allison 1935).

Measurements were carried out on small crystals of rock salt (both natural and ground) to demonstrate the practical applicability of the method. The results obtained with one of the specimens (size $0{\cdot}93 \times 0{\cdot}93 \times 0{\cdot}221\,\text{mm}^3$) are shown in table 4. The relative values of the structure factors were calculated on the basis of the formula

$$\rho_\perp{}' \propto \frac{A|F_{\text{obs}}|^2}{\sin 2\theta}(100-\epsilon),$$

Table 4

hkl	$\rho_\perp{}'$ (arbitrary units)	A	ϵ (%)	F'_{obs}	F_{obs}	F (Renninger CuK_α)	F (Witte and Woelfel MoK_α)
200	584	0·2337	27	17·4	20·4	20·55	20·19
220	252	0·1838	18	15·0	16·6	16·75	—
400	180	0·2360	0	12·7	12·7	12·70	12·45

where $\rho_\perp{}'$ is the observed integrated reflection for normal polarization in the presence of extinction, A the absorption factor, and ϵ the percentage of extinction as estimated from the experimental variation of $\rho_\phi{}'/\rho_\perp{}'$. In the table F'_{obs} and F_{obs} are respectively the observed structure factors before and after correcting for extinction. The values were scaled so that $F_{\text{obs}}(400)$, which was found to have negligible extinction, is equal to the absolute value at room temperature due to Renninger (1952)

As there is no exact theory of primary extinction in real crystals, it is not possible to make a precise estimate of the errors involved in neglecting higher order terms in (14). However, applying the existing formulae it

may be shown that (21) is valid to a good accuracy when the extinction (primary or secondary) is not greater than 25% (Chandrasekhar 1960). The method can, therefore, be used for correcting for extinction errors in crystal analysis.

Acknowledgments

I am indebted to Professor Sir Lawrence Bragg, F.R.S., and Professor Dame Kathleen Lonsdale, F.R.S., for advice and encouragement.

References

Allison, S. K., 1932, *Phys. Rev.*, **41,** 1.
Authier, A., and Warren, B. E., 1956, *J. appl. Phys.*, **27,** 1382.
Batterman, B. W., 1959, *Phys. Rev. Letters*, **2,** 47.
Bragg, W. H., 1914, *Phil. Mag.*, **27,** 881 ; 1915, *Phil. Trans. Roy. Soc.* A, **215,** 253 ; 1921, *Proc. Phys. Soc. Lond.*, **33,** 304.
Bragg, W. L., 1949, *The Crystalline State*, Vol. 1 (London : Bell).
Bragg, W. L., Darwin, C. G., and James, R. W., 1926, *Phil. Mag.*, **1,** 897.
Bragg, W. L., James, R. W., and Bosanquet, C. H., 1921, *Phil. Mag.*, **41,** 309 ; 1921, *Ibid.*, **42,** 1 ; 1922, *Ibid.*, **44,** 433.
Bragg, W. L., and West, J., 1928, *Z. Kristallogr.*, **69,** 118.
Chandrasekaran, K. S., 1955, *Acta Cryst.*, **8,** 361 ; 1959, *Ibid.*, **12,** 916.
Chandrasekhar, S., 1956, *Acta Cryst.*, **9,** 954 ; 1960, *Ibid.*, **13,** 588.
Chandrasekhar, S., and Weiss, R. J., 1957, *Acta Cryst.*, **10,** 598.
Cochran, W., 1953, *Acta Cryst.*, **6,** 260.
Compton, A. H., and Allison, S. K., 1935, *X-rays in Theory and Experiment* (New York : Van Nostrand).
Darwin, C. G., 1914, *Phil. Mag.*, **27,** 675 ; 1922, *Ibid.*, **43,** 800.
Ekstein, H., 1951, *Phys. Rev.*, **83,** 721.
Evans, R. C., Hirsch, P. B., and Kellar, J. N., 1948, *Acta Cryst.*, **1,** 124.
Ewald, P. P., 1917, *Ann. Phys., Lpz.*, **54,** 519.
Freeman, A. J., and Weiss, R. J., 1959, *Phil. Mag.*, **4,** 1086.
Gatineau, L., and Mering, J., 1956, *C. R. Acad. Sci., Paris*, **242,** 2018.
Gay, P., Hirsch, P. B., and Kellar, J. N., 1952, *Acta Cryst.*, **5,** 7.
Hirsch, P. B., 1956, *Progress in Metal Physics*, **6,** 275 (London and New York : Pergamon Press).
Hirsch, P. B., and Ramachandran, G. N., 1950, *Acta Cryst.*, **3,** 187.
Hume-Rothery, W., Brown, P. J., Forsyth, J. B., and Taylor, W. H., 1958, *Phil. Mag.*, **3,** 1466.
James, R. W., 1925, *Phil. Mag.*, **49,** 585 ; 1955, *The Optical Principles of Diffraction of X-rays* (London : Bell).
James, R. W., Brindley, G. W., and Wood, R. G., 1929, *Proc. Roy. Soc.*, A, **125,** 401.
James, R. W., and Firth, E. M., 1927, *Proc. Roy. Soc.*, A, **117,** 62.
Jellinek, F., 1958, *Acta Cryst.*, **11,** 626.
Lang, A. R., 1953, *Proc. Phys. Soc., Lond.* B, **66,** 1003.
Lonsdale, K., 1947 a, *Miner. Mag.*, **28,** 14 ; 1947 b, *Phil. Trans. Roy. Soc.* A, **240,** 219 ; 1948, *Acta Cryst.*, **1,** 12.
Parratt, L. G., 1932, *Phys. Rev.*, **41,** 561.
Ramaseshan, S., and Ramachandran, G. N., 1953, *Acta Cryst.*, **6,** 364 ; 1954, *Proc. Indian Acad. Sci.* A, **39,** 20.
Renninger, M., 1934, *Z. Kristallogr.*, **89,** 344 ; 1952, *Acta Cryst.*, **5,** 711.
Robinson, B. W., 1933, *Proc. Roy. Soc.* A, **142,** 422.

Sakisaka, Y., 1930, *Proc. math. phys. Soc. Japan*, **12,** 189.
Vand, V., 1955, *J. appl. Phys.*, **26,** 1191.
Waller, I., 1926, *Ann. Phys., Lpz.*, **79,** 261.
Weiss, R. J., and De Marco, J. J., 1958, *Rev. Mod. Phys.*, **30,** 59; 1959, *Phys. Rev. Letters*, **2,** 148.
Williamson, G. K., and Smallman, R. E., 1955, *Proc. Phys. Soc., Lond.* B, **68,** 577.
Witte, H., and Woelfel, E., 1958, *Rev. Mod. Phys.*, **30,** 47.
Zachariasen, W. H., 1945, *The Theory of X-ray Diffraction in Crystals* (New York: Wiley).

Crystal Stability and the Theory of Ferroelectricity

By W. Cochran
Crystallographic Laboratory, Cavendish Laboratory, Cambridge

Abstract

The phenomenon of ferroelectricity in pseudo-cubic crystals is discussed in terms of the normal modes of vibration. It is shown that the parameters which determine the lattice vibrations of a diatomic ionic crystal may be chosen in such a way that the crystal will exhibit ferroelectric properties, and that ferroelectric or anti-ferroelectric transitions may be regarded as the result of an instability of the crystal for a certain normal mode of vibration. The theory is extended to apply to other cubic crystals, including barium titanate, and the concepts of 'ionic polarizability' and 'a polarizability catastrophe' are discussed in terms of lattice dynamics. Certain of the parameters which appear in Devonshire's phenomenological theory of ferroelectricity are found to be expressible in terms of atomic parameters. Values for the latter which are physically reasonable are found to account quite well for the dielectric properties of barium titanate and for the relative movements of the atoms which occur at the cubic-tetragonal transition. The lowest dielectric dispersion frequency is calculated to be about 3×10^{11} c.p.s. for barium titanate, and to be a function of temperature in the cubic phase. Other predictions of the theory are discussed.

§ 1. Introduction

The main thesis of this paper is that a ferroelectric or an anti-ferroelectric transition in certain crystals is the result of an instability of the crystal for a certain normal mode of vibration, and can be treated as a problem in lattice dynamics. We therefore begin with an outline of the conditions for stability of a crystal, and of the theory of the lattice dynamics of simple ionic crystals of the sodium chloride or of the caesium chloride type. In § 2 we show that it is possible to choose the parameters which determine the lattice dynamics of such a crystal in a way that will cause it to exhibit the properties of a ferroelectric crystal of the barium titanate type. Section 3 is concerned with some general results on the lattice dynamics and dielectric properties of cubic crystals; in § 4 it is shown that these results are considerably simplified for crystals which are 'diagonally cubic' in symmetry. In § 5 we consider the problem of the lattice dynamics of $BaTiO_3$, and the conditions for the three ferroelectric transitions. Finally we discuss possible experimental tests of the theory.

It may be shown that a cubic crystal with one atom in the (primitive) unit cell is stable for homogeneous deformations if the elastic constants satisfy the conditions $c_{44} > 0$, $c_{11} > 0$, $c_{11}^2 - c_{12}^2 > 0$, $c_{11} + 2c_{12} > 0$. This however does not ensure the stability of the crystal against other types of small deformation, indeed it does not even ensure the stability of a crystal with more than one atom per unit cell against all types of homogeneous

deformation. Born and Huang (1954) point out that a crystal will be stable for all small deformations if all the normal modes have real frequencies.

In the Born–von Kármán theory of lattice dynamics the energy perturbation of a crystal, as a result of small displacements of the nuclei, is assumed to be

$$\Phi = -\tfrac{1}{2} \sum_{lKx} \sum_{l'K'y} \Phi_{xy}(lK, l'K') u_x(lK) u_y(l'K'). \quad . \quad . \quad . \quad (1.1)$$

Here $u(lK)$ is the displacement of the Kth nucleus in the lth unit cell, and $\Phi_{xy}(lK, l'K')$ may be called a force constant between atoms (lK) and $(l'K')$. The equations of motion, when expressed in terms of normal coordinates, lead to relations such as

$$m_K \omega^2 U_x(K) = \sum_{K'y} M_{xy}(KK')\, U_y(K'). \quad . \quad . \quad . \quad . \quad (1.2)$$

In order to obtain these results each displacement is expressed as a sum of displacements of the type

$$U_x(K) \exp i\,(\mathbf{q} \,.\, \mathbf{r}\,(lK) - \omega t)$$

where $\mathbf{q}$ is the wave vector $(q = 2\pi/\lambda)$ and ω the circular frequency $(2\pi\nu)$ of a normal mode of vibraton, and $\mathbf{r}\,(lK)$ is the equilibrium position of an atom (lK) whose mass is m_K. The quantities $M_{xy}(KK')$ will be referred to as coefficients, they are functions of $\mathbf{q}$ and of the force constants, defined by

$$M_{xy}(KK') = -\sum_{l'} \Phi_{xy}(lK, l'K') \exp i\,\mathbf{q} \,.\, (\mathbf{r}(l'K') - \mathbf{r}(lK)). \quad (1.3)$$

In the particular case where $q = 0$ each coefficient $M_{xy}(KK')$ is, apart from a change of sign, simply a sum of force constants. Such sums may conveniently be referred to as force constants per atom between Bravais arrays, since they determine the forces which act when all atoms of the same type (i.e. having the same index K) are given equal displacements.

The condition for the solubility of the set of Eqns. (1.2) is

$$\begin{vmatrix} M_{xx}(11) - m_1\omega^2 & M_{xy}(11) \ldots . M_{xz}(1n) \\ \ldots\ldots\ldots\ldots\ldots & M_{xy}(KK') \ldots\ldots\ldots \\ M_{zx}(n1) \ldots\ldots\ldots\ldots & M_{zz}(nn) - m_n\omega^2 \end{vmatrix} = 0.$$

The solution of this equation gives the dispersion relation, that is, ω as a function of $\mathbf{q}$. For each value of $\mathbf{q}$ there are of course a number of values of ω, in general $3n$, where n is the number of atoms per unit cell. The condition $\omega^2 > 0$ is satisfied for any value of $\mathbf{q}$ if all the principal minors of the $3n \times 3n$ matrix whose elements are the corresponding coefficients $M_{xy}(KK')$, are positive. A full account of the theory is given by Born and Huang (1954); the above summary mainly serves the purpose of introducing quantities which appear frequently in subsequent sections.

It has been shown by Power (1942) that a crystal having a face-centred cubic structure, with one atom in the unit cell, is stable for all deformations if it is stable for homogeneous deformations, that is, in this case, if the elastic constants satisfy the conditions mentioned in our second paragraph. Force constants between nearest neighbour atoms only were taken into

account in Power's investigation. Thompson (1953) has discussed the melting of an ionic crystal in terms of the Born–von Kármán theory, but only the possibility of an instability against acoustic modes of vibration was considered. We show later that it is possible for an ionic crystal to be stable for certain homogeneous deformations, and to exhibit quite usual values for its elastic constants, and yet be unstable or nearly so for certain other normal modes of vibration.

The theory of the lattice dynamics of ionic crystals having the sodium chloride type of structure has been developed by Kellermann (1940) and others, using methods due largely to Born and his collaborators. It has recently been extended by Woods *et al.* (1960) to take into account the polarizability of the ions and the fact that the short-range 'overlap' force between ions depends on their state of polarization, and conversely. The comparative success of this theory in accounting for the dispersion relations of sodium iodide (Woods *et al.* 1960) and also of germanium (Brockhouse and Iyengar 1958, Cochran 1959 b), leaves no doubt that the dipole moment of an atom in a crystal is not entirely determined by the effective field, but also directly by the displacements and dipole moments of neighbouring atoms. Previous work on the theory of ferroelectricity has not taken this feature into account. The theory of Woods, Cochran and Brockhouse was developed by considering each ion to consist of a core, coupled by an isotropic force constant to a shell which represents the outer electrons (Dick and Overhauser 1958). It was, however, pointed out that the same final results may be obtained by expressing the energy perturbation (eqn. (1.1)) as a quadratic function of the nuclear displacements *and* the atomic dipole moments. In this paper we shall use the nomenclature of the shell model, as it is the simpler of the two types of approach.

For certain crystals the problem of deriving the normal modes of vibration in terms of the force constants is greatly simplified when the wave-vector $\mathbf{q}$ is in a symmetry direction, such as [100], [110] or [111] for the sodium chloride type of structure. This comes about from the fact that when $\mathbf{q}$ is along [100] for example, the direction of displacement of the atoms in a normal mode is determined by the symmetry of the crystal and not by the force constants. The displacements can only be parallel to [100] (longitudinal mode) or parallel to [010] or [001] (transverse modes), and all atoms in any one (100) lattice plane move in phase. The force constants involved may then be regarded as force constants between planes of atoms, and the problem becomes similar to that of the linear chain, which provides the standard introduction to lattice dynamics. In other words the set of eqns. (1.2) reduces to three separate sets, and the sixth-order determinant factors to give three equations each of order two, of which one gives the dispersion relation for the longitudinal mode and the others give identical solutions for the two transverse modes, (when $\mathbf{q}$ is parallel to [100]). A further simplification is possible when $q = 0$. For any such mode all atoms of the same type have the same displacement and the only force constant involved, for a diatomic crystal, is that between the two Bravais arrays of atoms such as sodium and chlorine. It is with such modes of vibration

that we are concerned in this paper, since they determine the dielectric properties of a crystal.

We illustrate the above remarks, and the effect of using a shell model for a polarizable atom, by deriving in an elementary way the frequency of the transverse optic mode for which $q=0$, in a diatomic cubic crystal. For simplicity only the negative ion will be taken to be polarizable, and the non-Coulomb forces (such as 'overlap' forces and covalent bonds) will be assumed to act through the shell, and not the core, of the negative ion (a quite general derivation is given in a later section). There are then three Bravais arrays, comprising respectively the positive ions and the cores and shells of negative ions. Their equations of motion, for this particular mode, may be written

$$\left.\begin{aligned} m_1\ddot{u}_1 &= R_0(v_2-u_1)+\frac{4\pi}{3}PZe, \\ m_2\ddot{u}_2 &= k(v_2-u_2)+\frac{4\pi}{3}PXe, \\ 0 &= k(u_2-v_2)+R_0(u_1-v_2)+\frac{4\pi}{3}PYe. \end{aligned}\right\} \quad . \quad . \quad . \quad (1.4)$$

Here u_1, u_2 and v_2 are the displacements from their equilibrium positions of positive ions and the cores and shells respectively of negative ions. Ze, Xe and Ye are the corresponding charges, where $e=+4{\cdot}80\times10^{-10}$ e.s.u. and $X+Y+Z=0$. The forces have been separated into Coulomb forces, which depend on the polarization P, and short-range forces specified by a force constant R_0 (in the notation of later sections $R_0=R_{11}=-R_{12}$) per atom between arrays displaced a relative amount v_2-u_1 (shells and positive ions), and a force constant k between the shell and core of a negative ion. The third equation specifies that the shells always occupy positions of equilibrium corresponding to the instantaneous configuration of the nuclei. The direction of $\mathbf{q}$ may be thought of as along [100], with the atoms displaced parallel to [001]. On writing

$$u_1=U_1\exp(-i\omega t), \text{ etc.}, \quad P=\mathscr{P}\exp(-i\omega t),$$

and rearranging the equations, one obtains

$$\left.\begin{aligned} m_1\omega^2U_1 &= R_0(U_1-U_2)+R_0(U_2-V_2)-\frac{4\pi}{3}\mathscr{P}Ze, \\ m_2\omega^2U_2 &= R_0(U_2-U_1)+R_0(V_2-U_2)+\frac{4\pi}{3}\mathscr{P}Ze, \\ 0 &= R_0(U_2-U_1)+(k+R_0)(V_2-U_2)-\frac{4\pi}{3}\mathscr{P}Ye \end{aligned}\right\} \quad . \quad . \quad (1.5)$$

or on eliminating V_2-U_2,

$$\left.\begin{aligned} m_1\omega^2U_1 &= R_0'(U_1-U_2)-\frac{4\pi}{3}\mathscr{P}Z'e, \\ m_2\omega^2U_2 &= R_0'(U_2-U_1)+\frac{4\pi}{3}\mathscr{P}Z'e, \end{aligned}\right\} \quad . \quad . \quad . \quad . \quad (1.6)$$

where

$$R_0' = \frac{kR_0}{k+R_0} < R_0, \quad Z' = Z + \frac{YR_0}{k+R_0} < Z. \quad . \quad . \quad . \quad (1.7)$$

However from $\mathscr{P} = (e/v)(ZU_1 + XU_2 + YV_2)$, (where v = unit cell volume), and the third of eqns. (1.5), one finds that

$$\mathscr{P}\left\{1 - \frac{4\pi(Ye)^2}{3v(k+R_0)}\right\} = \frac{Z'e}{v}(U_1 - U_2). \quad . \quad . \quad . \quad . \quad (1.8)$$

Consider now the situation when an effective field $E = \mathscr{E}\exp(-ipt)$ exists in the crystal, and the frequency p is such that the cores do not move appreciably. The equilibrium of any shell is determined by

$$\mathscr{E}Ye = (k+R_0)V_2$$

and the polarization is given by

$$\mathscr{P} = \frac{YeV_2}{v},$$

from which we see that the electronic polarizability α_e of the negative ion, on the basis of the shell model, is

$$\alpha_e = \frac{\mathscr{P}v}{\mathscr{E}} = \frac{(Ye)^2}{k+R_0}. \quad . \quad . \quad . \quad . \quad . \quad . \quad (1.9)$$

The polarizability is, however, related to the high-frequency dielectric constant ϵ_e by the Clausius–Mossotti formula

$$\frac{4\pi\alpha_e}{3v} = \frac{\epsilon_e - 1}{\epsilon_e + 2}. \quad . \quad . \quad . \quad . \quad . \quad . \quad . \quad (1.10)$$

so that eqn. (1.8) becomes

$$\mathscr{P} = \frac{Z'e(\epsilon_e+2)(U_1 - U_2)}{3v} \quad . \quad . \quad . \quad . \quad . \quad (1.11)$$

On substituting this value of $\mathscr{P}$ into eqns. (1.6) and eliminating U_1 and U_2, one obtains

$$\mu\omega_T^2 = R_0' - \frac{4\pi(\epsilon_e+2)(Z'e)^2}{9v}. \quad . \quad . \quad . \quad . \quad (1.12)$$

The suffix T has been added to emphasize that we are dealing with a *transverse* optic mode, and $\mu = m_1m_2/(m_1+m_2)$. It should be noted that the replacement of R_0 and Ze in eqn (1.12) by effective values R_0' and $Z'e$ does not result from the fact that the ions are polarizable in an electric field, but from the fact that dipoles are generated by the short-range interaction in the course of the lattice vibrations. The frequency of the longitudinal optic mode for which $q = 0$ can be derived in the same way, taking into account the presence of a macroscopic field $-4\pi P$ in addition to the Lorentz field $(4\pi/3)P$ (Born and Huang 1954). The result obtained is

$$\mu\omega_L^2 = R_0' + \frac{8\pi(\epsilon_e+2)(Z'e)^2}{9v\,\epsilon_e}. \quad . \quad . \quad . \quad . \quad . \quad (1.13)$$

Equations (1.12) and (1.13) have already been obtained by Woods *et al.* (1960) as special cases of the dispersion relation (ω as a function of $\mathbf{q}$) which

applies when **q** is in a symmetry direction. This more general relation is found to involve only the parameters R_0, Z, Z' and α_e, provided that the short-range interaction is between nearest-neighbour atoms only (a restriction which we did not make in deriving (1.12) and (1.13), which are also independent of Z). The parameter R_0 is then related to the compressibility β by $R_0 = 6r_0/\beta$, where r_0 is the nearest-neighbour distance in a sodium chloride type structure. With $Z = 1$ all the parameters involved are therefore determined by the compressibility β and the static and high-frequency dielectric constants ϵ_s and ϵ_e respectively of the material. The dispersion relations determined by experiment for sodium iodide are in rather good agreement with the theory (Woods *et al.* 1960).

A relation between the frequencies ω_L and ω_T and the dielectric constants ϵ_s and ϵ_e was first derived by Lyddane *et al.* (1941); it is

$$\frac{\omega_L^2}{\omega_T^2} = \frac{\epsilon_s}{\epsilon_e}. \quad . \quad . \quad . \quad . \quad . \quad . \quad . \quad . \quad . \quad (1.14)$$

The significance of this result for the theory of ferroelectricity appears to have been overlooked, except by Fröhlich (1949), who makes a brief comment. From eqns. (1.14) and (1.12) we see that $\epsilon_s = \infty$ if

$$R_0' = \frac{4\pi(\epsilon_e + 2)(Z'e)^2}{9v}.$$

For a real alkali halide crystal these two quantities are of the same order of magnitude, but R_0' is about twice as great as the other. If they were equal, the crystal would be just unstable for the transverse optic mode of wave-number zero. It is interesting to note that this condition may be approached without the crystal becoming unstable for any other mode of vibration, even when the short-range forces act only between nearest neighbours. A numerical calculation has been made, using the formulae given by Woods *et al.* (1960) with $\beta = 7{\cdot}16 \times 10^{-12}$ c.g.s., $\alpha_e = 0{\cdot}01$ v, $Z' = Z = 1$ and values for the remaining parameters (such as r_0) which correspond to those of sodium chloride. The above value of β is about twice as great as the true value. The calculated dispersion relations are then as shown in fig. 1. Most frequencies are comparatively normal, but ω_T is just zero. A slight decrease in the value of β would raise ω_T to a positive value, and reduce ϵ_s to a finite value. The fact that all frequencies are real in this instance when **q** is in a symmetry direction does not of course prove that all are real for general values of **q**, but an examination of Kellermann's results (1940) makes this seem very likely. In any case such an instability or near-instability, arising first for the T.O. mode of wave-number zero, is more likely to occur when there are also short-range force constants between other than nearest-neighbour atoms. If for example there is a short-range interaction between neighbouring positive ions, all frequencies are increased, except when $q = 0$. A detailed algebraic analysis of this point will not be given, as the situation may be understood physically as follows: in an optic mode of wave-number zero the two Bravais arrays carrying type 1 (positive) and type 2 (negative) ions remain undistorted,

Fig. 1

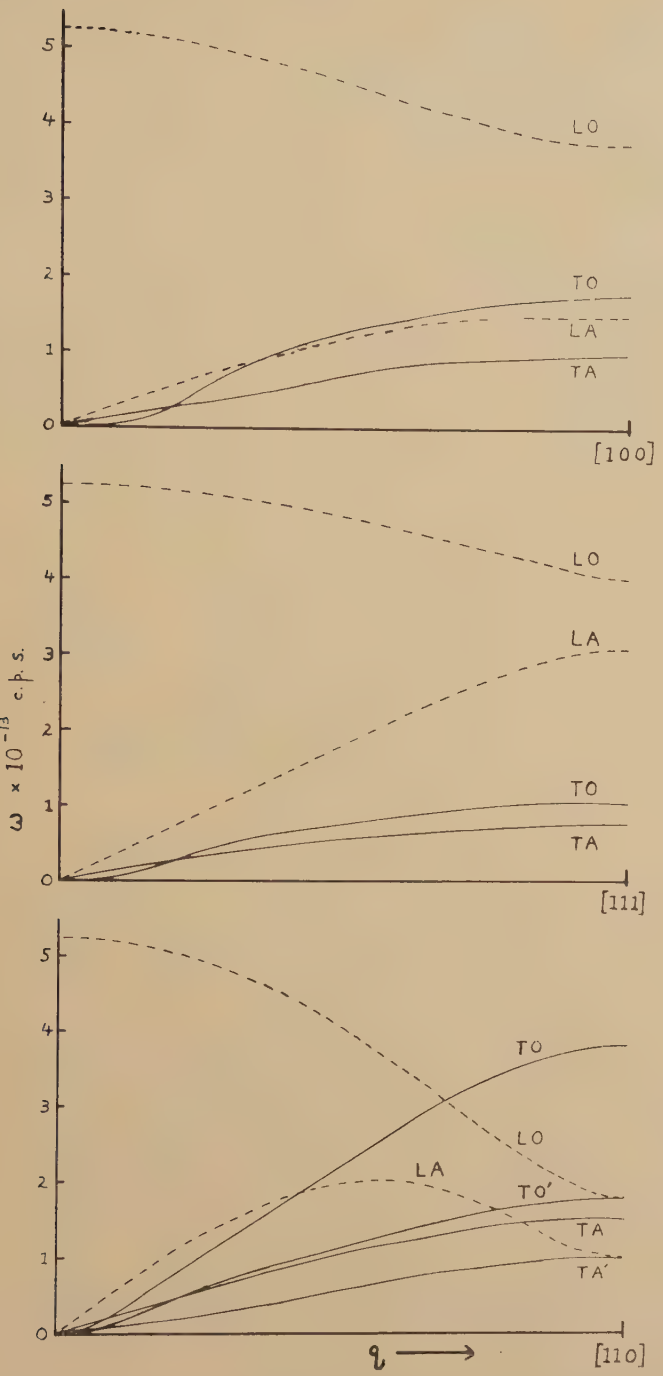

Frequency ω versus wave-vector $\mathbf{q}$ for $\mathbf{q}$ in each of three symmetry directions. Except when $\mathbf{q}$ is in the [110] direction, each transverse mode is degenerate. The parameters determining $\omega(\mathbf{q})$ have been chosen so that the frequency of the T.O. mode is zero when $\mathbf{q}=0$.

and vibrate against one another. Any force constants between atoms of the same type are therefore ineffective and eqns. (1.12) and (1.13) remain valid. All other modes of vibration involve a distortion of one or (usually) both Bravais arrays, and their frequencies will be raised by suitable force constants between like atoms. It is therefore possible in principle for all normal modes to exhibit quite usual values of ω, except for the T.O. mode at, and near to, $q=0$.

An instability may arise for a value of **q** other than zero. For example the equations of Woods *et al.* (1960) may be used to show that in certain circumstances a crystal of the caesium chloride type will become unstable against a transverse mode for which **q** is at the point $(\frac{1}{2}, 0, 0)$ in reciprocal space. In this mode the atoms move as shown in fig. 2, with *one* Bravais array remaining undistorted. By analogy with results which we give in the next section, this type of instability would result in a transition to an antiferroelectric phase. However, we shall not deal with the topic of antiferroelectricity in this paper.

Fig. 2

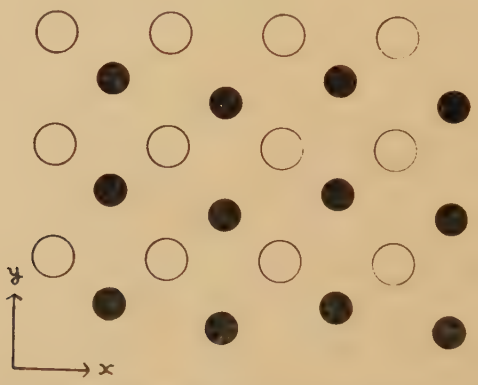

Movement of the atoms in a CsCl type of structure in a transverse mode for which **q** is at the point $(\frac{1}{2}, 0, 0)$ in reciprocal space. The wavelength of the vibration is thus twice the unit cell dimension.

To summarize, an ionic crystal having the NaCl or CsCl type of structure may in principle exhibit quite a normal relation between frequency and wave-number except in a limited range of values of **q**. An abnormally low value of ω can occur in the T.O. mode when $q=0$, and in other modes for a few other values of **q** which depend on the crystal structure but which inspection shows will usually occur when **q** is in a symmetry direction and at the boundary of the Brillouin zone.

§ 2. Ferroelectricity in Simple Ionic Crystals

No alkali halide in practice exhibits ferroelectric properties, but for the purposes of illustration we continue to consider this type of structure. Suppose the force constants are such that

$$\mu\omega_{\mathrm{T}}^2 = R_0' - \frac{4\pi(\epsilon_e+2)(Z'e)^2}{9v} \quad . \quad . \quad . \quad . \quad (1.12)$$

is close to zero, but other frequencies are comparatively high. Until now, our results have been based on the harmonic approximation. It is however known (see for example Leibfried 1955) that one effect of the anharmonicity of the lattice vibrations is to make parameters such as R_0 linearly temperature-dependent. The unit cell volume v exhibits a similar dependence for the same reason, and on the basis of the shell model at least, this will also be the case for Z'. Accordingly we write

$$1-\frac{4\pi(\epsilon_e+2)(Z'e)^2}{9vR_0'}=\frac{\mu\omega_T^2}{R_0'}=\gamma(T-T_c) \quad . \quad . \quad . \quad (2.1)$$

where γ is a temperature coefficient of the same order of magnitude as the volume coefficient of expansion, and T_c is the temperature at which the crystal will just become unstable. For the sake of simplicity in subsequent discussion we shall think of R_0' as being independent of temperature, so that the other term in eqn. (1.12) is responsible for the temperature variation—this is not of course a necessary assumption. From eqns. (1.12), (1.13) and (1.14) one finds that

$$\epsilon_s-\epsilon_e=\frac{4\pi(\epsilon_e+2)^2(Z'e)^2}{9v\mu\omega_T^2} \quad . \quad . \quad . \quad . \quad . \quad . \quad . \quad (2.2)$$

which is one of Szigeti's equations (1949, 1950). We therefore have, from eqn. (2.1), that

$$\epsilon_s=\epsilon_e+\frac{4\pi(\epsilon_e+2)^2(Z'e)^2}{9vR_0'\gamma(T-T_c)} \quad . \quad . \quad . \quad . \quad . \quad . \quad . \quad (2.3)$$

Comparing this with the Curie–Weiss law in the form

$$\epsilon_s=\epsilon'+\frac{4\pi\mathscr{C}}{T-T_c}$$

(see for example Känzig (1957), p. 24), we identify the constant ϵ' as ϵ_e, while the Curie constant is

$$\mathscr{C}=\frac{(\epsilon_e+2)^2(Z'e)^2}{9vR_0'\gamma}\simeq\frac{(\epsilon_e+2)}{4\pi\gamma} \quad . \quad . \quad . \quad . \quad . \quad (2.4)$$

If the crystal is not to disrupt exponentially with time, a transition to another structure must take place at or above the Curie temperature T_c, and the transition must have the effect of raising ω_T. This will be the case if the short-range force between the two Bravais arrays is neither precisely harmonic, as we have already assumed, nor precisely isotropic. Guided by Devonshire's work (1949, 1951, 1954), we take the short-range effective potential between the two Bravais arrays, when the cores are displaced a relative distance $\mathbf{u}$, to be

$$\Phi_R=\tfrac{1}{2}R_0'(u_x^2+u_y^2+u_z^2)+\tfrac{1}{4}B(u_x^4+u_y^4+u_z^4)+\tfrac{1}{6}B'(u_x^6+u_y^6+u_z^6)$$
$$+\tfrac{1}{2}B''(u_x^2u_y^2+u_y^2u_z^2+u_z^2u_x^2). \quad . \quad . \quad . \quad . \quad . \quad . \quad . \quad . \quad . \quad (2.5)$$

The assumed dependence of Φ_R on $\mathbf{u}$ is physically reasonable, and only the presence of the fourth term calls for comment. Its probable physical origin will be pointed out later. The frequency of transverse vibrations of

small amplitude will still be given by eqn. (1.12), and ϵ_s of eqn. (2.2) will be the dielectric constant for small applied field.

For the present we restrict **u** to be in the [001] direction. In fig. 3(*a*) we plot the restoring force

$$R_0'u + Bu^3 + B'u^5$$

and the displacing Coulomb force

$$\frac{4\pi(\epsilon_e + 2)(Z'e)^2 u}{9v}$$

against u (remembering that $u = u_z$). The curvature of the former force is much exaggerated, and we have taken B to be negative. From eqn. (1.12)

Fig. 3

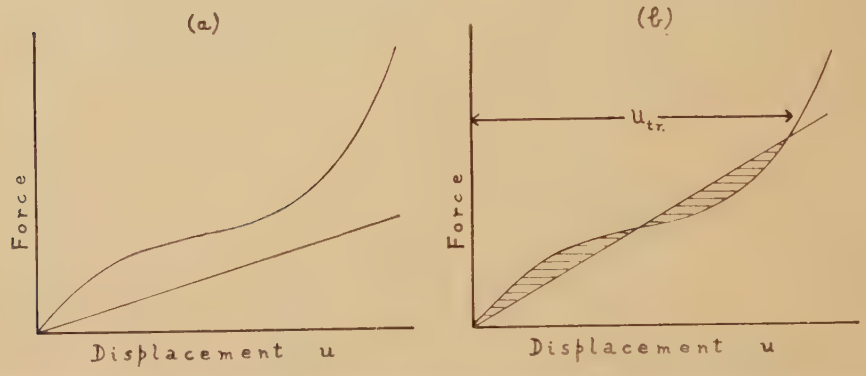

Restoring force and displacing force (straight line) as a function of displacement u. (*a*) Temperature above the transition temperature, (*b*) at the transition temperature.

the value of ω_1^2 is proportional to the difference of slope of the two lines at the origin, while the value of ϵ_s is inversely proportional to the same quantity. As the temperature decreases, the slope of the lower line increases until the two lines intercept at a finite value of u as well as at the origin. Stable, but anharmonic, oscillations of the two Bravais arrays about this value of u are possible. This represents a first-order transition to a phase having tetragonal symmetry. The transition will not however take place until the free energies of the two phases are equal. This will in fact occur at a temperature T_{tr} such that the areas shown shaded in fig. 3 (*b*) are equal to one another. Above the temperature T_{tr} the cubic crystal is stable, between T_{tr} and T_c it is metastable and below T_c it is unstable. At the transition the relative displacement of the two Bravais arrays is u_{tr} (fig. 3 (*b*)), and the new value of ϵ_s is inversely proportional to the difference in slopes at $u = u_{tr}$ of the two lines of fig. 3 (*b*). Diagrams similar in principle are of course already familiar from Devonshire's phenomenological theory of ferroelectricity, but the interpretation given here is different. Our object in choosing the expression (2.5) for the short-range potential was of

course to show that the atomic mechanism which we propose here leads to Devonshire's theory. This has already been foreshadowed by Devonshire's own work (1949), in which however the atoms were taken to move independently of one another (the Einstein model of a crystal). The same is true of Slater's theory (1950). Since the publication of a short note on this subject (Cochran 1959 c) I have received the manuscript of an unpublished paper by P. W. Anderson (1958). By an analysis based on lattice dynamics Anderson arrives at conclusions similar in principle to those given above; in particular he associates a ferroelectric transition with an abnormally low transverse optic mode of vibration at $q=0$, resulting from the near-cancellation of short-range and Coulomb interactions.

We next consider the behaviour of the crystal in a static applied electric field $\mathbf{E}_A$, and the connection with Devonshire's theory. Since the frequency of the applied field is zero, there is no distinction between $\mathbf{u}$ and $\mathbf{U}$, or between $\mathbf{P}$ and $\mathscr{P}$. To emphasize the fact that we are dealing with static displacements we shall use $\mathbf{u}$ and $\mathbf{P}$. The effective field is given by

$$\mathbf{E}=\mathbf{E}_A+\frac{4\pi}{3}\mathbf{P}. \quad . \quad . \quad . \quad . \quad . \quad . \quad . \quad . \quad (2.6)$$

The equilibrium displacement of the two arrays is then determined by the balance between short-range and electrostatic forces, expressed by

$$Z'e\,E_z=R_0'\,u_z+B\,u_z^3+B'\,u_z^5+B''\,u_z(u_x^2+u_y^2) \quad . \quad . \quad . \quad (2.7)$$

and two similar equations.

The polarization is given by

$$P_z=\frac{(\epsilon_e+2)Z'e\,u_z}{3v}+(E_A)_z\,\frac{(\epsilon_e-1)}{4\pi} \quad . \quad . \quad . \quad . \quad (2.8)$$

and two similar equations.

That Z' and not Z should appear in eqn. (2.7) has been shown by Woods *et al.*, (1960). It also follows from eqn. (4.6), derived later. Equation (2.8) is a special case of the general eqn. (3.33), derived later. From eqns. (2.7) and (2.8) we have that

$$Z'e\left\{(E_A)_z+\frac{4\pi(\epsilon_e+2)Z'eu_z}{9v}+\tfrac{1}{3}(E_A)_z(\epsilon_e-1)\right\}=R_0'\,u_z+B\,u_z^3+B'\,u_z^5 +B''\,u_z(u_x^2+u_y^2).$$

Using eqn. (2.1) we therefore have

$$\tfrac{1}{3}(E_A)_z(\epsilon_e+2)Z'e=R_0'\gamma(T-T_c)u_z+B\,u_z^3+B'\,u_z^5+B''\,u_z(u_x^2+u_y^2)$$

which with the use of eqns. (2.8) and (2.4) leads to

$$(E_A)_z\left\{1+\frac{(\epsilon_e-1)(T-T_c)}{4\pi\mathscr{C}}\right\}=\frac{(T-T_c)}{\mathscr{C}}\,P_z+\frac{3}{(\epsilon_e+2)Z'e}\{B\,u_z^3+B'\,u_z^5 +B''\,u_z(u_x^2+u_y^2)\}. \quad . \quad (2.9)$$

The term

$$\frac{(\epsilon_e-1)(T-T_c)}{4\pi\mathscr{C}}$$

is less than $\gamma(T-T_c)$ and may therefore be neglected compared with unity. To about the same accuracy we can now eliminate u_z from eqn. (2.9) by using eqn. (2.8), neglecting the second term on the right-hand side of the latter. We then obtain the approximate result

$$(E_A)_z = \frac{(T-T_c)}{\mathscr{C}} P_z + v^3 g^4 (BP_z^3 + B'' P_z (P_x^2 + P_y^2)) + v^5 g^6 B' P_z^5. \quad (2.10)$$

We have introduced the abbreviation

$$g = \frac{3}{(\epsilon_e + 2) Z' e} \quad . \quad . \quad . \quad . \quad . \quad . \quad . \quad (2.11)$$

In Devonshire's (1954) notation, the change of the free energy function G_1 at constant temperature and zero stress is

$$dG_1 = (E_A)_x dP_x + (E_A)_y dP_y + (E_A)_z dP_z.$$

From eqn. (2.10) and the two corresponding equations, therefore

$$G_1 = \frac{(T-T_c)}{2\mathscr{C}} (P_x^2 + P_y^2 + P_z^2) + \tfrac{1}{4} B v^3 g^4 (P_x^4 + P_y^4 + P_z^4)$$
$$+ \tfrac{1}{6} B' v^5 g^6 (P_x^6 + P_y^6 + P_z^6) + \tfrac{1}{4} B'' v^3 g^4 (P_x^2 P_y^2 + P_y^2 P_z^2 + P_z^2 P_x^2).$$
$$. \quad . \quad . \quad . \quad . \quad . \quad . \quad (2.12)$$

The Gibbs free energy per unit volume is $G_1 - E_A P$. Equations (2.10) and (2.12) are identical with those of Devonshire's, which have been found to be in good agreement with the behaviour of an unstressed crystal of, for example, barium titanate. In the thermodynamic theory the coefficients of the second, third and fourth terms are usually written respectively as $\frac{1}{4}\xi$, $\frac{1}{6}\zeta$ and $\frac{1}{4}\lambda$, so we may establish the following connections between macroscopic and atomic parameters:

$$\xi = B v^3 g^4, \quad \zeta = B' v^5 g^6, \quad \lambda = B'' v^3 g^4. \quad . \quad . \quad . \quad . \quad . \quad (2.13)$$

Using the above expression for the free energy, or more simply by considering the external mechanical work done in causing the transition, one can show that the temperature of the cubic-tetragonal transition is such that the shaded areas of fig. 3 (*b*) are equal. It follows of course from Devonshire's work that if the constants B, B' and B'' are suitably chosen the crystal will make three successive transitions as the temperature decreases, with the spontaneous polarization successively directed along [001], [011], and [111].

There are approximations in the above discussion in addition to those we have pointed out. In discussing the interaction with an applied field we have singled out the T.O. mode of wave-number zero, and ignored all others. However, by introducing anharmonic terms in the restoring force, we have destroyed the normality of the modes which alone makes this procedure admissible. Also in discussing the free energy we have ignored the fact that a change in the value of ω_T at a transition implies a change in the frequency distribution of the modes. Neither approximation is likely to be important in practice; we show later that the anharmonic terms will have a negligible direct effect on frequencies large compared with ω_T.

Furthermore our assumption is that only frequencies with wave-number near zero are appreciably changed at a transition, and such modes make a negligible contribution to the frequency distribution (see formula (6.24) of Born and Huang (1954)).

In principle the axis, (001), (010) or (100), along which polarization developed at the first transition, would depend on the shape of the crystal, if the instability developed for q exactly equal to zero. There is however a point involved here which requires a fuller investigation than we make in this paper. It has been shown by Born and Huang (1954) that when the effect of retardation is included in the electrostatic interaction, the limiting frequency ω_T is not the frequency at $q=0$, i.e. infinite wavelength, but at values of the wavelength small compared with the dimensions of the crystal but large compared with the unit cell dimensions. For greater

Fig. 4

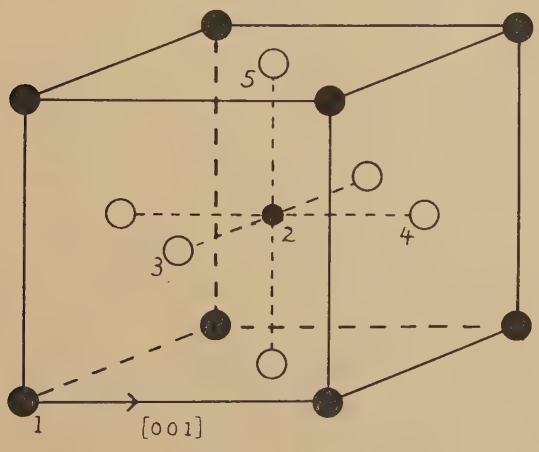

Numbering of the atoms in $BaTiO_3$. The open circles represent oxygens, the smallest circle represents titanium. The [001] direction is horizontal.

wavelengths there are two T.O. branches, of which one goes to ω_L at q exactly zero, and the other to zero. This suggests that an instability will first develop for a mode whose wavelength is relatively large, but which is smaller than the crystal dimensions. This further suggests that the instability would develop at the anti-nodes and trigger a transition into domains of alternate polarization. It is of course well known that there are other considerations which favour a domain structure.

We now return to a discussion of the transitions in terms of atomic rather than macroscopic parameters. It may readily be shown that

$$\mu\omega_T^2 = \frac{3B^2}{16B'}$$

just before the first transition, and that the relative 'jump' of the atoms at this transition, in going to the tetragonal phase, is

$$u_{\mathrm{tr}} = \left(\frac{3|B|}{4B'}\right)^{1/2}.$$

The spontaneous polarization immediately after the transition is given by

$$P = \frac{u_{\mathrm{tr}}}{gv}.$$

The Curie constant is given by eqn. (2.4), while the difference between the transition and Curie temperatures is

$$T_{\mathrm{tr}} - T_{\mathrm{c}} = \frac{3B^2 \mathscr{C} v g^2}{16B'}.$$

The values of ϵ_{s} are approximately

$$(\epsilon_{\mathrm{s}})_{\max} = \frac{64\pi B'}{3g^2 v|B|}, \text{ just before the transition,}$$

$$\epsilon_{\mathrm{s}} = \tfrac{1}{4}(\epsilon_{\mathrm{s}})_{\max}, \text{ just after the transition,}$$

$$= \frac{3}{32}(\epsilon_{\mathrm{s}})_{\max}, \text{ at the Curie temperature.}$$

The same relations between a number of these quantities can of course be established using Devonshire's theory, since our model leads to the same relation between E_{A} and P. However, the phenomenological theory does not establish any connection between the dielectric properties, the displacement of the atoms, and the frequencies of the lattice vibrations.

We next consider the question of how ω_{T} will change at the transition. Since the crystal becomes tetragonal there will in fact be two distinct frequencies $(\omega_{\mathrm{T}})_c$ and $(\omega_{\mathrm{T}})_a$ which correspond to displacement vectors parallel to the crystallographic c and a axes respectively. These frequencies may be expected to differ considerably since in a CsCl type of structure for example the relative displacement of the two lattices along the c axis will increase the repulsive interaction for vibration in this direction more than for vibration in a perpendicular direction, so that $(\epsilon_{\mathrm{s}})_c < (\epsilon_{\mathrm{s}})_a$, while $(\omega_{\mathrm{T}})_c > (\omega_{\mathrm{T}})_a$. If one ignores the fact that the crystal will be piezoelectric in the tetragonal phase, so that no distinction is made between the 'clamped' and 'free' dielectric constants, it may readily be shown that

$$\mu(\omega_{\mathrm{T}}^2)_c = \frac{3B^2}{4B'}$$

just after the transition, while the value at the Curie temperature is $2B^2/B'$. For an actual crystal ω_{T}^2 may be expected to be inversely proportional to the value of the *clamped* dielectric constant, so that the above formulae should be regarded as setting a lower limit only.

It is interesting to note that it is possible to choose reasonable numerical values for the parameters γ, B, B', B'' and Z' so that a diatomic crystal exhibits dielectric properties in fairly good quantitative agreement with those of barium titanate.

It is not difficult to show that the transitions will be of the second order if B (eqn. (2.5)) is positive—this is well known from Devonshire's theory. In principle the minimum value of ω_T is then zero, just as in principle the maximum value of ϵ_s is infinite. Near the transition the linear term in the short-range force will be almost cancelled by the electrostatic force and the vibration will be very anharmonic. Devonshire also points out that if the electrostrictive change of unit cell dimensions could be prevented (by clamping the crystal) the quantity ξ (and therefore B, eqn. (2.13)) would be positive. The treatment given here does not take *directly* into account the electrostrictive changes of unit cell dimensions, but it seems clear that they are in fact taken into account indirectly by taking $B<0$ and $B''\neq 0$ (eqn. (2.5)). At the first transition, the relative displacement of the atoms increases the short-range interaction for vibrations in the [001] direction. This may be expressed by writing the appropriate short-range force constant, defined as the coefficient of $\frac{1}{2}u_z^2$ in eqn. (2.5) with $u_x=u_y=0$, as

$$(R_0')_z=R_0'\left\{1+\frac{B}{2R_0'}u_z^2+\frac{B'}{3R_0'}u_z^4\right\}.$$

The increased proximity of the atoms would be expected to give $B>0$, however an *expansion* of the crystal in the z-direction, which would necessarily be an even function of u_z, would produce the opposite effect. After the transition the short-range force constant for vibration in the x-direction (the coefficient of $\frac{1}{2}u_x^2$ in eqn. (2.5) with $u_x=u_y=0$) is

$$(R_0')_x=R_0'\left\{1+\frac{B''}{2R_0'}u_z^2\right\}.$$

This result, with $B''>0$ and of the same order of magnitude as $-B$, is of the form that is to be expected if it in fact originates from a *contraction* of the crystal in the x-direction, which again will be an even function of u_z.

The second and third transitions may be described in terms of crystal stability as follows. At the first transition $(R_0')_x$ and $(R_0')_y$ increase discontinuously, $(\epsilon_s)_a$ decreases discontinuously and the corresponding transverse optic frequency increases and will at first continue to increase with decreasing temperature as u_z increases. However, this quantity tends eventually to level off—its variation with temperature is similar to that of the spontaneous polarization shown in fig. 5. At the same time the electrostatic interaction steadily increases relative to the short-range interaction, as expressed by eqn. (2.1), so that the crystal tends to become unstable against transverse optic modes with displacement vectors along [010] or [100], and eventually makes a transition with atomic movements in one or other of these directions, raising all values of ω_T in the process. By symmetry the relative atomic displacement is now directed along [011], say. Increase of the relative displacement with decreasing temperature at first tends to stabilise the crystal against vibrations directed along [100], but for the same reason as before a third transition will eventually take place, with the relative displacement finally along [111].

Fig. 5

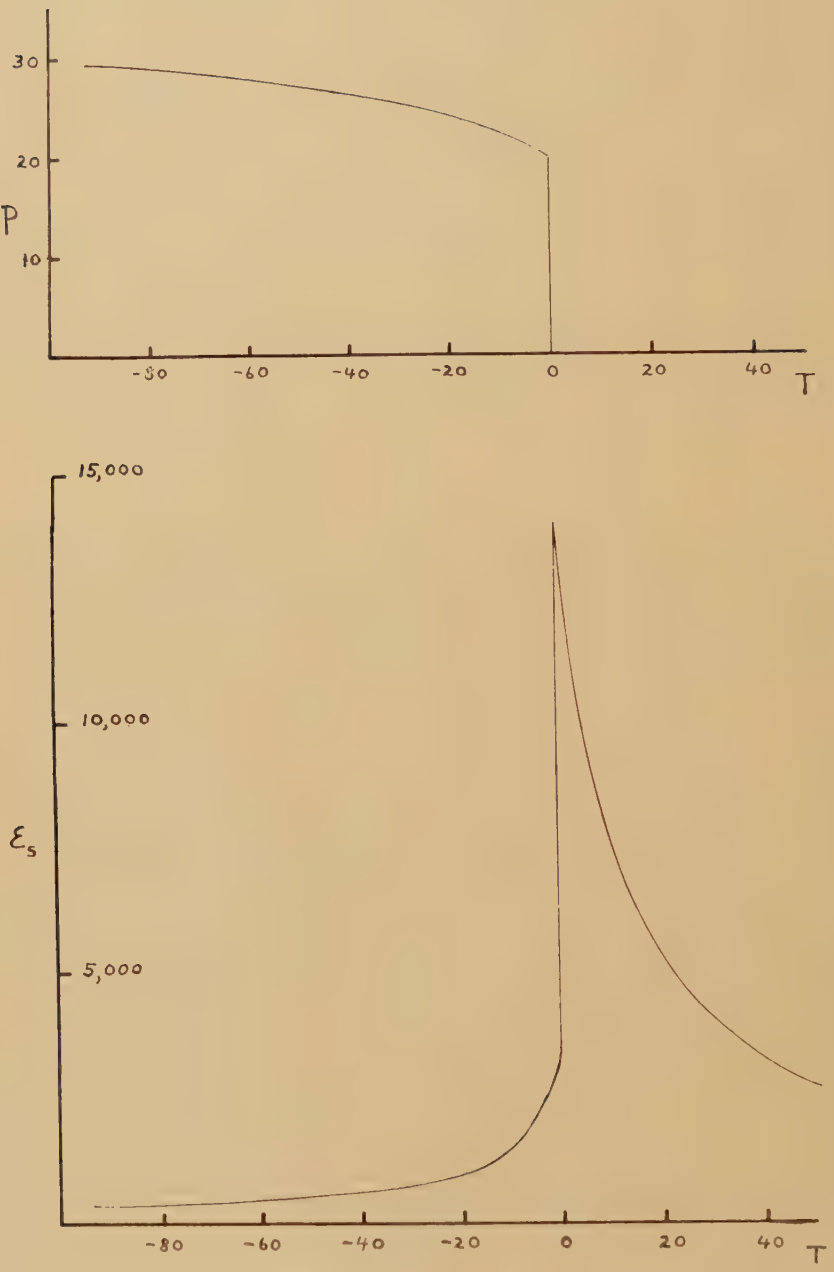

Calculated values of the spontaneous polarization in micro-coulombs per square centimetre and of the static dielectric constant as a function of temperature. The temperature is measured in °c from the transition temperature.

The properties of a diatomic crystal have been discussed in some detail in terms of the crystal-stability theory, because most of the problems which arise are the same as are met in a similar treatment of barium titanate. The general procedure, and the physical assumptions which are made, may however be more clearly understood in the context of the present section.

§ 3. Dielectric Properties of Cubic Crystals

Many of the formulae of previous sections, in particular the Lyddane–Sachs–Teller relation (eqn. (1.14)) which is of central importance for the theory, apply only to diatomic cubic crystals in which each atom has surroundings of tetrahedral symmetry (Born and Huang 1954, p. 103). A crystal having this symmetry, which we shall refer to as diagonally cubic (Born and Göppert-Meyer 1933), but with n atoms in the (primitive) unit cell has in general, for $q=0$, n transverse modes (each is degenerate) and n longitudinal modes. One of each is an acoustic mode, to which we give subscript 1, with $\omega_1=0$. The writer has shown (Cochran 1959 a) that the result corresponding to eqn. (1.14) is then

$$\frac{\epsilon_s}{\epsilon_e}=\prod_{j=2}^{n}\frac{(\omega_j^2)_L}{(\omega_j^2)_T}. \qquad (3.1)$$

In the derivation it was assumed that the dipole moment of an atom depends only on the effective field. However, we show later in this section that the effect of short-range interaction between the electrons is taken into account (for $q=0$) if charges and force constants are replaced by effective values (eqns. (4.7) and (4.8)). By making use of this result the proof referred to above is readily extended, and it is found that (3.1) is valid for any diagonally cubic crystal. We give in the Appendix a derivation of eqn. (3.1) for other cubic crystals including $BaTiO_3$. The crystal is imagined as composed of n cores comprising the nuclei and inner electrons, and any number of shells representing the outer electrons. Each unit (core or shell) exerts short-range harmonic forces of quantum origin on neighbouring units when they are relatively displaced, and also purely Coulomb forces on units throughout the crystal. We have put this derivation in an appendix because of its length, and because the notation differs somewhat from that of the remainder of this section.

We now consider the lattice dynamics, for $q\to 0$, of a cubic crystal of any space group, subject to the limitation that it is possible to find a direction for $\mathbf{q}$ such that the displacements in any mode of vibration are determined in directon by crystal symmetry. (The limiting values of ω for each mode, as $q\to 0$, are independent of the direction of $\mathbf{q}$ for a cubic crystal, but the above restriction ensures that any mode considered is purely transverse or purely longitudinal). We first of all consider transverse modes. We shall assume that the polarizability of each atom can be adequately represented by treating it as a core and *one* shell, although this is not a necessary restriction. The usual treatment, in which the dipole moment is simply the product of polarizability and effective field, is included as a special case,

as we show later in § 5. By making use of the fact that for $q=0$ all the atoms of the same type move together, one can write down equations analogous to those of § 1 (eqns. (1.5)) as follows:

$$m_K\omega^2 U_K = \sum_{K'\neq K}\{D_{KK'}(U_{K'}-U_K)+X_K X_{K'} C_{KK'}(U_{K'}-U_K)\} + \sum_{K'\neq K}\{F_{KK'}(V_{K'}-U_K)+X_K Y_{K'} C_{KK'}(V_{K'}-U_K)\} + k_K(U_K-V_K)+X_K Y_K C_0(V_K-U_K). \quad . \quad . \quad . \quad (3.2)$$

The displacement of the Kth type of core is $U_K \exp(-i\omega t)$, and of the corresponding shell, $V_K \exp(-i\omega t)$. (The time-dependent factor cancels from all equations and will not be explicitly mentioned in future.) The charge on a core is $X_K e$, and on the corresponding shell, $Y_K e$, so that the ionic charge is $Z_K e=(X_K+Y_K)e$. The corresponding electronic dipole moment is thus $Y_K e(V_K-U_K)$. The force constant between a core and a shell is k_K. Since $q=0$ we again have to deal with force constants between Bravais arrays, for example $D_{KK'}(U_{K'}-U_K)$ is the restoring force, other than Coulomb force, acting on each core of type K and originating from all cores of type K'. Similarly $F_{KK'}(V_{K'}-U_K)$ denotes a core-shell force, and in the equation which follows $S_{KK'}(V_{K'}-V_K)$ denotes a shell–shell force. The 'Coulomb coefficients' $C_{KK'}$ would all have the value $-(4\pi e^2/3v)$ if the crystal were diagonally cubic. (The values appropriate to $BaTiO_3$ will be quoted later.) The value of C_0 is $-(4\pi e^2/3v)$. We now take the mass of each shell to be negligible so that the equation for its equilibrium is

$$0=\sum_{K'\neq K}\{S_{KK'}(V_{K'}-V_K)+Y_K Y_{K'} C_{KK'}(V_{K'}-V_K)\} + \sum_{K'\neq K}\{F_{KK'}(U_{K'}-V_K)+Y_K X_{K'} C_{KK'}(U_{K'}-V_K)\} + k_K(V_K-U_K)+X_K Y_K C_0(U_K-V_K). \quad . \quad . \quad . \quad . \quad . \quad (3.3)$$

In writing down these equations we have been careful to express all forces in terms of the *relative* displacements of cores and/or shells. The importance of this in considering the Coulomb interaction has been emphasized by Cohen (1951) and by Takagi (1953). We now *define*

$$D_{KK}=-\sum_{K'\neq K} D_{KK'} \quad . \quad . \quad . \quad . \quad . \quad . \quad (3.4)$$

and similarly for F and S, and

$$Z_K C_{KK}=-\sum_{K'\neq K} C_{KK'} Z_{K'}. \quad . \quad . \quad . \quad . \quad . \quad (3.5)$$

We also introduce a coordinate

$$W_K=V_K-U_K \quad . \quad . \quad . \quad . \quad . \quad . \quad . \quad . \quad (3.6)$$

so that the electronic dipole moment is $eY_K W_K$, and we also define

$$R_{KK'}=D_{KK'}+S_{KK'}+2F_{KK'} \quad . \quad . \quad . \quad . \quad . \quad . \quad . \quad (3.7)$$

and

$$T_{KK'}=S_{KK'}+F_{KK'}. \quad . \quad . \quad . \quad . \quad . \quad . \quad . \quad . \quad (3.8)$$

These latter quantities are a generalization of the 'coefficients' defined by Woods *et al.* (1960) and by Cochran (1959 b). In the present instance, where they apply only for $q=0$, it is more convenient to refer to them as short-range force constants per atom between Bravais arrays. The physical meaning of $R_{KK'}$ for example is that if the lattices K and K' were displaced a relative distance $U_{K'}-U_K$, with the atoms behaving as rigid non-polarizable units, the short-range force on each atom would be $R_{KK'}(U_{K'}-U_K)$. On adding together eqns. (3.2) and (3.3), and using definitions (3.4) to (3.8), one obtains eventually

$$m_K \omega^2 U_K = \sum_{K'} \{(R_{KK'} + Z_K C_{KK'} Z_{K'}) U_{K'} + (T_{KK'} + Z_K C_{KK'} Y_{K'}) W_{K'}\} \quad (3.9)$$

while eqn. (3.3) can be rewritten as

$$\begin{aligned} 0 = \sum_{K'} \{(T_{KK'} + Y_K C_{KK'} Z_{K'}) U_{K'} + (S_{KK'} + Y_K C_{KK'} Y_{K'}) W_{K'}\} \\ + \{k_K + F_{KK} + Y_K X_K (C_{KK} - C_0)\} W_K. \quad . \quad . \quad . \quad . \quad . \quad . \quad . \quad (3.10) \end{aligned}$$

These are the dynamical equations with the atomic coordinates and dipole moments serving as generalized coordinates, a procedure first suggested in another context by Mashkevich and Tolpygo (1957). Using similar methods one can obtain expressions for the effective fields at the Kth core, or at the Kth shell. The results are

$$\left.\begin{aligned} -e(\mathscr{E}_{\text{core}})_K &= \sum_{K'} \{C_{KK'} (Z_{K'} U_{K'} + Y_{K'} W_{K'})\} + (C_0 - C_{KK}) Y_K W_K, \\ -e(\mathscr{E}_{\text{shell}})_K &= \sum_{K'} \{C_{KK'} (Z_{K'} U_{K'} + Y_{K'} W_{K'})\} + (C_{KK} - C_0) X_K W_K. \end{aligned}\right\} \quad (3.11)$$

These two fields are equal only in a crystal which is diagonally cubic, when $C_0 = C_{KK}$, or if an atom is uncharged, when $Y_K = -X_K$.

These equations can be concisely expressed in matrix notation. For example we define

$$\mathbf{R} = \begin{bmatrix} R_{11} & R_{12} \ldots . R_{1n} \\ R_{21} & R_{22} \ldots . R_{2n} \\ \ldots\ldots\ldots\ldots \\ R_{n1} & R_{n2} \ldots . R_{nn} \end{bmatrix}.$$

This matrix is symmetrical and of order n. It is however of rank $(n-1)$ because the sum of the elements in any row or column is zero (eqns. (3.4) and (3.7)). The matrix whose element is $Z_K C_{KK'}$ is similarly of rank $(n-1)$, although the matrix $\mathbf{C}$, whose element is $C_{KK'}$, is not necessarily of rank less than n. We also define a matrix whose element is given by

$$\mathscr{S}_{KK'} = S_{KK'} + \delta_{KK'} \{k_K + F_{KK} + X_K Y_K (C_{KK} - C_0)\} \quad . \quad (3.12)$$

that is, $\mathscr{S}$ is the sum of $\mathbf{S}$ and a diagonal matrix. While $\mathbf{S}$ is singular, $\mathscr{S}$ is non-singular. We shall use subscripts d, r and c to distinguish diagonal,

row and column matrices. The absence of a subscript will denote a square matrix. For example

$$\mathbf{m}_d = \begin{bmatrix} m_1 & 0 \ldots\ldots 0 \\ 0 & m_2 \ldots . 0 \\ \ldots\ldots\ldots\ldots\ldots \\ 0 & 0 \ldots\ldots m_n \end{bmatrix}.$$

Equations (3.9) and (3.10) then become

$$\omega^2 \mathbf{m}_d \mathbf{U}_c = (\mathbf{R} + \mathbf{Z}_d \mathbf{C} \mathbf{Z}_d)\mathbf{U}_c + (\mathbf{T} + \mathbf{Z}_d \mathbf{C} \mathbf{Y}_d)\mathbf{W}_c, \quad . \quad . \quad (3.13)$$

$$0 = (\mathbf{T} + \mathbf{Y}_d \mathbf{C} \mathbf{Z}_d)\mathbf{U}_c + (\mathscr{S} + \mathbf{Y}_d \mathbf{C} \mathbf{Y}_d)\mathbf{W}_c. \quad . \quad . \quad (3.14)$$

On eliminating $\mathbf{W}_c$ between these equations, one obtains

$$\omega^2 \mathbf{m}_d \mathbf{U}_c = \mathbf{M}' \mathbf{U}_c$$

where $$\mathbf{M}' = \mathbf{R} + \mathbf{Z}_d \mathbf{C} \mathbf{Z}_d - (\mathbf{T} + \mathbf{Z}_d \mathbf{C} \mathbf{Y}_d)(\mathscr{S} + \mathbf{Y}_d \mathbf{C} \mathbf{Y}_d)^{-1}(\mathbf{T} + \mathbf{Y}_d \mathbf{C} \mathbf{Z}_d). \quad (3.15)$$

The quantities $M'_{KK'}$ may be regarded as effective force constants between Bravais arrays. The inverse matrix is to be formed by the usual rules. The matrix $\mathbf{M}'$ is of order n, and can be shown to be symmetrical and of rank $(n-1)$. In principle the values of ω for transverse modes are now given as solutions of the characteristic equation

$$\begin{vmatrix} M_{11}' - m_1\omega^2 & M_{12}' \ldots\ldots\ldots M_{1n}' \\ M_{21}' & M_{22}' - m_2\omega^2 \ldots . M_{2n}' \\ \ldots\ldots\ldots\ldots\ldots\ldots\ldots\ldots\ldots\ldots \\ M_{n1}' & M_{n2}' \ldots\ldots\ldots M_{nn}' - m_n\omega^2 \end{vmatrix} = 0. \quad (3.16)$$

(Although we have been considering only the situation for $q = 0$, the approach is readily generalized so as to apply to any value of q, with $\mathbf{q}$ in a direction such that the displacements are fixed in direction by crystal symmetry. It will not be necessary to do this here.)

The condition for the crystal to become unstable and thus make a ferroelectric transition has now also been obtained. It will be remembered that for the crystal to be stable against this vibration mode, all principal minors of $\mathbf{M}'$ must be positive. A solution $\omega_1^2 = 0$ is always obtained since Det $\mathbf{M}' = 0$, this is however merely the frequency of the acoustic mode. A second solution $\omega_2^2 = 0$ will be obtained when the determinant of a principal minor of order $(n-1)$ just vanishes. It can be shown that because the elements of $\mathbf{M}'$ satisfy the condition $\sum_{K'} M'_{KK'} = 0$, all principal minors of order $(n-1)$ are equal, hence it does not matter which we choose. We shall use the symbol $[\mathbf{M}']$ for a principal minor of $\mathbf{M}'$ of order $(n-1)$. Thus the condition for the crystal to make a transition to a ferroelectric phase is

$$\text{Det}\,[\mathbf{M}'] = 0. \quad . \quad . \quad . \quad . \quad . \quad . \quad . \quad . \quad (3.17)$$

If the transition is of the first order, the transition will occur as Det $[\mathbf{M}']$ approaches zero.

Relation (3.17) may be confirmed in another way. We make use of a theorem given in text books on the theory of matrices (see, for example

Aitken 1939, p. 88), namely that the sum of the products of the characteristic roots of a matrix of order n, taken $(n-1)$ at a time, is equal to the sum of the n principal minors of order $(n-1)$. If we divide the Kth row of $\mathbf{M}'$ by m_K the matrix obtained has characteristic roots which are just the values of ω^2. Applying the above theorem, and remembering that all principal minors of $\mathbf{M}'$ of order $(n-1)$ are equal, one obtains

$$\sum_{j=1}^{n} \frac{(\omega_1^2 \omega_2^2 \ldots . \omega_n^2)}{\omega_j^2} = \sum_{K=1}^{n} \frac{m_K}{(m_1 m_2 \ldots m_n)} \mathrm{Det}\,[\mathbf{M}']. \quad . \quad (3.18)$$

However, we know that $\omega_1 = 0$ (the acoustic mode), so all terms except one on the left of this equation are zero, giving

$$\prod_{j=2}^{n} \omega_j^2 = \sum_{K=1}^{n} \frac{m_K}{(m_1 m_2 \ldots . m_n)} \mathrm{Det}\,[\mathbf{M}']. \quad . \quad . \quad . \quad (3.19)$$

Since we are considering transverse modes, reference to eqn. (3.1) now confirms that the condition for $\epsilon_s = \infty$ is $\mathrm{Det}\,[\mathbf{M}'] = 0$.

One can obtain explicit expressions for the dielectric constants ϵ_e and ϵ_s in terms of the matrices defined above. Consider a field $\mathscr{E}_A \exp(-ipt)$ applied to the crystal in such a way that there is no depolarizing field. The equations of motion then lead to the results

$$p^2 \mathbf{m}_d \mathbf{U}_c = (\mathbf{R} + \mathbf{Z}_d \mathbf{C} \mathbf{Z}_d)\mathbf{U}_c + (\mathbf{T} + \mathbf{Z}_d \mathbf{C} \mathbf{Y}_d)\mathbf{W}_c - e\mathscr{E}_A \mathbf{Z}_c, \quad (3.20)$$

$$0 = (\mathbf{T} + \mathbf{Y}_d \mathbf{C} \mathbf{Z}_d)\mathbf{U}_c + (\mathscr{S} + \mathbf{Y}_d \mathbf{C} \mathbf{Y}_d)\mathbf{W}_c - e\mathscr{E}_A \mathbf{Y}_c. \quad (3.21)$$

These equations describe a forced vibration, and are analogous to (3.13) and (3.14) which described a free vibration.

The polarization in the crystal is given quite generally by

$$\mathscr{P} = \frac{e}{v} \sum_K (Z_K U_K + Y_K W) \quad . \quad . \quad . \quad . \quad . \quad (3.22)$$

or in matrix notation

$$\mathscr{P} = \frac{e}{v} (\mathbf{Z}_r \mathbf{U}_c + \mathbf{Y}_r \mathbf{W}_c). \quad . \quad . \quad . \quad . \quad . \quad . \quad (3.23)$$

On eliminating $\mathbf{W}_c$ between (3.21) and (3.23) one obtains

$$\mathscr{P} = \frac{e}{v} \{(\mathbf{Z}_r - \mathbf{Y}_r(\mathscr{S} + \mathbf{Y}_d \mathbf{C} \mathbf{Y}_d)^{-1}(\mathbf{T} + \mathbf{Y}_d \mathbf{C} \mathbf{Z}_d))\mathbf{U}_c$$
$$+ e\mathscr{E}_A \mathbf{Y}_r(\mathscr{S} + \mathbf{Y}_d \mathbf{C} \mathbf{Y}_d)^{-1} \mathbf{Y}_c\}. \quad (3.24)$$

Suppose now the frequency p is sufficiently high that the cores do not move ($\mathbf{U}_c = 0$) and the polarization results entirely from the movement of the electrons. Then

$$\frac{\mathscr{P}}{\mathscr{E}_A} = \frac{\epsilon_e - 1}{4\pi} = \frac{e^2}{v} \mathbf{Y}_r(\mathscr{S} + \mathbf{Y}_d \mathbf{C} \mathbf{Y}_d)^{-1} \mathbf{Y}_c \quad . \quad . \quad . \quad (3.25)$$

from eqn. (3.24). For a general value of p, we have by eliminating $\mathbf{W}_c$ between (3.21) and (3.20) that

$$e\mathscr{E}_A \{\mathbf{Z}_c - (\mathbf{T} + \mathbf{Z}_d \mathbf{C} \mathbf{Y}_d)(\mathscr{S} + \mathbf{Y}_d \mathbf{C} \mathbf{Y}_d)^{-1} \mathbf{Y}_c\} = (\mathbf{M}' - p^2 \mathbf{m}_d)\mathbf{U}_c \quad (3.26)$$

where $\mathbf{M}'$ is defined by eqn. (3.15). Inspection of eqns. (3.24) and (3.26) shows that they can be written simply as

$$\mathscr{P} = \frac{e}{v}\mathbf{Z}_r''\mathbf{U}_c + \frac{\epsilon_e - 1}{4\pi}\mathscr{E}_A \quad . \quad . \quad . \quad . \quad . \quad (3.27)$$

and

$$e\mathscr{E}_A\mathbf{Z}_c'' = (\mathbf{M}' - p^2\mathbf{m}_d)\mathbf{U}_c \quad . \quad . \quad . \quad . \quad . \quad (3.28)$$

where the apparent charge Z_K'' is defined by the two equivalent expressions

$$\left.\begin{aligned}\mathbf{Z}_c'' &= \mathbf{Z}_c - (\mathbf{T} + \mathbf{Z}_d\mathbf{C}\mathbf{Y}_d)(\mathscr{S} + \mathbf{Y}_d\mathbf{C}\mathbf{Y}_d)^{-1}\mathbf{Y}_c,\\ \mathbf{Z}_r'' &= \mathbf{Z}_r - \mathbf{Y}_r(\mathscr{S} + \mathbf{Y}_d\mathbf{C}\mathbf{Y}_d)^{-1}(\mathbf{T} + \mathbf{Y}_d\mathbf{C}\mathbf{Z}_d).\end{aligned}\right\} \quad (3.29)$$

The value of $(\epsilon_s - 1)/4\pi$ may now be obtained by setting $p = 0$ and eliminating $\mathbf{U}_c$ between eqns. (3.27) and (3.28). The elimination is not entirely straightforward because $\mathbf{M}'$ is singular. However, by using the method described towards the end of the Appendix, one finds

$$\frac{\mathscr{P}}{\mathscr{E}_A} = \frac{\epsilon_s - 1}{4\pi} = \frac{e^2}{v}[\mathbf{Z}_r'']\,[\mathbf{M}']^{-1}[\mathbf{Z}_c''] + \frac{\epsilon_e - 1}{4\pi}$$

or

$$\frac{\epsilon_s - \epsilon_e}{4\pi} = \frac{e^2}{v}[\mathbf{Z}_r'']\,[\mathbf{M}']^{-1}[\mathbf{Z}_c''] \quad . \quad . \quad . \quad . \quad . \quad (3.30)$$

where as before $[\mathbf{M}']$ is a principal minor of $\mathbf{M}'$ of order $n-1$. If the nth row and column are omitted from $\mathbf{M}'$ to give $[\mathbf{M}']$, the corresponding element Z_n'' is omitted from $\mathbf{Z}_r''$ to give $[\mathbf{Z}_r'']$, etc. The expressions (3.25) and (3.30) for what may be called the electronic and ionic susceptibilities respectively are somewhat similar in form. It may readily be shown that the right-hand side of eqn. (3.30) becomes infinite when Det $[\mathbf{M}'] = 0$, thus confirming the result which was given as eqn. (3.17).

The ionic susceptibility may also be expressed in a form which is directly comparable with that derived from the phenomenological treatment of Born and Huang (1954). We begin from eqns. (3.15), (3.27) and (3.28), written respectively in the form

$$m_K\omega_j^2 U_{Kj} = \sum_{K'} M'_{KK'}U_{K'j}, \quad . \quad . \quad . \quad . \quad . \quad (3.31)$$

$$e\mathscr{E}_A Z_K'' = \sum_{K'} M_{KK'}'U_{K'} - p^2 m_K U_K \quad . \quad . \quad . \quad . \quad (3.32)$$

and

$$\mathscr{P} = \frac{e}{v}\sum_K Z_K''U_K + \frac{\epsilon_e - 1}{4\pi}\mathscr{E}_A. \quad . \quad . \quad . \quad . \quad . \quad (3.33)$$

In eqn. (3.31) it is now necessary to distinguish the displacements of the atoms in different modes of free vibration; this is done by writing U_{Kj} for the displacement of the Kth atom in the j'th (transverse optic) mode. $\mathscr{P}_j$ will denote the corresponding polarization. U_K and $\mathscr{P}$ on the other hand denote the displacement and polarization in the course of a forced vibration which results from an external field $\mathscr{E}_A\exp(-ipt)$. We now express each U_K as a linear combination of the U_{Kj}, thus

$$U_K = \sum_j a_j U_{Kj}. \quad . \quad . \quad . \quad . \quad . \quad . \quad . \quad (3.34)$$

On substituting into (3.32), and using (3.31), therefore,

$$e\mathscr{E}_A Z_K'' = m_K \sum_j a_j U_{Kj}(\omega_j^2 - p^2),$$

so that

$$e\mathscr{E}_A \sum_K Z_K'' U_{Kj'} = \sum_{Kj} m_K U_{Kj'} a_j U_{Kj}(\omega_j^2 - p^2). \quad . \quad . \quad (3.35)$$

However, the orthogonality relations (see Born and Huang 1954, p. 298) give the result

$$\sum_K m_K U_{Kj} U_{Kj'} = 0 \quad \text{unless } j = j',$$

so that eqn. (3.35) reduces to

$$e\mathscr{E}_A \sum_K Z_K'' U_{Kj} = a_j(\omega_j^2 - p^2) \sum_K m_K U_{Kj}^2.$$

However,

$$\mathscr{P}_j = \frac{e}{v} \sum_K Z_K'' U_{Kj},$$

from (3.33) and the fact that there is no applied field for a free vibration. As an abbreviation, write

$$\sigma_j = \sum_K m_K U_{Kj}^2. \quad . \quad . \quad . \quad . \quad . \quad . \quad . \quad . \quad (3.36)$$

We then have

$$\mathscr{E}_A v \mathscr{P}_j = a_j(\omega_j^2 - p^2)\sigma_j \quad . \quad . \quad . \quad . \quad . \quad . \quad (3.37)$$

so from (3.34)

$$U_K = \mathscr{E}_A v \sum_j \frac{\mathscr{P}_j U_{Kj}}{\sigma_j(\omega_j^2 - p^2)}.$$

From this equation, using (3.33), we finally obtain

$$\mathscr{P} = \mathscr{E}_A v \sum_j \frac{\mathscr{P}_j^2}{\sigma_j(\omega_j^2 - p^2)} + \frac{\epsilon_e - 1}{4\pi} \mathscr{E}_A. \quad . \quad . \quad . \quad . \quad . \quad (3.38)$$

It follows immediately that the ionic susceptibility, for $p = 0$, is given by

$$\frac{\epsilon_s - \epsilon_e}{4\pi} = v \sum_j \frac{\mathscr{P}_j^2}{\sigma_j \omega_j^2}. \quad . \quad . \quad . \quad . \quad . \quad . \quad . \quad (3.39)$$

Later we shall make practical use of this simple result.

Equation (3.37) also gives the dielectric constant ϵ_p for any frequency p as

$$\frac{\epsilon_p - \epsilon_e}{4\pi} = v \sum_j \frac{\mathscr{P}_j^2}{\sigma_j(\omega_j^2 - p^2)}. \quad . \quad . \quad . \quad . \quad . \quad . \quad (3.40)$$

The more important results which we have obtained in this section are eqns. (3.25) and (3.30) for ϵ_e and ϵ_s respectively in terms of atomic parameters, and the condition (3.17) for the crystal to become unstable, which coincides with $(\omega_2)_T = 0$ and $\epsilon_s = \infty$.

§ 4. Dielectric Properties of Diagonally Cubic Crystals

Many of the results given in § 3 assume a simpler and more useful form when the crystal is diagonally cubic. The simplifying situation is that the effective field is the same at every atom, so that one may deal with the

dielectric properties in terms of polarizability instead of susceptibility.

Equations (3.20) and (3.21) become

$$\left.\begin{aligned} p^2\mathbf{m}_d\mathbf{U}_c &= \mathbf{R}\mathbf{U}_c + \mathbf{T}\mathbf{W}_c - e\mathscr{E}\mathbf{Z}_c \\ 0 &= \mathbf{T}\mathbf{U}_c + \mathscr{S}\mathbf{W}_c - e\mathscr{E}\mathbf{Y}_c \end{aligned}\right\} \quad . \quad . \quad . \quad . \quad (4.1)$$

where the effective field $\mathscr{E}$ is given by $\mathscr{E}_A + (4\pi/3)\mathscr{P}$. Proceeding in exactly the same way as before, one finds that at high frequencies

$$\frac{\mathscr{P}}{\mathscr{E}} = \frac{\alpha_e}{v} = \frac{e^2}{v}\mathbf{Y}_r\mathscr{S}^{-1}\mathbf{Y}_c \quad . \quad . \quad . \quad . \quad . \quad . \quad (4.2)$$

where α_e is defined as the total electronic polarizability per unit cell. For general values of p, on the other hand, one finds on eliminating $\mathbf{W}_c$ between eqns. (4.1), and from the general definition of $\mathscr{P}$ (eqn. (3.22)) that

$$\mathscr{P} = \frac{e}{v}(\mathbf{Z}_r - \mathbf{Y}_r\mathscr{S}^{-1}\mathbf{T})\mathbf{U}_c + \frac{\alpha_e}{v}\mathscr{E} \quad . \quad . \quad . \quad . \quad (4.3)$$

and

$$e\mathscr{E}(\mathbf{Z}_c - \mathbf{T}\mathscr{S}^{-1}\mathbf{Y}_c) = (\mathbf{R} - \mathbf{T}\mathscr{S}^{-1}\mathbf{T} - p^2\mathbf{m}_d)\mathbf{U}_c. \quad . \quad . \quad (4.4)$$

These equations may be written simply as

$$\mathscr{P} = \frac{e}{v}\mathbf{Z}_r'\mathbf{U}_c + \frac{\alpha_e}{v}\mathscr{E} \quad . \quad . \quad . \quad . \quad . \quad . \quad (4.5)$$

and

$$e\mathscr{E}\mathbf{Z}_c' = (\mathbf{R}' - p^2\mathbf{m}_d)\mathbf{U}_c. \quad . \quad . \quad . \quad . \quad . \quad . \quad (4.6)$$

The effective charges Z_K' which have been introduced are given by the equivalent expressions

$$\left.\begin{aligned} \mathbf{Z}_r' &= \mathbf{Z}_r - \mathbf{Y}_r\mathscr{S}^{-1}\mathbf{T}, \\ \mathbf{Z}_c' &= \mathbf{Z}_c - \mathbf{T}\mathscr{S}^{-1}\mathbf{Y}_c, \end{aligned}\right\} \quad . \quad . \quad . \quad . \quad . \quad . \quad (4.7)$$

and the effective short-range force constants $R_{KK'}'$ are given by

$$\mathbf{R}' = \mathbf{R} - \mathbf{T}\mathscr{S}^{-1}\mathbf{T}. \quad . \quad . \quad . \quad . \quad . \quad . \quad (4.8)$$

It may readily be shown that the effective charges and effective force constants satisfy respectively the relations

$$e\sum_K Z_K' = 0 \quad \text{and} \quad \sum_{K'} R_{KK'}' = 0,$$

as do the true ionic charges and force constants. The effective charge Z_K' is not the same as the apparent charge Z_K'' which we defined in the previous section. For a crystal which is not diagonally cubic only the concept of apparent charge is valid; for a crystal which is diagonally cubic the two are related by

$$Z_K'' = \tfrac{1}{3}(\epsilon_c + 2)Z_K'. \quad . \quad . \quad . \quad . \quad . \quad . \quad (4.9)$$

The total polarizability of the crystal per unit volume, α_s/v, is defined as the ratio $\mathscr{P}/\mathscr{E}$ at zero frequency. Setting $p=0$ in eqn. (4.6) and eliminating $\mathbf{U}_c$ between eqns. (4.5) and (4.6), remembering that the matrix $\mathbf{R}'$ is singular, one obtains

$$\mathscr{P}=\mathscr{E}\left(\frac{e^2}{v}[\mathbf{Z}_r'][\mathbf{R}']^{-1}[\mathbf{Z}_c']+\frac{\alpha_e}{v}\right)$$

and therefore

$$\alpha_s=e^2[\mathbf{Z}_r'][\mathbf{R}']^{-1}[\mathbf{Z}_c']+\alpha_e. \quad . \quad . \quad . \quad . \quad . \quad (4.10)$$

This equation gives the ionic polarizability $\alpha_i=\alpha_s-\alpha_e$ in terms of the atomic parameters. The concept of ionic polarizability has often been used previously, but has usually been based on the Einstein model of a crystal in which the atoms move independently of one another. It has sometimes therefore been regarded as a concept of doubtful validity (Megaw 1952, Känzig 1957). It is worth noting that we have been able to legitimize the concept only for crystals which are diagonally cubic. Our expression for α_i does not at first sight appear to support the observation by Roberts (1949) that ionic polarizability is an additive property of the atoms involved. Although we shall not pursue this topic here, closer investigation shows that, at least for the alkali halides, there is no discrepancy. It can be shown from eqn. (4.2) that electronic polarizability is an additive property of the atoms involved provided that the diagonal elements of the matrix $\mathscr{S}$ are large compared with the other elements of this matrix. These points will be discussed in more detail elsewhere.

Next we discuss the free vibrations, for $q=0$, of a diagonally cubic crystal. By analogy with eqn. (4.6), these are given by

$$\omega^2\mathbf{m}_d\mathbf{U}_c=\mathbf{R}'\mathbf{U}_c-e\mathscr{E}\mathbf{Z}_c' \quad . \quad . \quad . \quad . \quad . \quad . \quad (4.11)$$

where $\mathscr{E}=(4\pi/3)\mathscr{P}$ for a transverse optic mode of vibration. As before, $\mathscr{P}$ is given by eqn. (4.5). From this equation we have, using eqn. (1.10), that

$$\mathscr{P}=\frac{(\epsilon_c+2)}{3v}e\mathbf{Z}_r'\mathbf{U}_c. \quad . \quad . \quad . \quad . \quad . \quad . \quad (4.12)$$

From eqn. (4.11) therefore,

$$\omega^2\mathbf{m}_d\mathbf{U}_c=\mathbf{R}'\mathbf{U}_c-\frac{4\pi(\epsilon_c+2)e^2}{9v}\mathbf{Z}_r'\mathbf{U}_c\mathbf{Z}_c'. \quad . \quad . \quad . \quad (4.13)$$

As usual, the condition of solubility of this set of equations gives the values of ω_T. It is found that eqn. (4.13) may equally well be written as

$$\omega^2\mathbf{m}_d\mathbf{U}_c=\mathbf{M}'\mathbf{U}_c$$

where

$$\mathbf{M}'=\mathbf{R}'-\frac{4\pi(\epsilon_e+2)e^2}{9v}\mathbf{Z}_d'\mathscr{I}\mathbf{Z}_d' \quad . \quad . \quad . \quad . \quad (4.14)$$

and $\mathscr{I}$ is a square matrix with every element equal to unity. As before, the condition for the crystal to become unstable against a transverse optic mode of vibration is

$$\text{Det}\,[\mathbf{M}']=0. \quad . \quad . \quad . \quad . \quad . \quad . \quad . \quad . \quad (3.17)$$

We now make use of a result explained in the Appendix, where it is also used. In the present context it is, from (4.14), that

$$\mathrm{Det}\,[\mathbf{M}'] = \mathrm{Det}\,[\mathbf{R}']\left(1 - \frac{4\pi(\epsilon_e+2)e^2}{9v}\,[\mathbf{Z}_r'][\mathbf{R}']^{-1}[\mathbf{Z}_c']\right). \quad . \quad (4.15)$$

Thus the crystal becomes unstable when

$$\frac{4\pi(\epsilon_e+2)\alpha_i}{9v} = 1$$

from eqns. (4.10) and (4.15). This is however the same as

$$\frac{4\pi\alpha_s}{3v} = 1,$$

so that the terms 'instability' and 'polarizability catastrophe' are synonymous, for a diagonally cubic crystal.

The results given in this section reduce to the corresponding results given in § 2 when there are two atoms per unit cell.

§ 5. Application to Barium Titanate

We shall first discuss Slater's (1950) theory of the mechanism of ferroelectricity in $BaTiO_3$ in the light of results given in the previous section. In Slater's theory the following assumptions and simplifications are made:

(1) The atoms do not move from their equilibrium positions, but to compensate for this the electronic polarizability of the Ti atom is increased at low frequencies. The added polarizability is taken to be the ionic polarizability.

(2) The dipole moment of each atom is taken to be the product of its polarizability and the effective field at the nucleus.

With the atoms numbered as in fig. 4 the following set of equations then applies:

$$\left.\begin{aligned} E_1 &= f_0P_1 + f_{12}P_2 + \ldots + f_{15}P_5, \\ E_2 &= f_{21}P_1 + f_0P_2 + \ldots + f_{25}P_5, \text{ etc.} \end{aligned}\right\} \quad . \quad . \quad . \quad . \quad . \quad (5.1)$$

Here P_1 is the component of the polarization P caused by the Ba atoms, etc., so that assumption (2) gives

$$P_1 = \alpha_1 E_1/v. \quad . \quad . \quad . \quad . \quad . \quad . \quad . \quad . \quad (5.2)$$

The value of f_0 is $4\pi/3$, while $f_{KK'}$ is related to $C_{KK'}$ of the previous section by the identity

$$C_{KK'} = -(e^2/v)f_{KK'}.$$

The condition for a ferroelectric transition is that the polarization should become finite in zero applied field. From eqns. (5.1) and (5.2) the condition for this is

$$\begin{vmatrix} f_0 - v/\alpha_1 & f_{12} & \ldots\ldots & f_{15} \\ f_{21} & f_0 - v/\alpha_2 & \ldots\ldots & f_{25} \\ \ldots & \ldots & \ldots & \ldots \\ f_{51} & f_{52} & & f_0 - v/\alpha_5 \end{vmatrix} = 0. \quad . \quad . \quad (5.3)$$

This equation is the basis of Slater's numerical calculations. Since the ionic polarizability is simply added to the electronic polarizability, eqn. (3.25) is the correct result to use for purposes of comparison. The dielectric constant calculated from this equation will be infinite if

$$\mathrm{Det}\,(\mathscr{S}+\mathbf{Y}_{\mathrm{d}}\mathbf{C}\mathbf{Y}_{\mathrm{d}})=0. \qquad . \quad . \quad . \quad . \quad . \quad . \quad . \quad (5.4)$$

Assumption (2) requires that each shell is coupled only to the core of the same atom, so from eqn. (3.12)

$$\mathscr{S}_{KK'}=\delta_{KK'}\{k_K+Y_K X_K(C_{KK}-C_0)\}.$$

The first row of the determinant (5.4) is therefore, for example,

$$k_1+Y_1X_1(C_{11}-C_0)+Y_1{}^2C_{11},\quad Y_1Y_2C_{12}.\ldots.Y_1Y_5C_{15}.$$

We may now take all Y_K to be equal, and determine each polarizability $\alpha_K=Y_K{}^2e^2/k_K$ by suitable choice of the force constant k_K. Now on the basis of the shell model the dipole moment is determined not by the field at the nucleus, but by that at the shell. In general these are unequal (eqn. (3.11)). Hence to fit assumption (2) completely using a shell model, we must take k_K and Y^2 to be large, so that core and shell are never appreciably separated, but α_K remains finite. But since $X_K+Y_K=Z_K$ and Z_K remains finite, X_K tends to $-Y_K$. Consequently we take

$$Y_1=Y_2=\ldots.=-X_1=-X_2.\ldots.$$

On multiplying the first row of the determinant (5.4) by $-v/(Ye)^2$ it is now found to be identical with the first row of the determinant (5.3), and similarly for the other rows. Conditions (5.3) and (5.4) are therefore the same when the parameters of the shell model are chosen so that it behaves in the way required by assumption (2), and the conditions required by assumption (1) are also satisfied. This part of Slater's theory may therefore be said to be a special case of the general theory given in § 3. The assumptions made are open to criticism however. The way in which ionic polarizability is introduced is equivalent to coupling each titanium ion to its equilibrium position in the crystal, rather than to the other ions. The neglect by Slater of non-Coulomb interaction between the electrons—short-range force constants between the shells, in the nomenclature of the shell model—may have resulted in an incorrect picture of the situation in another respect, as we attempt to show later by qualitative reasoning.

The elements of the matrix $\mathbf{C}$ are as follows for $BaTiO_3$:

C_{11}	C_0	C_0+C_A	C_0-2C_A	C_0+C_A
C_0	C_{22}	C_0-C_B	C_0+2C_B	C_0-C_B
C_0+C_A	C_0-C_B	C_{33}	C_0+C_A	C_0+C_A
C_0-2C_A	C_0+2C_B	C_0+C_A	C_{44}	C_0+C_A
C_0+C_A	C_0-C_B	C_0+C_A	C_0+C_A	C_{55}

where $C_0=-(4\pi e^2/3v)$ as before, $C_A=-4{\cdot}334(e^2/v)$ and $C_B=-15{\cdot}04(e^2/v)$. Using eqn. (3.5) one can show that $C_{11}=C_{22}=C_0$, but that the value of the remaining diagonal elements depends on the values assumed for the ionic

charges. It may readily be shown however that $C_{33}=C_{55}$, and it will be seen from the above figures that $C_{3K}=C_{5K}$. It is clear from fig. 4 that this arises from the identical environment of the oxygen atoms 3 and 5 with respect to displacement of the other atoms along [001], and that this relation extends to the elements of all the other matrices, e.g. $R_{3K}=R_{5K}$, $R_{33}=R_{55}$, etc. It follows that for a transverse mode with **q** along [100] and the displacements along [001], $U_3=U_5$ and $W_3=W_5$, that is, lattices 3 and 5 are completely equivalent and move as one. It follows that the dynamical equations can be simplified. For example, consider the Coulomb terms $\mathbf{Z}_d\mathbf{C}\mathbf{Z}_d$ of eqn. (3.13). Those which occur in the first of the dynamical equations will be

$$Z_1(Z_1C_{11}U_1+Z_2C_{12}U_2+Z_3C_{13}U_3+Z_4C_{14}U_4+Z_5C_{15}U_5).$$

We may now add the third and fifth terms, giving a term appropriate to a single atom with a charge $2Z_3$. We may similarly add together the third and fifth equations to give an equation appropriate to an atom of mass $2m_3$, and so on. The net result is to reduce every matrix from order 5 to order 4. There are therefore only four transverse modes of different frequency at $q=0$, and since one is acoustic, there are three transverse optic modes. The same is true of longitudinal modes. This conclusion agrees with that of Last (1957) who showed in another way that $BaTiO_3$ has only three modes which are 'infra-red active'.

Unfortunately this appears to be as far as an *exact* theoretical treatment of the problem can be taken at the present time. The equations of § 3 are of course exact to the extent that a shell model for the atoms in $BaTiO_3$ is valid, but our knowledge of the forces between the atoms and even of the ionic charges is too slight for any numerical calculation to be directly based on the general equations. We are therefore forced to make some approximations. The structure analyses of tetragonal $BaTiO_3$ and $PbTiO_3$ (Shirane *et al.* 1957, Shirane *et al.* 1955) show that within the limits of experimental error the oxygen framework is undistorted after the ferroelectric transition. This remarkable result suggests that the oxygen atoms are linked by comparatively strong covalent bonds, since after a transition with the atoms moving in the |001| direction, the effective field at sites 3 and 5 is quite different from that at site 4. The structure analysis strongly suggests, if it does not actually prove, that in the T.O. mode of lowest frequency the oxygen nuclei move as a single unit with $U_3=U_4=U_5$. If we accept this as a fact, then, for this mode only, the matrices **R** and $\mathbf{Z}_d\mathbf{C}\mathbf{Z}_d$ can be reduced from order 4 to order 3. Reduction of the other matrices is not permissible unless $W_3=W_4=W_5$. We have already seen that $W_3=W_5$, but on the basis of Slater's theory the dipole moments produced at sites 3 and 4 by a movement of titanium are oppositely directed. However, the situation is completely altered if we take into account short-range forces between the electrons. The oxygen atoms cannot be directly linked by covalent bonds, but must be linked through the titanium, in other words it seems probable that the corresponding shells are connected by

comparatively large force constants and the matrix elements S_{23}, S_{24}, S_{25} and T_{23}, T_{24}, T_{25} are all large. It is conceivable that the shell of the titanium ion is in fact more strongly linked to the shells of the surrounding oxygens than to the titanium core. In the above circumstances there is then necessarily a tendency towards equilization of W_3 and W_4, and this will be enhanced by the movement of barium in the same direction as titanium. While the exact equality of W_3 and W_4 is unlikely, we propose as an approximation to ignore any difference. For the T.O. mode of lowest frequency all the matrices can then be contracted to become of order 3. When this is done it is found that the resulting Coulomb coefficients all have the value $-4\pi e^2/(3v)$, or in other words the crystal behaves as if it were diagonally cubic. That this should be so is in fact clear on considering fig. 4 with the proviso that sites 3, 4 and 5 are to be equivalent in displacement and dipole moment. In setting $W_3 = W_4$, as distinct from $U_3 = U_4$, we have in fact gone beyond what is warranted by the direct experimental evidence; the chief justification for this assumption is the satisfactory results to which it leads. The situation is of course much simplified by this approximation, for we can now make use of the relatively simple equations derived in § 4.

We now use suffix o to denote the group of oxygens so that

$$m_o = 3m_3, \quad Z_o = 3Z_3, \quad R_{10} = R_{13} + R_{14} + R_{15}, \quad \text{etc.}$$

The simplest approach is now to consider the static dielectric constant, which is given by

$$\epsilon_s = \frac{3 + 8\pi(\alpha_e + \alpha_i)}{3 - 4\pi(\alpha_e + \alpha_i)}.$$

From the general result

$$\alpha_i = e^2[\mathbf{Z}_r'][\mathbf{R}']^{-1}[\mathbf{Z}_c']$$

we have in this instance

$$\alpha_i = \frac{e^2((Z_1')^2 R_{22}' + (Z_2')^2 R_{11}' - 2Z_1' Z_2' R_{12}')}{R_{11}' R_{22}' - (R_{12}')^2}.$$

The condition for the dielectric constant ϵ_s to follow a Curie–Weiss law in the cubic phase is then found to be

$$1 - \frac{4\pi e^2(\epsilon_e + 2)\{(Z_1')^2 R_{22}' + (Z_2')^2 R_{11}' - 2Z_1' Z_2' R_{12}'\}}{9v\{R_{11}' R_{22}' - (R_{12}')^2\}} = \gamma(T - T_c) \quad (5.5)$$

where the temperature coefficient γ is related to the Curie constant $\mathscr{C}$ by eqn. (2.4), as before. Equation (5.5) is closely analogous to eqn. (2.1), which applied to a diatomic crystal, and the mechanism which we mentioned in § 2 will serve equally well to explain the temperature variation of the quantity on the left of eqn. (5.5)—that is, anharmonicity of the lattice vibrations will cause a linear change with temperature of the parameters which appear in the 'harmonic' theory. The condition for a ferroelectric transition is that the left-hand side of eqn. (5.5) should approach zero. The same result may be obtained from the condition $(\omega_2)_T \to 0$. The fact that the crystal does not become completely unstable can be explained by

postulating an explicit expression for the anharmonic terms involving relative motion of the titanium and oxygen atoms. The equilibrium of the system is then determined by the equations

$$eZ_1'E_z = R_{11}'(u_1-u_0)_z + R_{12}'(u_2-u_0)_z,$$
$$eZ_2'E_z = R_{12}'(u_1-u_0)_z + R_{22}'(u_2-u_0)_z + B(u_2-u_0)_z^3 + B'(u_2-u_0)_z^5 + B''(u_2-u_0)_z\{(u_2-u_0)_x^2 + (u_2-u_0)_y^2\}. \quad . \; . \; . \quad (5.6)$$

The field E includes any applied field E_Λ. The validity of this approach was discussed in § 2. Additional anharmonic terms involving the relative movement of barium and oxygen could be included, but we prefer to introduce no more parameters than are necessary to account for the observed behaviour. Equation (4.5) now gives

$$P_z v = eZ_1'(u_1-u_0)_z + eZ_2'(u_2-u_0)_z + \alpha_e E_z. \quad . \; . \; . \; . \; . \quad (5.7)$$

The use of u, P and E in place of U, $\mathscr{P}$ and $\mathscr{E}$ is intended to emphasize the fact that we are considering static displacements, in eqns. (5.6) and (5.7). There are of course similar equations with the suffices permuted. The approximate solution of the above equations, when eqn. (5.5) is taken into account, is

$$(E_\Lambda)_z = \frac{(T-T_c)P_z}{\mathscr{C}} + Bv^3g^4P_z^3 + B'v^5g^6P_z^5 + B''v^3g^4P_z(P_x^2+P_y^2) \quad . \; . \; . \; . \quad (5.8)$$

together with similar equations for $(E_\Lambda)_y$ and $(E_\Lambda)_z$. The derivation is very similar to that given in § 2, and the definition of g is now found to be

$$g = \frac{3(Z_2'R_{11}' - Z_1'R_{12}')}{e(\epsilon_e+2)\{(Z_1')^2R_{22}' + (Z_2')^2R_{11}' - 2Z_1'Z_2'R_{12}'\}}. \quad . \quad (5.9)$$

Apart from the difference in the definition of g, eqn. (5.8) is the same as was found to apply to a diatomic crystal. These equations are the same as would be obtained by assuming that the free energy is given by

$$G_1 = \frac{(T-T_c)}{2\mathscr{C}}(P_x^2+P_y^2+P_z^2) + \tfrac{1}{4}\zeta(P_x^4+P_y^4+P_z^4) + \tfrac{1}{6}\zeta(P_x^6+P_y^6+P_z^6) + \tfrac{1}{2}\lambda(P_x^2P_y^2+P_y^2P_z^2+P_z^2P_x^2). \quad (5.10)$$

It follows from the known success of Devonshire's theory that if atomic parameters are chosen so as to give suitable values for $\mathscr{C}$, ξ, ζ and λ, the theory given here will give dielectric properties in good agreement with those of $BaTiO_3$. It remains only to investigate whether the required atomic parameters are of a reasonable magnitude. We shall make numerical calculations only for the cubic-tetragonal transition, since it is known that with $\lambda \simeq -\xi$, i.e. $B'' \simeq -B$, the other transitions may be accounted for quantitatively. By using eqns. (5.5) to (5.9) it is found that the parameters

which determine the properties of the crystal in the neighbourhood of the upper transition are γ, B, B', d_1, d_2 and $Z_1' d_1 + Z_2' d_2$, where

$$d_1 = \frac{Z_1' R_{22}' - Z_2' R_{12}'}{R_{11}' R_{22}' - (R_{12}')^2} \text{ and } \quad d_2 = \frac{Z_2' R_{11}' - Z_1' R_{12}'}{R_{11}' R_{22}' - (R_{02}')^2} .$$

Thus it is not necessary to fix values for the individual effective charges and effective short-range force constants. It is however to be expected that R_{12}' will be small compared with R_{11}' or R_{22}', since the barium and titanium atoms are not nearest neighbours, but that R_{11}' and R_{22}' will be of the same order of magnitude. Thus for the sake of definiteness we have taken $R_{12}' = 0$ and $R_{11}' = R_{22}'$ in the numerical calculations, which were made using values of the parameters chosen so as to give best agreement with observation. These values are $\gamma = 4{\cdot}57 \times 10^{-5}$ per °C, $B = -7{\cdot}81 \times 10^{20}$ c.g.s., $B' = 5{\cdot}83 \times 10^{38}$ c.g.s., $R_{11}' = R_{22}' = 2{\cdot}83 \times 10^5$ dyne cm^{-1}, $Z_1' = 1{\cdot}20$ and $Z_2' = 2{\cdot}40$. The values used for ϵ_e and v were 5·76 and 64 Å^3 respectively. The results of the calculation are given in table 1, and are compared with the corresponding experimental values. The calculated variations with temperature of the spontaneous polarization and the static dielectric constant are shown in fig. 5.

Table 1. Calculated and Measured Values of Various Quantities. The last four entries are calculated for $T = T_{tr}$

	$\mathscr{C}$	ξ	ζ	$(T_{tr} - T_c)$
Calculated	$1{\cdot}35 \times 10^4$ c.g.s.	$-10{\cdot}5 \times 10^{-13}$ c.g.s.	$2{\cdot}30 \times 10^{-22}$ c.g.s.	12·1 °K
Measured	$1{\cdot}35 \times 10^4$	$-\ 6{\cdot}8 \times 10^{-13}$	$2{\cdot}28 \times 10^{-22}$	11
	$1{\cdot}32 \times 10^4$	$-10{\cdot}8 \times 10^{-13}$		14
	ϵ_s	P	$(u_1 - u_0)$	$(u_2 - u_0)$
Calculated	$1{\cdot}40 \times 10^4$	19·5 μ-coul. cm^{-2}	0·05 Å	0·10 Å
Measured	$\sim 10^4$	18·0	0·07 Å	0·13 Å

The measured values are as collected by Känzig (1957); where more than one reliable value is available, both are quoted. The experimental values of $(u_1 - u_0)$ and of $(u_2 - u_0)$ were not determined at the transition temperature and should therefore be reduced somewhat for comparison. In giving the above figures the small relative movements of the oxygens have of course been ignored.

From the results given in table 1 and fig. 5, it is clear that the theory accounts rather well for many of the properties of $BaTiO_3$ and that it does so with parameters which are physically reasonable. The values of γ and of Z_1' and Z_2' scarcely require comment, although it should be remembered that the two latter are not the true ionic charges. The physical meaning of R_{22}' is that it is the short-range force exerted on a titanium atom when all the titanium nuclei are displaced the same (small) unit distance, the other nuclei remaining fixed in their equilibrium positions. The value of the

corresponding quantity for germanium has been found to be $1{\cdot}82\times10^5$ (Cochran 1959 b), while for the alkali halides it ranges from about $1{\cdot}0\times10^5$ for LiF to about $2{\cdot}5\times10^4$ for RbI. Thus the value used here is of the correct order of magnitude. The relative values of R_{22}', B and B' correspond to a very small departure from the harmonic approximation. This is shown in table 2, where the components of the force

$$R_{22}'(u_2-u_0)+B(u_2-u_0)^3+B'(u_2-u_0)^5$$

are set out. It is clear that there is no question of a second minimum in the short-range potential between the titanium and oxygen atoms.

Table 2

(u_2-u_0)	$R_{22}'(u_2-u_0)$	$B(u_2-u_0)^3+B'(u_2-u_0)^5$
0·1 Å	$2{\cdot}83\times10^{-4}$ dynes	$-1{\cdot}98\times10^{-7}$ dynes
0·2	$5{\cdot}66\times10^{-4}$	$+1{\cdot}24\times10^{-5}$
0·3	$8{\cdot}49\times10^{-4}$	$+1{\cdot}21\times10^{-4}$

We next consider the question of the numerical value of $(\omega_2)_T$ in the cubic phase. If this is known for example at the transition temperature, it can be calculated at any higher temperature from $(\omega_2)_T^2\propto(T-T_c)$. Since ϵ_s is some 2500 times greater than in a normal ionic crystal, $(\omega_2)_T$ at its lowest must be some 50 times lower than 'normal'. Two infra-red absorption frequencies have been measured by Last (1957) for $BaTiO_3$, at approximately $1{\cdot}0\times10^{13}$ and $1{\cdot}5\times10^{13}$ c.p.s. (we quote numerical values of $\nu=\omega/(2\pi)$). It is significant that Last did not detect a third absorption frequency. From the specific heat, Last predicted that it would be found at about $\nu=6{\cdot}7\times10^{12}$ c.p.s. We believe that this estimate is too high, and that the remaining frequency will be found to be, at its lowest, some 50 times less than the measured frequencies, in the neighbourhood of 2 or 3×10^{11} c.p.s. A more precise estimate may be made as follows. In § 3 it was found that the displacements U_K of the nuclei in an applied field may be written as a linear combination of the corresponding displacements U_{Kj} in the T.O. modes of free vibration, thus $U_K=\sum_j a_j U_{Kj}$, and that $a_j\propto\omega_j^{-2}$, for a static field. Thus when one mode ($j=2$) has a frequency much lower than the others, the relative displacements of the atoms in an applied field must be closely the same as in the low-frequency mode of vibration. Provided the anharmonic terms in the short-range force are relatively small, as we have found, the same is true of the displacement of the atoms at and after the cubic-tetragonal transition. Thus after the transition, the crystal preserves approximately the relative values of $\mathscr{P}_j$ and U_{Kj} appropriate to $j=2$. From eqn. (3.39) therefore, neglecting terms which involve ω_3 or ω_4, one has approximately

$$\epsilon_s(\omega_2)_T^2=\frac{4\pi v P^2}{\sigma}=\text{a constant},$$

where $(\omega_2)_T$ and ϵ_s are values appropriate to the cubic phase (at any temperature above T_{tr}), while P and σ are values appropriate to a temperature below T_{tr}, P being the spontaneous polarization and $\sigma = \sum_K m_K u_K^2$, where u_K is the displacement of an atom corresponding to this value of P. The atomic displacements are determined by the structure analysis of Shirane, Danner and Pepinsky (1957). Absolute displacements can be derived from the measured relative values by making use of the fact that the centre of mass is not displaced, and one finds $\sigma = 0{\cdot}693 \times 10^{-40}$ g cm^2. These are room-temperature displacements, so we take $P = 22{\cdot}0$ μ-coul. cm$^{-2} = 6{\cdot}6 \times 10^4$ e.s.u. Taking $\epsilon_s = 1{\cdot}2 \times 10^4$ as the maximum value of the dielectric constant in the cubic phase then gives the minimum value of $(\nu_2)_T$ as $3{\cdot}2 \times 10^{11}$ c.p.s., in good agreement with the earlier estimate.

Relaxation of the dielectric constant of $BaTiO_3$ has been reported at frequencies lower than 3×10^{10} c.p.s. (Känzig 1957). Recently, however, Benedict and Durand (1958) have made measurements on single crystals of the cubic phase, and found at a frequency of $2{\cdot}4 \times 10^{10}$ c.p.s. a dielectric constant identical with the static value. Measurements in the frequency range in which we expect the lowest dispersion frequency to be found would be difficult as it is in the millimetre wavelength range. H. Juretschke, R. Landauer and P. Sorokin have independently come to the conclusion that the lowest dispersion frequency for $BaTiO_3$ should be in the region of 10^{11} c.p.s., and should vary as $(T - T_c)^{1/2}$ (unpublished work communicated to me privately by Dr. Landauer). They also make the interesting suggestion that the low-frequency mode of vibration may in fact be 'overdamped'. Damping of the T.O. modes having $q = 0$ does not affect our analysis except to make eqn. (3.40) inapplicable in the neighbourhood of $p = \omega_j$. Our other results, including eqn. (3.39), are not affected even if one mode is overdamped.

A low-frequency mode (even if overdamped) should give rise to diffuse scattering of x-rays, since the intensity of diffuse scattering depends, among other things, on ω^{-2}. However, if the value of $(\omega_2)_T$ increases rather steeply away from $q = 0$, this intensity will be obscured by the Bragg peak and by the scattering from acoustic modes. This objection does not apply when ω is low for a value of q not equal to zero, which we have indicated as a characteristic of a cubic crystal near an antiferroelectric transition. For such a crystal there should be a region of thermal diffuse scattering around points in the reciprocal lattice where additional Bragg peaks will appear after the transition. The intensity of scattering should increase as the temperature is lowered towards the transition temperature.

A most thorough test of the theory developed in this paper would be provided by an experimental determination of the $\omega(\mathbf{q})$ relation for $BaTiO_3$ or a similar material, by neutron spectroscopy. In principle an investigation in the neighbourhood of $q = 0$ is all that is required, but an investigation over a range of values of $\mathbf{q}$ (possibly confined to the [100] direction) would be more useful. No neutron group with distinctive energy change would be scattered by an overdamped mode, and it seems likely that for $\mathbf{q}$ along

[100], only two T.O. modes would be detected near $q=0$, with the third possibly becoming apparent for larger values of $\mathbf{q}$.

The discussion in this paper has been confined to cubic crystals. It seems clear by analogy that for any crystal, with the possible exception of those in which an order-disorder transformation takes place, the problem of the onset of ferroelectric or antiferroelectric properties is in principle a problem in lattice dynamics, and that a high dielectric constant must always be associated with an optic mode of vibration of low frequency. In a crystal of low symmetry, such as Rochelle Salt, it will not be possible to treat the problem of the stability of this mode as one involving a determinant of order n, the full $3n \times 3n$ determinant must be used. The reason is that no mode is constrained by crystal symmetry to be purely transverse or longitudinal. For the same reason the frequencies of the optic vibrations for $q \to 0$ may not coincide with the dielectric dispersion frequencies (Born and Huang 1954). The situation is further complicated by the fact that free and clamped dielectric constants have to be distinguished in all phases. Nevertheless there seems to be experimental evidence for a relation of the form $\omega^{-2} \propto \epsilon_s$, where ϵ_s is the clamped dielectric constant and ω is the lowest dispersion frequency. Measurements made by Akao and Sasaki (1955) of the temperature dependence of the dielectric relaxation frequency of Rochelle salt are in at least qualitative agreement with such a result, and the measured frequency was relatively very low—in the region of 2×10^9 c.p.s.

Acknowledgments

Much of this work was done during the tenure of a fellowship from Atomic Energy of Canada, to whom I express my thanks, and also to the University of Cambridge for granting me a year's leave of absence. I am grateful to various colleagues who helped with advice and criticism, particularly to Dr. Brockhouse who introduced me to the subject of lattice dynamics.

APPENDIX

In the following derivation the cores and shells are treated on the same basis—each unit has a finite mass m_K, charge Z_K and displacement U_K, so that the notation differs from that of § 3. There are n cores and $Q-n$ shells. The equation corresponding to (3.13), for transverse modes, is now simply

$$\omega^2 \mathbf{m}_d \mathbf{U}_c = (\mathbf{R} + \mathbf{Z}_d \mathbf{C} \mathbf{Z}_d) \mathbf{U}_c. \quad . \quad . \quad . \quad . \quad . \quad (A\,1)$$

As in § 3, using the result (3.19), one finds

$$(\omega_2^2 \omega_3^2 \ldots . \omega_Q^2)_T = \sum_{K=1}^{Q} \frac{m_K}{(m_1 m_2 \ldots . m_Q)} \mathrm{Det}\,[\mathbf{M}] \quad . \quad . \quad (A\,2)$$

where $[\mathbf{M}]$ is a principal minor of order $(Q-1)$ of a matrix which in the present notation is

$$\mathbf{M} = \mathbf{R} + \mathbf{Z}_\mathrm{d}\,\mathbf{C}\,\mathbf{Z}_\mathrm{d}. \quad . \quad . \quad . \quad . \quad . \quad . \quad . \quad . \quad . \quad (\mathrm{A}\,3)$$

Reference to Born and Huang (1954) shows that for a purely longitudinal mode with $q=0$ there is a macroscopic field $-4\pi\mathscr{P}$ to be taken into account. When this is done it is found that eqn. (A 1) still applies, but with each matrix element $C_{KK'}$ replaced by $C_{KK'}+4\pi e^2/v$. It follows that

$$(\omega_2{}^2\omega_3{}^2\ldots\omega_Q{}^2)_\mathrm{L} = \sum_{K=1}^{Q} \frac{m_K}{(m_1 m_2 \ldots m_Q)}\,\mathrm{Det}\,[\mathbf{N}] \quad . \quad . \quad (\mathrm{A}\,4)$$

where $\mathbf{N}$ is defined by (A 3), but with each $C_{KK'}$ replaced by $C_{KK'}+4\pi e^2/v$. As an abbreviation, write this as $C_{KK'}+b$, and consider the determinant

$$\mathrm{Det}\,\mathbf{N} = \begin{vmatrix} M_{11}+bZ_1{}^2 & M_{12}+bZ_1Z_2 \ldots\ldots\ldots\ldots \\ M_{21}+bZ_2Z_1 & M_{22}+bZ_2{}^2 \ldots\ldots\ldots\ldots \\ \ldots\ldots\ldots\ldots\ldots\ldots\ldots\ldots\ldots\ldots\ldots\ldots \\ \ldots\ldots\ldots\ldots\ldots\ldots\ldots\ldots\ldots\ldots\ldots\ldots & M_{QQ}+bZ_Q{}^2 \end{vmatrix}.$$

On multiplying out, it is found to be equal to

$$\mathrm{Det}\,\mathbf{M} + bZ_1 \begin{vmatrix} Z_1 & M_{12}\ldots\ldots \\ Z_2 & M_{22}\ldots\ldots \\ \ldots\ldots\ldots\ldots \\ Z_Q & M_{Q2}\ldots M_{QQ} \end{vmatrix} + bZ_2 \begin{vmatrix} M_{11} & Z_1\ldots\ldots \\ M_{21} & Z_2\ldots\ldots \\ \ldots\ldots\ldots\ldots \\ M_{Q1} & Z_Q\ldots\ldots M_{QQ} \end{vmatrix} + \ldots\ldots$$

which may be written as

$$\mathrm{Det}\,\mathbf{N} = (\mathrm{Det}\,\mathbf{M})(1 + b\,\mathbf{Z}_\mathrm{r}\,\mathbf{M}^{-1}\,\mathbf{Z}_\mathrm{c}).$$

The same relation is found to hold when principal minors of order $(Q-1)$ are involved. We suppose that in each case the principal minor is obtained by omitting the nth row and column, and that $[\mathbf{Z}_\mathrm{r}]$ for example represents $\mathbf{Z}_\mathrm{r}$ with Z_n omitted, so that

$$\mathrm{Det}\,[\mathbf{N}] = (\mathrm{Det}\,[\mathbf{M}])\left(1 + \frac{4\pi e^2}{v}\,[\mathbf{Z}_\mathrm{r}][\mathbf{M}]^{-1}[\mathbf{Z}_\mathrm{c}]\right).$$

Therefore from eqns. (A 1) and (A 4),

$$\frac{(\omega_2{}^2\ldots\omega_Q{}^2)_\mathrm{L}}{(\omega_2{}^2\ldots\omega_Q{}^2)_\mathrm{T}} = 1 + \frac{4\pi e^2}{v}\,[\mathbf{Z}_\mathrm{r}][\mathbf{M}]^{-1}[\mathbf{Z}_\mathrm{c}]. \quad . \quad . \quad . \quad (\mathrm{A}\,5)$$

We next consider the conditions for the equilibrium of each unit in an externally-applied static field E_A, with no depolarizing field. They are simply

$$eE_\mathrm{A}\,\mathbf{Z}_\mathrm{c} = \mathbf{M}\,\mathbf{U}_\mathrm{c}. \quad . \quad . \quad . \quad . \quad . \quad . \quad . \quad . \quad . \quad (\mathrm{A}\,6)$$

Now we take the origin to be the displaced position of core n, and write

$$eE_\mathrm{A}[\mathbf{Z}_\mathrm{c}] = [\mathbf{M}]\,[\mathbf{u}_\mathrm{c}{}^*]$$

where $u_K{}^* = U_K - U_n$, in the present notation. Now the polarization may be written

$$P = \frac{e}{v}\,[\mathbf{Z}_\mathrm{r}][\mathbf{u}_\mathrm{c}{}^*] = \frac{e^2E_\mathrm{A}}{v}\,[\mathbf{Z}_\mathrm{r}][\mathbf{M}]^{-1}[\mathbf{Z}_\mathrm{c}]. \quad . \quad . \quad . \quad (\mathrm{A}\,7)$$

(The obvious derivation, from (A 6) and the equation

$$P = \frac{e}{v}\,\mathbf{Z}_{\mathrm{r}}\,\mathbf{U}_{\mathrm{c}}$$

leads to the result

$$P = \frac{e^2 E_{\mathrm{A}}}{v}\,\mathbf{Z}_{\mathrm{r}}\,\mathbf{M}^{-1}\,\mathbf{Z}_{\mathrm{c}},$$

which is indeterminate since $\mathbf{M}$ is singular.)

From eqn. (A 7) and the definition of ϵ_{s} we have

$$\epsilon_{\mathrm{s}} = 1 + \frac{4\pi e^2}{v}\,[\mathbf{Z}_{\mathrm{r}}][\mathbf{M}]^{-1}[\mathbf{Z}_{\mathrm{c}}]$$

$$= \prod_{j=2}^{Q} \frac{(\omega_j^{\,2})_{\mathrm{L}}}{(\omega_j^{\,2})_{\mathrm{T}}}, \quad \text{from eqn. (A 5).}$$

The above derivation may now be repeated, with the frequency of the applied field taken to be in the range of visible light, that is, above a frequency involving resonance of the cores, but below any involving the shells. The cores do not then move or contribute to the polarization. The effect is the same as if the field were static, but the cores were clamped in position by the elements R_{11}, R_{22} . . . . R_{nn} all becoming infinite. The dielectric constant involved is then ϵ_{e}. A derivation similar to that given above then leads to

$$\epsilon_{\mathrm{e}} = \prod_{j=n+1}^{Q} \frac{(\omega_j^{\,2})_{\mathrm{L}}}{(\omega_j^{\,2})_{\mathrm{T}}}$$

and therefore finally

$$\frac{\epsilon_{\mathrm{s}}}{\epsilon_{\mathrm{e}}} = \prod_{j=2}^{n} \frac{(\omega_j^{\,2})_{\mathrm{L}}}{(\omega_j^{\,2})_{\mathrm{T}}}. \qquad \text{. . . . . (3.1)}$$

The weakness of the above derivation is that it involves electronic dispersion frequencies, ω_{n+1} to ω_Q. A shell model cannot be an adequate approximation in this frequency range, although it should be noted that these frequencies do not appear in the final result, which involves only the frequencies ω_2 to ω_n which are in the infra-red frequency range or lower. The same final result can be derived quite rigorously for a diagonally cubic crystal, or for a cubic crystal in which the atoms are not polarizable, so that $\epsilon_{\mathrm{e}} = 1$. There is therefore a strong presumption that the final result is independent of any particular model, as has been shown by Born and Huang (1954) to be the case when $n = 2$.

Corresponding results can be derived by the method given above for crystals of lower symmetry, always provided that there are directions for which the polarization of each mode is determined by crystal symmetry. For example, eqn. (3.1) applies to a tetragonal crystal whose space group is $P4/mmm$, provided that the frequencies correspond to modes whose displacement vectors are directed along the same axis, say the c-axis, while ϵ_{s} and ϵ_{e} also refer to this axis. This means that for the longitudinal modes, $\mathbf{q}$ is parallel to c, but for the transverse modes, $\mathbf{q}$ is perpendicular to c.

References

Aitken, A. C., 1939, *Determinants and Matrices* (Edinburgh: Oliver & Boyd)

Anderson, P. W., 1958, paper given at All-Union Conference on Dielectrics, Moscow.

Akao, H., and Sasaki, T., 1955, *J. chem. Phys.*, **23,** 2210.

Benedict, T. S., and Durand, J. L., 1958, *Phys. Rev.*, **109,** 1091.

Born, M., and Göppert-Mayer, M., 1933, *Handb. Phys.*, Vol. 24, 2nd edition, Chap. 4.

Born, M., and Huang, K., 1954, *Dynamical Theory of Crystal Lattices* (Oxford: University Press).

Brockhouse, B. N., and Iyengar, P. K., 1958, *Phys. Rev.*, **111,** 747.

Cochran, W., 1959 a, *Z. Kristallogr.*, **112,** 465; 1959 b, *Proc. roy. Soc.* A, **253,** 260; 1959 c, *Phys. Rev. Letters*, **3,** 412.

Cohen, M. H., 1951, *Phys. Rev.*, **84,** 369.

Devonshire, A. F., 1949, *Phil. Mag.*, **40,** 1040; 1951, *Ibid.*, **42,** 1065; 1954, *Advanc. Phys.*, **3,** 85.

Dick, B. G., and Overhauser, W., 1958, *Phys. Rev.*, **112,** 90.

Fröhlich, H., 1949, *Theory of Dielectrics* (Oxford: Clarendon Press).

Känzig, W., 1957, *Solid State Physics*, **4,** 1 (New York: Academic Press Inc.).

Kellermann, E. W., 1940, *Phil. Trans. roy. Soc.*, **238,** 513.

Last, J. T., 1957, *Phys. Rev.*, **105,** 1740.

Leibfried, G., 1955, *Encyclopaedia of Physics*, Vol. 7, Part I, edited by S. Flugge (Berlin: Springer-Verlag).

Megaw, H. D., 1952, *Acta Cryst.*, **5,** 739.

Mashkevich, V. S., and Tolpygo, K. B., 1957, *J. exp. theor. Phys., Moscow*, **32,** 520. (Translation: *Soviet Physics, JETP*, **5,** 435.)

Power, S. C., 1942, *Proc. Camb. phil. Soc.*, **38,** 62.

Roberts, S., 1949, *Phys. Rev.*, **76,** 1215.

Shirane, G., Danner, H., Pepinsky, R., 1957, *Phys. Rev.*, **105,** 856.

Shirane, G., Pepinsky, R., and Frazer, B. C., 1955, *Phys. Rev.*, **97,** 1179.

Slater, J. C., 1950, *Phys. Rev.*, **78,** 748.

Szigeti, B., 1949, *Trans. Faraday Soc.*, **45,** 155; 1950, *Proc. roy. Soc.* A, **204,** 52

Takagi, Y., 1953, *Proc. Int. Conf. Theor. Phys., Kyoto and Tokyo*, p. 824.

Thompson, J. H. C., 1953, *Phil. Mag.*, **44,** 131.

Woods, A. D. B., Cochran, W., and Brockhouse, B. N., 1960, *Phys. Rev.* (to be published).

The Statistical Model and Nuclear Level Densities

By Torleif Ericson†
Department of Physics and Laboratory of Nuclear Science,
Massachusetts Institute of Technology, Cambridge,
Massachusetts‡

CONTENTS

---

† On leave from Institute of Theoretical Physics, Lund, Sweden.

‡ Present address : CERN, Geneva, Switzerland. This work is supported in part through AEC Contract AT–(30–1)–2098 by funds provided by the U.S. Atomic Energy Commission, the Office of Naval Research and the Air Force Office of Scientific Research.

§ 1. Introduction

Nuclear reactions fall naturally into two principal classes, the fast reactions and the slow reactions, according to the time scale on which they occur. The fast reactions take place with typical reaction times of the order of the time it takes for the incident particle to pass the nucleus. The wavelength of the incident particle in nuclear matter is in most cases so short compared to nuclear dimensions that it must be expected to explore the individual constituents of the target nucleus. Its trajectory can in this approximation be considered as classical and it will only affect the nuclear matter in the immediate neighbourhood of this trajectory during the reaction time. A typical example of this type of reaction is the nucleon–nucleon collision, in which the incident particle collides with one of the nucleons in the target and ejects this nucleon. Because the incident particle does not interact with the nucleus as a whole but only with a small part of it, the emitted particle will take up an essential part of the momentum of the incident particle giving rise to typical angular distributions. Furthermore, because of the nearly negligible time difference in the emission process there will occur strong coherence and interference effects. These fast reactions, usually called direct interactions have been intensively studied in the last years and have been the subject of several articles of general nature (e.g. Austern 1959, Butler and Hittmair 1957, Kerman *et al.* 1959).

According to the above the typical time of a fast reaction process is $2R/v$ where R is the nuclear radius and v the velocity of the incident particle inside the nucleus. Expressed in some more convenient units it is thus about $\beta^{-1}A^{1/3}\,10^{-23}$ sec, where β is the velocity in units of c and A is the mass number.

The fast reactions may be considered as one extreme of our description of nuclear reactions. The other extreme is provided by the slow reactions. Instead of immediate emission of a particle after the initial interaction of the projectile, both the projectile and the particle with which it interacted can remain inside the nucleus and give rise to new interactions. Thus, by the subsequent scattering, the energy and momentum initially brought in will diffuse through the nucleus and eventually be transferred to the nucleus as a whole.

Obviously the emission of particles is possible during this entire process. After each interaction, however, the memory of the incident particle will be less; its energy and momentum will be split up between more particles. The angular distribution, though still preferentially forward peaked, will be less pronouncedly so. This intermediate stage in the nuclear reaction is probably the most commonly observed in practice; depending on its state of development it will have more or less of the fast characteristics. When finally the energy and momentum (as well as angular momentum) only characterize the system as a whole, and the memory of the initial mode of formation has been lost, we are dealing with the Compound Nucleus (N. Bohr 1936, N. Bohr and Kalckar 1937). This is the reaction we will

call slow. The reaction is then slow compared to the characteristic nuclear relaxation time for equilibrium due to the collisions between the nucleons.

The actual value of the relaxation time in the nucleus is not known; it can only be crudely estimated. A perturbation of nuclear matter will have a typical propagation velocity of the order of the average nucleon velocity inside the nucleus; the relaxation time may thus be expected to be of the order of one or two orders of magnitude longer than the time it would take an average nucleon to traverse the nucleus, i.e. about $A^{1/3} \times 10^{-21}$ to $A^{1/3} \times 10^{-20}$ sec. We must therefore expect decays taking place more rapidly than a time of this order to be partly characterized by the features of the fast reactions.

A typical feature of the emission from an equilibrium system is that it is entirely characterized by the constants of the motion of the system and its size and shape; it is completely independent of the details of its formation (N. Bohr 1936). The study of the emissions from such a system can therefore never shed any light on the exact mechanism which produced the equilibrium system in the first instance. This situation is very classical; it implies in particular that there are no phase relations between the formation and decay modes and that the decay of the Compound Nucleus is governed by phase space. There is thus an ergodic statement for this kind of a system, that every configuration will appear with equal weight. Two classical systems exhibit an extremely close analogy to the Compound Nucleus. These are the heated liquid drop from which particles evaporate, and the radiation from a black body (the analogy with the black body is only adequate for emission. The incident particle does not necessarily form an equilibrium system in all cases.) In both of these cases the emission is governed by the statistical characteristic of the system, the temperature, which determines the shape of the energy spectrum and the average energy of the emission. A particularly important feature is the low value of the temperature compared to the total excitation energy, which reflects the sharing of this energy among many degrees of freedom. This feature is also typical of the nuclear emission, which has relatively low kinetic energy in general compared to the total excitation energy.

There are, however, several important differences between classical systems and the nucleus. First, in the case of the classical system only a small fraction of the total excitation energy is carried away by the evaporation of one particle or the radiation of one photon. In the nuclear case, however, the system is essentially changed already by one particle emission; the emission of a secondary particle of the same kind becomes even energetically impossible in many cases. As a consequence it becomes important to distinguish in which system the nuclear 'temperature' is to be measured, in that of the intermediate system or in the residual nucleus after emission, a distinction of no consequence in the classical case. Secondly, a classical system has properties which are governed not by one quantum state but by a superposition of a large number of states, which are overlapping in energy. The nuclear system may or may not have this property.

The incident particle has mostly an energy spread which is many times larger than the spacing between the levels in the Compound Nucleus. The recurrence time for a wave packet with an energy spread much larger than the level spacing formed of the excited states is exactly $2\pi(h/D)$ for non-overlapping, equidistant levels of spacing D and should in general be of this order of magnitude. If the width of the levels is much smaller than the level distance, the lifetime is much longer than the recurrence time, and the assumption of independence of formation and decay modes will be fulfilled (Weisskopf 1950). The occurrence of this type of equilibrium system has no classical correspondence. It is typically met in neutron resonances and in the first few MEV of excitation above the neutron binding energy. With increasing excitation energy of the Compound Nucleus the lifetime becomes shorter and shorter as more and more decay channels become available. The levels become less defined and will start overlapping. It is then no longer possible to make any general statement about an equilibrium system based on the recurrence time. In this region different states will in general interfere and affect, for example, the angular distribution of the emitted particles. The incident beam will however average these effects over a region of energy even in the case of rather good experimental resolution and an additional average is often performed if transitions to the continuum region of levels in the residual nucleus are studied. The phases between the different transition amplitudes interfere ; due to the fluctuations in the energy range over which the averaging takes place there can then be a negligibly small contribution from cross terms as compared to diagonal terms when the square of the amplitude is averaged. The underlying approximation is that of random phases for the matrix elements. A more detailed discussion of the features of this approximation is given in § 11. In this sense an equilibrium system can again be achieved. This system is completely analogous to the classical liquid drop and radiating black body. The two classical examples show clearly that equilibrium systems can exist in the region of overlapping levels.

Experimentally few attempts have been made to establish the existence of a nuclear equilibrium state (Ghoshal 1950 ; John 1956, Kelly 1950). The classical results of Ghoshal based on a study of the excitation functions for the products of ^{64}Zn formed by α-particles incident on ^{60}Ni and protons on ^{63}Cu are shown in fig. 1. If an equilibrium system has been formed the relative yield of the different products should be the same for a compound system of the same excitation energy, independently of how the system was excited. The qualitative aspects of the curves show indeed such a behaviour, when the curves are compared as a function of excitation energy. There is however a slight discrepancy of unknown origin. The best agreement is obtained if the excitation energy for the proton induced reaction is allowed to be about 1·6 MEV higher than that corresponding to the α-induced reaction, when the experimental Q-value is used. The excitation function experiments show that there is not a strong difference between the decay ratios of the two reactions.

A considerably more stringent test of the independence hypothesis should be provided by the shape of the energy spectra of particles, which are emitted from the same Compound System formed in different ways. These energy spectra should have shapes which are independent of the mode of formation, at least in so far as no restrictions on the decay are imposed by angular momentum conservation. In this case it should also be possible to compare the probability of direct interaction to Compound Nucleus processes†.

Fig. 1

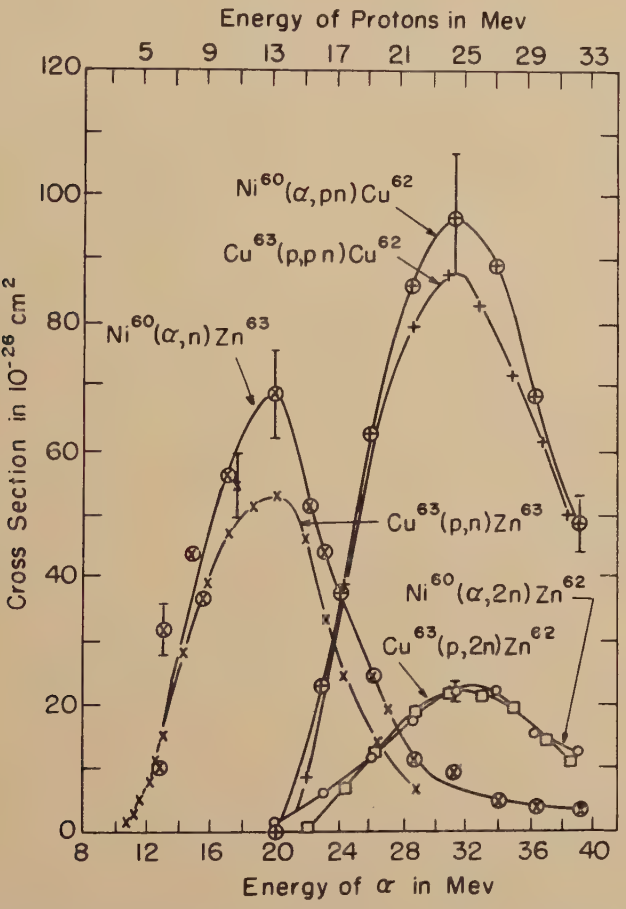

Experimental cross sections for (p, n), $(p, 2n)$ and (p, pn) reactions on ^{63}Cu and for (α, n), $(\alpha, 2n)$ and (α, pn) on ^{60}Ni plotted against E_p and E_α respectively. The same Compound Nucleus, ^{64}Zn, may be formed in both cases. The scale of E_p has been shifted 7 Mev with respect to E_α. After Ghoshal (1950).

† The energy spectra of α–particles emitted from the Compound System ^{60}Ni formed by the reactions Fe (α, α') Fe (Lassen) and ^{59}Co (p, α) ^{56}Fe (Brady and Sherr 1960) have the same shape within the experimental uncertainty. We are indebted to Professor R. Sherr and Dr. N. O. Lassen for privately communicating these unpublished results.

When the excitation energy is increased even further the lifetime of the Compound System will ultimately be shorter than the nuclear relaxation time. It is then no longer possible to treat formation and decay mode separately; the reaction must in this limit always be considered to be fast. When such excitation energies have been reached the concept of slow reactions is no longer useful. It is thus always necessary to compare the lifetime of the Compound Nucleus, which can be calculated, to the relaxation time in order to determine if the conditions for an equilibrium system are fulfilled.

The description of a nuclear reaction in terms of the decay of an equilibrium system of long lifetime in which phase relations can be neglected is called the 'Statistical Model' (Weisskopf 1937, Weisskopf and Ewing 1940). It is the purpose of this article to examine and discuss different aspects of this model and its predictions, as well as some related properties of the excited nucleus. The most obvious importance of the statistical model is that it provides the opposite extreme limit to the direct interactions. As an asymptotic limit it should be studied in complete detail so that its predictions are precisely known and deviations can easily be established. It has long been recognized that the statistical theory qualitatively predicts the major part of nuclear reaction cross sections. The reason for this is mainly that the decay of an equilibrium system is governed by the available phase space. Quantitatively its predictions have not been much studied and its usefulness in that respect is still largely unknown.

The purpose of the present article is to present a treatment of the different aspects of the Statistical Model and nuclear level densities from a theoretical point of view. As a consequence we will not refer to experimental material unless this has an immediate bearing on the theoretical discussion. Our aim is thus not to give the best sets of parameters which presently describe the experiments, but rather to expose the connection of these parameters to other nuclear properties and to achieve an understanding of the general features of the model and its consequences.

§ 2. General Features of Nuclear Level Densities

Almost any reaction has a tendency to produce a result that depends on the phase space available after the reaction. In the case of an equilibrium system the loss of memory of the formation mode leads to a decay which, as discussed in §§ 4 and 5, is governed entirely by phase space. A dominating part in the phase space in a nuclear reaction is played by the density of levels in the residual nucleus. Before proceeding further we will therefore discuss the general properties which are known or expected of nuclear level densities and review the present theoretical situation.

The outstanding experimental feature of nuclear level densities is their extremely rapid increase with excitation energy. It is well known that typical spacings between the first excited states above the ground state in medium weight and heavy elements are of the order of a tenth or some

tenths of MEV. When the excitation energy is increased into the MEV region it is also well known that the complexity of the nuclear spectra becomes greatly increased and that the spacing between the levels is considerably decreased compared to that near the ground state. Studies of medium weight elements, where the individual states still can be resolved for several MEV show that this decrease with energy quickly attains orders of magnitudes. Indeed the decrease in spacings has the characteristics of an approximately exponential decrease or a decrease inversely proportional to a rather high power of the excitation energy. Again this same fact is demonstrated by the spacings of the neutron resonances usually observed at excitation energies of 6–8 MEV. In spite of the fact that only a small fraction of the total number of states can be excited by s-wave neutrons, due to angular momentum and parity selection rules, the spacings are extremely small compared to the spacings near ground state. In the region of heavy elements the resonances are spaced about four to five orders of magnitude closer than the levels at low excitation, corresponding to up

Fig. 2

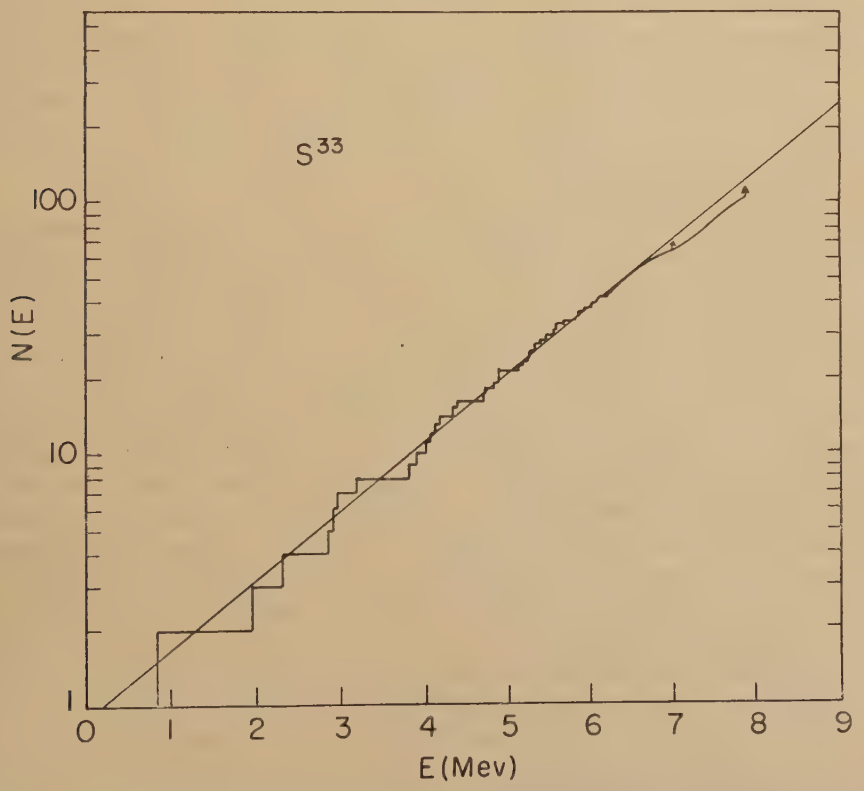

The total number of states up to excitation energy E, $N(E)$, vs. E for ^{33}S. The arrows indicate estimated number of unresolved levels. After Ericson (1959).

to millions of levels per MeV. This again proves that the level density must have an essentially exponential increase with excitation energy. It is therefore natural to study it on a logarithmic scale. As an illustration of this rapid increase of the number of states we have plotted the total number of states $N(E)$ as a function of the excitation energy E for ^{33}S, which is such a light element that the individual states are known to quite high excitation (fig. 2, Ericson 1959). The dense spacing of the levels in the highly excited nucleus has also been verified directly by other means as, for example, by proton resonances.

The comparison between the spacings of highly excited nuclear levels in neutron resonances at the same excitation energy has furthermore revealed that the level density is strongly influenced by nuclear shell structure. The density of resonances for magic or nearly magic nuclei is thus one to three orders of magnitude smaller than between the shells at the same excitation energy. The more detailed analysis of this effect indicates rather strongly that it is related to the larger low energy single particle spacings in the magic nuclei rather than to a shift of the entire energy scale of the excited nucleus (Newton 1956 a, Cameron 1958 a, Ericson 1958 b, El Nadi and Wafik 1959). A clear-cut demonstration of this is however still lacking. Thus there is a strong probability that the nucleus even at 6–8 MeV retains some of the basic properties of its spectrum at low excitation. It is not known to what energies shell effects still will play an important role; it might be expected that their influence will disappear slowly with increasing excitation (Rosenzweig 1957 b, Ericson 1958 b).

The striking difference in the low-energy spectra of odd and even nuclei has been known for a long time. While the odd nuclei show a number of states which often can be identified with shell model configurations, the neighbouring even nuclei have practically no states in the same region of excitation, and the few observed states can be associated with collective excitations of the nucleus, rotations and vibrations (A. Bohr and Mottelson 1953). This state of affairs remains to an energy of about 1 MeV in a heavy nucleus. At this energy the spectrum of the even nucleus rapidly becomes complex and a number of states appear. The region of energy in the even nucleus in which only the collective excitations appear is called the nuclear energy gap; its existence is associated with the existence of pairing correlations in the nucleus (A. Bohr *et al.* 1958). The sudden appearance of many states just above the gap can thus naively be regarded as the ' breaking of a pair '; the large number of states is then a consequence of the many different ways into which the unpaired particles can be rearranged. The difference in the spectra of odd and even nuclei is not only confined to the region near the nuclear ground state. It can be inferred from the spacings of neutron resonances. A direct demonstration is most easily obtained by a direct comparison of the number of levels as a function of excitation energy for neighbouring nuclei of odd and even character. Figure 3 demonstrates this quantity for odd, odd mass, and even nuclei in the iron region (Ericson 1959). The odd–even effect seems mainly to cause a shift of the effective excitation energy between the odd

and even nuclei. The magnitude of this shift is close to the value of the pairing energy as determined from nuclear binding energies in this region.

Fig. 3

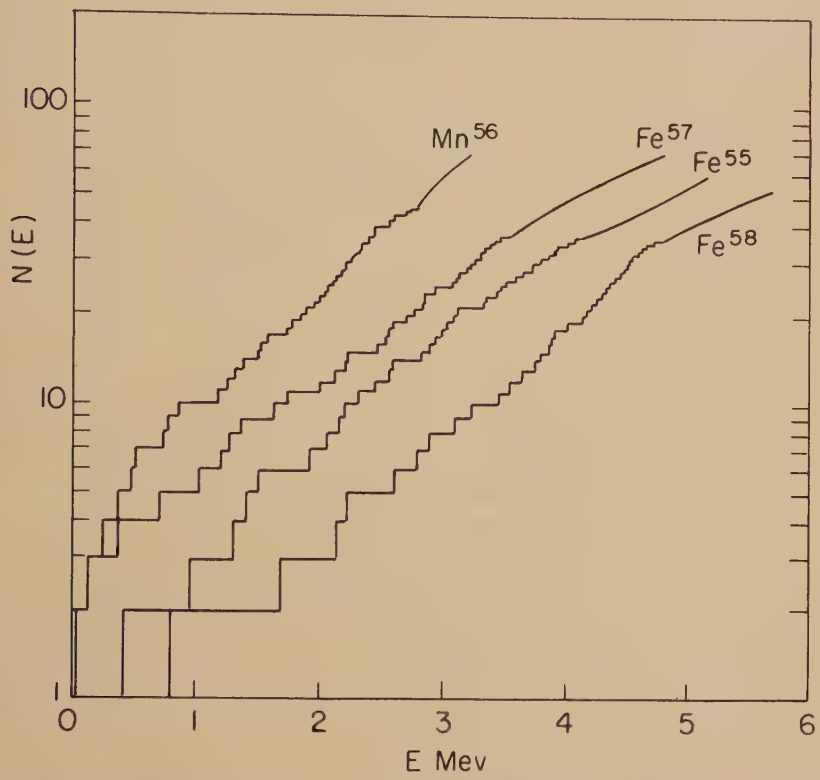

The total number of states up to excitation energy E for ^{56}Mn, ^{55}Fe, ^{57}Fe and ^{58}Fe vs. E. The experimental resolution is somewhat higher in the case of ^{56}Mn than for the rest. The figure compares the total number of states for odd, odd mass and even nuclei. After Ericson (1959).

In view of the dependence of the level density on shell structure and the appearance of the odd–even effect we must conclude that the average spectrum of the excited nucleus still retains some individual behaviour characteristic of the particular nucleus studied and that such features are not entirely averaged away. Besides the features of the nuclear level densities as discussed above there exists additional information on the distribution of spins in the excited nucleus and on the detailed variation of the level density with energy. These properties are however as yet not as well explored as the ones discussed. Further experimental data on the dependence of the level density on spin and energy are highly desirable.

It must be required of any satisfactory theoretical description of nuclear level densities that it can explain and reproduce the basic features as discussed above. In order to assure a common description of the nucleus near its ground state and at high excitation it is tempting to try to apply

models which have proved their usefulness for low energy phenomena, to the excited nucleus. We will shortly see that the experiments do not permit too much leeway in the choice of a basis for the description. Near its ground state the nucleus has most of the properties of a system of independent Fermions, though the residual interactions manifesting themselves, e.g. in the collective excitations, are far from negligible. The great success of the shell model (Mayer and Jensen 1955) strongly demonstrates the validity of this picture. Compared, for example, to the shell model, we can immediately conclude from the experimentally known rapid increase of the level density with energy, that it is not possible to describe the highly excited levels as one-particle levels; the spacing of such levels would remain essentially constant. It is rather characteristic of the excitation of several nucleons simultaneously so that the excitation energy no longer is concentrated on one single nucleon. The larger complexity of the resulting spectrum is thus due to the many different ways into which the given excitation energy can be distributed among several excited nucleons. It is easy to convince oneself on the basis of a very simple model which can be solved exactly, that this indeed gives a very rapid increase of the number of states with energy. Consider a sea of only one kind of independent Fermions, and let the Fermions have one-particle levels which are equally spaced with a spacing d. The excited states of this system will thus always appear at multiples of d, sd, and will in general be degenerate. At excitation energy 0 we have one state only, the ground state, at energy d we have also one state produced by exciting the particle in the highest state, at energy $2d$ there are two states, one produced by exciting the particle in the highest state two steps and one by producing a hole by exciting the particle in the next highest state two steps, at energy $3d$ there are four states and so on. In fig. 4 we show a typical configuration of such a system and in fig. 5 we show the number of states at excitation sd as a function of sd. The exact solution of this problem was obtained and tabulated by Euler (1753) by the use of recursion formulas.

We thus see that the rapid increase of the number of states with energy is basically only a result of the additivity or quasi-additivity of the energies of the Fermion states. In general we should expect it to be a feature of any system which on the average can be described by degrees of freedom, 'elementary excitations', which have additive energies. It is of course not necessary for the states, as in our simple model, to appear as highly degenerate states at specific energies. The residual interactions due to the part of the Hamiltonian not described by a simple shell model potential will not change the shell model character of the states very strongly at low excitation energy because of their large spacing. They will, however, profoundly change the character of the highly excited states, which have small spacings. They will remove degeneracies which are not due to exact quantum numbers, and they will lead to the occurrence of very mixed wave functions. In this spirit it is not appropriate to ask about a single excited state, if it can be represented on the basis of a certain nuclear model. It is only possible to ask such questions about the average

Fig. 4

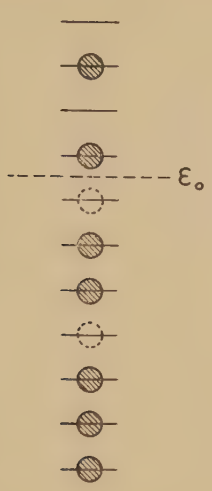

Typical excited configuration for an equidistantly spaced Fermi system of one kind of particles. Two particles are excited, two holes have been created; the excitation is $7d$.

Fig. 5

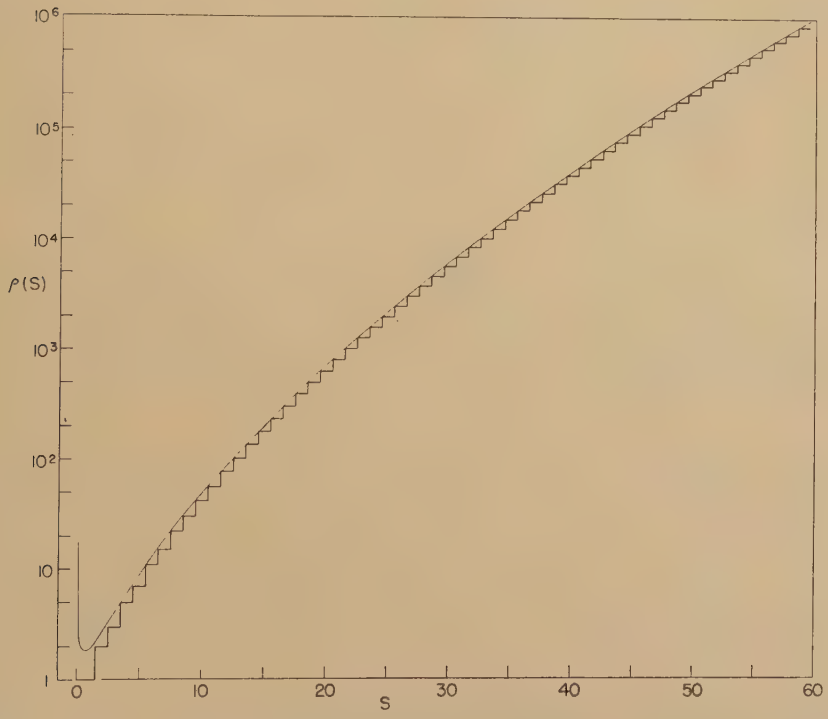

The exact level density per unit single particle spacing $\rho(s)$ for a Fermi system of one kind of particles with equidistant single particle levels vs. excitation energy s in units of this spacing. The solid smooth curve is the approximate solution (3.12), based on the continuous approximation and the saddle point method.

properties of the level density, such as the number of states per unit energy, distribution of spin-values, etc. It should be noted, however, that the residual interactions never create or destroy energy levels; it is therefore possible for the interactions to have a small average effect.

The existence of a correlation between the shell model single particle spacing and the spacing of neutron resonances suggests strongly that the appropriate model for the description of the excited nucleus must be intimately related to the ordinary shell model. On the other hand, the existence of the odd–even effect also shows that it is necessary to go beyond the very simplest shell model aspect. The detailed attempts of descriptions which take such features into account will be discussed in the next section.

In the sense we have outlined above the problem of calculation of nuclear level densities is essentially a combinatorial problem, or in other words, statistical mechanics. The analogy with statistical mechanics is so complete that a large part of the vocabulary about level densities has been directly taken over from thermodynamics. There is, however, a fundamental difference. The nuclear system has at low excitation energy, in the region below 10–15 MeV, a very small number of excited particles. On the other hand, the usual results of statistical mechanics apply to large systems, where the number of excited particles can be regarded as large even at 'low' excitation energy, and the results actually represent asymptotic expressions. As a typical example, the concept of temperature cannot be defined with greater accuracy than the spacing between the states, and is thus not completely well defined in the nuclear case. We must therefore re-examine the statistical approach to see at what points greater exactitude is required, and to what extent the analogy permits us to make general statements. We want to emphasize that the thermodynamic analogy is extremely useful for many qualitative arguments (cf. § 4) if used judicially.

Suppose we are dealing with a system of eigen-values E_1, E_2, ..., E_i, ... corresponding to a Hamiltonian $\mathscr{H}$. We will entirely neglect the width of the states, an approximation that is extremely good up to energies slightly above the neutron binding energy and which for higher excitation energies should have little influence on the average spectrum. We define a partition function $Z(\beta)$ by

$$Z(\beta) = \sum_i e^{-\beta E_i} = \mathrm{Tr}\, e^{-\beta \mathscr{H}}. \qquad (2.1)$$

The level density $\rho(E)$ can be represented as a sum of Dirac delta functions, one for each nuclear state,

$$\rho(E) = \sum_i \delta(E - E_i) = \mathrm{Tr}\, \delta(E - \mathscr{H}), \qquad (2.2)$$

which averaged over an energy interval containing many states will agree with the usual notion of the level density as a smoothly varying function. Equation (2.1) can be expressed in terms of the level density of eqn. (2.2) as

$$Z(\beta) = \int_0^\infty \rho(E)\, e^{-\beta E}\, dE. \qquad (2.3)$$

A formal expression for the level density can therefore immediately be expressed by the Laplace transform of the partition function:

$$\frac{1}{2\pi i}\int_{-i\infty}^{i\infty} Z(\beta)\, e^{\beta E}\, d\beta = \mathrm{Tr}\,\frac{1}{2\pi i}\int_{-i\infty}^{i\infty} e^{\beta(E-\mathscr{H})}\, d\beta = \mathrm{Tr}\,\delta(E-\mathscr{H}) = \rho(E). \quad (2.4)$$

A knowledge of the partition function is thus equivalent to a knowledge of the level density. Equation (2.4) can be largely simplified by applying the method of steepest descent to the evaluation of the Laplace transform†. The integrand of (2.4) has a minimum for β_0 determined by

$$-\frac{d}{d\beta_0}\ln Z(\beta_0) = E \quad . \quad . \quad . \quad . \quad . \quad . \quad (2.5)$$

and the level density is then approximately

$$\rho(E) = \frac{\exp\{\ln Z(\beta_0) + \beta_0 E\}}{\left(2\pi \dfrac{d^2 \ln Z(\beta_0)}{d\beta_0{}^2}\right)^{1/2}}. \quad . \quad . \quad . \quad . \quad . \quad (2.6)$$

The quantity which enters in the exponent of eqn. (2.6) is the entropy S of the system as defined in statistical mechanics

$$S = \ln Z(\beta_0) + \beta_0 E. \quad . \quad . \quad . \quad . \quad . \quad . \quad (2.7)$$

The value of β at the minimum is in statistical mechanics identified with the inverse of the temperature t of the system

$$t = \beta_0{}^{-1}. \quad . \quad . \quad . \quad . \quad . \quad . \quad . \quad . \quad (2.8)$$

The usual relation between entropy and energy will thus be valid:

$$\frac{dS}{dE} = \frac{d}{dE}\left[\ln Z(\beta_0) + \beta_0 E\right] = \frac{d\beta_0}{dE}\frac{d}{d\beta_0}\ln Z(\beta_0) + \beta_0 + E\frac{d\beta_0}{dE} = \beta_0 = \frac{1}{t}, \quad (2.9)$$

using the definition (2.7) of the entropy and eqn. (2.5). We can therefore express the level density of eqn. (2.6) completely generally as

$$\rho(E) = \frac{e^S}{\left(-2\pi \dfrac{dE}{d\beta_0}\right)^{1/2}}. \quad . \quad . \quad . \quad . \quad . \quad (2.10)$$

We notice that the level density in this approximation has become a smooth function, and that it therefore has been averaged by the application of the method of steepest descent. The region over which this average takes place is determined by the width η of the saddle point

$$\eta^{-1} = \sqrt{\left(-\frac{dE}{d\beta_0}\right)}. \quad . \quad . \quad . \quad . \quad . \quad . \quad (2.11)$$

The average is determined by the ordinary weighting factors of statistical mechanics. The averaging procedure implies in particular that minor fluctuations and variations of the level density cannot be described in this approximation.

In statistical mechanics it is usual to neglect the variation of the denominator of eqn. (2.10) as a function of energy compared to the much more

† For a simple discussion of the saddle point method see Morse and Feshbach (1953) p. 437.

rapid variation of the exponent. This is an approximation that should be good as long as the excitation energy is much larger than the temperature. This procedure is not very satisfactory in the nuclear case; the nuclear temperature is not negligible compared to the excitation energy at most excitations. The inclusion of the denominator in (2.10) is also necessary in order to study the value of the level density. We therefore conclude that while thermodynamics may provide guidance for the behaviour of the level density, especially at high excitations, deviations must be expected at low excitations. It is, however, convenient to use the language of thermodynamics; we will thus refer to the natural logarithm of the average level density as the 'nuclear entropy' and let its derivative with respect to the energy define the 'nuclear temperature' T.

$$\frac{1}{T} = \frac{d}{dE} \ln \rho(E). \qquad (2.12)$$

We point out that it is possible to associate several different temperatures to the nucleus at the same excitation energy. The definition (2.12) or the entire technique involving the method of steepest descent could equally well have been applied to a set of levels in the nucleus having a special property such as given parity or angular momentum; each such class of states will have a temperature, in general different from that of the other classes. These temperatures will tend to the same value at high excitations.

As in statistical mechanics it is advantageous to consider the grand partition function instead of the simple partition function (2.1). Instead of considering only the set of states characterized by given values of some quantum numbers M_k, we consider all states of all possible values of M_k simultaneously. The quantum numbers M_k may in particular be the number of neutrons N or protons Z in the nucleus or the projection of the total angular momentum on the z-axis. We will for simplicity consider, only one quantum number, N, which may be the neutron number. The nuclear states characterized by N are the $E_i(N)$. The grand partition function is defined as

$$Z(\beta, \alpha) = \sum_{i,\nu} \exp\{\alpha\nu - \beta E_i(\nu)\} \qquad (2.13)$$

with a corresponding level density

$$\rho(E, N) = \sum_{i,\nu} \delta(\nu - N)\, \delta(E - E_i(\nu)). \qquad (2.14)$$

The level density is again the Laplace transform of the partition function

$$\rho(E, N) = \frac{1}{(2\pi i)^2} \int_{-i\infty}^{i\infty} \int_{-i\infty}^{i\infty} Z(\beta, \alpha)\, e^{\beta E - \alpha N}\, d\beta\, d\alpha. \qquad (2.15)$$

By application of the method of steepest descent to this integral we obtain the approximate expression for the level density

$$\rho(E, N) = \frac{\exp\{\ln Z(\beta_0, \alpha_0) + \beta_0 E - \alpha_0 N\}}{2\pi(-\det A)^{1/2}}. \qquad (2.16)$$

The saddle point β_0, α_0, is determined again by the condition that the integrand is minimum:

$$\left.\begin{aligned} E + \frac{\partial}{\partial \beta_0} \ln Z(\beta_0, \alpha_0) = 0, \\ N - \frac{\partial}{\partial \alpha_0} \ln Z(\beta_0, \alpha_0) = 0, \end{aligned}\right\} \quad . \quad . \quad . \quad . \quad (2.17)$$

and

$$\det A = \begin{vmatrix} \dfrac{\partial^2 \ln Z(\beta_0, \alpha_0)}{\partial^2 \beta_0}, & \dfrac{\partial^2 \ln Z(\beta_0, \alpha_0)}{\partial \beta_0 \partial \alpha_0}, \\ \dfrac{\partial^2 \ln Z(\beta_0, \alpha_0)}{\partial \alpha_0 \partial \beta_0}, & \dfrac{\partial^2 \ln Z(\beta_0, \alpha_0)}{\partial {\alpha_0}^2}. \end{vmatrix} \quad . \quad . \quad (2.18)$$

The parameter α_0 is conveniently expressed by the chemical potential μ defined as

$$\alpha_0 = \beta_0 \mu. \quad . \quad . \quad . \quad . \quad . \quad . \quad . \quad . \quad (2.19)$$

We notice that the level density $\rho(E, N)$ of eqn. (2.16) is a continuous variable of both E and N in this approximation, so that an averaging procedure in both E and N has been performed.

In the preceding paragraphs we have established in a rather detailed way the strong correspondence between the techniques of statistical mechanics and those of the theory of nuclear level density. In particular we have seen that a knowledge of the partition function is equivalent to a complete knowledge of the level density. On the other hand, it must be emphasized that the equivalence of the formalism does not *per se* characterize the nuclear level density. In the establishing of the preceding relations no physical assumption entered regarding the system; the levels of the system were completely arbitrary. In particular it is not possible to make statements like "the nuclear temperature is an increasing function of energy"; indeed it is not difficult to suggest a model of the nucleus bearing a strong resemblance to the shell model for which the nuclear temperature as defined in eqn. (2.12) will even become negative in a certain energy interval†.

Additional information about the physical nature of the system, has therefore to be introduced in order to make any theoretical conclusion about the behaviour of the level density. The most satisfactory procedure for the calculation would be to start directly from the nucleon–nucleon interactions. Few attempts have been made in this direction (Bardeen and Feenberg 1938, Bloch 1954) due to the complexity of the finite many-body problem. Some recent treatments of the many-body problem

† It is of course possible to obtain a temperature in complete analogy to statistical mechanics if the level density is known as a function of energy. The partition function is determined as a function of β from eqn. (2.3). The temperature can then be determined as a function of E by eqn. (2.5). This definition is not so useful in nuclear physics due to an insufficient experimental knowledge of the level density and also because the level density itself is the quantity of primary interest.

using statistical analogies indicate that progress may be made along these lines (Bloch and de Dominics 1958, 1959, Martin and Schwinger 1959). The ordinary procedure is therefore instead to make use of known properties of the nucelus at low excitation, and to extend the low energy picture to higher excitation. In particular, as we discussed in the beginning of this section, both the experimental level densities and the success of the shell model indicate that the nucleons to a first approximation should be regarded as moving independently in an average potential. In the next section we will discuss the application of these ideas to specific models for the level density.

§ 3. Models for Nuclear Level Densities

In the beginning of the preceding section we found that the variation of the level density with energy is that typical of a system which has a large number of degrees of freedom. As a consequence the models for the description of the nuclear level densities mostly picture the nucleus as a gas of Fermions which have a quasi-additive spectrum. Thus the nucleus has been considered as a system of free neutrons and protons confined to the nuclear volume (Bethe 1936, 1937, v. Lier and Uhlenbeck 1937, Lang and Le Couteur 1954, Rosenzweig 1957 a), as nucleons moving in a shell model potential (Bloch 1954, Newton 1956 a, Cameron 1958 a, Rosenzweig 1957 b, Ross 1957, Ericson 1958 b) and as nucleons with residual pairing interactions in a deformed well potential (Ericson 1958 a, b; Strutinski 1959, Lang and Le Couteur 1960). In all of these cases it is possible to express these models in terms of elementary excitations of a Fermion system. The philosophy of these approaches is to replace the complicated nucleon–nucleon interactions by an average potential; this is a reasonable procedure, particularly as we are only interested in the average validity of such a picture. In view of this it is necessary to develop general methods for the theoretical study of the level density of such systems. We will not go into detailed aspects of these considerations which necessarily are of a rather mathematical nature, but refer the reader to the literature (Bloch 1954, Ericson 1958 b).

In so far as we need general methods, we will arbitrarily choose the formalism of the latter reference.

In general a system of independent Fermions will have one-Fermion levels ϵ_1, ϵ_2, $-$, $-$, ϵ_s, $-$, $-$. A configuration of the Fermion system is characterized by the occupation numbers n_s of these states, and these occupation numbers can only take values 0 and 1 because of the exclusion principle. Thus, the total number of Fermions N and the energy of the system E are given by

$$\left.\begin{aligned} \textstyle\sum_s n_s &= N, \\ \textstyle\sum_s n_s \epsilon_s &= E. \end{aligned}\right\} \quad \ldots\ldots\ldots \quad (3.1)$$

We can associate a single particle level density $g(\epsilon)$ with the set of states ϵ_s

$$g(\epsilon) = \textstyle\sum_s \delta(\epsilon - \epsilon_s) \quad \ldots\ldots\ldots \quad (3.2)$$

similarly to eqn. (2.2). Furthermore the grand partition function (2.13) expressed with eqn. (3.1) becomes

$$Z(\beta,\alpha)=\sum_{\text{all } n_s}\exp-\{\beta\sum_s n_s\epsilon_s-\alpha\sum_s n_s\}=\Pi_s(1+e^{\alpha-\beta\epsilon_s}). \qquad (3.3)$$

Taking the natural logarithm of eqn. (3.3) we then use eqn. (3.2) to write the result as an integral

$$\ln Z(\beta,\alpha)=\sum_s\ln(1+e^{\alpha-\beta\epsilon_s})=\int_0^\infty g(\epsilon)\ln(1+e^{\alpha-\beta\epsilon})\,d\epsilon. \quad . \quad . \quad (3.4)$$

In the ground state all the one-Fermion levels ϵ_1, ϵ_2, $-$, $-$, ϵ_N are filled; the rest are empty. We define the Fermi energy ϵ_0 to be

$$\frac{\epsilon_N+\epsilon_{N+1}}{2}$$

and can then use eqn. (3.2) to write

$$\int_0^{\epsilon_0} g(\epsilon)\,d\epsilon=N\,; \quad \int_0^{\epsilon_0}\epsilon g(\epsilon)\,d\epsilon=E_0 \quad . \quad . \quad . \quad . \quad (3.5)$$

where E_0 is the ground state energy. The integral in eqn. (3.4) can now be identically re-expressed by splitting it into two parts, one from 0 to $\mu=\alpha/\beta$ and one from μ to ∞:

$$\begin{aligned}\ln Z(\alpha,\beta)&=\int_0^\infty\{g(\mu+\epsilon)+g(\mu-\epsilon)\}\ln(1+e^{-\beta\epsilon})\,d\epsilon+\beta\int_0^\mu g(\epsilon)(\mu-\epsilon)\,d\epsilon\\&=-\beta E_0+\alpha N+\int_0^\infty\{g(\mu+\epsilon)+g(\mu-\epsilon)\}\ln(1+e^{-\beta\epsilon})\,d\epsilon\\&\quad+\beta\int_{\epsilon_0}^\mu g(\epsilon)\,(\mu-\epsilon)\,d\epsilon. \quad . \quad . \quad . \quad . \quad . \quad . \quad . \quad . \quad . \quad (3.6)\end{aligned}$$

We observe in doing this transformation that $g(\epsilon)=0$ for $\epsilon<0$ according to the definition (3.2). In eqn. (3.6) we have achieved a form of the partition function which explicitly displays the dependence on the number of Fermions in the system, which thus may be eliminated (cf. Ericson 1958 b). The nuclear Fermi system is highly degenerate. The great majority of the configurations corresponds to partitions in which the available energy is split up among several excited Fermions which each carry a rather small amount of excitation energy and the actual finiteness of the nuclear well depth is irrelevant. At very high excitation energies the average energy per excited nucleon becomes a sizeable fraction of the depth of the potential and it is no longer possible to treat the nucleus as degenerate. The special effects which then occur have been discussed by v. Lier and Uhlenbeck (1937) and Rosenzweig (1957 a). Important deviations from the features of the degenerate system should not occur until the excitation energy reaches values of several hundreds of MeV. At those energies questions of the self-consistency of the approach will constitute a more serious problem and we will therefore not treat this point. As a consequence of this it is only necessary to describe the single particle level density $g(\epsilon)$ accurately in a rather small region around the Fermi energy ϵ_0. For regions ϵ which are outside the neighbourhood of the Fermi energy we can describe $g(\epsilon)$ in a rather arbitrary way without affecting the result, and the most convenient one is usually used.

3.1. *The Equidistant Spacing Model*

A very simple model, which at the same time is the prototype for the behaviour of several Fermi gas models, is that in which the one-Fermion levels all are equidistant with a spacing d (Bethe 1936). The one-Fermion states are thus d, $2d$, $-$, sd, $-$. To evaluate the corresponding partition function we make the *continuous* approximation for the density function.

$$g(\epsilon) = g_0 = d^{-1}. \qquad (3.7)$$

We have justified this approximation even in the region of $\epsilon < 0$ by the arguments of the preceding page.

The evaluation of the partition function is now immediate.

$$\ln Z(\beta, \alpha) = -\beta E_0 + \alpha N + 2\frac{\pi^2}{12} g_0 \beta^{-1} + \frac{\beta g_0}{2}(\mu - \epsilon_0)^2. \qquad (3.8)$$

We introduce the excitation energy of the system

$$U = E - E_0 \qquad (3.9)$$

and proceed according to eqns. (2.16)–(2.18) to evaluate the level density by the method of steepest descent from eqn. (3.8). We obtain the relations

$$\mu = \epsilon_0,$$

$$U - \frac{\pi^2}{6} g_0 \beta^{-2} - \frac{g_0}{2}(\mu^2 - \epsilon_0^2) = 0, \qquad (3.10)$$

so that

$$U = \frac{\pi^2}{6} g_0 \beta^{-2} = \frac{\pi^2}{6} g_0 t^2, \qquad (3.11)$$

where t corresponds to the thermodynamic temperature. The level density is given by the expression

$$\rho(U) = \frac{e^{2\left(\frac{\pi^2}{6} g_0 U\right)^{1/2}}}{\sqrt{(48)}\, U}. \qquad (3.12)$$

The corresponding problem when there are two Fermion systems (neutrons and protons) can be solved analogously. If the equidistant spacings are d_n and d_p, the average total single Fermion density g_0 is

$$g_0 = {d_n}^{-1} + {d_p}^{-1} = g_n + g_p. \qquad (3.13)$$

The excitation energy is

$$U = \frac{\pi^2}{6} g_0 t^2 \qquad (3.14)$$

and the level density is

$$\rho(U) = g_0 \left(\frac{{g_0}^2}{4 g_n g_p}\right)^{1/2} \frac{6^{1/4}}{12} \frac{e^{2\left(\frac{\pi^2}{6} g_0 U\right)^{1/2}}}{(g_0 U)^{5/4}}. \qquad (3.15)$$

It should be noted that ${g_0}^2/4 g_n g_p$ usually is close to unity.

In this approximation the equidistant spacing model thus gives a remarkably simple expression for the level density. At high excitation the exponential factor in eqns. (3.12) and (3.15) is dominating. This has led to the commonly found statement that level densities should vary with energy as $\exp 2(aU)^{1/2}$, where a is a constant. According to the above it must be emphasized that this statement is valid only for high excitations and for a model similar to the one considered, i.e. with a fairly well-defined average single Fermion spacing near the Fermi levels. At low excitation

and for systems which have anomalies in the spacing near the Fermi energy deviations are to be expected.

It is interesting to compare the approximate solution (3.12) to the exact solution of the same model, a problem solved in a different context by Euler (1753). Figure 5 shows the remarkable agreement even down to the lowest energies. For excitation energies of the order $U \simeq d$ the approximate solution is no longer valid, which might have been anticipated as the temperature concept has little meaning for excitation energies smaller than the single Fermion spacing. Lang and Le Couteur (1954) have improved the analytical expressions for the level density for this model, so that a finite result is obtained as U goes to zero. The experimental accuracy and the approximation of equidistant levels do not seem to necessitate higher accuracy than that implied by the simple expressions of eqns. (3.12) and (3.15), if it is kept in mind that they are valid only for $U > g_0^{-1}$.

Similarly as in statistical mechanics, it is useful to introduce the average occupation numbers, $\bar{n}_s$, corresponding to the configurations of eqn. (3.1),

$$\bar{n}_s = \frac{1}{1+\exp\beta(\epsilon_s-\mu)}. \quad . \quad . \quad . \quad . \quad . \quad (3.16)$$

For the simple model we have discussed we therefore have immediately that the average number of excited degrees of freedom, i.e. excited nucleons and their corresponding holes, is

$$\bar{n} = 2g_0 t \ln 2 \quad . \quad . \quad . \quad . \quad . \quad . \quad . \quad . \quad (3.17)$$

and the average excitation energy $\bar{\epsilon}$ of these is

$$\bar{\epsilon} = \frac{U}{\bar{n}} = \frac{\pi^2}{12 \ln 2} t \quad . \quad . \quad . \quad . \quad . \quad . \quad . \quad (3.18)$$

according to eqn. (3.14). The particles responsible for the bulk of the configurations will therefore come from a region of the order of the temperature around the Fermi level, as, according to eqn. (3.18), the average excitation energy of the excited degrees of freedoms is of this order of magnitude. It is therefore sufficient to have an accurate knowledge of the single Fermion density $g(\epsilon)$ in a region of this order around the Fermi energy. In view of this the equidistant spacing model should be a good approximation for the description of systems for which the average value of $g(\epsilon)$ in a region of the order of t around ϵ_0 will be a slowly varying function of t; it will not be adequate if there is an anomalous structure in the spacing around ϵ_0 so that the average depends sensitively on how the average is performed. The latter situation is for example met in models in which the single Fermion spectrum has an energy gap at the Fermi energy.

It is sometimes useful to have crude estimates of the level densities associated with the excitation of p particles and h holes in the equidistant spacing model. If we neglect that the particles (or holes) may coincide in the same single particle level, which is a good approximation as long as $p^2 g_0^{-1}$ and $h^2 g_0^{-1}$ are small compared to U, the corresponding level density can be estimated to be

$$\rho(U\,;\,p,h) = \frac{g_0{}^{p+h}\, U^{p+h-1}}{p!\,h!\,(p+h-1)!}.$$

3.2. *Angular Momentum Distribution*

In the considerations so far we have made no reference to the angular momentum or parity distribution of the level density. A knowledge, especially of the former, is indispensible for the theoretical understanding of the statistical nuclear reaction (cf. § 5), but also for comparing the theoretical level density of a particular model with the level density of neutron resonances. These resonances, excited by s-wave neutrons, are subject to strong angular momentum and parity selection rules and can only have spin $|j_i \pm \frac{1}{2}|$, where j_i is the target nucleus spin. The calculation of the distribution of angular momenta is usually made by the technique of chemical potentials as discussed above (Bethe 1937, Bloch 1954); we will use the notion of random coupling of angular momenta, which is equivalent, but gives a physically clearer picture.

In addition to being characterized by the energy ϵ_s, the single Fermion states are also characterized by the projection of the angular momentum on the z-axis, m_s, or in the case of deformed nuclei, on the nuclear symmetry axis, Ω_s (Nilsson 1955). The case of deformed nuclei will be discussed later. The corresponding single Fermion level density should therefore have been written $g(\epsilon, m)$ rather than $g(\epsilon)$. The average occupation numbers $\bar{n}_s$ of eqn. (3.16) should therefore also be labelled by m_s. There is an equal probability for $+m_s$ and $-m_s$, so that $g(\epsilon, m) = g(\epsilon, -m)$ and there is a corresponding equality in the average occupation number for $+m_s$ and $-m_s$. As a consequence of this, the average value of the projection of the total angular momentum, $\bar{M}$, which is obtained as the sum of all the projections m_s for every state multiplied by its probability of occupation, $\bar{n}_s$, must be 0. Therefore, if all occupation numbers had their exact average values, the system would have total angular momentum 0; the occurence of other angular momenta must be due to fluctuations of the occupation numbers away from their average values (cf. Le Couteur and Lang 1959).

The probability ν_s that a Fermion in state s does not have the average occupation number $\bar{n}_s$, is the probability of occupation of the state, $\bar{n}_s$, multiplied by the probability of finding the state empty, $1-\bar{n}_s$, so that

$$\nu_s = \bar{n}_s(1-\bar{n}_s) = \frac{e^{\beta(\epsilon_s-\mu)}}{(1+e^{\beta(\epsilon_s-\mu)})^2}. \quad . \quad . \quad . \quad . \quad (3.19)$$

The average number of particles and holes which are excited away from the mean occupation numbers can therefore be obtained from eqn. (3.19) exactly similarly as the average number of excited particles $\bar{n}$ of eqn. (3.17) is obtained from eqn. (3.16) and is

$$\nu = g_0 t. \quad . \quad . \quad . \quad . \quad . \quad (3.20)$$

Each one of these ν excited particles and holes has a probability $p(m)$ for different m-values. The average value of m, $\langle m \rangle$, is obviously 0, while the average value of m^2, $\langle m^2 \rangle$, will differ from 0:

$$\left.\begin{aligned} \langle m \rangle &= \int_{-\infty}^{+\infty} p(m) m \, dm = 0, \\ \langle m^2 \rangle &= \int_{-\infty}^{-\infty} p(m) m^2 \, dm. \end{aligned}\right\} \quad . \quad . \quad . \quad . \quad . \quad (3.21)$$

The value of $\langle m^2 \rangle$ is to a good approximation a function of the Fermi energy only. It can easily be calculated, e.g. within a single level of spin j where for large j it becomes $j^2/3$, or within a major shell of the shell model. We will later discuss $\langle m^2 \rangle$ on the basis of the WKBJ approximation, but have at this point only need for its existence.

The projection of the total angular momentum, M, on the z-axis of the system is the sum of the projections of the ν excited particles. These projections can have both different signs and different values. We now apply the idea of random coupling to this system, so that the distribution of M can be regarded as the result of the random values of the projections of the ν excited particles and holes with the condition of eqn. (3.21) . The well-known central limit theorem of statistics then implies that the distribution of M-values for large ν asymptotically becomes a Gaussian, $\exp\{-M^2/2\sigma^2\}$, with a mean square deviation

$$\sigma^2 = \nu \langle m^2 \rangle = g_0 t \langle m^2 \rangle \quad . \quad . \quad . \quad . \quad . \quad . \quad (3.22)$$

by eqn. (3.20).

The density of states of a certain M is thus asymptotically related to the total level density of every possible M by

$$\rho(U, M) = \frac{\rho(U)}{\sqrt{(2\pi\sigma^2)}} e^{-\frac{M^2}{2\sigma^2}} . \quad . \quad . \quad . \quad . \quad (3.23)$$

It is also possible to obtain this result by introduction of an additional chemical potential in the partition function (3.3). Our derivation of eqn. (3.23) emphasizes, however, that this is only an asymptotic form valid for large ν. To illustrate this point, consider the case when $p(m)$ is given by a rectangular distribution, a constant equal to $1/2h$ in the interval $(-h, h)$, 0 outside. This may be thought of as the $p(m)$ for a shell model level of given large spin h. For two particles the distribution function for M, $p_2(M)$, has a triangular shape

$$p_2(M) = \left\{ \begin{array}{ll} \frac{1}{(2h)^2}(2h - |M|); & |M| < 2h, \\ 0 \quad ; & |M| > 2h, \end{array} \right\} \quad . \quad . \quad . \quad (3.24)$$

already beginning to resemble the Gaussian. For ν particles the distribution function $p_\nu(M)$ is

$$p_\nu(M) = \frac{1}{(2h)^\nu} \frac{1}{(\nu-1)!} \sum^k (-)_k \binom{\nu}{k} [M + h(\nu - 2k)]^{\nu-1}, \quad . \quad (3.25)$$

where the sum is performed as long as $M + h(\nu - 2k) > 0$. These polynomials converge rapidly to the form (3.23) with increasing ν. Our present experimental knowledge about angular momentum distributions is not sufficient to detect deviations from the Gaussian distribution. There are indications, however, that this will become an increasing problem at low excitations and in medium weight elements where the number of excited particles is small. In particular, the Gaussian of eqn. (3.23) will not be adequate for very large values of M. Because a finite number of particles cannot couple to arbitrarily large spin, the distribution function is then exactly 0.

From eqn. (3.23) the density of states of given spin j can be obtained by observing that this is the difference between the level density of spin $M=j$ and $M=j+1$. Thus

$$\rho(U,j)=\rho(U,M=j)-\rho(U,M=j+1)\simeq\frac{(2j+1)\,\rho(U)}{2(2\pi)^{1/2}\,\sigma^3}\,e^{-\frac{j(j+1)}{2\sigma^2}} \qquad (3.26)$$

To each of the states of spin j in eqn. (3.26) there obviously exist $(2j+1)$ sub-states corresponding to the magnetic quantum numbers.

The approximation in eqn. (3.26) is excellent for a very large range of values of j. To see this, take the ratio between the middle term of eqn. (3.26) and its approximate value, the righthand side. This ratio should be close to unity for the approximation to be useful. The ratio is given by $\sinh x/x$ with $x=(j+\frac{1}{2})/2\sigma^2$, which is close to unity for $(j+\frac{1}{2})\ll 5\sigma^2$. The range of validity is so large that the mathematical breakdown of approximation (3.26) occurs for larger values of j than those for which eqn. (3.23) (on which the approximation is performed) becomes invalid. In order to obtain a crude estimate of the magnitude of spin values for which the Gaussian distribution is inadequate, suppose that the particles responsible for the spin all have a maximum projection $\sqrt{\langle m^2\rangle}$ on the z-axis and neglect the exclusion principle. The corresponding value of the total maximum spin $j_0=\nu\sqrt{\langle m^2\rangle}=\sigma^2/\sqrt{\langle m^2\rangle}$ by eqn. (3.22). For values of $j>j_0$ the Gaussian approximation above is doubtful. The values of j_0 can be estimated by different means but its value is not strongly dependent on the method used. We notice that this value of j_0 easily fulfills the requirement for the validity of approximation (3.26); this approximation is therefore unimportant compared to the approximation (3.23). The limit to the validity of the Gaussian distribution is not only of academic interest. Nuclear reactions involving large angular momenta and emission of several particles or phonons already sample the spin-distribution at or close to j_0 in the last stages of the deexcitation process.

The derivation of eqn. (3.26), by passing through the consideration of a random coupling of projections along a z-axis, which does not appear in the final result, does not reveal the true character of the result. The natural viewpoint is to consider the coupling of the angular momenta to be random *in space*. For the discussion we will assume the angular momenta to be classical vectors. With each of the ν excited particles and holes there is then associated a vector which can have any spatial direction. If no spatial direction of the system is preferred and if $\langle m^2\rangle$ is the mean square of the projection of the individual spins on some arbitrary axis, the density of states of spin $\mathbf{j}$ and energy U, $\rho(U,\mathbf{j})$, is

$$\rho(U,\mathbf{j})=\frac{\rho(U)}{(2\pi\nu\langle m^2\rangle)^{3/2}}\,e^{-\frac{j^2}{2\nu\langle m^2\rangle}}, \qquad . \quad . \quad . \quad . \quad (3.27)$$

so that the number of states in an interval dU of energy and with spin in a volume element $d^3\mathbf{j}$ is $\rho(U,\mathbf{j})dU\,d^3\mathbf{j}$. The number of all states at energy U with spin between j and $j+dj$, $\rho_1(U,j)\,dj$, is thus obtained by multiplying

eqn. (3.27) by the volume of the spherical shell of radius j, $4\pi j^2\,dj$:

$$\rho_1(U, j)\,dj = \frac{(2j)^2\rho(U)}{2(2\pi)^{1/2}\sigma^3} e^{-\frac{j^2}{2\sigma^2}} dj \quad . \quad . \quad . \quad . \quad . \quad (3.28)$$

with σ^2 defined in eqn. (3.22). Equation (3.28) contains the density of all levels of spin j, therefore also the $(2j+1)$ degeneracy connected with the magnetic quantum number of a level of spin j. To compare with our previous result of eqn. (3.26) we therefore divide eqn. (3.27) by $2j$ and apply Kramers's rule for going from a classical angular momentum to a quantal one; j then corresponds to $j+\frac{1}{2}$ and j^2 to $j(j+1)$. With these substitutions in eqn. (3.28) we have for the density of states of spin j, magnetic quantum numbers excluded, $\rho(U, j)$,

$$\rho(U, j) = \frac{(2j+1)\rho(U)}{2(2\pi)^{1/2}\sigma^3} e^{-\frac{j(j+1)}{2\sigma^2}} \quad . \quad . \quad . \quad (3.29)$$

in agreement with eqn. (3.26). From this derivation it becomes obvious that the origin of the factor $(2j+1)$ in eqn. (3.26) is due to the volume element $d^3\mathbf{j}$ in the phase space of the angular momentum and it must therefore be regarded as completely geometrical.

Equation (3.27) suggests that it should be possible to associate a rotational energy and a moment of inertia $\mathscr{T}$ with the nucelar spin distribution. Suppose that the density of states with angular momentum 0 is $\rho_0(U)$. These states have no angular momentum and therefore describe a non-rotating system. If this system is given an angular momentum $\hbar\mathbf{j}$ we can expect an energy

$$\frac{\hbar^2\mathbf{j}^2}{2\mathscr{T}}$$

to go into rotational motion and the energy available for intrinsic excitation is thus $U-(\hbar^2\mathbf{j}^2/2\mathscr{T})$. The density of states of spin $\mathbf{j}$ is then

$$\rho(U, \mathbf{j}) = \rho_0\left(U - \frac{\hbar^2\mathbf{j}^2}{2\mathscr{T}}\right). \quad . \quad . \quad . \quad . \quad . \quad (3.30)$$

As we have discussed previously, the level density has an essentially exponential increase with energy. As long as the rotational energy is small we can therefore make use of this and expand eqn. (3.30) as

$$\rho(U, \mathbf{j}) \simeq \rho_0(U)\, e^{-\frac{\hbar^2}{2\mathscr{T}T}\mathbf{j}^2}, \quad . \quad . \quad . \quad . \quad . \quad (3.31)$$

where T is the nuclear temperature of eqn. (2.12). Comparing this to eqn. (3.27) we see that they are identical if we put

$$\rho_0(U) = \frac{\rho(U)}{(2\pi\nu\langle m^2\rangle)^{3/2}} \quad . \quad . \quad . \quad . \quad . \quad . \quad (3.32)$$

and

$$\sigma^2 = \nu\langle m^2\rangle = \frac{\mathscr{T}T}{\hbar^2} \quad . \quad . \quad . \quad . \quad . \quad . \quad (3.33)$$

which can be taken as the definition of the moment of inertia from the spin distribution. If we furthermore recall that at high excitation the nuclear

temperature T and the thermodynamic temperature t will tend to the same value, we obtain from eqn. (3.22)

$$\mathcal{T} = \hbar^2 g_0 \langle m^2 \rangle, \quad . \quad . \quad . \quad . \quad . \quad . \quad . \quad . \quad (3.34)$$

valid for the equi-distant spacing model in the continuous approximation.

We have previously emphasized the strong similarity between the emission of particles from a classical liquid drop and the excited compound nucleus. With the introduction of a moment of inertia as in eqn. (3.30) the analogy applies equally well to rotating systems as will be seen in detail in § 5. A rotating, classical liquid drop in thermal equilibrium has a rigid body moment of inertia. In view of this it should be expected that the nuclear moment of inertia tends towards the rigid body value at high excitation. Bloch (1954) has shown that the semi-classical WKBJ approximation applied to eqn. (3.34) gives this result for nucleons moving independently in an external central potential. The proof goes as follows:

A Fermi gas of particles in an external potential $V(r)$ has a mass-density $\mu(r)$ given by

$$\mu(r) = 4 \cdot \frac{4\pi}{3} [2M(\epsilon_0 - V(r))]^{3/2} \cdot M h^{-3} \quad . \quad . \quad . \quad . \quad (3.35)$$

at a point r, if M is the nucleon mass and ϵ_0 the Fermi energy. The total number of nucleon states of angular momentum l and energy less than ϵ_0 is

$$N_l(\epsilon_0) = \frac{4}{\pi} \int_{r_0}^{r_1} dr \left[\frac{2M}{\hbar^2} \left(\epsilon_0 - V(r) - \frac{l^2}{r^2} \right) \right]^{1/2} \quad . \quad . \quad . \quad (3.36)$$

where r_0 and r_1 are the classical turning points. The density of states with projection m on the z-axis is thus

$$g(\epsilon_0, m) = \int_{|m|}^{l_{\max}} \frac{d}{d\epsilon_0} N_l(\epsilon_0)\, dl \quad . \quad . \quad . \quad . \quad . \quad (3.37)$$

where $l_{\max}$ is the maximum classically allowed l-value. The moment of inertia $\mathcal{T}$ of eqn. (3.34) is thus

$$\mathcal{T} = \hbar^2 g_0 \langle m^2 \rangle = \hbar^2 \int_{-\infty}^{+\infty} g(\epsilon_0, m) m^2\, dm = \tfrac{2}{3} \int_0^R r^2 \mu(r)\, d\tau = \mathcal{T}_{\text{rigid}} \quad (3.38)$$

by elementary integration. Here $d\tau$ is the volume element and R is the nuclear radius defined as the point where $V(r)$ becomes equal to ϵ_0. The moment of inertia depends therefore in this limit on the mass distribution; for an infinite square well the rigid moment of inertia is

$$\mathcal{T}_{\text{rigid}} = \frac{2}{5} MAR^2. \quad . \quad . \quad . \quad . \quad . \quad . \quad (3.39)$$

The fact that we can associate a moment of inertia and a rotational energy with the nucleus in this way, does not imply that it is possible to make these statements for the individual states; it does not mean that it is possible to split the nuclear Hamiltonian into an intrinsic and a rotational part as in the unified model (A. Bohr 1952, A. Bohr and B. R. Mottelson 1953). In this case the rotation must instead be considered an average property of many nuclear states, as with a classical equilibrium system. The moment of inertia as applied to the highly excited nucleus must not be confused with moments of inertia for nuclei in or near their ground states.

These quantities are not necessarily related, and in contrast to nuclei in their ground states it is not certain that the moments of inertia of the excited nuclei are reduced. The discussion of the spin distribution above shows that its general character is not very model dependent. The dependence of a particular model is mainly in the value of the associated moment of inertia. This moment of inertia has recently been determined from experiments for certain medium-weight elements (Ericson and Strutinski 1958, Ericson 1959, Douglas and MacDonald 1959) and seems approximately to be given by the rigid body value. This result can however not yet be considered as established.

3.3. *Parity Distribution*

The argument of random coupling that we used to obtain the spin distribution can also be utilized to obtain a crude estimate of the distribution of parity. Again, the parity distribution is due to fluctuations in occupation number. The single Fermion states can have parity either $(+1)$ or (-1). If there is an odd number of Fermions in $(-)$ -parity states the resulting parity of the system is (-1). Thus, if there are ν excited Fermions which have a probability p_- for negative parity and $p_+ = 1 - p_-$ for positive parity, we conclude the following: the probability of finding k of the ν Fermions in negative parity states and the rest in positive parity states is

$$\binom{\nu}{k}(1-p_-)^{\nu-k}\, p_-{}^k,$$

if ν is an integer. The probability of negative parity, P_-, is thus obtained by summing this probability over the values of k which correspond to negative parity, i.e. odd values of k.

$$P_- = \sum_{\text{odd } k}\binom{\nu}{k}(1-p_-)^{\nu-k}\, p_-{}^k = \frac{1-(1-2p_-)^\nu}{2}. \quad . \quad . \quad (3.40)$$

This relation is strictly true only for integer values of ν. We observe that for even and odd nuclei ν is always an even number; for odd mass nuclei it is an odd number. In order to apply this result also to non-integer average values of ν we therefore should re-express eqn. (3.40) as

$$P_- = \frac{1-\epsilon(|1-2p_-|)^\nu}{2}\ ;\ P_+ = 1 - P_- \quad . \quad . \quad . \quad (3.41)$$

$$\epsilon = \left\{\begin{array}{lll} 1 & & \text{for even and odd nuclei,} \\ 1 & p_- < \tfrac{1}{2} & \\ -1 & p_- > \tfrac{1}{2} & \text{odd mass nuclei.} \end{array}\right\}$$

From these expressions we conclude that even a small admixture of negative parity or vice versa leads to a nearly equal probability of both parities. As an example: for 20% admixture and $\nu = 6$ we obtain $P_+ = 0{\cdot}52$ and $P_- = 0{\cdot}48$.

In the remainder of this section we will discuss the most important of the special models on which the theoretical study of nuclear level densities is based. We will emphasize the problems and inadequacies connected with

the models. This must not conceal the fact that the behaviour of the level density is understood qualitatively, in many respects even quantitatively, on the basis of these models, even though the description is not yet complete. The parameters of the models are closely related to other nuclear properties; the discrepancies between the predictions of these models and experiments must therefore be considered to be significant and they indicate features which go beyond these descriptions and the extent to which low energy nuclear models remain a valid description at high excitation.

3.4. *The Free Gas Model*

The model which historically has had the largest impact on the interpretation of experiments is Bethe's free gas model (Bethe 1936, 1937, Lang and Le Couteur 1954). The nucleus is considered as a free Fermi gas of neutrons and protons of both spins confined to move in a volume $V=(4\pi/3)R^3$. The Fermi energy is thus given by the phase space occupied in the ground state

$$V\frac{4\int_0^{\epsilon_0}4\pi p^2\frac{dp}{d\epsilon}d\epsilon}{h^3}=A. \qquad (3.42)$$

The Fermi energy is thus

$$\epsilon_0=\left(\frac{3}{\pi}\right)^{2/3}\frac{9}{4}\frac{\hbar^2}{2Mr_0^2} \qquad (3.43)$$

where M is the nucleon mass and r_0 the nucleon radius. The density of single particle states at the Fermi level is

$$g_0=\frac{3}{2}\frac{A}{\epsilon_0}. \qquad (3.44)$$

The level density is given by eqn. (3.15) with the parameters above; the difference between neutron and proton single particle spacing is neglected, so that the factor $g_0^2/4g_ng_p=1$. The distribution of spin among the nuclear levels is given by eqn. (3.29) with σ^2 from eqn. (3.33) with the rigid body value of the moment of inertia, $\mathscr{I}=\frac{2}{5}MAR^2$. The two parities are supposed to occur with equal probability.

The final level density in this model is thus given by

$$\rho(U,j)=\frac{\pi}{3}(2j+1)e^{-\frac{\hbar^2}{2\mathscr{I}t}j(j+1)}\cdot\frac{1}{32\sqrt{2}}\frac{\hbar^3}{\mathscr{I}^{3/2}}\left(\frac{A}{\epsilon_0}\right)^{1/2}\frac{e^{\pi\left(\frac{AU}{\epsilon_0}\right)^{1/2}}}{U^2} \qquad (3.45)$$

The thermodynamic temperature t is given by eqns. (3.14) and (3.44) as

$$t=\left(\frac{fU}{A}\right)^{1/2} \qquad (3.46)$$

where $f=(4/\pi^2)\epsilon_0$. The corresponding nuclear temperature T is obtained from eqns. (2.12) and (3.45) to be

$$\frac{1}{T}=\frac{1}{t}-\frac{2}{U}. \qquad (3.47)$$

Thus this model predicts nuclear temperatures which at high excitations are given asymptotically by eqn. (3.46). As the Fermi energy does not

depend on mass number the temperature will decrease as a function of A for the same excitation energy and the level density will increase with A. An appropriate value of the constant f seems presently to be about 10 MeV with an uncertainty of the order of 25%, which corresponds to a Fermi energy of 25 MeV.

It is the very nature of this model that it describes the overall behaviour of the level density and its gross structure throughout the periodic table rather than the behaviour of the level density of any particular nucleus. It will therefore never describe shell effects or odd–even effects; the fluctuations in the average value of g_0 are not accounted for and the predictions of this model must therefore be taken as a guide rather than a detailed description. The virtue of this model is its extreme simplicity.

The effect of nuclear surface oscillations have been included in this model (Lang and Le Couteur 1954). Present data have not been able to decide on the existence of this effect; we therefore refer to the original paper.

3.5. *The Newton–Cameron Model*

In view of the marked shell effects in the observed level densities it is tempting to substitute the shell model (Mayer and Jensen 1955) for the free gas model. The importance of shell effects was first emphasized by Bloch (1954), who developed general methods to deal with the mathematical problem. The main difficulty in obtaining numerical results lies in the treatment of the single particle level density. A convenient approximation, first introduced by Newton (1956 a) and later used also by Cameron (1958 a), is obtained from the observation that the important region of the single particle spacing is in a small region of the order of the temperature $t=\beta^{-1}$ around the Fermi level; it should therefore be possible to use the simple results of the equi-distant spacing model provided the exact single particle level density $g(\epsilon)$ is replaced by a suitably taken average over a region of this order. The dominating factor in the level density is the exponential factor of eqn. (2.16) for any independent particle model; the importance of this term thus suggests that the proper weighting factor for an average is that referring to this term, which we see from eqn. (3.6) to be of the form

$$\omega(\epsilon)=\ln\left(1+\exp\left[-\beta(|\epsilon-\mu|)\right]\right). \quad . \quad . \quad . \quad . \quad (3.48)$$

In practice the chemical potential μ is assumed to coincide with the Fermi energy ϵ_0. The average density $\overline{g_0(t)}$ is then

$$\overline{g_0(t)}=\frac{\int_{-\infty}^{+\infty} g(\epsilon)\ln\left(1+\exp\left[-\frac{|\epsilon-\epsilon_0|}{t}\right]\right)d\epsilon}{\int_{-\infty}^{+\infty}\ln\left(1+\exp\left[-\frac{|\epsilon-\epsilon_0|}{t}\right]\right)d\epsilon} \quad . \quad . \quad (3.49)$$

This average expression is regarded as the appropriate g_0 to be used eqn. (3.11) from which the temperature t can again be determined in terms of the known excitation energy U. An iterative procedure is applied and when $\overline{g_0(t)}$ becomes uniquely determined it is used for g_0 in eqn. (3.15). This approximation implicitly assumes: (1) that the chemical potential can

be replaced by the Fermi level, which is often a very good approximation, (2) that $\overline{g_0(t)}$ is a slowly varying function of t and does not depend strongly on the exact procedure used for the average. This procedure is that used by Newton. Cameron applies the same technique to average single particle level *spacings* instead of single particle level *densities* in order to improve agreement with experiments. This procedure is theoretically somewhat less justified.

The angular momentum dependence of the level density is in both cases introduced similarly as for the free gas model.

While the odd–even effect has no natural place in a shell model with non-interacting particles, it can be partially acccounted for by shifting the effective excitation energy of odd and even nuclei (cf. fig. 3). Newton and Cameron therefore regard the odd nucleus as representing a nucleus with an excitation energy appropriate for the shell model calculation while the ground states of the even and odd mass nuclei have been depressed by an amount similar to the corresponding odd–even shift in the semi-empirical mass formula (Metropolis and Reitwiesner 1950, Cameron 1957). The effective excitation energy is therefore reduced in this case by these pairing energies. While this is a good phenomenological description it is uncertain whether pairing effects, which presumably are cooperative effects, can be accounted for simply by such shifts, and should not be accounted for even in the further description.

One of the main objectives of these authors is to obtain a quantitative description of the spacings of neutron resonances. It is thus necessary to obtain some explicit expression for the single particle levels to perform the average of eqn. (3.49). In the shell model the total angular momentum $j_s = |l_s \pm \frac{1}{2}|$ of the states is a good quantum number; Newton observes that the density of such single particle shell-model states for large A becomes equal to $\alpha A^{2/3}$, where α is a constant, if the nucleus is considered as a square well with a radius $R = r_0 A^{1/3}$. The exact single particle level density $g(\epsilon)$ refers to both neutrons and protons and includes also the degeneracy of the states due to magnetic quantum numbers. Each of the shell-model states is obviously $(2j_s+1)$-fold degenerate or nearly degenerate in magnetic quantum number and the corresponding single particle level density is thus approximated by

$$g(\epsilon) \simeq 2\alpha A^{2/3}(j_N + j_Z + 1). \qquad (3.50)$$

Here j_N and j_Z are the spins of the neutron and proton shell model states which correspond to the particular $A = N + Z$. The appropriate values of j_N and j_Z are obtained from Klinkenberg's shell-model level scheme (1952) based on a study of nuclei in or near their ground states. The expression (3.50) can now be averaged according to eqn. (3.49). The constant α is left to be determined from experiments.

The characteristic feature of this treatment is that shell effects enter only through the spins j_N and j_Z and not at all due to the variation in spacing of the shell model states. As a consequence of this the magic shell

effects in Newton's treatment occur just before the closed shells due to low values of j_N and j_Z in that region.

So as to introduce shell structure in a more natural way, Cameron determined single particle orbits from his semi-empirical mass formula (1957) which is fitted to known nuclear mass excesses. To calculate single particle orbits from this formula he neglects the variation of the Coulomb and Coulomb exchange forces as the orbits of the first excited states in a shell-model do not change its volume; he also neglects the pairing term in the mass formula as representing a cooperative effect outside the shell model. From the remaining part of the mass-excess $M^1(Z, A)$ it is then possible to define a proton-orbit spacing $d(Z)$ by

$$d(Z) = M^1(Z, A) - 2M^1(Z-1, A-1) + M^1(Z-2, A-2) \qquad (3.51)$$

and similarly for the neutron spacing $d(N)$, as long as this formula is applied close to the valley of beta stability. While Newton makes use of an adjustable constant to determine his spacings, Cameron uses the values of the spacing as obtained from eqn. (3.51).

In the further comparison with experiments these authors make use of an important approximation. They observe that the spins of neutron resonances almost always are low. Thus, it should be justifiable to replace the exponential cut-off factor of eqn. (3.29) by unity as long as $j \ll \sigma$, so that the spin distribution of neutron resonances becomes approximately proportional to $2j+1$. Furthermore they observe that the moment of inertia $\mathscr{T}$, related to σ by eqn. (3.33) may well be reduced below its rigid body value. They therefore adopt the procedure of regarding the reduction factor as an adjustable constant, the same for all nuclei, but keeping the A-dependence of $\mathscr{T}$. (In the actual articles this argument is carried out on $\langle m^2 \rangle$, but is otherwise identical). Therefore,

$$\mathscr{T} = aA^{5/3}. \qquad . \quad . \quad . \quad . \quad . \quad . \quad . \quad . \quad . \quad (3.52)$$

The fit to the experimentally observed neutron resonances can now be carried out most accurately; the mean square deviation factor of the Newton expression is 3, of the Cameron one 1·7 for the ratio $\rho_{\text{exp}}/\rho_{\text{calc}}$. Especially the fit to the region of magic numbers, where the neutron resonance spacings differ from the spacings between shells by factors of up to 10^3 is greatly improved. The reduction factor for the moment of inertia is, however, in both cases large. Thus, the numerical coefficient of Newton corresponds to a ratio of the moment of inertia to the rigid body value of 0·13, that of Cameron of 0·03 with $r_0 = 1{\cdot}2$ Fermis (Douglas and McDonald 1959)†. This reduction is so large that the neglect of the cut-off term in angular momentum is not justified. These reduction factors would imply that in medium-weight elements only neutron resonances of spin 0 or $\frac{1}{2}$ could occur in practice. The small value of the moment of inertia seems to reflect the use of a too large single particle spacing, as these effects tend to compensate.

† We are indebted to Dr. McDonald for pointing out to us that another statement about this ratio (Ericson 1959) contains a calculational error.

As a whole the formulae obtained by Newton and Cameron represent the best fit at present to neutron resonances and they are recommended if the level density is needed in the neighbourhood of neutron binding energies and no experimental evidence is available. They cannot be considered reliable if the excitation energies vary by several MeV or more from this energy. The dependence on angular momentum can be ameliorated simply by using an exponential cut-off factor $e^{-\frac{j(j+1)}{2\sigma^2}}$ with σ^2 given by eqn. (3.33) and the rigid body moment of inertia (cf. Cameron 1959).

3.6. *The Rosenzweig Effect*

It has been emphasized by Rosenzweig (1957 b, 1959; cf. also Margenau 1941) that the pure shell model should lead to a marked effect in the level density depending on to what extent the last shell is filled in the ground state. Thus if a sub-shell in the shell model has a degeneracy and is filled by k particles, these can be rearranged in $n!/k!(n-k)!$ different, degenerate configurations at zero excitation energy. There is therefore a considerably larger number of rearrangement possibilities when the shell is half-filled than when there is only one particle in it. The number of rearrangement possibilities is symmetrical in the number of holes and particles of the last shell. At higher excitation this phenomenon will still exist in so far as the shell-model description is appropriate. It will gradually decrease with energy as the single particle level spacings become small compared to the temperature. Rosenzweig has shown that this effect is describable to a good approximation as a simple shift of the excitation energy in eqn. (3.15) changing it into the effective excitation energy U^1.

$$U^1 = U + \frac{n^2 d_n}{12} - \frac{d_n}{2}\left(k_n - \frac{n}{2}\right)^2 + \frac{p^2 d_p}{12} - \frac{d_p}{2}\left(k_p - \frac{p}{2}\right)^2 \quad . \quad . \quad (3.53)$$

where d_n and d_p are the previous mean spacings between states and n and p are the degeneracies of the last-filled neutron and proton shells. The expression (3.53) was derived for an exactly soluble model consisting of equi-distant shell-model levels with the same degeneracy. The solution is expected to be similar in the general case. In particular, this effect is still expected to be easily discernible at excitation energies of the order of the neutron binding energy (though more exact expressions than the approximation (3.53) may have to be used). The effect seems to be present in the neighbourhood of the closed shell $Z = 50$, where the closure of the highly degenerate $g^{9/2}$ proton shell is favourable for its existence. It has been searched for in other parts of the periodic system but no definite conclusion about its existence has been possible in these cases.

The Rosenzweig effect must be expected to be smaller than what might be first thought for two reasons. First the degeneracy is due to the spin-magnetic quantum number of the levels. From our previous discussion of the spin distribution (eqns. (3.25) and (3.29)) we conclude that of the total number of states in the half-filled shell a large number have high spin values, while the range of spin values will be much smaller when there is only

one particle in the shell. As the comparison of the number of states is usually done for nuclei with the same spin value (or reduced to the same spin value), the actual number of recombinations for the half-filled shell is reduced more strongly than that of the unfilled shell, decreasing the effect. Secondly, the large degeneracy of the ground state in the case of a half-filled shell is removed by the residual interactions which in particular must be expected to lead to a certain depression of the ground state with respect to the unperturbed value. This effect is not present in the unfilled shell. There will thus be a reduction of the effective excitation energy for the half-filled shell, again reducing this shell-effect. This may explain why the effect which should be of very general nature is easily discernible only in the most favourable cases. The occurrence of the effect at $Z = 50$ is, however, clear in spite of these reduction factors.

3.7. *The Newson Model*

Newson (1959) has recently tried a phenomenological description of the neutron resonance spacings in terms of a very special set of shell model excitations. Observing that the spacing between major shells is large, about 2 MeV/nucleon, he attributes the most important excitations to rearrangements within the partially filled major shells. Of all possible such configurations he only retains the pair excitations $(m, -m)$ of nucleons which have same, but opposite projection of angular momentum on the z-axis. In addition he also considers complex pair excitations, i.e. configurations in which such pairs have been excited to the next higher major shell or excited out of the next lower major shell. With these types of excitations only and with the *a posteriori* assumption of a spin distribution proportional to $(2j+1)$ it is possible to account for the regularities in the spacings of neutron resonances with good accuracy, using only one adjustable parameter, the spacing between 'pair excitations'. The physical basis for the inclusion of only these special types of excitations is not clear, nor is it presently possible to conclude whether this procedure has any deeper significance. In order to draw such conclusions it is first necessary to consider the angular momentum distribution, variation of the level density with excitation energy, etc., on the basis of this model and confront these results with experiments. We believe that the major result of Newson's model, the good description of the variation of level spacings from nucleus to nucleus, may be a rather general consequence of the shell model and that this result may be rather independent of the special model used. This indicates the desirability of a more accurate evaluation of level densities on the basis of the ordinary shell model with the inclusion of the variation in distance between the shell model levels and the Rosenzweig effect.

Ericson (1958 b) has discussed the general effect of shell structure as a function of excitation energy. The ratio of the level density of nuclei with half-filled and filled major shells is a rapidly increasing function of excitation energy up to an energy of the order of $g_0(\hbar\omega)^2/4\pi^2$, where the ratio reaches its maximum value. Here g_0 is the overall average single particle

level density and $\hbar\omega$ the spacing between the oscillator shells which is about $40A^{-1/3}$ MeV. The energy of full development of the shell effect is thus of the order of 10–15 MeV in heavy nuclei. At higher excitations the ratio is a slowly decreasing function which eventually becomes unity. At low excitation energies the shell effect, with the exception of the Rosenzweig phenomenon, is well described by eqn. (3.15) using a single particle level density averaged over a region of the order of the nuclear temperature; at excitations higher than $g_0(\hbar\omega)^2/4\pi^2$ it may be described by the same equation with a constant single particle level density g_0 but with an excitation energy counted from a fictitious ground state (cf. eqn. (3.53)).

3.8. *The Pairing Model*

While we thus see that the shell model accounts successfully for many effects of the level density, it does not touch on the problem of residual interactions, the effects of which have to be introduced *a posteriori*. From the marked odd–even effect (see fig. 3) we see that these interactions are far from negligible; a realistic model should therefore automatically give this feature, and should also be appropriate for a description of the main features of the nuclear spectrum close to the ground state.

The unified model for deformed nuclei provides a suitable frame within which the effects of the part of the residual interactions which are due to pairing forces can be studied (A. Bohr 1952, A. Bohr and Mottelson 1953, Nilsson 1955, A. Bohr *et al.* 1958). The low-energy spectra of the deformed nuclei have two kinds of excitations according to this model; collective excitations, i.e. rotations and vibrations, and single particle excitations. The single particle states arise from the motion of a nucleon in the deformed average potential. They are characterized by the projection Ω_s of the angular momentum on the nuclear symmetry axis; the states are doubly degenerate in $\pm\Omega_s$, since the reversal of the motion around the symmetry axis does not change the dynamics. The detailed distribution of single particle states has been studied by Nilsson (1955).

For the purpose of discussing the effect of pairing interactions on level densities the detailed behaviour of the model is not necessary. Ericson (1958 a) has used the following simple picture. The single particle levels are assumed to be equidistant, as is indicated to a rather good approximation by the Nilsson (1955) level scheme in the region of strongly deformed nuclei. Since two nucleons in the same degenerate orbit will have a large overlap of their wave functions, it should require an additional energy to break this pair and excite the two nucleons into unpaired orbits. This pairing energy is therefore of the ordinary Goeppert-Mayer type (1955). The pairing energy is taken to be a constant, 2δ, though in general it must depend on the character of the state. From this point of view the breaking of μ pairs will use an energy $2\mu\delta$ of the total excitation energy U. After the subtraction of this energy the system can thus be regarded as a system of ordinary shell model character but with the additional condition that exactly μ pairs are broken, a problem which can be solved by the previous methods.

Since an orbit with two paired nucleons will contribute no projection of angular momentum on the nuclear symmetry axis, this contribution is due to the unpaired nucleons only. As in the case discussed earlier (eqn. 3.23) these projections will couple at random and yield a distribution for $K = |\sum_s \Omega_s|$ which is proportional to $\exp[-K^2/2\overline{K^2}]$, in terms of the average value of K^2, $\overline{K^2}$, at this excitation energy. We can in analogy with eqn. (3.33) express $\overline{K^2}$ in terms of the average number of unpaired particles, ν, and the average value of Ω_s^2 for one particle, K_1^2.

$$\overline{K^2} = \nu K_1^2. \quad . \quad . \quad . \quad . \quad . \quad . \quad . \quad . \quad . \quad (3.54)$$

To get an estimate of K_1 we can evaluate it for the last filled oscillator shell giving

$$K_1^2 = \frac{K_m^2}{6} \quad . \quad . \quad . \quad . \quad . \quad . \quad . \quad . \quad (3.55)$$

where K_m is the maximum spin value in that oscillator shell.

We recall from the previous discussion of angular momentum distributions in spherically symmetric nuclei, that it was possible to associate these with a moment of inertia (eqn. (3.33)). In this case we can introduce a moment of inertia correspondingly; it has to be taken with respect to the nuclear symmetry axis, because it is associated with the projections K on this axis (the ordinary collective moment of inertia is taken about an axis perpendicular to the symmetry axis) (cf. Halpern and Strutinski 1958, Strutinski 1956). Denoting this moment of inertia by $\mathscr{T}_\parallel$

$$\overline{K^2} = \nu K_1^2 = \frac{\mathscr{T}_\parallel T}{\hbar^2}. \quad . \quad . \quad . \quad . \quad . \quad . \quad . \quad (3.56)$$

At very high excitations, where pairing effects become unimportant, this moment of inertia tends to the rigid body value; at lower excitation its value is reduced below this limit, because the pairing energy reduces the number of unpaired particles.

From the known single particle level spacing, the known pairing energy and the known value of K_1, it is thus possible to calculate the density of intrinsic states at excitation energy U and with projection K on the symmetry axis. We will not reproduce the expression for this quantity, which is somewhat complicated, but refer to eqn. (3.3) *et seq.* of the original paper. In analogy with the situation near the nuclear ground state, each of these intrinsic states may be considered the parent of collective states. The vibrational states may be neglected due to their large spacing, which makes them account for only a rather small fraction of the total level density. The rotational states account on the average for a part

$$E_{\text{rot}} = \frac{\hbar^2}{2\mathscr{T}_\perp}\,(I(I+1) - K^2) \quad . \quad . \quad . \quad . \quad (3.57)$$

of the total excitation energy U, where $\mathscr{T}_\perp$ is the moment of inertia *perpendicular* to the symmetry axis. The density of states of spin I and projection K is thus by eqns. (3.56) and (3.57)

$$\rho_{IK}(U) \simeq \rho_{I=0\,K=0}(U) \exp\left[-\frac{\hbar^2}{2\mathscr{T}_\perp T}\,I(I+1) - \frac{\hbar^2}{2T}\left(\frac{1}{\mathscr{T}_\parallel} - \frac{1}{\mathscr{T}_\perp}\right)K^2\right]. \quad (3.58)$$

This form for the level density is useful in the interpretation of fission (cf. § 9). Each I can have all the values of the projection smaller than I, so that the density of states of spin I is

$$\rho_I(U) = \sum_{K \leqslant I} \rho_{IK}(U) \simeq \int_0^{I+\frac{1}{2}} \rho_{IK}(U)\, dK . \quad . \quad . \quad . \quad . \quad (3.59)$$

For small values of I the level density is thus proportional to $(2I+1)$ as is to be expected on account of the previous geometrical interpretation of this factor.

This model, which has no free parameters, gives a very good agreement with the experimental neutron resonances in this form. The odd–even effect enters naturally due to the pairing energy, and may be described as follows. The even–even nucleus behave similarly to the odd–odd once a pair has been broken and the same number of unpaired particles results in both cases. This costs an additional energy of 2δ. The odd mass nuclei are intermediate and an energy of δ is expected to produce the same situation. This gives the rules for relating the different level densities.

$$\left.\begin{aligned} \rho_{\text{odd}}(U) &= \rho_{\text{even}}(U+\delta), \\ \rho_{\text{odd-odd}} &= \rho_{\text{even}}(U+2\delta), \end{aligned}\right\} \quad . \quad . \quad . \quad . \quad (3.60)$$

valid for $U \gg \delta$.

It should be noted that already the intrinsic states provide a complete set of wave functions for the description of this model; the collective states can be built up from linear combinations of the intrinsic states, and in a certain sense this model therefore accounts for the same state twice. There is however a quasi-orthogonality between intrinsic and collective states close to the nuclear ground state; thus this model provides a useful approximation in so far as this quasi-orthogonality persists on the average at excitation energies near the neutron binding energy. In other words, the model remains valid as long as the collectiveness of the rotational wave function implies a rather strong lowering of energy compared to the intrinsic states which make up the linear combination.

Lang and Le Couteur (1959) have recently made an elegant investigation of the same model under the assumption that the entire level density is due to the intrinsic states only; thus the level density necessarily will be smaller than above with the same parameters. They first derive the level density of all spin states (corresponding to the level density of all intrinsic states in the Ericson treatment) and give a closed expression for this quantity using the same approximations as Eriscon, i.e. constant single particle spacings and constant pairing energies. The resulting approximate formula for the total level density $P(U)$ is

$$\left.\begin{aligned} P(U) &= \frac{\exp\left\{\dfrac{2U}{t} - \dfrac{\pi^2}{8} g_0 a e^{-a/t} + 1\right\}}{12(\pi t)^{5/2}(\frac{1}{6}g_0)^{3/2}} \\ U &= \tfrac{1}{6} g_0 \pi^2 t^2 \{\tfrac{1}{4} + \tfrac{3}{4}(1 + a/t)e^{-a/t}\} - t, \\ a &= 0{\cdot}874\delta. \end{aligned}\right\} \quad . \quad (3.61)$$

The angular momentum distribution is obtained by consideration of the probability of occupation and the average occupation numbers of the single particle states. In the direction of the nuclear symmetry axis only the unpaired particles contribute to the projection of the angular momentum; the probability of finding unpaired particle in the state ϵ_s is

$$p_s = \frac{2e^{\beta(\mu-\epsilon_s-\delta)}}{1+2e^{\beta(\mu-\epsilon_s-\delta)}+e^{2\beta(\mu-\epsilon_s)}}. \quad . \quad . \quad . \quad . \quad . \quad . \quad . \quad . \quad (3.62)$$

The average value of the total projection along the symmetry axis is thus

$$\overline{K^2} = \sum_s p_s \Omega_s^2 = \mathscr{T}_{\text{rigid}}\left(\lambda \cot\lambda + \eta \frac{d}{t}\right)t, \quad . \quad . \quad . \quad (3.63)$$

where

$$\cos\lambda = e^{-\beta\delta}$$

and

$$\eta = \begin{cases} 0 & \text{even nuclei,} \\ 1 & \text{odd mass nuclei,} \\ 2 & \text{odd nuclei.} \end{cases}$$

The rigid moment of inertia is that of the spherical nucleus. The term proportional to η arises from the particles which are unpaired even in the ground state.

While the pairs do not contribute to the angular momentum along the nuclear axis, they will in general have an angular momentum in the plane perpendicular to this direction. The contribution to the angular momentum, $\mathbf{Q}$, in this direction is thus due to both paired and unpaired particles. In the case of an even nucleus the total angular momentum of the system will be 0, if all the occupation numbers of the states have exactly their mean values; the angular momentum distribution will hence arise from the fluctuations of the occupation numbers from their mean values.

With the occupation number n_{s+} for the state s with projection $+\Omega_s$ on the symmetry axis and with n_{s-} for projection $-\Omega_s$ we have

$$\overline{n_{s+}^2} = \bar{n}_{s+}; \quad \overline{n_{s-}^2} = \bar{n}_{s-} \quad . \quad . \quad . \quad . \quad . \quad . \quad . \quad (3.64)$$

for the average value of the occupation numbers. The explicit form for $\bar{n}_{s+}$ and $\bar{n}_{s-}$ is

$$\bar{n}_{s+} = \bar{n}_{s-} = \frac{e^{\beta(\mu-\epsilon_s-\delta)}+e^{2\beta(\mu-\epsilon_s)}}{1+2e^{\beta(\mu-\epsilon_s-\delta)}+e^{2\beta(\mu-\epsilon_s)}}. \quad . \quad . \quad . \quad . \quad . \quad . \quad (3.65)$$

The expectation value of $\mathbf{Q}$ is obviously 0; the average value of its square due to the fluctuations is

$$\overline{Q^2} = \sum_s (j_{xs}^2 + j_{ys}^2)(\overline{n_{s+}^2} - \bar{n}_{s+}^2 + \overline{n_{s-}^2} - \bar{n}_{s-}^2), \quad . \quad . \quad . \quad . \quad (3.66)$$

where $\mathbf{j}_s$ is the single particle spin and the symmetry axis is taken as z-axis.

Under the assumption of deformations so small that they do not change the average value of $j_x^2 + j_y^2$ from the value for a spherical nucleus, this can be expressed in moments of inertia as

$$Q^2 = \mathscr{T}_{\text{rigid}}\left(1 + \lambda \cot\lambda + \eta \frac{d}{t}\right) = 2\mathscr{T}_{\perp} t, \quad . \quad . \quad . \quad . \quad (3.67)$$

which determines the distribution of angular momenta†.

† The rest of the discussion differs from the presentation by Lang and Le Couteur, though the conclusion is identical.

In the classical approximation the distribution of the projection K along the symmetry axis must be

$$\rho_K dK \propto e^{-\frac{\hbar^2}{2\mathscr{T}_{\|}t}K^2} dK. \quad . \quad . \quad . \quad . \quad . \quad . \quad . \quad (3.68)$$

The random coupling of the excited pairs and unpaired particles in the plane perpendicular to the axis gives the distribution of Q as

$$\rho_Q dQ \propto dQ_x dQ_y e^{-\frac{\hbar^2}{2\mathscr{T}_{\perp}t}(Q_x^2+Q_y^2)} \propto Q\, dQ e^{-\frac{\hbar^2}{2\mathscr{T}_{\perp}t}Q^2}. \quad (3.69)$$

Since $I^2 = Q^2 + K^2$, we have $Q\,dQ = I\,dI$ for fixed K. The distribution over both K and I is thus

$$\rho_{IK} dK\, dI \propto e^{-\frac{\hbar^2}{2\mathscr{T}_{\|}t}K^2 - \frac{\hbar^2}{2\mathscr{T}_{\perp}t}(Q_x^2+Q_y^2)} dK\, dQ_x dQ_y \propto e^{-\frac{\hbar^2}{2\mathscr{T}_{\perp}t}K^2 - \frac{\hbar^2}{2\mathscr{T}_{\perp}t}Q^2} dK Q\, dQ$$

$$\propto e^{-\frac{\hbar^2}{2\mathscr{T}_{\perp}t}I^2 - \frac{\hbar^2}{2t}\left(\frac{1}{\mathscr{T}_{\|}} - \frac{1}{\mathscr{T}_{\perp}}\right)K^2} dK I\, dI. \quad . \quad . \quad . \quad . \quad (3.70)$$

From the point of view that *all* states are represented by this equation, it will also contain the degeneracy of magnetic quantum numbers, $2I+1$, so that the actual distribution should have dropped such a factor. Therefore, in the quantal form and normalized

$$\rho_{IK}(U) = \frac{1}{4(2\pi)^{1/2}} \frac{\hbar^3}{(\mathscr{T}_{\perp}^2 \mathscr{T}_{\|})^{1/2}} \frac{1}{t^{3/2}} e^{-\frac{\hbar^2}{2\mathscr{T}_{\perp}t}I(I+1) - \frac{\hbar^2}{2t}\left(\frac{1}{\mathscr{T}_{\|}} - \frac{1}{\mathscr{T}_{\perp}}\right)K^2} P(U).$$

$$. \quad . \quad . \quad . \quad . \quad . \quad . \quad . \quad . \quad (3.71)$$

A factor of $\frac{1}{2}$ has been inserted so as to let $\rho_{IK}(U)$ refer to states of one parity only.

The distribution over I only is most easily obtained by observing that eqn. (3.70) has to be averaged over all possible directions of the symmetry axis in space. The total volume accessible in the angular momentum phase space must remain constant, so that we only have to replace the ellipsoidal volume determined by $\mathscr{T}_{\|}$ and $\mathscr{T}_{\perp}$ by the same spherical volume corresponding to an effective moment of inertia $\mathscr{T}_{\mathrm{eff}}$:

$$\mathscr{T}_{\mathrm{eff}} = \mathscr{T}_{\|}^{1/3} \mathscr{T}_{\perp}^{2/3} \quad . \quad . \quad . \quad . \quad . \quad . \quad (3.72)$$

with the spin distribution

$$\rho_I(U) = \frac{1}{4(2\pi)^{1/2}} \frac{\hbar^3}{\mathscr{T}_{\mathrm{eff}}^{3/2}} \frac{1}{t^{3/2}} (2I+1) e^{-\frac{\hbar^2}{2\mathscr{T}_{\mathrm{eff}}t}I(I+1)} P(U). \quad . \quad (3.73)$$

The comparison of the density of neutron resonances shows that in order to obtain agreement between these and the predictions of the model with pairing energies and conventional values of the single particle spacing, it would be necessary to reduce the value of δ considerably below the value necessary to account for the odd–even effect. At present it does not seem possible to obtain a fit to experiments by any reasonable values of single particle spacings and pairing energies, as long as the pairing energy is kept constant. This extremely interesting result is a clear indication that either the effective pairing energies are reduced with increasing excitation, which would not be unexpected, or that it is necessary to retain the complete analogy with the low energy spectrum as in the calculation of Ericson.

The models discussed so far are the principal current models for level densities; they have been worked out in detail and are well determined in terms of parameters which can be associated with other nuclear properties.

In addition there exists a number of other models aiming at explaining a particular feature. The indeterminate nature of most of these models makes it extremely difficult to ascertain their relative value, in particular as they usually are of phenomenological nature. We will dwell further only on some of these models of current interest.

Hurwitz and Bethe (1951) suggested that shell effects and odd–even effects on the level density should be accounted for phenomenologically by using a characteristic level different from the ground state and expressing the excitation energy with respect to this level. This conjecture seems well verified in the case of odd–even effect. (Newton 1956 a, Ericson 1958 a,b, 1959) (see fig. 3); the work of El Nadi and Wafik (1958) who attempted to use the semi-empirical mass formula including shell effects in a verification of this hypothesis, indicates that important shell effects will still remain which are not explained by the characteristic level.

3.9. *The Nuclear Phase Transition*

Some general features of systems with pairing interactions have been considered by Ericson (1958 b). It is shown that in general any system which has an additive single particle spectrum with an anomaly at the Fermi level that suppresses the excitation of unpaired particles, will lead to a relation between odd and even level densities according to eqn. (3.60). It is not of importance if pairs can be excited near the ground state or if they are suppressed by an effect similar to the pairing energy as in the case of an energy gap model (A. Bohr *et al.* 1958). The reason for this effect is that unpaired particles in the ground state are nearly equivalent to the even nucleus excited to an energy which has an equivalent number of unpaired particles, i.e. for one and two unpaired particles an energy δ and 2δ. Because of this it is also to be expected that this shift of energy will remain even if the average pairing energy $\bar{\delta}$ will go to 0 at higher excitations. We must therefore conclude that while it is necessary to use a nuclear model which includes the odd–even shift, it will in general not be possible to obtain additional information about the structure of the excited nucleus from this effect; it is rather connected with the behaviour of the nucleus at low excitation. Additional information can only be obtained from an actual comparison of predicted and observed level densities.

It is also pointed out by Ericson (1958 b) that in so far as there exists an energy gap or a pairing energy which does not depend on excitation energy, we must expect the temperature to vary more slowly with excitation energy than implied by eqn. (3.14) for equidistantly spaced single particle states, for all but the very lowest excitation energies. This effect is some-what similar to the constancy of the temperature which would result if

the nucleus is considered as a melting system (Weisskopf 1953, Trainor and Dixon 1956). Experimental evidence indicates a *nuclear* temperature (cf. eqn. (2.12)), which is approximately constant as a function of energy below 10 MeV in some medium weight elements (Fulbright *et al.* 1959, Ericson 1959, Brady and Sherr 1960). It is not yet possible to conclude that this effect is due to a nuclear melting because even the equidistant spacing model yields a *nuclear* temperature which is rather slowly varying for low excitation. The rather meagre experimental evidence indicates that the constancy of the nuclear temperature is more pronounced near closed shells.

Ross (1957) has analysed level densities in terms of the equidistant spacing model with the aim of extracting the corresponding single particle spacing. In the analysis she used the spin distribution (3.29) with a

Fig. 6

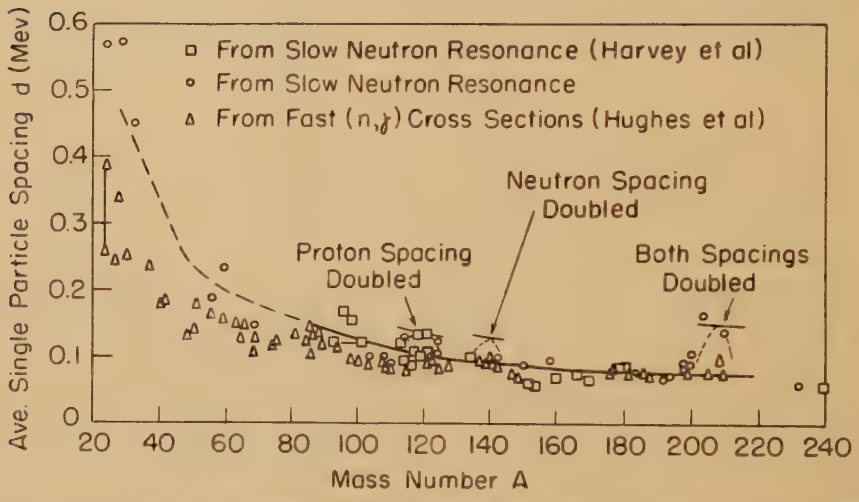

Single particle level spacings d as derived from experimental slow neutron resonances and (n, γ) cross sections and analysed according to the equidistant spacing model with rigid body moment of inertia (eqns. (3.15), (3.29) and (3.33)). The uncertainty in the points obtained from (n, γ) cross sections is considerably larger than in those from slow neutron resonances. The solid curve is a theoretical single particle level spacing essentially corresponding to that of the free Fermi gas with $r_0 = 1{\cdot}4$ Fermis. After Ross (1957).

corresponding moment of inertia (eqns. (3.33) and (3.39)) appropriate for a nuclear square well potential. No corrections for odd–even effects or shell effects were included. This way of analysis emphasizes the gross value and gross variation of the single particle spacing; it suppresses nearly all minor fluctuations. As an example, the well-established odd–even effect is not observable in this analysis. The low value of the single particle spacings which obtains in this way (fig. 6) is surprising in view of the strong pairing effects near the nuclear ground state; these

empirically derived single particle spacings $d = d_n d_p/(d_n + d_p)$ are of the same order as the spacings of single particle states as determined from nuclear spectroscopy once the degeneracy in magnetic quantum number is accounted for. The influence of pairing interactions would have tended to increase the spacings derived by Ross to values larger than the spectroscopic spacings if persisting to high excitation. This is in agreement with the previously discussed result of the pairing model, that there is a deficiency of states if constant pairing energies are used compared to the actually observed number. Only when a systematic lowering of collective states is assumed is agreement obtained. We are therefore led to the conclusion that either (1) pairing interaction effects decrease with increasing excitation and have little influence at excitation energies of the order of neutron binding energies, or (2) a separation between collective excitations and single particle excitations has still an average validity even at high excitation as in the Ericson treatment.

While it is possible that both of these possibilities are realized in different parts of the periodic system, the first of the two seems more attractive. This is particularly so in view of the recent description of pairing forces as analogous to the interactions giving rise to superconductivity (A. Bohr *et al.* 1958, Belyaev 1959, Soloviev 1959, Mottelson 1959).

In the case of a superconducting metal the electrons having momentum $(\mathbf{k}, -\mathbf{k})$ interact so as to form a quasi-bound pair state (Cooper 1956; Bardeen *et al.* 1957). Electrons in such paired configuration interact coherently with other pairs, exploiting a small part of the total Hamiltonian. The elementary excitations of the superconducting system are no longer even approximately determined by the simple Fermi sphere. The excitation of a pair of electrons or the breaking of a pair of electrons are both suppressed by an energy gap similar to the nuclear pairing energy. With increasing excitation the existence of excited pairs and broken electron pairs will more and more prevent the coherent scattering because of the exclusion principle, leading to a second order phase transition characterized by the disappearance of the energy gap. This transition takes place at a critical temperature; at higher temperatures the system will be in its normal state.

In the case of deformed nuclei the degenerate states characterized by the angular momentum projection $(+\Omega_s, -\Omega_s)$ on the nuclear symmetry axis strongly resemble the electron pairs of opposite momentum. These pairs can again scatter into unoccupied states of the same type, the interaction being usually considered to take place in the last major shell. The coherent scattering changes the spectrum of low lying excitations from $|\epsilon_s - \epsilon_0|$ into

$$E_s = \sqrt{[(\epsilon_s - \epsilon_0)^2 + \delta^2]} \quad . \quad . \quad . \quad . \quad . \quad . \quad (3.65)$$

where δ is a pairing energy due to the coherence. The excitation of a particle from a pair state r to a state s will cost an energy $E_r + E_s$, i.e. to a first approximation an energy of 2δ, if the states r and s are close to the Fermi level. Similarly the excitation of a pair in state s costs an energy

$2E_s$, again an energy of the order of 2δ. Thus both the excitation of pairs and the breaking of pairs are suppressed by this new pairing energy and it is no longer possible to regain the pairing energy by reforming a broken pair in another orbit. With increasing excitation the increasing number of broken pairs will reduce the total numer of states into which pairs can be scattered, thus reducing the effective value of δ. Again we must expect that at a critical energy, determined by the number of unpaired nucleons, the coherence will disappear and the pairing energy will become zero. This picture of the pairing forces seems to describe the low-energy pairing effects well. No detailed study of this model for higher excitations exists at present. Qualitatively we must expect some kind of nuclear phase transition to occur. The nuclear phase transition will certainly not have the sharpness of the transition in a superconductor due to the finiteness of the number of particles. It should manifest itself by a more rapid increase of the level density in the transition region and by a sudden increase in the moment of inertia associated with the spin distribution. The probable energy region of this transition must on account of the previous evidence be expected to be low and at least for heavy nuclei below the neutron binding energy. Tentative estimates based on a complete analogy with super-conductivity indicate transition energies to be of the order of 2–3·5 MeV for odd mass heavy nuclei.

Above the transition energy it should thus be possible to use the ordinary shell model to describe level densities; the excitation energy should not be counted from the ordinary ground state, but from a 'characteristic level', the exact position of which is not known at present.

3.10. *Conclusion*

The theoretical results on nuclear level densities are of two different types. First are the results of a general nature which do not depend critically on the detailed model. Such are the mainly exponential increase of the level density with energy, the qualitative influence of nuclear shell structure, the distribution of spins among the states and the odd–even effect. The understanding of these effects is rather complete and no major changes in our description of the way they arise is to be expected.

Second are the results connected with the actual *number* of states in an energy interval, the normalization of the level density. These predictions depend strongly on the detailed model used for the description and on the parameters, and they therefore provide sensitive tests of the validity of the model. Above we have presented arguments that the shell model without pairing interactions seems to provide an adequate description at the neutron binding energy with empirical values of the single particle spacing. The major present problem is therefore to obtain a detailed understanding of how the low-energy spectrum with essential pairing effects develops into the highly excited system with little average effect. We have given qualitative arguments for this based on present notions of pairing interactions which naturally seem to lead to a disappearance of

the pairing energy. Any definite conclusion must however await a detailed theoretical and experimental study of the properties of level densities below the neutron binding energy.

§ 4. The Evaporation Approximation

In any nuclear reaction there is a certain probability for the formation of a Compound Nucleus, which has a long lifetime compared to the nuclear relaxation time. The internal motion of the Compound Nucleus is completely randomized except for the exact quantum numbers, energy, angular momentum, etc. We will for the further discussion of this section assume that no restrictions are imposed by angular momentum conservation. These effects will be treated in detail in the next section.

The existence of a well-defined intermediate state of the Compound Nucleus permits the application of the principle of detailed balance; the transition probability from a state a to a state b, w_{ab}, is related to the transition probability from the state b to the state a, w_{ba} by

$$\rho_a w_{ab} = \rho_b w_{ba}^* \quad . \quad . \quad . \quad . \quad . \quad . \quad . \quad (4.1)$$

where ρ_a and ρ_b are the density of states a and b and the star on w_{ba} indicates the time-reversed transition, i.e. the transition in which all velocities and orbital angular momenta have changed sign.

The application of eqn. (4.1) to the Compound Nucleus is immediate, if the states have such a long lifetime that their width is much smaller than the level spacing. In the case of highly excited Compound Nuclei, which are often studied in nuclear reactions, the levels have large widths and overlap. In this case it is not possible to study the excited nucleus for a longer time than its lifetime and the uncertainty in energy is the corresponding width Γ. The principle of detailed balance (4.1) has in this case a meaning only as applied to the average transition probability for this energy interval.

The application of eqn. (4.1) to the case when several levels are within the width Γ is in general complicated due to the occurence of interference effects between the matrix elements. It might however be expected that the matrix elements have randomly distributed phases due to the randomized nature of the Compound Nucleus. This assumption is the basis of the Statistical Model. With this assumption the determination of cross sections averaged over an incident energy much larger than Γ will not depend on interference effects; all cross terms will disappear and the angular distribution becomes symmetrical around 90°. Interference effects will still occur, however, if the energy determination is better than the level width. A further discussion is found in § 11.

The statistical assumption of random phases has the consequence that the Compound Nucleus can be considered as a nearly classical system, as interference affects are the typical effects of wave mechanics, and such effects no longer occur in this approximation. In this case the Compound Nucleus is entirely analogous to a classical equilibrium system which is

decaying, the heated liquid drop or the radiation from a black body. These systems, both classical, are characterized, like all classical systems, by strongly overlapping levels. The case of radiation from a black surface is particularly similar. If radiation is incident on a hole in a nearly black box, there is a small but finite probability for emission after one or a few reflections within the box and this emission will still retain some phase and energy characteristics of the incident beam, corresponding to the direct interactions. The major part is reflected in a complicated way, comes to thermal equilibrium with the system and is finally emitted in a manner governed by phase space. The fact that both evaporation and black body radiation are determined by phase space makes it obvious that this is also a basic property of Compound Nucleus decay.

To see this we apply the principle of detailed balance (4.1) (Weisskopf 1937). Let the state a represent the intermediate Compound System which has a level density ρ_C. We denote the probability per unit time of emitting a particle ν with an energy E_ν by $P_\nu(E_\nu)$. The emitted particle has a statistical weight factor $g_\nu = 2s_\nu + 1$ due to its spin; it has velocity v_ν and momentum p_ν. The residual nucleus has excitation energy E_ν^* and a cross section for absorbing particles ν into the compound state, $\sigma_\nu^*(E_\nu)$. The nucleus and the particle are enclosed in a box of volume V. The probability of capture of particle ν by the nucleus is $v_\nu \sigma_\nu^*(E_\nu)/V$. The corresponding density of states is the phase space factor

$$g_\nu \frac{4\pi p_\nu^2}{h^3} \frac{dE_\nu}{dp_\nu} V$$

for the captured particle multiplied by the level density $\rho_\nu(E_\nu^*)$ of the residual nucleus. Observing that

$$\frac{dE_\nu}{dp_\nu} = v_\nu$$

we immediately have

$$\rho_C P_\nu(E_\nu) = g_\nu \frac{4\pi p_\nu^2}{h^3} \sigma_\nu^*(E_\nu) \rho_\nu(E_\nu^*). \quad . \quad . \quad . \quad . \quad . \quad (4.2)$$

We implicitly assumed an infinitely heavy target nucleus; the derivation should have been performed for a finite nucleus in the Centre-of-Mass system. Expressing the particle energy E_ν as channel energy rather than particle energy and replacing the velocity v_ν by the relative velocity between target and projectile the same expression results.†

The total probability of decay P is the sum of all particle probabilities of decay over all energies and all kind of particles.

$$P = \sum_\nu \int P_\nu(E_\nu)\, dE_\nu. \quad . \quad . \quad . \quad . \quad . \quad . \quad (4.3)$$

† We draw attention to the fact that in several currently used tables of cross-sections (Blatt-Weisskopf 1952, Shapiro 1953) the channel energy is called ' particle energy '. We are indebted to R. Sherr and E. Henley for pointing this out.

In an actual process the intermediate compound state is formed with a certain cross-section $\sigma_C(a)$. The cross section for a specific emission is therefore determined by the competition of a particular mode with all possible modes and is therefore the cross section $\sigma_C(a)$ multiplied by the relative probability of emission.

$$\sigma(a;\ E_\nu) = \sigma_C(a)\frac{P_\nu(E_\nu)}{P}, \quad . \quad . \quad . \quad . \quad . \quad . \quad . \quad (4.4)$$

which we write explicitly by eqn. (4.2) as

$$\sigma(a;\ E_\nu) = \sigma_C(a)\frac{g_\nu p_\nu{}^2 \sigma_\nu{}^*(E_\nu)\rho_\nu(E_\nu{}^*)}{\sum_\nu g_\nu \int_0^\infty p_\nu{}^2 \sigma_\nu{}^*(E_\nu)\rho_\nu(E_\nu{}^*)\,dE_\nu}, \quad . \quad . \quad . \quad (4.5)$$

which is referred to as the Weisskopf–Ewing formula (1940).

Equation (4.5) contains most of the characteristics of the statistical decay. The decay is independent of the way in which the compound state was initially formed; this feature depends however on the explicit assumption of no angular momentum restrictions and is not generally valid. The dynamics of the decay process are entirely contained in the inverse cross-section $\sigma_\nu{}^*(E_\nu)$, while the remainder of the factors are due to the available phase-space. The dominating influence in the inverse cross-section is due to the penetrabilities and in this sense we can regard the Statistical Model as a phase space description of the decay including the effects of barrier penetration. The usefulness of the model is essentially due to the generality of the phase-space concept and to the fact that the density of states in the intermediate nucleus is irrevelant in so far as the experimental energy resolution is many times the average width of the states (overlapping levels) or contains many states (non-overlapping levels). The weakness of the description is the occurrence of inverse cross sections which refer to excited states, for these cannot be determined experimentally. In particular it is not evident that the size, shape or barrier penetrabilities of the excited nucleus will be the same as in the ground state. Such effects will be discussed in some detail in § 6. The remaining characteristic feature of eqn. (4.5) is the occurrence of the level density of the residual nucleus. In the preceding sections we have discussed the theory of this quantity, which permits a direct comparison between theory and experiments. It should be noticed, however, that eqn. (4.5) contains ratios of level densities and that it will therefore mainly give the variation of the level density with energy. Furthermore, the experiments which give the most useful information on the level density are the energy spectra of emitted particles which according to eqn. (4.5) contain the factor $\sigma_\nu{}^*(E_\nu)\rho_\nu(E_\nu{}^*)$. Therefore, the inverse cross section is not separated from the level density. The usual procedure is to divide out, not the unknown inverse cross section, but the cross section $\sigma_\nu(E_\nu)$ for the nucleus in its ground state. The remaining quantity therefore consists, not only of the level density, but also of the ratio $\sigma_\nu{}^*(E_\nu)/\sigma_\nu(E_\nu)$. The influence of this quantity can be studied by comparing different reactions leading to the same residual

nucleus by emissions of different kinds of particles. At present there seems to be little evidence for strong deviations from ground state cross-sections for excitation energies below 50 MeV.

In spite of these principal difficulties, the generality of the phase space description is such that the Compound Nucleus description is rather satisfactory for a very large class of nuclear reactions. In the entire description it avoids explicit reference to the detailed dynamics of the emission process and to the possibility of preformation of the emitted particle inside the nucleus. These quantities are implicitly contained in the inverse cross section, and in particular it is not possible to introduce preformation as an additional and separate concept.

It should also be noticed that there has been no specification as to what kind of particles are emitted. As a consequence the Statistical Model, being mainly a phase space model, also encompasses the emission of complex, heavy particles and even of fission (Fong 1956), if the available phase space for these processes becomes large. We refer to later sections.

There exists a purely classical approximation to eqn. (4.5), the evaporation approximation, which makes the analogy with evaporation from a classical liquid drop complete. This approximation is extremely useful, when used discriminately, to obtain first estimates of cross sections, excitation functions and shapes of the energy spectra of the emitted particles, although it is certainly not accurate enough for a detailed description.

The evaporation approximation involves two assumptions: (1) The nucleus is considered as a classical black body which absorbs all particles incident on its surface. The particles are considered to have completely classical trajectories so that in the absence of barriers the cross section would be completely geometrical; with Coulomb barriers B_ν the inverse cross-section is in this approximation

$$\sigma_\nu^*(E_\nu) = \left\{ \begin{array}{ll} 0 & \text{for} \quad E_\nu < B_\nu, \\ \pi R^2 \left(1 - \frac{B_\nu}{E_\nu}\right) & \text{for} \quad E_\nu > B_\nu, \end{array} \right\} \quad . \; . \; . \quad (4.6)$$

(Blatt and Weisskopf 1952). (2) The nuclear temperature (eqn. (2.12)) is taken to be a constant in the relevant region of emission, so that the level density $\rho_\nu(E_\nu^*)$ can be approximated by $\rho_\nu(U_\nu) e^{-\frac{E\nu}{T}}$, where $E_\nu^* = U_\nu - E_\nu$.

If the object is to obtain a first orientation of the cross sections or relative cross sections, the nuclear radius R and the nuclear temperature T may be considered the same in the different residual nuclei, as long as the Coulomb barriers are not concerned. This approximation is somewhat more restrictive than the preceding.

Introducing the non-relativistic channel energy for particles $p_\nu^2/2\mu_\nu = E_\nu$ with μ_ν the reduced mass of particle ν into eqn. (4.5) we can write (neglecting γ-emission)

$$\sigma(a\,;\; E_\nu) = \sigma_C(a) \frac{g_\nu \mu_\nu E_\nu \sigma_\nu^*(E_\nu) \rho_\nu(E_\nu^*)}{\sum_\nu g_\nu \mu_\nu \int_0^\infty E_\nu \sigma_\nu^*(E_\nu) \rho_\nu(E_\nu^*) dE_\nu} \quad . \; . \; . \; . \; . \quad (4.7)$$

In the evaporation approximation the distribution in energy of the emitted particles is therefore

$$\sigma(a;\ E_\nu) \propto \left\{ \begin{array}{ll} 0 & \text{for} \quad E_\nu < B_\nu, \\ (E_\nu - B_\nu) e^{-\frac{E_\nu}{T}} & \text{for} \quad E_\nu > B_\nu. \end{array} \right\} \quad . \ . \ . \quad (4.8)$$

Particularly, in the case of neutrons for which there is no Coulomb barrier, it is given by

$$\sigma(a;\ E_n) \propto E_n e^{-\frac{E_n}{T}}, \quad . \ . \ . \ . \ . \ . \ . \quad (4.9)$$

which is exactly the Maxwellian energy distribution of particles evaporated from a liquid, which has given the name to this approximation and the name evaporation spectrum to eqn. (4.5). The typical shape of evaporation spectra is thus the low value below the Coulomb barrier, the rapid rise in the neighbourhood of the barrier with a maximum which, in the case of eqn. (4.8), is at an energy

$$E_{\nu m} = B_\nu + T. \quad . \ . \ . \ . \ . \ . \ . \ . \ . \quad (4.10)$$

The average energy $\bar{E}_\nu$ is similarly obtained to be

$$\bar{E}_\nu = B_\nu + 2T. \quad . \ . \ . \ . \ . \ . \ . \ . \ . \quad (4.11)$$

At energies of the emitted particle larger than $E_{\nu m}$ the cross section decreases exponentially. We want, however, to emphasize, that, in the case of charged particles, the actual maximum of the spectrum due to the tunneling effect occurs even below the classical barrier in many cases (cf. § 6).

A similar estimate can be made for the spectrum of evaporated γ-rays. The main part of the evaporated γ-rays is usually dipole radiation. The inverse cross-section is therefore proportional to E_γ for γ-energies that are such that the compound state energy is well below the dipole giant resonance energy of 15–20 MeV. The phase space factor ${p_\gamma}^2$ of eqn. (4.5) is in this case proportional to ${E_\gamma}^2$ so that the spectrum of γ-rays is

$$\sigma(a;\ E_\gamma) \propto {E_\gamma}^3 e^{-\frac{E\gamma}{T}} \quad . \ . \ . \ . \ . \ . \quad (4.12)$$

with a maximum energy

$$E_{\gamma m} = 3T, \quad . \ . \ . \ . \ . \ . \ . \ . \quad (4.13)$$

and a mean energy

$$\bar{E}_\gamma = 4T. \ . \ . \ . \ . \ . \ . \ . \ . \ . \quad (4.14)$$

In the remainder of this section we will discuss gross-features of cross sections on the basis of the evaporation approximation. It must be kept clearly in mind that these estimates represent simple tendencies for relative cross sections and are intended for orientation only. In this discussion we will neglect the emission of γ-rays as compared to particle emission, a procedure which is justified for excitation energies of the Compound Nucleus higher than a few MeV above the neutron binding energy. This discussion therefore does not immediately apply to capture reactions. The total cross section for emission of a particle ν is obtained by substituting the evaporation approximation into eqn. (4.7) and integrating over all energies of the emitted particle. We carry the integration over the energy E_ν up to the limit $+\infty$, because the exponential

decrease of the spectrum implies that this procedure introduces only small errors. With the same nuclear radii and temperatures we therefore get for the cross section $\sigma(a\,;\ \nu)$ initiated by a process a;

$$\sigma(a\,;\ \nu)=\sigma_C(a)\frac{g_\nu\mu_\nu\rho_\nu(U_\nu-B_\nu)}{\sum_\nu g_\nu\mu_\nu\rho_\nu(U_\nu-B_\nu)} \quad . \quad . \quad . \quad . \quad (4.15)$$

Here U_ν is the maximum possible energy of the residual nucleus after emission of the particle ν and is therefore determined by the reaction Q-value,

$$U_\nu=E_a+Q_{a\nu} \quad . \quad . \quad . \quad . \quad . \quad . \quad . \quad . \quad . \quad (4.16)$$

with E_a the incident channel energy. In writing the level densities in eqn. (4.15) as $\rho_\nu(U_\nu-B_\nu)$ we have explicitly used the assumption of a constant nuclear temperature. Equation (4.15) can be still further simplified by observing that the level densities of neighbouring nucleides are very similar but for the odd–even effect (eqn. 3.60). In the preceding section we showed that the odd–even effect was equivalent to a shift in the excitation energy by an amount closely equal to the pairing energy as entering in nuclear binding energies.

We introduce the notation δ_ν for this shift, so that

$$\delta_\nu=\left\{\begin{array}{ll} 0 & \text{for even residual nuclei,} \\ \delta & \text{for odd mass residual nuclei,} \\ 2\delta & \text{for odd residual nuclei.} \end{array}\right\} \quad . \quad . \quad (4.17)$$

Introducing eqns. (4.16) and (4.17) into eqn. (4.15) we therefore obtain in this approximation

$$\sigma(a\,;\ \nu)=\sigma_C(a)\frac{g_\nu\mu_\nu\exp\left\{\dfrac{Q_{a\nu}+\delta_\nu-B_\nu}{T}\right\}}{\sum_\nu g_\nu\mu_\nu\exp\left\{\dfrac{Q_{a\nu}+\delta_\nu-B_\nu}{T}\right\}}, \quad . \quad . \quad . \quad . \quad (4.18)$$

which is in a convenient form.

An interesting consequence of this odd–even effect in the nuclear level density, namely that the cross-sections $\sigma(a\,;\ \nu)$ should not vary appreciably with the oddness or evenness of the target, is apparent from eqn. (4.18). According to eqn. (4.18) the condition for this result is that

$$Q_{a\nu}+\delta_\nu-Q_{a\nu'}-\delta_{\nu'}=\text{const.}, \quad . \quad . \quad . \quad . \quad . \quad . \quad . \quad (4.19)$$

where the constant has to be independent of the decaying Compound Nucleus. In so far as the odd–even effect of the level density is describable by a shift in the excitation, which coincides exactly with the pairing energy, this is indeed so. As an illustration consider the decay of an even–even and an even–odd Compound Nucleus by α-particle and neutron emission. Denote the Q-values without pairing effects by $Q_{\alpha 0}$ and Q_{n0}. The expression of eqn. (4.19) is therefore in the case of an even-even nucleus $Q_{\alpha 0}+0-(Q_{n0}-2\delta)-\delta$, in the case of an even–odd nucleus it is $Q_{\alpha 0}+\delta-Q_{n0}-0$, and therefore in both cases $Q_{\alpha 0}-Q_{n0}+\delta$.

This result can easily be shown to be approximately valid even outside the evaporation approximation, and it applies also to capture reactions. In considering this effect we neglected the differences in pairing energies

for neutrons and protons. If, as seems probable, the odd–even shift is the sum of half the pairing energies of the odd nucleons, the effect will still be valid even in regions of large differences of proton and neutron pairing energies. Discontinuities in pairing energies should be noticeable, however.

We can state this rule in the following way:

The combined pairing effects in binding energies and level densities cancel in such a way that evaporation cross sections become approximately independent of pairing effects.

While no systematic attempt at verifying this rule has been made, it has been observed that (p, α) cross sections in medium weight elements do not show odd–even regularities (Fulmer and Cohen 1958). The effect should provide one of the best means of indirect study of the odd–even shift of the level density.

The shape of the energy spectrum of the emitted particles as given by eqn. (4.5) will in general depend on the excitation energy of the Compound Nucleus. If the inverse cross section $\sigma_\nu^*(E_\nu)$ depends neligibly on excitation energy and the nuclear temperature T is a constant over the pertinent range of excitation the shape of the spectrum is proportional to

$$\sigma(a;\ E_\nu) \propto E_\nu \sigma_\nu^*(E_\nu)\, e^{-\frac{E_\nu}{T}}, \qquad . \ . \ . \ . \quad (4.20)$$

which does not depend on the excitation energy of the Compound Nucleus. Variation of the shape of the energy spectrum with excitation energy is thus evidence that one or both of these assumptions are invalid.

§ 5. The Statistical Model and Angular Momentum Conservation

In the preceding section we considered the decay of an equilibrium system with the explicit assumption that no restrictions were imposed by angular momentum conservation. In this section we will investigate to what extent this approximation can be considered valid and extend the treatment to the general case.

While discussing the statistical assumption of randomly interfering matrix elements we noted that this assumption made the analogy between the decay of the Compound System and the decay of the classical equilibrium system complete. This approximation does not by itself imply that all effects of the non-commutativity of operators can be neglected; in particular, quantum effects due to spin and angular momentum will still exist. The classical nature of the statistical assumption has, however, the consequence that the effects of angular momentum conservation can be perfectly well understood from completely classical considerations simply by regarding all angular momenta as classical vectors, neglecting the intrinsic spins $\frac{1}{2}\hbar$ of neutrons and protons. The results of this approximation are nearly always qualitatively and quantitatively right.† This has the

† The quantal results, in so far as the Compound Nucleus decays to a few definite states of the residual nucleus, have been treated by Wolfenstein (1951) and Hauser and Feshbach (1952). The latter article though apparently dealing with inelastic neutron scattering can with a few trivial changes be applied to more general reactions.

additional advantage of avoiding the Clebsch–Gordan formalism, which becomes difficult to handle when many and high angular momenta occur.

5.1. *Qualitative Considerations*

In the spirit of the statistical model as a phase space description of the decay of the equilibrium system, it is therefore natural to take angular momentum effects into account by the available angular momentum phase space.

Consider the decay of a Compound Nucleus which has been formed with angular momentum **I**. The emitted particle has an orbital angular momentum **l**, the residual nucleus a spin **j**. The conservation angular momentum requires

$$\mathbf{I}=\mathbf{l}+\mathbf{j}. \quad . \quad . \quad . \quad . \quad . \quad . \quad . \quad . \quad . \quad (5.1)$$

The assumption of the preceding section that the decay of the Compound Nucleus was independent of any restrictions arising from angular momentum conservation therefore implies that eqn. (5.1) should give rise to no restrictions on the direction or length of the orbital angular momentum **l** of the emitted particle. Such limitations are in general imposed because the value of the spin of the residual nucleus is not arbitrary. For a constant **I** we have the relation between the volume elements $d^3\mathbf{l}$ and $d^3\mathbf{j}$ of **l** and **j**:

$$d^3\mathbf{l}+d^3\mathbf{j}=0. \quad . \quad . \quad . \quad . \quad . \quad . \quad . \quad . \quad . \quad (5.2)$$

If, therefore, no restrictions are imposed on the volume element $d^3\mathbf{l}$ the same is true for $d^3\mathbf{j}$, which means that every unit volume of the phase space corresponding to **j** is equally probable. Therefore the probability of levels in the residual nucleus having spin between j and $j+dj$ is

$$\rho_j\, dj \propto 4\pi j^2\, dj. \quad . \quad . \quad . \quad . \quad . \quad . \quad . \quad . \quad (5.3)$$

Comparing this to the previous discussion of the distribution of spins among the levels in the excited nucleus (eqns. (3.27)–(3.29)) we find that the corresponding quantal distribution is

$$\rho_j \propto 2j+1, \quad . \quad . \quad . \quad . \quad . \quad . \quad . \quad . \quad . \quad (5.4)$$

which thus leads to a complete decoupling between the formation and decay models of the Compound Nucleus. Therefore, the neglect of angular momentum conservation is a good approximation only when the j-values corresponding to the effective values of I and l in the process are distributed according to eqn. (5.4).

The extreme opposite case obtains when the spin **j** of the residual nucleus is very small, so that the orbital angular momentum of the emitted particle has to align completely with the angular momentum of the Compound Nucleus by eqn. (5.1). As the orbital angular momentum is always perpendicular to the direction of motion of the particles, these will all be in the plane perpendicular to **l**. We can therefore describe their angular distribution by the Dirac delta function $\delta(\mathbf{n}\,.\,\mathbf{l})$, where **n** is the direction of emission. If the spin of the target nucleus is 0 or small, we can consider the angular momentum of the Compound Nucleus as entirely due to the orbital angular momentum of the incident particle and it is therefore

perpendicular to the incident beam. We have therefore to average the angular distribution, as given by the delta function above, over all directions perpendicular to the beam, i.e. over the azimuthal angle ϕ. The angular distribution for the aligned case, $W_a(\theta)$, is then

$$W_a(\theta) \propto \frac{1}{2\pi}\int_0^{2\pi} \delta(\mathbf{n}.\mathbf{I})\, d\phi = \frac{1}{\pi I \sin\theta} \quad . \quad . \quad . \quad . \quad (5.5)$$

where θ is the angle between the direction of emission and the beam direction. A typical feature of eqn. (5.5) is its large value for small $\sin\theta$. This occurs, because particles are emitted in the forward and backward direction for every direction of **I**, when the alignment is complete, and is therefore due to a 'piling up' effect. Therefore even a small decoupling of **l** from **I** will smear the angular distribution near the beam direction, while it remains essentially unchanged elsewhere, removing the discontinuity.

We will now discuss the qualitative aspects of the angular distribution in more general cases. At present we will neglect any dynamical effects, which will effect the penetrabilities of the outgoing particles. These are taken to be constant.

If the emitted particle leaves the residual nucleus in a state of definite spin j_f, the conservation of angular momentum, eqn. (5.1), obviously implies that **l** has to end on a sphere of radius j_f around **I** (see fig. 7). Thus, while **l** still is essentially aligned with **I**, it is decoupled from **I** by the freedom to end anywhere on this sphere. There will therefore be a maximum decoupling angle, ϑ_0, determined by

$$\sin\vartheta_0 = \frac{j_f}{I}. \quad . \quad . \quad . \quad . \quad . \quad . \quad . \quad . \quad . \quad (5.6)$$

Fig. 7

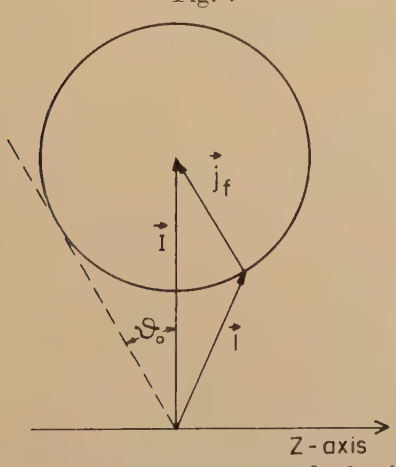

Coupling of angular momentum vectors in case of a 0 spin target and a residual nucleus of spin j_f. The orbital angular momentum **l** of the emitted particle is restricted to lie on a sphere of radius j_f around the end point of the angular momentum I of the incident particle. The decoupling angle ϑ_0 is the angle between **I** and a tangent to the sphere.

Because of the decoupling, the angular distribution (5.5) will now be smeared near the beam direction within an angle of the order of the decoupling angle. For directions far from the beam direction the angular distribution is nearly unchanged and is still close to $1/\sin\theta$. For constant penetrabilities the angular distribution can be obtained explicitly (Ericson 1960) in this limit

$$W(\theta) \propto \begin{cases} 1 & \text{for} \quad \sin\theta < \sin\vartheta_0 = \dfrac{j_f}{I} \\ \dfrac{2}{\pi} \arcsin \dfrac{j_f}{I \sin\theta} & \text{for} \quad \sin\theta > \sin\vartheta_0 = \dfrac{j_f}{I} \end{cases} \quad . \quad . \quad (5.7)$$

which clearly expresses the features obtained from the qualitative discussion (see fig. 8) The characteristic of this asymptotic geometric angular distribution is the constancy for angles $\sin\theta < \sin\vartheta_0$ and the minimum at 90°. For $\sin\vartheta_0 > 1$ it reduces to the isotropic distribution. In this case dynamic effects become important and can even give rise to a maximum at 90°. As this article mainly deals with the decay of the Compound Nucleus to many levels in the residual nucleus, we will refrain from the further

Fig. 8

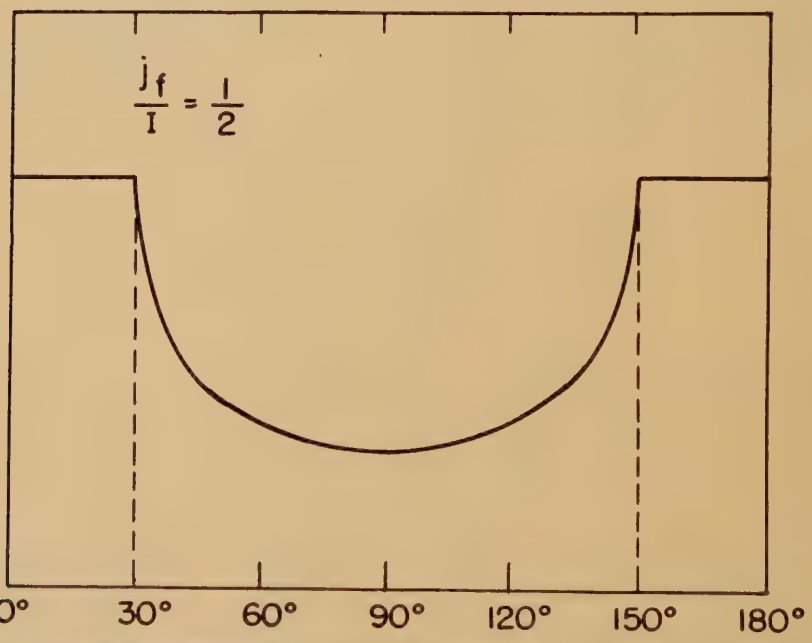

Classical angular distribution of particles emitted in the case of a 0 spin target and a residual nucleus of spin j_f. The transmission coefficients of the emitted particles are assumed independent of its orbital angular momentum. The ratio between the spin of the residual nucleus j_f and the angular momentum I of the Compound Nucleus is $\frac{1}{2}$. In the quantal case the angular distribution will be more smeared in the neighbourhood of the decoupling angle. After Ericson (1960).

discussion of different cases of transitions to one level in the residual nucleus and refer to the literature (Wolfenstein 1951, Hauser and Feshbach 1952, Ericson 1960).

In the case of transitions to many states in the residual nucleus, it is more appropriate to study the angular distribution for fixed value of the angular momentum l of the emitted particle and varying lengths of the spin j of the residual nucleus. The exponential cut-off factor in the spin distribution of the level density, eqns. (3.27)–(3.29), will again tend to align **l** and **I** to within a decoupling angle ϑ_0. When **l** is only weakly decoupled from **I**, we can estimate this angle as follows: the probability of reaching residual states of spin **j** is proportional to $\exp\{-j^2/2\sigma^2\}$. Thus by eqn. (5.1) the probability of **l** making an angle ϑ with **I** is determined by

$$e^{-\frac{(\mathbf{l}-\mathbf{I})^2}{2\sigma^2}} = e^{-\frac{(l-I)^2}{2\sigma^2}-\frac{lI}{\sigma^2}(1-\cos\vartheta)} \simeq e^{-\frac{(l-I)^2}{2\sigma^2}} e^{-\frac{lI}{2\sigma^2}\vartheta^2} = e^{-\frac{(l-I)^2}{2\sigma^2}} e^{-\frac{\vartheta^2}{\vartheta_0^2}} . \quad (5.8)$$

for small ϑ. This therefore determines the decoupling angle ϑ_0 to be of the order

$$\vartheta_0 \simeq \left(\frac{2\sigma^2}{lI}\right)^{\frac{1}{2}} . \quad (5.9)$$

As before the angular distribution will be smeared in a region of the order of ϑ_0 around the beam direction, while it has the character of $1/\sin\theta$ as in the aligned case for angles with $\sin\theta > \sin\vartheta_0$. We note that the relative emission probability is reduced by a factor r_{Il} defined as the effective solid angle $\Omega_0 = \pi\vartheta_0^2$ within which **l** lies, compared to the total solid angle 4π and multiplied by the reduction factor $\exp\{-(l-I)^2/2\sigma^2\}$. Thus

$$r_{Il} = \frac{\pi\vartheta_0^2}{4\pi} e^{-\frac{(l-I)^2}{2\sigma^2}} = \frac{\sigma^2}{2lI} e^{-\frac{(l-I)^2}{2\sigma^2}} . \quad (5.10)$$

Therefore not only the angular distribution is affected but also the total emission probability. This effect favours the emission of particles of angular momentum l close to I for large I.

In the discussion so far we have implicitly assumed that **l** has nearly the same direction as **I**, i.e. that the decoupling angle $\vartheta_0 \ll \pi/2$. In view of the strong directional correlation between these two vectors in this case we will call this the case of strong coupling of **l** to **I**. When the decoupling angle ϑ_0 becomes of the order of $\pi/2$, there is very little restriction on the direction of the orbital angular momentum **l** and the angular distribution becomes nearly isotropic. Because of the weak directional correlation between **l** and **I** we therefore call $\sin\vartheta_0 > 1$ the weak coupling case.

In the weak coupling limit it is useful to consider the emission of particles as analogous to the classical evaporation from a slowly rotating liquid drop. From our treatment of the distribution of spins among the levels in the excited nucleus we found that it was formally possible to take this into account by considering part of the excitation energy as being due to rotational motion (eqn. (3.30)); the moment of inertia associated with the rotation tends towards the rigid body value at high excitation (eqn. (3.38)).

In the discussion of the influence of angular momentum effects as due to the spin–cut-off factor σ in the level density, we could therefore as well have considered the angular momentum conservation (5.1) to be supplemented by energy conservation with rotational energy accounted for:

$$U = U_0 + \frac{\hbar^2}{2\mathscr{T}}\mathbf{j}^2. \quad . \quad . \quad . \quad . \quad . \quad . \quad . \quad . \quad (5.11)$$

Here U_0 is the excitation energy due to internal modes of excitation only. From eqn. (5.11) we conclude that the treatment in the previous section where angular momentum effects were neglected corresponds to the assumption of an infinite or very large moment of inertia in order that the residual nucleus acts as a reservoir to take up the angular momentum balance. This is in complete agreement with eqns. (5.2)–(5.4) which state that the nuclear spin-distribution is due to phase space only in the case of no angular momentum restrictions. (cf. eqn. (3.29)).

In order to study the deviations due to angular momentum conservation from the simple evaporation approximation of the preceding section we consider the rotational energy of eqn. (5.11) to be small. We make an expansion in the angular velocity $\boldsymbol{\omega} = \hbar\mathbf{I}/\mathscr{T}$ of the Compound System. In any measurable quantity we will only find terms proportional to powers of ω^2, because, averaging over the direction of spin $\mathbf{I}$ of the Compound Nucleus, $+\mathbf{I}$ and $-\mathbf{I}$, thus $\boldsymbol{\omega}$ and $-\boldsymbol{\omega}$, enter on an equal basis. The angular distribution of emitted particles will be symmetric about 90° for the same reason. The only quantity in ω^2 associated with the emitted particle is the fraction of the total rotational energy $(\mu R^2/\mathscr{T})E_{\text{rot}}$, due to this particle, when it is at the nuclear equator. Here $E_{\text{rot}} = \mathscr{T}\omega^2/2$ is the rotational energy of the Compound Nucleus. In order to make this expansion parameter dimensionless it has to be divided by the other characteristic energy of the particle, its average kinetic energy $2T$ just inside the nuclear surface. Using only the first correction term to the isotropic angular distribution we can approximately write the actual distribution

$$W(\theta) \propto 1 + \text{const.}\frac{\mu R^2}{\mathscr{T}}\frac{E_{\text{rot}}}{2T}.\cos^2\theta. \quad . \quad . \quad . \quad (5.12)$$

It will later be shown that the constant is unity. Similarly we can estimate the change in the average kinetic energy due to the rotation for the emission of neutrons. This depends on the same expansion parameter and is thus

$$\bar{E} \simeq 2T + \text{const.}\frac{\mu R^2}{\mathscr{T}}E_{\text{rot}} \quad . \quad . \quad . \quad . \quad . \quad (5.13)$$

and the constant will be shown to be $\frac{4}{3}$.

5.2. *Formal Solution of the Classical Approximation*

We will now proceed more formally and put the previous qualitative discussion in a quantitative form. The mathematical technique is that of Ericson and Strutinski (1958) and Ericson (1960). As before we neglect

the intrinsic spins of emitted particles compared to their orbital angular momenta, though we take them into account as statistical factors. We also neglect the spin of the target nucleus.

As in the preceding section the derivation makes use of the principle of detailed balance. Consider the decay of a compound system of angular momentum $\mathbf{I}$ by emission of a particle ν of energy E_ν and orbital angular momentum $\mathbf{l}$ in the direction $\mathbf{n}$. The residual nucleus is left with an excitation energy $E_\nu{}^*$ and a spin $\mathbf{j}$. The probability of decay per unit time by this emission is denoted by $P(\mathbf{I};\ E_\nu,\ \mathbf{n})$. We denote the density of states of angular momentum $\mathbf{I}$ in the Compound Nucleus by $\rho_c\,(\mathbf{I})$, the corresponding quantity in the residual nucleus of spin $\mathbf{j}$ by $\rho_\nu(E_\nu,\ \mathbf{j})$. Detailed balance applied to this classical problem therefore gives

$$\rho_c(\mathbf{I})\,P(\mathbf{I};\ E_\nu,\ \mathbf{n})\,dE_\nu\,d\Omega_\nu = \frac{d^3\mathbf{p}_\nu}{h^3}\,g_\nu v_\nu \int d\sigma_{\mathbf{l}}(\mathbf{n}, E_\nu) \int \delta^{(3)}(\mathbf{l}+\mathbf{j}-\mathbf{I})\,\rho_\nu(E_\nu{}^*,\ \mathbf{j})\,d^3\mathbf{j} \quad . \quad . \quad (5.14)$$

in analogy to eqn. (4.2). Here $d\sigma_{\mathbf{l}}(\mathbf{n}, E_\nu)$ is the pertinent inverse cross section, i.e. the cross section for capture into the compound state of particles incident on the excited residual nucleus with orbital angular momentum $-\mathbf{l}$ from the direction $-\mathbf{n}$, and $\delta^{(3)}(\mathbf{r})$ is the ordinary 3-dimensional Dirac delta function.

In the following we will use inverse transmission coefficients and cross sections for the emitted particles without explicit notation. The corresponding quantities for the incident particle refer to the nucleus in its ground state.

The partial inverse cross section $d\sigma_{\mathbf{l}}(\mathbf{n},\ E_\nu)$ can, following Ericson and Strutinski (1958), be expressed in terms of the scalar product of $\mathbf{l}$ and $\mathbf{n}$ and the Dirac delta function as (cf. eqn. (5.5) and earlier)

$$d\sigma_{\mathbf{l}}(\mathbf{n}, E_\nu) = \lambda\!\!\!^{-2}\delta(\mathbf{n}\,.\,\mathbf{l})\,\mathsf{T}_l^{(\nu)}(E_\nu)\,d^3\mathbf{l}, \quad . \quad . \quad . \quad . \quad (5.15)$$

which simply expresses the perpendicularity of the direction of motion to the orbital angular momentum. The dynamics of the problem are contained in the transmission coefficients $\mathsf{T}_l^{(\nu)}(E_\nu)$ for absorption of the lth partial wave.

The density of states $\rho_\nu(E_\nu{}^*,\ \mathbf{j})$ in eqn. (5.14) has been discussed in detail in § 3. The distribution of spins was there shown to be

$$\rho_\nu(E_\nu{}^*, \mathbf{j}) = \rho_\nu(E_\nu{}^*, 0)\,e^{-\frac{\hbar^2}{2\mathscr{T}_\nu T_\nu}\mathbf{j}^2} = \rho_\nu(E_\nu{}^*, 0)\,e^{-\frac{\mathbf{j}^2}{2\sigma_\nu{}^2}} = \frac{1}{\pi}\rho_{0\nu}(E_\nu{}^*)\,e^{-\frac{j(j+1)}{2\sigma_\nu{}^2}} \quad (5.16)$$

We will in different contexts make use of these forms. The last is the quantal correspondence.

If the transition, instead of taking place to many states as represented by eqn. (5.16), goes to an individual state of spin j_f, the corresponding density of spin-states is classically

$$\rho(\mathbf{j})\,d^3\mathbf{j} = \frac{\delta(j-j_f)}{\pi\,.\,2j}\,d^3\mathbf{j}. \quad . \quad . \quad . \quad . \quad . \quad . \quad (5.17)$$

This case has been treated in detail by Ericson (1960) and we refer to the original article.

We denote the differential cross section for particles emitted in the direction $\mathbf{n}$ with energy E_ν by $\sigma(\mathbf{n}, E_\nu)$. Just as we obtained the cross section for a reaction in the preceding section (eqn. (4.4)) by multiplying the total cross section for Compound Nucleus formation by the relative probability of decay, so we obtain the differential cross section $\sigma(\mathbf{n}, E_\nu)$ by multiplying the cross section for formation of the Compound Nucleus with angular momentum $\mathbf{I}$ by its relative probability of decay; the product is then integrated over all $\mathbf{I}$. We observe that the total probability of decay per unit time of a system of angular momentum $\mathbf{I}$, $P(\mathbf{I})$, as well as the total probability of emission of a particle ν with energy E_ν, $P(\mathbf{I}; E_\nu)$ must be independent of the orientation of the system.

We can therefore write the cross section

$$\sigma(\mathbf{n}, E_\nu) = \int \lambda_i^2 \, \delta(I_z) \mathsf{T}_I^{(i)} d^3\mathbf{I} \frac{P(\mathbf{I}; E_\nu, \mathbf{n})}{P(I)}$$

$$= \pi\lambda_i^2 \int_0^\infty 2I \mathsf{T}_I^{(i)} \frac{P(I; E_\nu)}{P(I)} dI \frac{1}{2\pi} \int_0^{2\pi} d\phi \frac{P(\mathbf{I}; E_\nu, \mathbf{n})}{P(I; E_\nu)} \quad . \quad . \quad . \quad (5.18)$$

Here $\mathsf{T}_I^{(i)}$ is the transmission coefficient for formation of the Compound Nucleus by the Ith partial wave of the incident particle; ϕ is the azimuthal angle describing the position of $\mathbf{I}$ perpendicular to the beam. We note in passing that eqn. (5.18) does not depend on the intermediate level density $\rho_c(\mathbf{I})$ provided there are states available.

The cross section in eqn. (5.18) therefore consists of a factor containing the angular dependence multiplied by the total cross section of corresponding angular momentum:

$$\sigma(\mathbf{n}, E_\nu) = \pi\lambda_i^2 \int_0^\infty 2I \mathsf{T}_I^{(i)} \frac{P(I; E_\nu)}{P(I)} W_I(\mathbf{n}, E_\nu) dI \quad . \quad . \quad (5.19)$$

with

$$W_I(\mathbf{n}, E_\nu) = \frac{1}{2\pi} \int_0^{2\pi} d\phi \frac{P(\mathbf{I}; E_\nu, \mathbf{n})}{P(I; E_\nu)} \quad . \quad . \quad . \quad . \quad . \quad (5.20)$$

The angular part $W_I(\mathbf{n}, E_\nu)$ is normalized so that

$$\int W_I(\mathbf{n}, E_\nu) d\Omega = 1. \quad . \quad . \quad . \quad . \quad . \quad . \quad . \quad (5.21)$$

We now apply eqns. (5.14) and (5.15) to obtain on explicit representation of $P(I; E_\nu) W_I(\mathbf{n}, E_\nu)$.

$$P(I; E_\nu) W_I(\mathbf{n}, E_\nu) = \frac{1}{2\pi} \int_0^{2\pi} d\phi P(\mathbf{I}; E_\nu, \mathbf{n})$$

$$= \frac{1}{\rho_c(I)} \frac{1}{2\pi} \int_0^{2\pi} d\phi \int\int \frac{1}{(2\pi)^2 \hbar} g_\nu \delta(\mathbf{n} \cdot \mathbf{l}) \mathsf{T}_l^{(\nu)}(E_\nu) \, \delta^{(3)}(\mathbf{l} + \mathbf{j} - \mathbf{I}) \rho_\nu(E_\nu^*, \mathbf{j}) \, d^3\mathbf{l} \, d^3\mathbf{j}.$$

$$. \quad . \quad . \quad . \quad . \quad . \quad . \quad . \quad . \quad (5.22)$$

The distribution of spins $\rho_\nu(E_\nu^*, \mathbf{j})$ is now substituted from eqn. (5.16).

The resulting integrals can be carried out explicitly (Ericson and Strutinsk 1958) yielding

$$P(I;E_\nu)W_I(\mathbf{n},E_\nu)=\frac{g_\nu\rho_\nu(E_\nu{}^*,0)}{\rho_c(I)\hbar}\int_0^\infty 2l\mathsf{T}_l^{(\nu)}(E_\nu)e^{-\frac{I^2+l^2}{2\sigma_\nu{}^2}}j_0\left(i\frac{Il}{\sigma_\nu{}^2}\right)W_{Il}(\mathbf{n},E_\nu)\,dl \quad . \quad . \quad . \quad (5.23)$$

where $j_0(x)=\dfrac{\sin x}{x}$ and $W_{Il}(\mathbf{n},E_\nu)$ is the angular distribution for given I and l. The latter is given by

$$W_{Il}(\mathbf{n},E_\nu)=\frac{1}{4\pi}\frac{\sum_k(-)^k(4k+1)\left[\dfrac{(2k)!}{(2^k k!)^2}\right]^2 j_{2k}\left(i\dfrac{Il}{\sigma_\nu{}^2}\right)P_{2k}(\cos\theta)}{j_0\left(i\dfrac{Il}{\sigma_\nu{}^2}\right)} \quad (5.24)$$

with $j_n(x)$ spherical Bessel functions of order n. Thus by integrating eqn. (5.23) over the solid angle of the emitted particle

$$P(I;E_\nu)=\frac{1}{\rho_c(I)}\frac{g_\nu\rho_\nu(E_\nu{}^*,0)}{\hbar}\int_0^\infty 2l\mathsf{T}_l^{(\nu)}(E_\nu)e^{-\frac{I^2+l^2}{2\sigma_\nu{}^2}}j_0\left(i\frac{Il}{\sigma_\nu{}^2}\right)dl. \quad . \quad . \quad (5.25)$$

Substitution of eqns. (5.23) and (5.25) into eqn. (5.19) and the observation that the total probability of decaying is obtained by summing over all different emitted particles and their energies gives finally

$$\sigma(\mathbf{n},E_\nu)=\pi\lambda_i{}^2\int_0^\infty 2I\mathsf{T}_I^{(i)}\,dI \times \frac{g_\nu\rho_\nu(E_\nu{}^*,0)\displaystyle\int_0^\infty 2l\mathsf{T}_l^{(\nu)}(E_\nu)e^{-\frac{I^2+l^2}{2\sigma_\nu{}^2}}j_0\left(i\frac{Il}{\sigma_\nu{}^2}\right)W_{Il}(\mathbf{n},E_\nu)dl}{\sum_\nu g_\nu\displaystyle\int_0^\infty dE_\nu\rho_\nu(E_\nu{}^*,0)\int_0^\infty 2l\mathsf{T}_l^{(\nu)}(E_\nu)e^{-\frac{I^2+l^2}{2\sigma_\nu{}^2}}j_0\left(\frac{Il}{\sigma_\nu{}^2}\right)dl}. \quad (5.26)$$

Equation (5.26) represents the entire solution to the Compound Nucleus reaction when the decay goes to the statistical region of many levels. It should be noted that the quantity σ_ν which enters in this equation depends on the excitation energy of the residual nucleus.

5.3. *Special Limits*

The remainder of this section will be devoted to a discussion of different approximations of eqn. (5.26), in particular the weak and strong coupling limits discussed earlier, and of its region of applicability. We will also briefly discuss some of the information which is obtainable by the particular effects of angular momentum conservation in the statistical decay.

The parameter which determines whether the angular momentum of the emitted particle, **l**, is strongly or weakly coupled to the rotation is the value of $Il/\sigma_\nu{}^2$ as compared to unity for the effective values of l and I,

$$\left.\begin{array}{ll} Il/\sigma_\nu{}^2\gg 1 & \text{for strong coupling,} \\ Il/\sigma_\nu{}^2\ll 1 & \text{for weak coupling.}\end{array}\right\} \quad . \quad . \quad . \quad (5.27)$$

The physical reason for these limits was discussed earlier in terms of the decoupling angle ϑ_0 (eqn. 5.9) as compared to $\pi/2$; the formal reason

results from eqns. (5.24) and (5.26) and corresponds to taking the limits of the spherical Bessel functions $j_n(ix)$ which are functions of the parameter Il/σ_ν^2:

$$\left.\begin{aligned} j_n(ix) &\to \frac{i^n e^x}{2x} \quad \text{when} \quad x \to \infty, \\ j_n(ix) &\to \frac{i^n x^n}{(2n+1)!!} \quad \text{when} \quad x \to 0. \end{aligned}\right\} \quad . \quad . \quad (5.28)$$

The complete decoupling limit obtains if $\sigma_\nu \to \infty$ in which case eqn. (5.24) becomes

$$W_{Il}(\mathbf{n}, E_\nu) \longrightarrow \frac{1}{4\pi}, \quad . \quad . \quad . \quad . \quad . \quad . \quad . \quad (5.29)$$

yielding complete isotropy. Similarly, applying this limit to eqn. (5.26) and recalling that the total inverse cross section $\sigma_\nu^*(E_\nu)$ is

$$\sigma_\nu^*(E_\nu) = \frac{\pi}{k_\nu^2} \int_0^\infty 2l \mathsf{T}_l^{(\nu)}(E_\nu)\, dl, \quad . \quad . \quad . \quad . \quad . \quad . \quad (5.30)$$

we immediately obtain

$$\sigma(\mathbf{n}, E_\nu) = \sigma^{(i)} \frac{1}{4\pi} \frac{g_\nu k_\nu^2 \sigma_\nu^*(E_\nu) \rho_\nu(E_\nu^*, 0)}{\Sigma_\nu g_\nu \int_0^\infty k_\nu^2 \sigma_\nu^*(E_\nu) \rho_\nu(E_\nu^*, 0)\, dE_\nu}, \quad . \quad . \quad (5.31)$$

in agreement with eqn. (4.5) and again verifying that no angular momentum restrictions are imposed on the decay, if the level density has a distribution of spins proportional phase space.

In the strong coupling limit the substitution of the asymptotic expansion (5.28) of the spherical Bessel functions into eqn. (5.24) gives

$$W_{Il}(\mathbf{n}, E_\nu) \to \frac{1}{4\pi} \Sigma_k (4k+1) \left[\frac{(2k)!}{(2^k k!)^2}\right]^2 P_{2k}(\cos\theta) = \frac{1}{2\pi^2 \sin\theta}, \quad . \quad (5.32)$$

which is the angular distribution of eqn. (5.5) characteristic of complete alignment of **l** with **I**. In the spirit of eqn. (5.10) the relative emission probability is reduced by a factor r_{Il} due to the correlation of **l** and **I** as compared to the decoupled case. Simple inspection of eqn. (5.26) yields this fraction as

$$r_{Il} = e^{-\frac{I^2+l^2}{2\sigma_\nu^2}} j_0\left(i\frac{Il}{\sigma_\nu^2}\right). \quad . \quad . \quad . \quad . \quad . \quad . \quad . \quad (5.33)$$

This quantity is obviously unity for $\sigma_\nu \to \infty$; for $Il/\sigma_\nu^2 \ll 1$ it becomes

$$r_{Il} \longrightarrow \frac{\sigma_\nu^2}{2Il} e^{-\frac{(I-l)^2}{2\sigma_\nu^2}}, \quad . \quad . \quad . \quad . \quad . \quad . \quad . \quad (5.34)$$

in accordance with eqn. (5.10).

The weak coupling limit is obtained by applying the expansion of eqn. (5.28) to eqn. (5.26) for I and l smaller than σ_ν. Retaining only terms

in Il/σ_ν^2 which give rise to deviations from isotropy to first surviving order we obtain for the resulting angular distribution

$$W(\mathbf{n}, E_\nu) \simeq 1 + \frac{\overline{I^2}\,\overline{l^2}}{12\sigma^4} P_2(\cos\theta), \quad . \quad . \quad . \quad . \quad . \quad (5.35)$$

where the average values of I^2 and l^2 have been obtained by the use of the weighting factors

$$\frac{2I\mathsf{T}_I^{(i)}}{\int_0^\infty 2I\mathsf{T}_I^{(i)}\,dI} \quad \text{and} \quad \frac{2l\mathsf{T}_l^{(\nu)}(E_\nu)}{\int_0^\infty 2l\mathsf{T}_l^{(\nu)}(E_\nu)\,dl}$$

While the validity of the approximation (5.35) in principle depends on the smallness of both I and l compared to σ_ν its range of validity is in practice usually determined by the smallness of Il compared to σ_ν^2. In many reactions $I \gg l$, which usually follows from the strong decrease in energy of the emitted particles as compared to the energy of the incident particles. The extended validity is due to the strong cancellation between factors of the type $e^{-\frac{I^2}{2\sigma_\nu^2}}$ which occur in both numerator and denominator of eqn. (5.26). This approximate cancellation is due to the slow variation of σ_ν^2 with excitation energy.

Applying the sharp cut-off approximation, i.e. using transmission coefficients which are unity in the classically allowed region and 0 outside, we obtain

$$\overline{l^2} = \tfrac{1}{2} l_{\max}^2 = \frac{\mu_\nu (E_\nu - B_\nu) R^2}{\hbar^2}, \quad . \quad . \quad . \quad . \quad (5.36)$$

where μ_ν is the mass of the emitted particle and R the nuclear radius.

Therefore the evaporation approximation applied to eqn. (5.37) to obtain the average value $\overline{l_T^2}$ over the entire spectrum yields

$$\overline{l_T^2} = \frac{2\mu_\nu T R^2}{\hbar^2}. \quad . \quad . \quad . \quad . \quad . \quad . \quad . \quad (5.37)$$

Introducing this result as well as the rotation interpretation of the spin cut-off factor σ_ν (eqn. (3.33)) the average angular distribution $W(\mathbf{n})$ can be written

$$W(\mathbf{n}) \simeq 1 + \tfrac{1}{3} \frac{\mu_\nu R^2}{\mathscr{T}} \frac{\hbar^2 \overline{I^2}}{2\mathscr{T} T} P_2(\cos\theta) = 1 + \tfrac{1}{3} \frac{\mu_\nu R^2}{\mathscr{T}} \frac{E_{\mathrm{rot}}}{T} P_2(\cos\theta), \quad (5.38)$$

which is in agreement with eqn. (5.12).

Similarly and in the same approximation we may ask for the average change of kinetic energy of neutrons evaporated, due to the angular momentum of the Compound Nucleus. In an entirely analogous manner we obtain the average kinetic energy in direction $\mathbf{n}$, $\overline{E(\mathbf{n})}$

$$\overline{E(\mathbf{n})} \simeq 2T\left\{1 + \frac{\overline{I^2}\,\overline{l_T^2}}{12\sigma_\nu^4}(2 + P_2(\cos\theta))\right\} = 2T + \tfrac{2}{3} \frac{\mu_\nu R^2}{\mathscr{T}} E_{\mathrm{rot}}(2 + P_2(\cos\theta)), \quad (5.39)$$

which averaged over all angles agrees with the qualitatively argued eqn. (5.13). The average energy is thus a function of the direction of emission.

We draw attention to the fact that the angular momentum effect can be considerable in the case of successive evaporations of particles (Ericson and Strutinski 1958). A highly excited nucleus is mostly de-excited by the emission of neutrons and protons, which do not carry off large angular momenta for energies close to the average evaporation energies. The decoupling angle ϑ_ν of eqn. (5.9) can therefore be large, indicating weak coupling of the direction of the angular momentum to the Compound Nucleus angular momentum. As a consequence the angular momenta of the first evaporated particles are both small and couple essentially at random, so that the direction and magnitude of the initial angular momentum will not be appreciably changed. In the last stage of the evaporation a large angular momentum has to be disposed of because only low spin states are available in the residual nucleus. The last particle will therefore be emitted strongly coupled to the initital spin giving rise to angular distributions close to $1/\sin\theta$. This effect can be important even when the angular momentum initially brought in is not very large. It has been observed in the (n, np)—reaction in medium weight elements, induced by 14 Mev neutrons (Allan 1959, analysed by Douglas and McDonald 1959).

An important aspect of effects of angular momentum conservation in the statistical decay is that it permits a determination of the spin cut-off factor σ_ν or, in other words, the moment of inertia which enters in the level density. The present data indicate that the nuclear moment of inertia is that of a rigid body if r_0 is taken to be 1·2 Fermis (Ericson and Strutinski 1958; Douglas and McDonald 1959) with an uncertainty of 20–30%. This is in agreement with an analysis by Ericson based on directly measured states as compared with levels of one spin only which gives similar results with similar accuracy (Ericson 1959). As previously emphasized (eqn. (3.39) f.f.) the appearance of a nearly rigid moment of inertia is not in disagreement with the values of moments of inertia found in nuclear spectroscopy; the moment of inertia which appears in the Statistical Model is not necessarily associated with a rotational spectrum and is an average property of many levels.

The case of a transition to individual states in the residual nucleus can be used for a study of nuclear level densities when they occur in competition with transitions to the statistical region. With increasing excitation of the Compound Nucleus, the probability of a transition to the statistical region increases proportionately to the level density relative to that of a single state and the cross section for transition to the individual state will therefore rapidly decrease. As any special mechanism which also populates the state will conceal the Compound Nucleus contribution, if it is small, the following discussion is probably mainly applicable to reactions induced by relatively low energy particles and γ-rays.

We will assume the decay to the statistical region to take place mainly by neutron emission, as is often but not always the case; angular momentum selection rules are mostly of neglibible effect due to the low

energy of the incident particle. In the evaporation approximation for the transition to the statistical region, we obtain the total cross section for a low spin target j_i, if the residual spin is j_f, to be (Ericson 1960)

$$\sigma(j_i \simeq 0\,;\, j_f) = \pi\lambda_i^2 \frac{\hbar^2}{2\mu_n R^2} \frac{\int_0^\infty \mathsf{T}_I^{(i)}\, dI\, g_\nu \int_{|I-j_f|}^{I+j_f} \mathsf{T}_l^{(\nu)}(E_\nu) dl}{g_n T^2 \rho_{0n}(U_n)} \quad . \quad . \quad . \quad (5.40)$$

Here U_n is the maximum possible energy after neutron emission and $\rho_{0n}(U_n)$ refers to the level density of 0 spin and both parities in the residual nucleus corresponding to neutron emission. Though this result is obtained in the classical approximation the main change to obtain the quantal form is the replacement of the integrals by sums. We observe that we have a method which in principle allows us to obtain the level density of 0 spin for excitation energies different from the neutron binding energies. It requires a crude knowledge of nuclear temperatures but is not very sensitive to this quantity. This method has never been used for a study of level densities, as far as is known to us.

The classical approximation of angular momenta as used in this section must be expected to be reliable as long as descriptions which violate the uncertainty principle are not attempted. In the case of cross sections the major change in going to quantum mechanics is the replacement of integrals by sums and the replacement of classical variables l and I by $l+\frac{1}{2}$ and $I+\frac{1}{2}$, l^2 and I^2 by $l(l+1)$ and $I(I+1)$, according to Kramers's rules. In the case of angular distributions it is also well known that these will quantally be described by sums of Legendre-polynomials which all have a degree less than or equal to the smaller of $2l$ and $2I$. Inspection of eqn. (5.24) for the angular distribution reveals immediately that the condition for this to be valid is

$$\left.\begin{aligned} &\frac{Il}{\sigma_\nu^2} \lesssim 2\min(I, l) \\ \text{or} \quad &\max(I, l) \lesssim 2\sigma_\nu^2. \end{aligned}\right\} \quad . \quad . \quad . \quad . \quad . \quad (5.41)$$

When this condition is no longer valid, the total cross section is still adequately described; the angular distribution has however a decoupling angle which is no longer determined by eqn. (5.9), but by $1/2\min(I, l)$; it is however correctly described for larger angles.

Douglas and McDonald (1959) have carried out computer calculations of the angular distributions, which correspond to the exponential cut-off in the spin distribution, retaining the exact Clebsch–Gordan coefficients. Their results indicate that the classical approximation produces results which agree closely with the exact solution.

§ 6. Inverse Cross Sections

A typical feature of the Statistical Model is the appearance of inverse cross sections and transmission coefficients, i.e. such quantities for particles incident on nuclei which are in excited states. These cross

sections and transmission coefficients contain the entire dynamics of the decay process.

For obvious reasons it is not possible to use highly excited nuclei as targets and deduce these cross sections experimentally; our knowledge of these quantities relies entirely on experiments involving Compound Nuclei and on theoretical expectations. The Statistical Model offers in principle a method of studying these cross sections and of deducing some properties of the excited nuclei therefrom.

The theory of inverse cross sections is not in a very satisfactory state at present. We will in the following examine the background of presently used inverse cross sections and in particularly determine how well these have to be known to allow conclusions about properties of the excited nucleus. We will furthermore discuss the special effects which may occur in the inverse cross sections, mostly due to different mechanisms for increasing the effective nuclear radius.

The tacit assumption which is inherent in all applications of the Statistical Model, whether referring to angular distributions or total cross sections, is that of smooth variation with incident energy. It is well known that experiments performed with high energy resolution in the region of non-overlapping levels exhibit not only resonances, but also strong variations of the resonance widths from level to level. A somewhat similar situation is to be expected in the region of overlapping levels though not yet displayed experimentally. The Statistical Model always assumes that such rapid variations have been averaged and that the resulting inverse cross-sections are smoothly varying with energy. The average may have been performed in the intermediate nucleus by using a fairly large energy spread in the incident beam, or it may arise by an average over many states in the final nucleus, or as is mostly the case, by both. The consequences of such averaging will be further discussed in § 11. In all cases the appropriate inverse cross section is the *average* cross section taken over many states; it has therefore a great similarity to the optical model reaction cross section (Feshbach *et al.* 1953). It differs from this by referring only to the formation of the Compound Nucleus instead of referring to all processes. In spite of this difference in principle, the practical difference is probably small. Particles emitted in the statistical decay have relatively low energy in the main part of the spectrum; thus neutrons are emitted with typical energies of $2T$, charged particles mostly with energies close to the Coulomb barrier (eqn. 4.10). These energies are still so low that the contribution of direct processes to the cross section is small when the target is in its ground state. The contribution of direct processes is probably small also when the target nucleus is in an excited state. The appropriate optical model and inverse cross sections should therefore be close.

The main difference between optical model and inverse cross sections is rather a difference in parameters. Nuclei in their ground state exhibit a rather strong transparency in nuclear reactions. This transparency is largely due to the exclusion principle which suppresses many otherwise

possible scatterings of the incident particle, and seems to be largely connected with the specially ordered character of nuclear ground states. Qualitatively we therefore expect an excited nucleus to be 'blacker' than in the ground state; the exclusion principle is of less importance due to the increased diffuseness of the nuclear surface in momentum space. One therefore expects the imaginary part of the optical model potential to be increased for the excited nucleus.

The approximation of the excited nucleus as a completely absorbing black body should therefore be considerably better for the excited than for the unexcited nucleus. Tabulations of cross sections for charged particles incident on a completely absorbing nuclear square well potential exist in several places in the literature (Shapiro 1953, Blatt and Weisskopf 1952, Thomas 1959) and have been used extensively in the analysis of spectra thought to be due to nuclear evaporation. Though we believe the argument for using such models for the analysis should be based on the reasoning above, it is also obvious that such models account well for the major part of penetrabilities and their variation with energy. All of these tables are calculated for spherical nuclei with sharp boundaries.

The increased use of computers in the analysis of evaporation spectra has led to the introduction of simple analytic approximations to the inverse cross sections. The most current of these is an amelioration of the simple sharp cut-off approximation (4.6) of the form

$$\sigma(E) \simeq \left\{ \begin{array}{ll} 0 & ; \quad E < kB, \\ \pi R^2(1+c)\left(1-\dfrac{kB}{E}\right); & E > kB, \end{array} \right\} \quad . \quad . \quad . \quad (6.1)$$

where c and k are adjustable parameters determined by the best fit of eqn. (6.1) to more exact tabulated cross sections. In particular, k is smaller than unity, so that particles can be emitted to some extent also below the classical barrier B. It is experimentally well known that charged particles frequently are emitted in abundance below or close to the classical Coulomb barrier. We draw attention to the fact that extreme care must be taken in using approximations to the inverse cross section in this region, if the actual shape of the spectrum is studied. The reason for this is that the inverse cross section for charged particles has a mainly exponential increase with energy below the barrier and is not well reproduced there by any sharp cut-off approximation. (The use of such an approximation in § 4 was only for qualitative discussions and to give a first orientation on total cross sections.) As a consequence the maximum in the energy spectrum of the emitted particles results from a delicate balance between two rapidly varying functions of energy, the increasing cross section and the exponentially decreasing level density. The exact condition for maximum is obtained from eqn. (4.7) by differentiation and is

$$\frac{d}{dE_\nu}\left[\ln E_\nu \sigma_\nu^*(E_\nu)\right] = \frac{1}{T} \quad . \quad . \quad . \quad . \quad . \quad . \quad (6.2)$$

where T is the nuclear temperature. As the nuclear temperature is unrelated to the inverse cross section, the maximum can easily fall below

the classical barrier. From eqn. (6.2) it is clear that it is necessary to use approximations to the inverse cross section which have correct *fractional* change in the neighbourhood of the maximum (6.2) in order to reproduce the shape of the spectrum correctly. The tabulated cross sections as cited previously do not suffer from the drawback of the sharp cut-off approximation.

The excited nucleus does not necessarily have the same size or shape as the nucleus in its ground state; even a classical body undergoes for instance a thermal dilatation with increasing excitation. In the nuclear case such changes may have a profound effect on the emission probability of charged particles, because a change of the effective radius will affect the height of the Coulomb barrier, usually reducing it. In this way particles will be emitted with energies that ordinarily would be forbidden. This is the reason for the discussion above of the exact conditions of the position of the maximum of the energy spectrum of the emitted particles. Before briefly discussing some different possible mechanisms for nuclear expansion, we emphasize the desirability that assumptions about the variation of nuclear level densities with energy are eliminated as far as possible from conclusions about nuclear expansion drawn from charged particle emission. This may be done by using level densities determined from neutron evaporation to the same residual nucleus.

The magnitude of the thermal dilatation of the nucleus has been estimated by Le Couteur (1950) on the basis of a model nucleus consisting of free particles with nucleon–nucleon interactions given by a Gaussian potential. He finds that the effective radius of the nucleus is changed from the undilated value R_0 to a radius R, where

$$\frac{R-R_0}{R_0} = 2{\cdot}5\left(\frac{t}{\epsilon_0\gamma}\right)^2 \quad . \quad . \quad . \quad . \quad . \quad . \quad . \quad (6.3)$$

in terms of the temperature t, the Fermi energy ϵ_0 and the reduction factor γ, which is the effective mass in units of the nucleon mass. This effect is small; at 400 MeV and $A = 100$ the thermal expansion of eqn. (6.3) is about 10% and at 40 MeV excitation 1% only.

In the excited nucleus the occupied particle orbits will extend further in space than in the ground state. This gives rise to an increased diffuseness of the nuclear radius which again may manifest itself by a reduced effective barrier. Lane and Parker (1960) have recently investigated this effect in the case of a plane nuclear surface of infinite extension. They find that the effect is very small in most cases, but increases with excitation energy. Bagge (1938) investigated the influence of surface waves on the emission of particles from a nucleus considered as a liquid drop. He found that a nucleus with an initially sharp surface will have an effective mass distribution with a diffuse surface at high excitation. For a nucleus of $A = 80$ the diffuseness region is about 20% of the nuclear radius at 200 MeV of excitation. In view of our greatly increased knowledge about nuclear surface waves, it would be desirable to have a modern reinvestigation of this effect which should be very important for highly excited nuclei.

As a whole there has been considerable difficulty of finding plausible effects which theoretically give rise to appreciable reductions of Coulomb barriers below 50 MeV of excitation. Experimentally there is at present no clear evidence for any energy dependent Coulomb barrier below approximately 50 MeV of excitation. The very strong variation with energy of the Coulomb barrier found in (p, α)-reactions (Fulmer and Cohen 1958, Fulmer and Goodman 1960) has not been found in (α, α')-reactions (Fulbright *et al.* 1959) and (p, α)-reactions (Brady and Sherr 1960) on neighbouring elements and with similar excitation energies and is thus in some doubt. At very high excitations where appreciable reductions are expected theoretically the evidence is not clear, but indicates strongly such reductions. The uncertainty of interpretation is mainly due to insufficient knowledge of level densities in this region.

§ 7. Multiple Emission of Particles

In this section we will only briefly discuss the problem of successive evaporation of particles, as this and connected questions are well covered in the current literature. This field has recently been reviewed by Le Couteur (1958), to whom we refer for earlier references. Later these problems have been studied by Monte Carlo calculations in a series of papers (Dostrovsky, Rabinowitz and Bivins 1958, Dostrovsky, Fraenkel and Rabinowitz 1958, 1960, Dostrovsky, Fraenkel and Friedlander 1959, Dostrovsky, Fraenkel and Winsberg 1959) and using analytic expressions by Le Couteur and Lang (1959). The reactions involving multiple emissions are of two types.

1. The relatively low energy reactions in which a Compound Nucleus is formed initially with high probability in the sense previously discussed.

2. The high energy reactions, in which the rapid incident particle first produces an initial cascade of other particles by direct collisions with the nucleons in the target nucleus, which can approximately be considered a gas of free Fermions (Goldberger 1948). While many of the particles in the cascade are ejected from the nucleus, a certain number stay inside, still colliding with other nucleons and ejecting some of these. When the energy of these particles is reduced to a few times 10 MeV the reflection at the nuclear surface becomes important and the system will tend to develop towards an equilibrium system in the previous sense. This equilibrium system will therefore be produced with a wide range of excitation energies and evaporation takes place in the same way as in case 1.

The multiple decay of an equilibrium system proceeds by the evaporation of a first particle, leaving the residual nucleus with a probability of different excitations determined by the energy of the evaporated particles and the reaction Q-values. From such an excited nucleus new particles are emitted with competition between different modes of de-excitation in the ordinary way until the entire excitation energy is disposed of. This process obviously takes place in such a way that energy and angular momentum is conserved for each step in the decay. While physically no new assumptions enter into this problem, the great complexity of the decay, when

many particles are emitted, leads to a relatively large uncertainty if parameters for level densities or inverse cross sections have to be determined. This is due to the unfolding which necessitates specific assumptions. The results are however qualitatively in very good agreement with statistical theory.

The problem of unfolding the complicated decay is even more acute when the incident particle initiates a primary cascade. In addition to the evaporation decay it is then necessary to obtain the initial distribution of excitation energies from which the statistical decay begins, which thus introduces an additional uncertainty. Also in this case there is a good general agreement with statistical theory both with respect to general trends of spectra, excitation functions and cross sections and to the extrapolated parameters of the nuclear level density.

An important practical method to evaluate the relative competition between different de-excitation modes is to follow a number of decays taken at random by a Monte Carlo technique. This yields a good idea of how often different decays occur. This technique was first applied by Rudstam (1956).

A problem which poses itself in this type of calculation is the energy at which the nucleus can be considered an equilibrium system. This energy is in part determined by the condition that the cascade particles should have attained a kinetic energy which is sufficiently low for them to be reflected at the nuclear surface, and particularly in reactions initiated by very high energy particles, by the condition that the equilibrium system must have a lifetime that is at least of the order of the nuclear relaxation time. It is not obvious that this latter condition can be fulfilled at excitation energies above 100 MeV. We will return to this question in the discussion of the lifetime of the Compound System in § 10.

§ 8. Emission of Complex Particles

As we have emphasized several times in the preceding sections, the decay of the intermediate Compound System is entirely governed by phase space in the Statistical Model. If we study processes with very small phase space, any application of the statistical theory has to be made with great care, because any special reaction mechanism to produce the same result can easily make much larger contributions. We can however expect the Statistical Model to give a lower limit at least, to the observed cross section if the bulk of the entire reaction passes through a Compound Nucleus. From the phase-space point of view there is no discrimination between the emission of neutrons, α-particles, ^{3}He or even heavier particles. We should even be able to produce heavy nuclei in their excited states, taking this picture to its extreme, so that fission should become a special case. In view of the special problems involved in fission we refer to the discussion in the next section.

While the emission of complex entities heavier than α-particles in general is disfavoured by high barriers and Q-values, it is on the other hand favoured

by statistical factors. Even if we do not consider the possibility of emission to excited states, inspection of eqn. (4.7) reveals that the statistical factor is $g_\nu \mu_\nu$ with $g_\nu = 2s_\nu + 1$ and μ_ν the mass of the particle. The mass factor is proportional to A and even the statistical weight due to the ground state spin is sometimes rather large. For example, the combined statistical weight for the ground state of ^{8}Li ($s_\nu = 2$) is twenty times larger than for neutrons. The calculations of the cross sections for the emission of complex particles is completely straight forward on the basis of the Statistical Model with the provision that excited states have to be included in the calculation with Q-values different from that of the ground state.

The production of complex particles like ^{6}He, Li, Be and B becomes appreciable when the projectile has energies of 100 Mev or more and is in magnitude of the cross section of the order of millibarns. This reaction mechanism for the production was first proposed by Camerini *et al.* (1952) and has since been investigated more in detail by Hudis and Miller (1958) and Dostrovsky *et al.* (1960). The agreement between calculated cross section and excitation functions and the experimental ones is surprisingly good. The experiments are all induced by very energetic protons so that the initial reaction is a cascade as discussed in the previous section, followed by a subsequent slower de-excitation. The lifetime of an equilibrium system on the basis of the Statistical Model itself (see § 10) is rather short for the relevant excitation energies; it is not evident that these results indicate the existence of a long-lived equilibrium system as an intermediate state, at least not in the sense we have discussed it previously. The agreement between evaporation theory and these experiments may rather be regarded as a pure phase space effect, as the phase space available to these complex particles is considerably larger than might have been thought off-hand. It is thus possible that we are here dealing with a case which indicates the usefulness of the Statistical Model regarded only as a phase space description. It may then have an approximative validity outside its ordinary range of applicability.

While the emission of particles heavier than α-particles occurs mainly at high excitation energies, it is possible to have 'curious' emissions at lower excitation. In addition to evaporation of D, ^{3}H and ^{3}He the phase space for the emission of the deuteron in its excited state, D^*, and of the hypothetical di-neutron, δ, two neutrons in a quasi-bound state, is not neligible. Both of these cases represent the same singlet two nucleon state. D^* is known to be a virtual state, unbounded by ~ 60 Kev. It has thus 2·3 Mev higher Q-value than the ground state. The penetrabilities being the same as for the ordinary deuteron we therefore immediately conclude that its relative probability of emission compared to ground state deuterons is of the order of $\frac{1}{3} e^{-\frac{2.3}{T}}$, if the nuclear temperature is a constant T. The factor $\frac{1}{3}$ is due to the statistical spin factors. The excited deuteron has of course a very short lifetime; the width of the virtual state is however sufficiently small that the proton and neutron should remain close to each other, until the emitted 'particle' has come many nuclear radii from the nucleus. It will then disintegrate into a free neutron and a free proton

with very similar energies and closely correlated in angle. An estimate of the relative cross section for the excited deuteron compared to the ground state deuteron gives about 3–10% in light and medium weight elements.

In the case of the possible di-neutron we again expect to be dealing with an unbound state, firstly because a bound or long-lived di-neutron has been searched for several times (Fenning and Holt 1948, Ferguson and Montague 1952, Cohen and Handley 1953), secondly because of the probable charge independence of nuclear forces. As before we expect this entity to reveal itself by a strong angular correlation of the outgoing neutrons. This process will occur in competition with the $(2n)$ emission from which it has to be separated. With the di-neutron state unbound by about 50 kev the angular correlation should be of the order of 10°. Comparing the di-neutron cross section to the $(2n)$ cross section we have, assuming geometrical inverse cross section for the di-neutron, a constant nuclear temperature and complete decay of the compound nucleus by secondary neutrons after emission of the first:

$$\frac{\sigma(\delta)}{\sigma(2n)} \simeq \frac{\rho_0}{\rho_n} e^{-\frac{B_n}{T}} . \quad . \quad . \quad . \quad . \quad . \quad . \quad . \quad . \quad (8.1)$$

ρ_0 and ρ_n are the factors describing the odd–even effect of the level densities in the residual nucleus after di-neutron and first neutron emission, B_n is the binding energy of the second neutron. Equation (8.1) represents a lower limit for the di-neutron cross section. While the ratio above is rather small, the strong angular correlation will increase the feasibility of observation considerably because the two successively emitted neutrons are nearly uncorrelated in angle. The percentage of di-neutrons to $(2n)$ emission increases also when the excitation energy of the intermediate nucleus is brought closer to the $(2n)$ threshold.

We want to emphasize that the above considerations about D^* and δ are not strongly model dependent and an emission of this kind should be associated with almost any reaction mechanism due to phase space. Even the relative percentages are probably not greatly different from the estimates.

§ 9. Statistical Fission

As in the case of emission of complex particles which we discussed in the preceding section, it is also possible to regard nuclear fission as being entirely governed by the phase space available after the process (Fong 1956). In the case of fission there need be little doubt that one of the essential conditions for statistical decay, a long lifetime of the intermediate system, is fulfilled. A phase-space description of the fission process is complete in the sense that it predicts the final result uniquely: angular distribution of the fragments, mass distribution, velocity distribution, number of neutrons emitted before and after fission, and even the ratio of fission to neutron emission, if the quantities which enter the description are known. On the other hand this description again avoids the question of a detailed dynamics of the process. While this probably is permissible in the previously discussed cases, it is not necessarily so in the case of fission. The relative slowness with which the nucleus passes the fission barrier gives the nucleus the possibility to remain in a quasi-equilibrium state, in which part of its

internal energy goes into potential energy. The nucleus can then be in a state at the saddle-point which is so ordered that the available phase space, which governs the process, is determined rather by properties at the saddle point than by the phase space of the final fission products. The saddle point may then provide a 'bottleneck' through which the process is forced to pass. This situation is particularly probable close to the fission threshold. The study of fission widths in this region has revealed that they fluctuate in a manner typical of a decay through one or a few channels in spite of the many decay possibilities available and in contrast to what is expected from a completely statistical decay.

This feature can be understood from the description of fission on the basis of the unified model of deformed nuclei (A. Bohr 1955). When the fissioning nucleus has reached the saddle-point, it has become cold and organized; it will then have the characteristics of a strongly deformed nucleus close to its ground state. In particular, there will be a quasi-spectrum of excited 'states' associated with the saddle-point. Each of these states will be specified by particular symmetry, angular momentum and projection of the angular momentum on the axis of the deformed nucleus, in complete analogy to the situation in ordinary deformed nuclei. The fission will therefore take place through these 'quasi-states'; it will be governed by the properties of the particular one of these channels which is responsible for the fission. After the nucleus has passed the saddle point, the further development of the system is expected to be governed mainly by the available phase space, though the specific properties of the fissioning channel still can influence the result.

As the excitation energy of the Compound Nucleus is increased well above fission threshold, it is again possible that the statistical arguments become valid due to the large density of virtual levels at the saddlepoint and their strong overlap in energy. It is in this spirit that we will examine fission as a statistical process.

Our approach will be the same as in the discussion in § 5, and we will include angular momentum conservation in the treatment. Certain aspects of the influence of angular momentum on statistical fission have been considered by Pick–Pichak (1958). The important difference from the previous discussion is that there now are *two* residual nuclei left in excited states with excitation energies E_1^* and E_2^* and spins $\mathbf{j}_1$ and $\mathbf{j}_2$. Thus, the total excitation energy U goes partly into the kinetic energy E of the fragments, partly into excitation energy $E^* = E_1^* + E_2^*$ of the fragments and partly into their binding energy. We can in analogy with eqn. (5.14) *et seq.* write the decay probability per unit time of the system of spin $\mathbf{I}$ with a level density $\rho_C(\mathbf{I})$ into excited nuclei of level densities $\rho_1(E_1^*, \mathbf{j}_1)$ and $\rho_2(E_2^*, \mathbf{j}_2)$ as

$$P_{12}(\mathbf{I};\, E,\, \mathbf{n})\, d\Omega_n\, dE = \frac{1}{\rho_C(\mathbf{I})} \frac{p^2 dp\, d\Omega_n}{\hbar^3} v_{12} \int \lambda\!\!\!^{-2} \delta(\mathbf{n}\,.\,\mathbf{l})\, \mathsf{T}_l^{(12)}(E)\, d^3\mathbf{l}$$
$$\times \int\int\int\int \delta^{(3)}(\mathbf{l} + \mathbf{j}_1 + \mathbf{j}_2 - \mathbf{I})\, \rho_1(E_1^*, \mathbf{j}_1)\, \rho_2(E_2^*, \mathbf{j}_2)$$
$$\times \delta(E^* - E_1^* - E_2^*)\, dE_1^*\, dE_2^*\, d^3\mathbf{j}_1\, d^3\mathbf{j}_2. \quad . \quad . \quad . \quad (9.1)$$

The penetrability $T_l^{(12)}(E)$ is that for shooting two excited nuclei towards each other in such a way that they amalgamate into a Compound Nucleus. Equation (9.1) can be considerably simplified with respect to the spin and angular momentum variables, if the most probably populated states in the residual nuclei are excited to well above the ground state. Application of the nuclear spin distribution as given by eqn. (5.17), i.e. the notion that part of the excitation energy is due to rotational motion, gives when introduced into $\rho_1(E_1^*, \mathbf{j}_1)$ and $\rho_2(E_2^*, \mathbf{j}_2)$

$$P_{12}(\mathbf{I};\, E,\, \mathbf{n}) = \frac{1}{\rho_C(I)} \frac{1}{4\pi^4 \hbar} \int_0^\infty \int_0^\infty \rho_{01}(E_1^*)\, \rho_{02}(E_2^*)\, \delta(E^* - E_1^* - E_2^*)$$
$$\times \int \mathsf{T}_l^{(12)}(E) \delta(\mathbf{n} \,.\, \mathbf{l})\, d^3\mathbf{l} \int\int \delta^{(3)}(\mathbf{l} + \mathbf{j}_1 + \mathbf{j}_2 - \mathbf{I})\, e^{-\frac{j_1^2}{2\sigma_1^2} - \frac{j_2^2}{2\sigma_2^2}} d^3\mathbf{j}_1\, d^3\mathbf{j}_2. \quad (9.2)$$

Introducing new variables with $\mathbf{j} = \mathbf{j}_1 + \mathbf{j}_2$ this integral can be integrated to the form

$$P_{12}(\mathbf{I};\, E,\, \mathbf{n}) = \frac{1}{\rho_C(I)} \frac{1}{4\pi^2 \hbar} \int_0^\infty \int_0^\infty \left(\frac{2\pi \sigma_1^2\, \sigma_2^2}{\sigma_1^2 + \sigma_2^2} \right)^{3/2} \rho_{01}(E_1^*)\, \rho_{02}(E_2^*)$$
$$\times \delta(E^* - E_1^* - E_2^*)\, dE_1^* dE_2^* \int\int \mathsf{T}_l^{(12)}(E)\, \delta(\mathbf{n} \,.\, \mathbf{l})\, \delta^{(3)}(\mathbf{l} + \mathbf{j} - \mathbf{I})$$
$$\times e^{-\frac{1}{2} \frac{j^2}{\sigma_1^2 + \sigma_2^2}} d^3\mathbf{j}\, d^3\mathbf{l}. \quad . \quad . \quad . \quad . \quad . \quad . \quad . \quad . \quad . \quad . \quad (9.3)$$

We have now brought the expression for the probability into a form which closely resembles that which occurs when one particle is emitted. The principal difference is the replacement of the level density of the single residual nucleus by the folded level density of the two residual nuclei and for the angular momentum effects the replacement of σ_ν^2 by the sum $\sigma_1^2 + \sigma_2^2$. It is thus possible to proceed from eqn. (9.3) to calculate angular distributions and the kinetic energy distributions of the fission fragments, if the penetrabilities $\mathsf{T}_l^{(12)}(E)$ are known. The cross section for fission results by substitution into eqn. (5.19). It is possible to take over most of the results from § 5.

We will however make an additional approximation. The angular momentum barrier is very low for fission and of the order of a few kev only. The restrictions on angular momentum due to the cut-off factors σ_1^2 and σ_2^2 in the residual nucleus are therefore of much larger importance than the change in penetrabilities; it should therefore be a good approximation to replace the penetrabilities $\mathsf{T}_l^{(12)}(E)$ by their value for $l = 0$, $\mathsf{T}_0^{(12)}(E)$, as long as the initially brought in angular momentum is not very high. After this replacement the penetration factor does not enter the integral over $\mathbf{l}$ and $\mathbf{j}$ in eqn. (9.3) and this can be integrated explicitly. The pertinent part of (9.3) in this repect is

$$\int\int \delta(\mathbf{n} \,.\, \mathbf{l})\, \delta^{(3)}(\mathbf{l} + \mathbf{j} - \mathbf{I})\, e^{-\frac{1}{2} \frac{j^2}{\sigma_1^2 + \sigma_2^2}} d^3\mathbf{j}\, d\mathbf{l}^3 = 2\pi(\sigma_1^2 + \sigma_2^2)\, e^{-\frac{1}{2} \frac{(\mathbf{n} \,.\, \mathbf{I})^2}{\sigma_1^2 + \sigma_2^2}}. \quad (9.4)$$

This clearly exhibits that the direction of emission **n** is preferably perpendicular to **I** as in the case of complete alignment. The decoupling angle h_0 is

$$\left(\frac{2(\sigma_1^2+\sigma_2^2)}{I^2}\right)^{1/2}.$$

If the orbital angular momentum of the projectile causing fission is entirely responsible for the spin **I** of the compound nucleus, we can easily average over all directions perpendicular to the beam direction. We will do this in a somewhat round-about way which exposes the extremely strong similarity to the result for the fission angular distribution in the unified model (A. Bohr 1955, Halpern and Strutinski 1958). Thus averaging eqn. (9.4) over the azimuthal angle of ϕ we have

$$\frac{1}{2\pi}\int_0^{2\pi} d\phi \int\int \delta(\mathbf{n}\,.\,\mathbf{l})\delta^{(3)}(\mathbf{l}+\mathbf{j}-\mathbf{I})\, e^{-\frac{1}{2}\frac{j^2}{(\sigma_1^2+\sigma_2^2)}} d^3\mathbf{j}\, d^3\mathbf{l}$$

$$= (\sigma_1^2+\sigma_2^2)\int_{-I\sin\theta}^{I\sin\theta} \frac{e^{-\frac{1}{2}\frac{m^2}{\sigma_1^2+\sigma_2^2}}}{I\sqrt{\left(\sin^2\theta-\frac{m^2}{I^2}\right)}}$$

$$= 2\pi(\sigma_1^2+\sigma_2^2)\, e^{-\frac{I^2\sin^2\theta}{4(\sigma_1^2+\sigma_2^2)}} J_0\left(i\frac{I^2\sin^2\theta}{4(\sigma_1^2+\sigma_2^2)}\right). \quad . \quad . \quad . \quad . \quad . \quad (9.5)$$

We have here denoted the projection of **j** on **n**, **n** . **j**, by m; $J_0(x)$ is the Bessel function of zeroth order and θ is the angle between the direction of emission and the beam direction. The eqn. (9.5) for the fission angular distribution is formally *identical* to the expression obtained by Halpern and Strutinski (1958); it differs only in the constant $\sigma_1^2+\sigma_2^2$ which they denote by K_0^2 and associate with the distribution of the projection K on the nuclear symmetry axis of the angular momentum (cf. eqns. (3.58) and (3.70)). It is thus apparent from eqn. (9.5) that the projection of the total angular momentum on the direction of motion of the fragments will have very similar restrictions in both unified and statistical fission.

Finally taking eqns. (9.3) and (9.5) together, the probability of fissioning into fragments 1 and 2 with kinetic energy E in centre of mass system is

$$P_{12}(I;E,\mathbf{n}) = \frac{1}{\rho_C(I)}\frac{1}{\pi^2\hbar}\mathsf{T}_0^{(12)}(E)\int_0^\infty\int_0^\infty\left(\frac{2\pi}{\sigma_1^2+\sigma_2^2}\right)^{1/2}\sigma_1^3\sigma_2^3\,\rho_{01}(E_1^*)\,\rho_{02}(E_2^*)$$

$$\times\delta(E-E_1^*-E_2^*)\, e^{-\frac{I^2\sin^2\theta}{4(\sigma_1^2+\sigma_2^2)}} J_0\left(i\frac{I^2\sin^2\theta}{4(\sigma_1^2+\sigma_2^2)}\right) dE_1^*\, dE_2^*. \quad (9.6)$$

The comparison of the decay probability of fission, eqn. (9.6), with eqns. (5.19) and (5.26), immediately gives the fission cross section. Assuming that the Compound Nucleus decays predominantly by neutron emission, which is not a good approximation close to neutron threshold but otherwise is often valid, and that angular momentum restrictions can be neglected in the neutron decay due to its low orbital angular momentum,

we obtain in the evaporation approximation for the neutrons that the total decay probability $P(I)$ is

$$P(I) \simeq P_n(I) = \frac{1}{\rho_C(I)} \frac{g_n 2\mu_n}{\hbar} \frac{T_n{}^2 R^2}{\hbar^2} \rho_n(U_n), \quad . \quad . \quad . \quad (9.7)$$

where U_n is the maximum excitation of the residual nucleus after neutron emission and T_n the nuclear temperature. Thus the ratio of the fission decay probability for the particular decay studied $P_{12}(I\,;\,E,\,\mathbf{n})$ to the total decay probability is

$$\frac{P_{12}(I\,;\,E,\,\mathbf{n})}{P(I)} \simeq \frac{1}{\pi} \frac{\hbar^2}{2\mu_n R^2} \frac{\mathsf{T}_0{}^{(12)}(E)}{g_n T_n{}^2 \rho_{0n}(U_n)} \int_0^\infty \int_0^\infty \left(\frac{2\pi}{\sigma_1{}^2 + \sigma_2{}^2} \right)^{1/2} \rho_{01}(E_1{}^*)\, \rho_{02}(E_2{}^*)$$

$$\times \delta(E^* - E_1{}^* - E_2{}^*) \times e^{-\frac{I^2 \sin^2\theta}{4(\sigma_1{}^2+\sigma_2{}^2)}} J_0\left(i \frac{I^2 \sin^2\theta}{4(\sigma_1{}^2+\sigma_2{}^2)} \right) dE_1{}^* dE_2{}^*.$$

$$. \quad . \quad . \quad . \quad . \quad . \quad . \quad (9.8)$$

Rather detailed comparison of the mass distribution, the distribution of kinetic energy of the fission fragments etc, neglecting angular momentum effects have been carried out by Fong (1956), Newton (1956) and Cameron (1958). While these calculations give reasonable overall agreement between the experimental results they are sensitive to the actual Q-values for the different fission modes and the form of the level densities which are used. It should be noted however that none of these quantities is arbitrary in principle and that this sensitivity is itself no argument against the statistical model for fission. On the other hand the pure Statistical Model for fission is certainly not applicable close to threshold, where the fission process is strongly indicated to pass via a 'cold' nucleus at the saddle point.

We want to emphasize that effects, which sometimes are thought to prove that fission occurs according to the unified model (A. Bohr 1955, Strutinski 1956), are also easily explained by the Statistical Model. We noted previously the analogy in the description of angular distributions where the result was identical but for a parameter. A comparison of the experimental value of this parameter, which corresponds to the analysis of Halpern and Strutinski (1958), shows that the use of rigid moments of inertia to calculate $\sigma_1{}^2 + \sigma_2{}^2$ from eqn. (3.33) yields approximately the same result. The difference in the two models is in their detailed quantitative predictions, rather than in their qualitative predictions, at high excitation. Similarly the appearance of strong fission anisotropies in reactions which first proceed by evaporation of neutrons (Halpern and Strutinski 1958, Griffin 1959) with subsequent fission is in complete accord as well with the Statistical Model as with the unified model. It is possible that studies of actual cross sections may provide a more crucial test of the validity of the model. We draw attention to the fact that the study of the emission of complex particles as discussed in the previous section may also throw light on the fission process, in particular on the existence or not of a 'bottle neck' for the process.

§ 10. Lifetime of the Compound State

The very basis of the Statistical Model is the assumption of a long-lived intermediate compound system. If this assumption is not valid the application of the principle of detailed balance from which we derived the theoretical expressions for cross sections, angular distributions, etc., is no longer permitted. It is also necessary for the system to have achieved equilibrium. This demonstrates the necessity to insure that the Statistical Model is internally consistent; that the lifetime is not shorter than the relaxation time. In the next section we will also see that the lifetime of the Compound System is intimately connected with the fluctuations of cross sections and angular distributions away from the mean values, which again necessitates an approximate knowledge of the lifetime.

We will in both cases need the lifetime estimates at fairly high excitation energies. In order to obtain a simple and useful, though somewhat crude expression, for the lifetime we observe that under these conditions neutron emission is most probable. The emission of protons is inhibited by the Coulomb barrier, but can sometimes become as probable as neutron emission in medium weight elements. Our estimates for neutrons only will therefore give an upper limit for the lifetime, mostly better than to within a factor of 2, but it is hardly expected to differ by more than this from the estimate. We furthermore observe that in the case of neutron emission angular momentum restrictions will not strongly influence the decay, and we will therefore neglect them.

The probability of decay per unit time for this case is given by eqn. (4.2). The inverse cross section for neutrons is closely approximated by πR^2, the maximum excitation energy of the residual nucleus is $U - B_n$, where U is the excitation energy of the Compound Nucleus and B_n the neutron binding energy. In the evaporation approximation the lifetime due to neutron emission, τ_n, is then

$$\frac{1}{\tau_n} = P_n = \frac{4\pi}{h^3} g_n 2M_n \pi R^2 \frac{\int_0^\infty E_n \rho_n(U - B_n - E_n) dE_n}{\rho_C(U)}$$

$$\simeq \frac{4\pi}{h^3} g_n 2M_n \pi R^2 \frac{\rho_n(U - B_n)}{\rho_C(U)} T^2, \qquad \ldots\ldots (10.1)$$

where T is the nuclear temperature. For the discussion of lifetimes and relaxation times in the nucleus the natural time scale is the passage time of a light signal through the nucleus, $2R/_C = A^{1/3} \times 10^{-23}$ sec. At high excitation we can regard the nuclear temperature as that typical of a free gas of particles and put the temperature $T = (10U/A)^{1/2}$ (eqn. (3.46)); we also introduce $R = r_0 A^{1/3}$ with $r_0 = 1{\cdot}4 \times 10^{-13}$ cm. The lifetime τ is then

$$\tau \simeq \tau_n \simeq \frac{200}{U - B_n} \frac{\rho_C(U)}{\rho_n(U - B_n)} \simeq \frac{200}{U - B_n} e^{\frac{Bn}{T}} \frac{\rho_C(U)}{\rho_n(U)} \qquad \ldots (10.2)$$

where the energy U is in MeV. The ratio $\rho_C(U)/\rho_n(U)$ contains the odd–even effect in the level density. In the further estimates we will neglect this factor.

According to eqn. (10.2) the lifetime of the Compound System of a typical nucleus of $A = 100$ and $B_n = 8$ MeV is about 50 000 times $2R/c$ at 18 MeV excitation ($T = 1$ MeV); at 200 MeV excitation ($T = 4{\cdot}5$ MeV) it is only about 6 times $2R/c$. The short lifetime at 200 MeV excitation shows clearly that at excitation energies of this magnitude there is serious doubt on the consistency of the Statistical Model; the lifetime is so short that there is no clear separation between fast and slow processes. The appropriate quantity with which to compare the lifetime is obviously the relaxation time. As the interactions cannot propagate faster than a light signal, the relaxation time is always larger than $2R/c$. A lower limit of the relaxation time is obtained by considering the interactions to propagate with a speed of the order of the average velocity of a nucleon or by the sound velocity in nuclear matter ($c/10$ to $c/3$) (Glassgold *et al.* 1959). Even in this case we can hardly expect an instantaneous equilibrium to be achieved and the relaxation time is thus larger than 5–10 times $2R/c$. Therefore as we reach excitation energies of the order of 100 MeV and higher the influence of nuclear non-equilibrium processes such as partial excitation of the nucleus (Bethe 1938) will become increasingly dominant.

We have several times emphasized that the Compound Nucleus when it represents a system which is averaged over a sufficiently large energy interval (cf. § 11) represents a complete analogy with a classical system. In particular, it is possible to associate a moment of inertia $\mathscr{T}$ (eqn. (3.33)) and an angular velocity $\omega = 2\pi/\tau_{\text{rot}}$ with it. We must require that the rotation time τ_{rot} of a classical equilibrium system is so long that the periphery does not attain light velocity; indeed it has even to be longer than the relaxation time. If we now compare the quantal expression for the angular momentum, $\hbar I$, to its classical value $\mathscr{T}\omega$, the rotation time is

$$\tau_{\text{rot}} = \frac{\mathscr{T} 2\pi}{\hbar I} \quad . \quad . \quad . \quad . \quad . \quad . \quad . \quad . \quad (10.3)$$

To get an estimate of the rotation time we replace the moment of inertia by the rigid body value for a spherical nucleus and express the result in units of $2R/c$:

$$\tau_{\text{rot}} \simeq 5 \ (A^{4/3}/I) > \tau_{\text{relaxation}}. \quad . \quad . \quad . \quad . \quad . \quad (10.4)$$

As we previously found that the relaxation time is at least of the order of 5–10 in these units and probably another order of magnitude larger, the relation (10.4) is not readily fulfilled in light elements and for high angular momenta. This is easily understood, because the peripheral collisions which have the highest angular momenta, are least likely to lead to Compound Nucleus formation. This is at least one of the reasons for the preponderance of direct interactions in the case of light elements. The limitations on the Statistical Model imposed by the rotation time are often more stringent than the lifetime restrictions. If the latter restriction is violated, we should not have much hope of describing angular distributions by the Statistical Model; it is still possible that a sufficiently high fraction of the process passes by Compound Nucleus formation to make it a useful description for total cross sections.

Recently Wilets (1959) has made an estimate of the relaxation time of the Compound Nucleus. He considers the nucleus as initially being in a particular state and that the probability of the system developing into other, more complicated states behaves analogously to diffusion. Thus, the real and virtual transitions will completely specify the probability of excitation of the other components at a later time, provided the decay of the system can be neglected, because the probability flux depends directly on the transition rate. The calculation is based on the unified model. The relaxation mechanism is ascribed to the coupling between particle and collective excitation modes. Assuming a nuclear level density which varies as $e^{2\sqrt{aU}}$ with the excitation energy U he obtains at high energy the relaxation time

$$\tau_{\text{relaxation}} \to \frac{14}{\pi^3} \frac{U^{3/2}}{V_0} \frac{a^{1/2}}{\omega_0} \cdot \cdot \cdot \cdot \cdot \cdot \cdot \cdot \quad (10.5)$$

Here V_0 is the depth of the nuclear well and $\hbar\omega_0 = 40\, A^{-1/3}$ Mev is the shell model oscillator frequency. The applicability of this formula is expected to be above 10 Mev of excitation. This relaxation time is surprisingly short; at 100 Mev of excitation it is still only of the order of 100 in our previous units.

This result should still be taken with some care, in particular as a number of approximations go into eqn. (10.5). It is still interesting that the relaxation time comes out to be very short. If this result could be more firmly established it would greatly increase our understanding of the Statistical Model and its limitations.

§ 11. Fluctuations of Cross Sections and Angular Distributions

We have previously emphasized several times the central role played by the concept of an average in the Statistical Model; in fact the assumption that cross sections can be regarded as smoothly varying functions of energy beside the assumption of a compound state must be considered as the very basis of this model. It has however little meaning to deal with averages, if there is no way of evaluating the fluctuations which inevitably are associated with the averages. These fluctuations may, at least in special cases, be so large as to render the entire treatment meaningless; they will also indicate deviations from the predictions based on the strictly averaged quantities. Thus, the appearance of such deviations must be considered a natural part of the model. In view of the importance of understanding the influence of fluctuations in the Statistical Model, it is surprising that this problem is untreated with the exception of the unpublished estimates by Feshbach (1955) and Lane and Lynn which refer to the region of non-overlapping levels. No estimates have been made for the continuum region. In this section we will therefore attempt to obtain the magnitude of the fluctuations and their effects in different cases.

In describing the fluctuations it is necessary first to describe the fluctuations which occur when the energy resolution of the incident beam is microscopically fine, and the reaction proceeds to a specific state of the

residual nucleus. With this knowledge it is then comparatively easy to estimate the fluctuations when the resolution of the beam is finite and when the transitions take place to many states. The Statistical Model describes the reaction in two steps, first the formation of the Compound Nucleus and secondly its decay. The cross section for a reaction going to a final state $|\alpha'\rangle$ from the initial state $|\alpha\rangle$ is proportional to the absolute square of the matrix element $\langle\alpha'|S|\alpha\rangle$, where S is the ordinary scattering matrix. The compound assumption implies that it is possible to split the S-matrix into a product $S_{\alpha'}f(E, \mathscr{H}_c)S_\alpha$, where S_α leads into the Compound System and $S_{\alpha'}$ out of it. The factor $f(E, \mathscr{H}_c)$ represents the probability amplitude with which compound states $|i\rangle$ (for which $\mathscr{H}_c|i\rangle = E_i|i\rangle$) are excited with energies different from the excitation energy E; the appearance of this factor is due to the energy uncertainty caused by the finite lifetime of the Compound Nucleus. The cross section $\sigma_{\alpha\alpha'}$ is thus proportional to

$$\sigma_{\alpha\alpha'} \propto |\langle\alpha'|S_{\alpha'}f(E, \mathscr{H}_c)S_\alpha|\alpha\rangle|^2. \quad . \quad . \quad . \quad . \quad . \quad (11.1)$$

We emphasize that the compound system does not necessarily consist of one state only; in the region of overlapping levels it consists of a large number of states and it is not possible without further assumptions to split the matrix elements of eqn. (11.1) into two independent, non-interfering parts.

The levels in the intermediate Compound Nucleus provide a complete set for the description of that system. If we try to express these levels as linear combinations of ordinary shell model states, for example, these combinations will be enormously complex as the close spacing of the states implies a strong mixing even with weak residual interactions. The vector $S_\alpha|\alpha\rangle$, which is a vector of fixed length in the vector-space spanned by all the state-vectors of the intermediate nucleus, has little to do with any particular one of these vectors, though correlations between them occur, if we study large enough energy regions. If we thus consider only the levels of the intermediate nucleus in a limited energy-interval, it is possible to regard that part of $S|_\alpha\alpha\rangle$ which is projected on $|i\rangle$ as being a vector with a random direction. The condition for this to be possible is obviously that the projection on this sub-space only represents a small part of the total length of $S_\alpha|\alpha\rangle$. A consequence of the assumption of random direction is that the projection of $S_\alpha|\alpha\rangle$ on any one of the vectors $|i\rangle$ can be considered a random number with a Gaussian distribution. The application of the idea of random matrix elements to the description of the fluctuations of widths and spacings of levels seen in neutron resonances has been very successful and we will use this approximation as the basis for our further discussion. For an up-to-date discussion of the present situation in this field we refer to Porter and Rosenzweig (1960), where previous references can be found.

A simple argument for the Gaussian distribution of the random matrix elements is obtained by considering rotations in the space spanned by

the vectors $|i\rangle$†. Suppose a vector of given length has a random direction in an N-dimensional space with projection x_j on the different orthogonal axes. The mean value of this projection is obviously 0 and the mean square of x_j^2 is the same for all axes, as none is singled out. We denote this mean square by a^2. There will be a probability distribution for x_j, $f(x_j)$, which must also be independent of the particular axis. The entire coordinate system is now rotated to a new random position. As the original vector was at random, it will still be at random with respect to the new axes and the probability distribution for the new projection x_j', $f(x_j')$, must be the same as before. Expressing the new projection x_j' in terms of the old x_j

$$x_j' = \sum_i \beta_{ji} x_i \quad . \quad . \quad . \quad . \quad . \quad . \quad . \quad . \quad . \quad (11.2)$$

where the β_{ji} are ordinary transformation coefficients for an orthonormal transformation and satisfy

$$\sum_i \beta_{ji}^2 = 1. \quad . \quad . \quad . \quad . \quad . \quad . \quad . \quad . \quad . \quad . \quad (11.3)$$

Thus we can regard x_j' in eqn. (11.2) as the sum of N random variables $\beta_{ji} x_i$, each with a mean value 0 and a mean square value $\beta_{ji}^2 a^2$. The sum of a large number of such terms is a typical random walk problem, which we discussed earlier in § 3 in connection with spin distributions. Essentially independent of the detailed distribution functions for the x_i the mean square for x_j' is given by

$$x_j'^2 = \sum_i \beta_{ji}^2 x_i^2 = a^2 \sum_i \beta_{ji}^2 = a^2, \quad . \quad . \quad . \quad . \quad . \quad . \quad . \quad . \quad (11.4)$$

and the distribution function is a Gaussian with this dispersion.

$$f(x_j) = \frac{1}{\sqrt{(2\pi a^2)}} e^{-\frac{x_j^2}{2a^2}}. \quad . \quad . \quad . \quad . \quad . \quad . \quad (11.5)$$

From this we conclude that the distribution $f(x_j)$ for the projections of a random vector on an axis in a many-dimensional system must be Gaussian. We notice that when the number of dimensions is large, the different projections can be considered as independent of the fixed length of the vector.

It can be immediately concluded from eqn. (11.5), that the square of a random projection, y_j, which is the quantity entering in the transition probability, has a Porter-Thomas distribution (1956)

$$g(y_j) = \frac{1}{\sqrt{(2\pi\bar{y})}} \frac{e^{-\frac{y_j}{2\bar{y}}}}{\sqrt{(y_j)}}. \quad . \quad . \quad . \quad . \quad . \quad . \quad (11.6)$$

This distribution is strongly fluctuating. Its mean value is $\bar{y}$, but the fluctuations give rise to a mean square deviation, $\overline{(y_j - \bar{y})^2}$, which is $2\bar{y}^2$.

† A somewhat similar argument based on rotations in configuration space is given by Porter and Rosenzweig (1960) for matrix elements of the residual interactions in the intermediate nucleus.

11.1. *Non-overlapping Levels*

We are now in a position to estimate the fluctuations in cross sections and angular distributions for the case of non-overlapping compound states. The reaction proceeds through specific resonances with definite spin and parity. Equation (11.1) can thus be simplified, because there is only one intermediate compound state $|i\rangle$. The cross section is proportional to

$$\sigma_{\alpha\alpha'} \propto |\langle \alpha' | S_{\alpha'} | i \rangle|^2 |\langle i | S_\alpha | \alpha \rangle|^2. \quad . \quad . \quad . \quad . \quad . \quad . \quad (11.7)$$

Both of the squared matrix elements in eqn. (11.7) will fluctuate independently according to the Porter-Thomas distribution. If eqn. (11.7) is averaged over N compound levels $|i\rangle$, each of which decays to n different states in the final nucleus over which we also average, the associated fluctuation away from the average cross section $\sigma_{\alpha\alpha'}$ is thus of the order

$$\sigma_{\alpha\alpha'} = \bar{\sigma}_{\alpha\alpha'} \left(1 \pm \frac{1}{\sqrt{N}} \pm \frac{1}{\sqrt{(nN)}} \right). \quad . \quad . \quad . \quad . \quad (11.8)$$

Thus, as far as the total cross section $\sigma_{\alpha\alpha'}$ is concerned, the average over final states has little influence on its fluctuations, because n is always larger than or equal to unity. The average is performed experimentally by using a beam with a spread of incident energy ΔE_i. The number of states in the Compound Nucleus, N, over which the average is performed is thus

$$N = \Delta E_i \rho_c. \quad . \quad . \quad . \quad . \quad . \quad . \quad . \quad . \quad (11.9)$$

Here ρ_c is the effective level density of the Compound Nucleus, i.e. with all effectively participating spins and parities. Similarly the average in the final state is performed over the n states which can be reached effectively from a particular compound level. The energy region over which the average is performed is due to the initial energy spread of the beam ΔE_i and to the final resolution ΔE_f. The number n is therefore

$$n = (\Delta E_i + \Delta E_f) \rho_f \quad . \quad . \quad . \quad . \quad . \quad . \quad (11.10)$$

where ρ_f is the appropriate effective level density for final states.

In order to discuss fluctuations in the angular distribution it is necessary to take the interference effects between different angular momenta properly into account; the simple eqn. (11.7) is no longer sufficient. We will use the formulation of reaction cross-sections for unpolarized targets by Blatt and Biedenharn (1952). The differential cross section is expressed in terms of the scattering amplitudes multiplied by geometrical factors. The properties we are going to exploit are extremely simple in spite of the rather complicated notation. Let J be the total angular momentum of the system, s and s' the channel spins of the initial and final states, I the orbital angular momentum of the incident particle, l the orbital angular

momentum of the outgoing particles and L the order of Legendre polynomials in the expansion of the angular distribution. The differential cross section can then be written

$$\frac{d\sigma_{\alpha\alpha'}}{d\Omega} \propto \sum_L B_L(\alpha' s' ; \alpha s) P_L(\cos\theta), \quad . \quad . \quad . \quad . \quad (11.11)$$

where $B_L\ (\alpha' s' ; \alpha s) =$

$$\frac{(-)^{s'-s}}{4} \sum_{I_1}\sum_{I_2}\sum_{l_1}\sum_{l_2} Z(I_1 J I_2 J ; sL) Z(l_1 J l_2 J ; s' L) \mathrm{Re}[S^{J*}_{\alpha' s' l_1 ; \alpha s I_1} S^{J}_{\alpha' s' l_2 ; \alpha s I_2}].$$

$$. \quad . \quad (11.12)$$

In eqn. (11.12) we have neglected the elastic scattering. The Z-coefficients are geometrical factors defined by Biedenharn *et al.* (1952); we will not use their explicit form, but only observe that the coefficients are 0, if the angular momenta do not obey triangular inequalities. In particular l_1 and l_2 as well as I_1 and I_2 have to couple to L, and $l_1 + l_2 - L$ and $I_1 + I_2 - L$ have to be even numbers.

An important consequence of eqn. (11.12) due to the fact that only one level of the Compound Nucleus enters the reaction, is that the order L of the Legendre polynomials necessarily is *even*. Consequently the angular distribution is always strictly symmetrical about 90°, if the levels are non-overlapping.

To obtain the fluctuations of the $B_L(\alpha' s' ; \alpha s)$ we observe that the Z-coefficients are slowly varying functions of the angular momenta, if these are large. We may thus apply a semi-classical approximation to the Z-coefficients and replace them by a continuous function $\bar{Z}(\bar{I}\bar{J}\bar{I}\bar{J} ; \bar{s}L)$, etc., when they are different from 0. Restricting the summations of eqn. (11.12) to include only permitted combinations of angular momenta, we can then take the geometrical coefficients outside the summation sign. Furthermore we split the scattering matrix into two parts as previously

$$S^{J}_{\alpha' s' l ;\ \alpha s I} = S^{J}_{\alpha' s' l ;\ i} S^{J}_{\alpha s I ;\ i} \quad . \quad . \quad . \quad . \quad . \quad (11.13)$$

where i denotes the compound state. Introducing this into eqn. (11.12) we can approximately write $B_L(\alpha' s' ; \alpha s)$ as

$$B_L(\alpha' s' ; \alpha s) \propto \bar{Z}(\bar{I}\bar{J}\bar{I}\bar{J} ; \bar{s}L) \bar{Z}(\bar{l}\bar{J}\bar{l}\bar{J} ; \bar{s}' L) |\textstyle\sum_l^{(L)} S^{J}_{\alpha' s' l ;\ i}|^2 |\sum_l^{(L)} S^{J}_{\alpha s I ;\ i}|^2$$

$$. \quad . \quad . \quad (11.14)$$

where the superscript (L) on the sums indicates that the restrictions implied by the Z-coefficients have to be taken into account. While eqn. (11.14) is only a crude approximation it should be quite sufficient for an estimate of the fluctuations.

The structure of eqn. (11.14) is extremely similar to eqn. (11.7) for the corresponding total cross section. As sums of random numbers again are random numbers, we conclude that the coefficients $B_L(\alpha' s' ; \alpha s)$ fluctuate in a completely similar manner to the corresponding total cross

section (which is proportional to $B_0(\alpha' s' ; \alpha s)$). While these coefficients thus have rather strong fluctuations, the angular distribution

$$W_{\alpha\alpha'}(\theta) = \frac{1}{\sigma_{\alpha\alpha'}} \frac{d\sigma_{\alpha\alpha'}}{d\Omega}$$

has a weaker variation. This is most easily seen when the channel spin in the incident channel is 0, so that the resonance is excited only by one orbital angular momentum I of the incident wave. In this case eqn. (11.14) reduces to

$$B_L(\alpha' s' ; \alpha 0) \propto Z(IIII ; 0L)\bar{Z}(\bar{I}\bar{I}\bar{I}\bar{I} ; \bar{s}' L)|\textstyle\sum_l^{(L)} S^I_{\alpha' s' l ; i}|^2 |S^I_{\alpha 0 I ; i}|^2 \quad . \quad . \quad . \quad (11.15)$$

The last term in the product, the formation probability of the state i, is thus just a multiplicative factor which is the same for all the B_L and it will not affect the angular distribution. The term $\sum_l^{(L)} S^I_{\alpha' s' l ; i}$ is the sum of random numbers, and thus a random number ; its square will thus fluctuate according to a Porter-Thomas distribution. Averaging over N states in the Compound Nucleus and n states in the final nucleus the fluctuation in the angular distribution is thus of the order

$$W(\theta) = \overline{W(\theta)}\left(1 \pm \frac{1}{\sqrt{(nN)}}\right). \quad . \quad . \quad . \quad . \quad (11.16)$$

By this fluctuation we mean that each coefficient in the expansion of $W(\theta)$ in Legendre polynomials will fluctuate by a factor $1/\sqrt{(nN)}$.

When the channel spin is not 0 for the target nucleus, the fluctuations in the angular distribution will increase somewhat compared to eqn. (11.16) ; they will, however, be smaller than the fluctuations of the total cross section. The angular distribution may even fluctuate less than implied by eqn. (11.16). The reason for this is that the matrix elements which determine the fluctuations of $B_L(\alpha' s' ; \alpha s)$ in eqn. (11.14) are correlated for different L-values. The matrix elements, which enter in the sum $\sum_l^{(L)} S^J_{\alpha' s' l ; i}$, are to a large extent the same for neighbouring values of L ; these matrix elements have thus also a tendency to act like a fluctuating multiplicative factor, which does not introduce rapid variations in the angular distribution.

As a conclusion for the fluctuations of reactions involving non-overlapping levels :

(1) The total cross section $\sigma_{\alpha\alpha'}$ has fluctuations determined essentially by the number N of compound levels over which the average is performed and does not depend strongly on additional averages in the residual nucleus.

(2) The angular distribution has considerably smaller fluctuations. The pertinent average is performed both over the N compound levels and over the n states in the residual nucleus reached from each compound level. Due to correlation effects the fluctuations are possibly even smaller.

11.2. *Overlapping Levels*

With increasing excitation energy the lifetime of the compound system, τ, decreases, and the corresponding uncertainty in energy of the compound nucleus $\Gamma = \hbar/\tau$ will thus increase. The energy uncertainty may then be so large that a large number of compound states are contained within it. We are then dealing with strongly overlapping levels and are in the energy region which is usually called the continuum. In the region of non-overlapping levels the reaction proceeds through one particular compound state, independent of the other. In contrast to this, the uncertainty in energy of the Compound nucleus in the continuum region makes it necessary to consider simultaneously transitions through all states within the region of energy-uncertainty and to take interference effects between these states into account.

The lifetime τ, which we calculated in the preceding section, is a slowly varying function of the excitation energy due to the strong averaging over the final states, which is implied, and the energy uncertainty Γ is therefore also slowly varying. In a certain sense Γ may be regarded as a width of the Compound Nucleus; it is however more appropriate to regard it as a 'coherence energy' within which it is necessary to treat matrix-elements between compound states $|i\rangle$ as coherent.

We can according to eqn. (11.1) write the cross section $\sigma_{\alpha\alpha'}$

$$\sigma_{\alpha\alpha'} \propto |\textstyle\sum_i \langle \alpha' | S_{\alpha'} | i \rangle f(E, E_i) \langle i | S_\alpha | \alpha \rangle|^2. \quad . \quad . \quad . \quad . \quad (11.17)$$

where $f(E, E_i)$ is the probability amplitude that the reaction passes by state $|i\rangle$. The probability amplitude is determined by the coherence energy Γ and has essentially a Lorentzian form:

$$|f(E, E_i)|^2 \propto \frac{1}{(E_i - E)^2 + \Gamma^2/4}. \quad . \quad . \quad . \quad . \quad (11.18)$$

Thus the eqn. (11.17) simply expresses that the reaction is assumed to pass through a Compound Nucleus in the region of overlapping levels. The important feature of eqn. (11.17) is not the detailed expression of the probability amplitude $f(E, E_i)$, but that it is approximately constant within the 'coherence energy' Γ and small outside. Thus only compound states within energies which differ less than Γ from the energy E of the system, will effectively participate in the sum of eqn. (11.17). We now make the assumption that the matrix elements $\langle \alpha' | S_{\alpha'} | i \rangle$ and $\langle i | S_\alpha | \alpha \rangle$ have random phases within energy intervals much larger than Γ. This assumption is thus less restrictive than the assumption of randomness. The product $\langle \alpha' | S_{\alpha'} | i \rangle \langle i | S_\alpha | \alpha \rangle$ has again a random phase; it can be shown that the sum of a large number of elements with random phases will be a random number with a Gaussian distribution. Thus, if there are many compound states within the 'coherence energy' the sum in eqn. (11.17) is a random number and the cross-section will fluctuate strongly for different final states.

The appearance of strong fluctuations for transitions to isolated states in the residual nucleus passing through a Compound Nucleus in the continuum region has an extremely interesting consequence. If the energy of the projectile is varied by an amount which is small compared to Γ, the sum of matrix-elements in eqn. (11.17) will be practically unchanged, because the states $|i\rangle$ which enter will nearly all be identical. As a consequence $\sigma_{\alpha\alpha'}$ will not vary appreciably for changes in the bombarding energy small compared to Γ (we assume infinite resolution in the beam). In order to obtain a different value of $\sigma_{\alpha\alpha'}$ it is necessary that the compound states $|i\rangle$ in eqn. (11.17) are entirely changed; this can be achieved only if the energy is varied by an amount which is at least of the order of Γ. Thus, if cross sections $\sigma_{\alpha\alpha'}$ are compared for incident energies which differ by more than Γ, the cross sections should be expected to exhibit strong fluctuations.

The fact that the cross section $\sigma_{\alpha\alpha'}$ varies only over regions of the order of Γ opens the possibility of experimental determination of the 'coherence energy' Γ, i.e. of the lifetime of the Compound Nucleus. This lifetime is predicted by the Statistical Model to be very short, often of the order of 10^{-18} to 10^{-20} sec. It is thus a lifetime of an order that is difficult to measure and it is of considerable interest to know if the predicted and actual lifetime are of the same order (cf. § 10).

In discussing the fluctuations of the averaged cross section it is important to keep in mind that the large number of compound states within the energy region Γ do not ameliorate the average; they must rather be treated as one for purposes of average. The average with resolution ΔE_i of the incident energy is therefore over N different degrees of freedom:

$$N = \Delta E_i/\Gamma \geqslant 1. \quad . \quad . \quad . \quad . \quad . \quad . \quad . \quad . \quad (11.19)$$

The average over the n states in the residual nucleus is independent of the average over the Compound System. The fluctuations are thus of the order

$$\sigma_{\alpha\alpha'} = \bar{\sigma}_{\alpha\alpha'}\left(1 \pm \frac{1}{\sqrt{(nN)}}\right), \quad . \quad . \quad . \quad . \quad . \quad . \quad (11.20)$$

where n is given by eqn. (11.10). This implies in particular that the total reaction cross section for which n is large will have only small fluctuations; the same is true for all cross sections of large n, as for example the energy spectrum of emitted particles when averaged over many states.

In order to estimate the fluctuations in the angular distribution we again make use of the formalism of Blatt and Biedenharn. The coefficients $B_L(\alpha's'\,;\,\alpha s)$ of eqn. (11.11) are in the general case

$$B_L(\alpha's'\,;\,\alpha s) = \frac{(-)^{s'-s}}{4} \sum_{J_1}\sum_{J_2}\sum_{l_1}\sum_{l_2}\sum_{l_1}\sum_{l_2} Z(I_1 J_1 I_2 J_2\,;sL) Z(l_1 J_1 l_2 J_2\,;s'L)$$

$$\mathrm{Re}\,[S^{J_1 *}_{\alpha' s' l_1\,;\,\alpha s I_1} S^{J_2}_{\alpha' s' l_2\,;\,\alpha s I_2}] \quad (11.21)$$

The difference between this and the preceding expression for non-overlapping levels (eqn. 11.12) is the occurrence of interference terms between different total angular momenta J_1 and J_2. By exactly the same argument

we applied to demonstrate the randomness of the sum over i in eqn. (11.17) and with the same assumption the matrix-element $S^J_{\alpha' s' l;\, \alpha s I}$ is a random number. We apply the same approximation to the Z-coefficients as previously and regard them as smoothly varying functions of the average values, $\bar{l}$, $\bar{J}$, $\bar{I}$, of the angular momenta, and take them outside the sums of eqn. (11.21), when non-zero. In contrast to the case of non-overlapping levels it is now important to consider parity conservation with care. Each matrix-element $S^J_{\alpha' s' l;\, \alpha s I}$ couples the state α to α' in such a way that $l+I$ is even if they have same parity, odd if they have opposite parity. We furthermore recall that l_1+l_2-L and I_2+I_2-L both must be even numbers. We can thus write eqn. (11.21) in analogy with eqn. (11.14) as

$$B_L(\alpha' s';\ \alpha s) \propto \bar{Z}(\bar{I}\bar{J}\bar{I}\bar{J};\ \bar{s}L)\bar{Z}(\bar{l}\bar{J}\bar{l}\bar{J};\ \bar{s}'L)$$

$$\times \begin{cases} \left|\sum_{\text{even } l}^{(L)}\sum_I^{(L)}\sum_J^{(L)} S^J_{\alpha' s' l,\, \alpha s I}\right|^2 + \left|\sum_{\text{odd } l}^{(L)}\sum_I^{(L)}\sum_J^{(L)} S^J_{\alpha' s' l;\ \alpha s I}\right|^2 & \text{for even } L, \\ 2\,\mathrm{Re}\ \left(\sum_{\text{even } l}^{(L)}\sum_I^{(L)}\sum_J^{(L)} S^{J*}_{\alpha' s' l;\ \alpha s I}\right)\left(\sum_{\text{odd } l}^{(L)}\sum_I^{(L)}\sum_J^{(L)} S^J_{\alpha' s' l;\ \alpha s I}\right) & \text{for odd } L. \end{cases} \quad \ldots \quad (11.22)$$

In the deviation of eqn. (11.22) it is implicitly assumed that the channel spin of the residual nucleus, s', is large. If both channel spins s and s' are small, the amplitude of the fluctuations will be partially damped particularly in the integrated cross-section, less in the angular distribution. From eqn. (11.22) we conclude that the coefficients $B_L(\alpha' s';\ \alpha s)$ fluctuate as much as the integrated cross section for even L; indeed we notice that the particular geometrical influence of the Z-coefficients tend to separate terms of odd and even l into independently squared terms, an effect that we neglected in the integrated cross-section and which will slightly reduce its fluctuation. The expression for the $B_L(\alpha' s';\ \alpha s)$ for odd L consists essentially of the same sums as for even L but multiplied instead of squared and summed. Its mean value is 0. Thus the fluctuations in the $B_L(\alpha' s';\ \alpha s)$ are of the order

$$B_L(\alpha' s';\ \alpha s) = \begin{cases} \overline{B_L(\alpha' s';\ \alpha s)}\left(1 \pm \dfrac{1}{\sqrt{(nN)}}\right) & \text{for even } L, \\ \pm\,\overline{B_{L\pm1}(\alpha' s';\ \alpha s)}\ \dfrac{1}{\sqrt{(nN)}} & \text{for odd } L. \end{cases} \quad \ldots \quad (11.23)$$

We notice that there is in general no symmetry of the angular distribution about 90° in this case in spite of the many intermediate levels; only by further averaging can the assymmetry term be made to disappear.

As in the case of non-overlapping levels there is a correlation between the values of $B_L(\alpha' s';\ \alpha s)$ for different L. In this case the correlation can be strong between the coefficients for different even values of L or different odd values of L separately, as is evident from eqn. (11.22). There is, however, no correlation in sign between the coefficients of the odd

Legendre polynomials and those of the even Legendre polynomials. The angular distribution in transitions to one state must therefore be expected to be strongly fluctuating due to this effect only.

As a summary of the fluctuation effects for many strongly overlapping levels:

(1) The total reaction cross section and any integrated cross section averaged over many final states will be smoothly varying with energy even with infinitely good resolution in the incident beam in agreement with ordinary continuum theory.

(2) The partial cross section to an isolated state will fluctuate strongly from state to state. It will also fluctuate with incident energy over energy regions larger than the coherence energy Γ.

(3) The angular distribution will be asymmetric about 90° due to interference terms which disappear when averaged over many states in the final nucleus or over an energy region large compared to Γ in the intermediate nucleus.

We have here attempted some crude estimates of the fluctuations of various quantities of the Statistical Model. We have made extensive use of the assumption of uncorrelated matrix-elements within small regions of energy. While this approximation has had great success in the region of neutron resonances, it is not necessarily good in general. In particular it is possible to imagine that the contribution from states which are far away in energy give a non-random coherent contribution in the region of overlapping levels or that approximate sum-rules are of importance within the region of the coherence energy. Little is at present known about such effects and the approximation of no correlations seems most in the spirit of the Statistical Model. The estimates of the fluctuations given are very crude and are intended as an orientation. A more detailed investigation is needed to obtain detailed quantitative predictions. We also want to emphasize that similar fluctuations will occur as a result of interference between direct interactions and Compound Nuclear reactions.

§ 12. Conclusion

The Statistical Model of nuclear reactions is in a rather peculiar situation. It is now nearly 25 years since N. Bohr (1936) first proposed the existence of a long-lived intermediate Compound Nucleus in nuclear reactions. In spite of the tremendous impact of this idea on nuclear physics, there has hardly been any attempt to establish whether such an intermediate system exists and under what circumstances it exists in the case of very highly excited nuclei. The very basis for the application of the Statistical Model has therefore not been established and its existence has not been subject to stringent tests.

The outstanding present problem of the Statistical Model is therefore to establish its region of applicability as a function of projectile, incident energy, and target nucleus. While a large number of experiments indicate many of the limitations qualitatively, the importance of this problem is such that it has to be settled without invoking arguments about level

densities and inverse cross sections. The typical experiments to determine the regions of validity should therefore use very general consequences of the intermediate system and should, for example, test the prediction of independence of formation and decay modes of the Compound Nucleus as well as possible. This may be achieved either by comparing excitation functions or by comparing the energy spectra of particles emitted in reactions corresponding to the same Compound Nucleus excited by different means. The latter method has the advantage of simultaneously displaying the non-compound contributions.

In any nuclear reaction there will always be a certain probability of Compound Nucleus formation. If this probability is small, the description in terms of the Statistical Model is still correct for that part of the reaction which passes by Compound Nucleus formation; this is, however, no longer a useful way of describing the process as a whole. The probability of Compound Nucleus formation is largely a question of the relative magnitude of the relaxation time for formation of an equilibrium system as compared to the lifetime of the nucleus in equilibrium. If the equilibrium system has a short lifetime compared to the relaxation time, the probability for its formation will be small and the process fast compared to the relaxation time. By systematic studies of the probability of formation of the Compound Nucleus under different circumstances, it should therefore be possible to establish a time-scale for the reactions and obtain estimates of the nuclear relaxation time. Somewhat similar information may be obtained by determinations of the lifetime of the equilibrium system from the fluctuation of the cross section with incident energy.

The theoretical description and understanding of the decay of the equilibrium system is rather complete, in so far as it can be ascertained that a Compound Nucleus has been formed. Our understanding is mainly due to the general nature of the principle of detailed balance, which leads to a description of the decay in which the phase space available for the decay products plays the dominating role. Nuclear level densities and inverse cross sections are important quantities in this phase-space description; while we may not have complete information on either of these quantities, they are both well-defined concepts and do not alter any features of the theory. Therefore, the Statistical Model can be used to obtain quantitative information about the excited nucleus: the properties of its level density, its Coulomb barrier, its lifetime, whenever it is possible to ascertain that a reaction proceeds predominantly by Compound Nucleus formation. As previously, a systematic study of the probability of Compound Nucleus formation under different circumstances should greatly increase the confidence in such quantities as determined from nuclear reactions. From a theoretical point of view it should be very useful, if level densities could be determined absolutely by statistical reactions, and not only their variation with energy. This may be possible by studies of transitions to individual states in the residual nucleus.

The information that nuclear reactions can give on the behaviour of nuclear level densities at relatively low energies is extremely important.

The present problems of nuclear level densities are connected with the transition of the spectrum of the nucleus near its ground state, strongly dominated by pairing effects, to the spectrum of the highly excited nucleus, which seems to be essentially of independent particle character. In order to achieve an understanding of this transition, it is thus highly desirable to know the detailed behaviour of the level density and its spin distribution between these two regions. While this information in part can be obtained by direct measurements of the states involved, the small spacing between states at higher excitation makes it necessary to rely on nuclear reactions in this region.

In a direct interaction process a particle is ejected immediately after the initial interaction of the projectile with the target; in a statistical process on the other hand this emission takes place only after the projectile has caused a long and complicated chain of collisions of the target nucleons. These two types of reactions are therefore the one-collision and the many-collision limits of the nuclear reaction. From this point of view it is therefore unnatural to regard these two limits as inherently opposed; they are only asymptotic limits of the same picture, and they are both present to lesser or larger extent in any reaction, as well as contributions from intermediate processes. The Statistical Model often implies small cross sections for certain reactions, even when the bulk of the total reaction process goes by Compound Nucleus formation. This may be due to unfavourable Q-values and Coulomb barriers; it may also occur in transitions to individual states due to their small statistical weight. In these cases it is only possible to ascertain that the Statistical Model predicts a minimum cross section. Any special type of reaction mechanism which yields the same result with higher cross section will automatically dominate this particular reaction. The occurrence of special processes with cross sections larger than the statistical cross section is by no means contrary to the Statistical Model; they have only been left out of this asymptotic description of the reaction. Only if the cross section becomes smaller than implied by the Statistical Model is any real discrepancy present.

The Statistical Model is sometimes regarded as predicting only the crude overall properties of nuclear reactions. In contrast to this, the model makes very definite and precise predictions, which have a very general basis theoretically. The uncertainty in the description is entirely due to the fact that it only predicts the decay of an equilibrium system and that other contributions are not accounted for. When it is known that the process proceeds by Compound Nucleus formation the Statistical Model is firmly founded theoretically. The analysis of the reaction according to this model then provides a very useful tool for the quantitative study of the properties of the excited nucleus.

Acknowledgments

I am deeply indebted to Professor V. Weisskopf and Professor H. Feshbach for numerous stimulating and enlightening discussions on various aspects of the Statistical Model.

References

Allan, D. L., 1959, *Nucl. Phys.*,**10,** 348.

Austern, N., 1960, *Fast Neutron Physics* II (New York : Interscience).

Bagge, E., 1938, *Ann. Phys., Lpz.*, **33,** 389.

Bardeen, J., Cooper, L. N., and Schrieffer, J. R., 1957, *Phys. Rev.*, **108,** 1175.

Bardeen, J., and Feenberg, E., 1938, *Phys. Rev.*, **54,** 809.

Belyaev, S. T., 1959, *Math.-fys. Medd.*, **31,** No. 11.

Bethe, H., 1936, *Phys. Rev.*, **50,** 332; 1937, *Rev. Mod. Phys.*, **9,** 69; 1938, *Phys. Rev.*, **53,** 675.

Biedenharn, L. C., Blatt, J. M., and Rose, M. E., 1952, *Rev. mod. Phys.*, **24,** 249.

Blatt, J. M., and Biedenharn, L. C., 1952, *Rev. mod. Phys.*, **24,** 258.

Blatt, J., and Weisskopf, V., 1952, *Theoretical Nuclear Physics* (New York: Wiley and Sons).

Bloch, C., 1954, *Phys. Rev.*, **93,** 1094.

Bloch, C., and de Dominicis, C., 1958, *Nucl. Phys.* **7,** 459; 1959, *Ibid.*, **10,** 509.

Bohr, A., 1952, *Math.-fys. Medd.*, **26,** No. 14; 1955, *Proceedings of the International Conference on the Peaceful Uses of Atomic Energy, Geneva* (New York: United Nations), Vol. 2, p. 151.

Bohr, A., and Mottelson, B. R., 1953, *Math.-fys. Medd.*, **27,** No. 16.

Bohr, A., Mottelson, B. R., and Pines, D., 1958, *Phys. Rev.*, **110,** 936.

Bohr, N., 1936, *Nature, Lond.*, **137,** 344.

Bohr, N., and Kalckar, F., 1937, *Math.-fys. Medd.*, **14,** No. 10.

Brady, F. P., and Sherr, R., 1960, *Bull. Amer. phys. Soc.* **5,** 249.

Butler, S. T., and Hittmair, O. H., 1957, *Nuclear Stripping Reactions* (New York: Wiley and Sons).

Cameron, A. G. W., 1957, *Canad. J. Phys.*, **35,** 1021; 1958 a, *Ibid.*, **36,** 1040; 1958, *Proceedings of the Second International Conference on the Peaceful Uses of Atomic Energy* (Geneva: United Nations), P/198; 1959, *Canad. J. Phys.*, **37,** 244.

Camerini, U., Lock, W. O., and Perkins, D. H., 1952, *Progress in Cosmic Ray Physics* (Amsterdam: North Holland Publishing Co.).

Cohen, B. L., and Handley, T. H., 1953, *Phys. Rev.*, **92,** 101.

Cooper, L. N., 1956, *Phys. Rev.*, **104,** 1189.

Dostrovsky, I., Bivins, R., and Rabinowitz, P., 1958, *Phys. Rev.*, **111,** 1659.

Dostrovsky, I., Fraenkel, Z., and Friedlander, G., 1959, *Phys. Rev.*, **116,** 683.

Dostrovsky, I., Fraenkel, Z., Rabinowitz, P., 1958, *Proceedings of the Second International Conference on the Peaceful Uses of Atomic Energy, Geneva* (Geneva : United Nations), P/1615; 1960, *Phys. Rev.*, **118,** 791.

Dostrovsky, I., Fraenkel, Z., and Winsberg, L., 1960, *Phys. Rev.*, **118,** 781.

Douglas, A. C., and McDonald, N., 1959, *Nucl. Phys.*, **13,** 382.

El Nadi, M., and Wafik, M., 1958/59, *Nucl. Phys.*, **9,** 22.

Ericson, T., 1958 a, *Nuc Phys.*, **6,** 62; 1958 b, *Ibid.*, **8,** 265. Errata 1958/59, **9,** 697; 1959, *Ibid.*, **11,** 481; 1960, *Ibid.*, **17,** 250.

Ericson, T., and Strutinski, V., 1958, *Nucl. Phys.*, **8,** 284. Addendum 1958/59, **9,** 689.

Euler, L., 1753, *Novi Commentarii Academiae Scientiarum Petropolitanae*, **3,** 125. Reprinted in Leonhardi Euleri Opera Omnia, Series I, Opera Mathematica, Vol. II, Commentationes Arithmeticae, Volumen primum, p. 254 (Berlin 1915).

Fenning, F. W., and Holt, F. R., 1950, *Nature, Lond.*, **165,** 722.

Ferguson, A. J., and Montague, J. H., 1952, *Phys. Rev.*, **87,** 215.

Feshbach, H., 1955, *Proceedings of Brookhaven Conference* (BNL Report–331).

Feshbach, H., Porter, C. E., and Weisskopf, V. F., 1953, *Phys. Rev.*, **90,** 166.

Fong, P., 1956, *Phys. Rev.*, **102,** 434.
Fulbright, H. W., Lassen, N. O., and Roy Poulsen, N. O., 1959, *Math.-fys. Medd.*, **31,** No. 10.
Fulmer, C., and Cohen, B., 1958, *Phys. Rev.*, **112,** 1672.
Fulmer, C., and Goodman, C., 1960, *Phys. Rev.*, **117,** 1339.
Ghoshal, S. N., 1950, *Phys. Rev.*, **80,** 939.
Glassgold, A. E., Heckrotte, W., and Watson, K., 1959, *Ann. Phys.*, **6,** 1.
Goldberger, M., 1948, *Phys. Rev.*, **74,** 1269.
Griffin, J. J., 1959, *Phys. Rev.*, **116,** 106.
Halpern, I., and Strutinski, V. M., 1958, *Proceedings of the Second United Nations International Conference on the Peaceful Uses of Atomic Energy, Geneva* (Geneva: United Nations), P/1513.
Hauser, W., and Feshbach, H., 1952, *Phys. Rev.*, **87,** 366.
Hudis J., and Miller, J., 1958, *Phys. Rev.*, **112,** 1322.
Hurwitz, H., Jr., and Bethe, H., 1951, *Phys. Rev.*, **81,** 898.
John, W., 1956, *Phys. Rev.*, **103,** 704.
Kelly, E. L., 1950, University of California (unpublished).
Kerman, A., McManus, H., and Thaler, R. M., 1959, *Ann. Phys.*, **8,** 551.
Klinkenberg, P. F. A., 1952, *Rev. mod. Phys.*, **24,** 63.
Lane, A. M., and Parker, K., 1960, *Nucl. Phys.*, **16,** 690.
Lane, A. M., and Lynn, J. E., Harwell Report A.E.R.E. T/R 2210.
Lang, J. M., and Le Couteur, K. J., 1954, *Proc. phys. Soc. Lond.*, A, **67,** 585; 1959, *Nucl. Phys.*, **14,** 21.
Le Couteur, K. J., 1950, *Proc. phys. Soc. Lond.*, A, **63,** 259; 1958, *Nuclear Reactions*, Vol. I, p. 138 (Amsterdam: North Holland Publishing Co.).
Le Couteur, K. J., and Lang, D. W., 1959, *Nucl. Phys.*, **13,** 32.
v. Lier, C., and Uhlenbeck, G. E., 1937, *Physica*, **4,** 531.
Margenau, H., 1941, *Phys. Rev.*, **59,** 627.
Martin, P. C., and Schwinger, J., 1959, *Phys. Rev.*, **115,** 1342.
Mayer, M. G., and Jensen, J. H. D., 1955, *Elementary Theory of Nuclear Shell Structure* (New York: Wiley and Sons).
Metropolis, N., and Reitwiesner, G., 1950, NP–1980.
Morse, P. M., and Feshbach, H., 1953, *Methods of Theoretical Physics* (New York : McGraw-Hill).
Mottelson, B. R., 1959, *The Many Body Problem* (Paris: Dunod), p. 283.
Newson, H., and Duncan, M., 1959, *Phys. Rev. Letters*, **3,** 45.
Newton, T. D., 1956 a, *Canad. J. Phys.*, **34,** 804; Errata 1957, **35,** 1400; 1956 b, Proceedings of the Symposium on the Physics of Fission, Chalk River Report CRP–642–A; Atomic Energy of Canada Report AECL–329.
Nilsson, S. G., 1955, *Math.-fys. Medd.*, **30,** No. 1.
Pick-Pichak, G. A., 1958, *Zhur. Eksptl. i Teoret. Fiz.*, **30,** 341.
Porter, C., and Rosenzweig, N., 1960, *Suomalaisen Tiedeakatemian Toimituksia* (in the press).
Porter, C., and Thomas, R. G., 1956, *Phys. Rev.*, **104,** 483.
Rosenzweig, N., 1957 a, *Phys. Rev.*, **105,** 950; 1957 b, *Ibid.*, **108,** 817.
Rosenzweig, N., Bollinger, L. M., Lee, L. L., and Schiffer, J. P., 1958, *Proceedings of the Second International Conference on the Peaceful Uses of Atomic Energy, Geneva* (Geneva: United Nations).
Ross, A. A., 1957, *Phys. Rev.*, **108,** 720.
Rudstam, S. G., 1956, *Spallation of Medium Weight Elements* (Uppsala).
Shapiro, M., 1953, *Phys. Rev.*, **90,** 171.
Soloviev, V. G., 1958/59, *Nucl. Phys.*, **9,** 655.
Strutinski, V. M., 1956 a, *Zhur. Eksptl. i Teoret. Fiz.*, **30,** 606; Transl. 1956 b, JETP, **3,** 638; 1958, *Comptes Rendus du Congres Internationale de Physique Nucléaire* (Paris : Dunod).

THOMAS, T. D., 1959, *Phys. Rev.*, **116,** 703.
TRAINOR, L. E. H., and DIXON, W. R., 1956, *Canad. J. Phys.*, **34,** 229.
WEISSKOPF, V. F., 1937, *Phys. Rev.*, **52,** 295; 1950, *Helv. phys. acta*, **23,** 187; 1953, *Proc. Amer. Acad. Arts Sci.*, **82,** 360.
WEISSKOPF, V. F., and EWING, D. H., 1940, *Phys. Rev.*, **57,** 472.
WILETS, L., 1959, *Phys. Rev.*, **116,** 372.
WOLFENSTEIN, L., 1951, *Phys. Rev.*, **82,** 690.

FOR USERS OF CALCULATORS

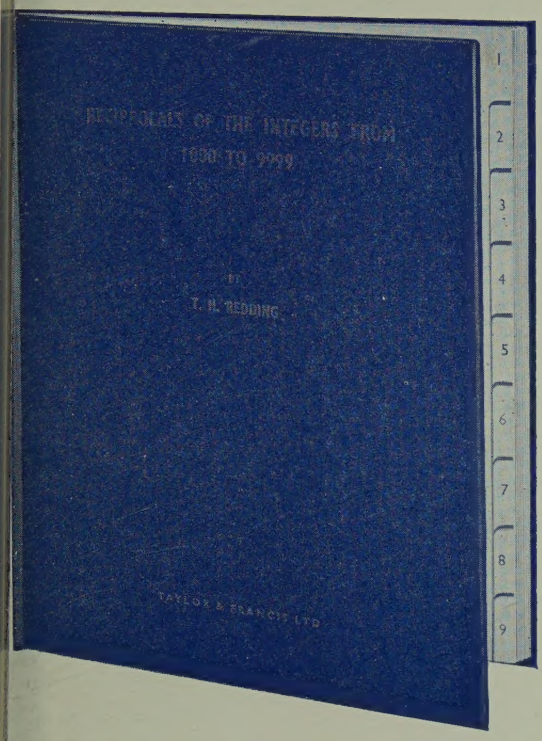

RECIPROCALS OF THE INTEGERS FROM 1000 TO 9999

By T. H. Redding
M.Sc.(Lond.), A.M.I.Mech.E., A.F.R.Ae.S.

Arranged for use with mechanical calculating machines to facilitate the evaluation of quotients and compound fractions

With an Appendix on mechanical barrel-setting calculators

These tables list the 10^6 multiples of the reciprocals of the integers 1000 to 9999 and are displayed as 1000 entries on each of nine double-page spreads which are thumb-indexed (1000 . . . , 2000 . . . , 3000 . . . , . . . etc) to facilitate rapid manipulation with one hand only. The entries are direct reading and are correct to the nearest integer in the third place of decimals.

Although suitable for general use, the tables have been prepared and arranged in a manner particularly suitable for use in conjunction with mechanical computing machines of the "barrel-setting" type in the evaluation of quotients and compound fractions. Equally the tables find application in effecting the evaluation of quotients on adding and listing machines when these incorporate a mechanism for automatically evaluating simple products.

In the first instance it was anticipated that an Appendix dealing with the advantages to be gained by the use of the reciprocal function in conjunction with such machines—and particularly with barrel-setting machines—would suffice to ensure the best use being made of the tables. The present 22-page *Appendix*, however, goes further than this, since the discussion of the tables is prefaced by a description of barrel-setting machines and their (simplest) method of operation in the evaluation of products, quotients and compound fractions. Thus, the description of each calculating procedure is followed by a numerical example with accompanying diagrams to illustrate the keyboard-displays at the beginning, the end, and at intermediate stages in the calculation. The machine-evaluation of series comprising the sum of a number of product or quotient-terms is also discussed. Generally it is hoped that the Appendix will serve as an introduction to mechanical methods of computation and that it will materially assist prospective purchasers in the choice of a machine.

A valuable guide to all users of Computers. Bound in blue publishers case, lettered on the front, with an 18 page table index. Printed on good quality paper for constant use.

Size 10 in. × 8 in.

Price 18s. 6d. *plus postage and packing* 1s. 3d.

Printed and Published by

TAYLOR & FRANCIS LTD

RED LION COURT, FLEET STREET, LONDON, E.C.4

Announcing the new publication

INSTRUMENT CONSTRUCTION

Translated from the Russian

Editor-in-chief: M. E. Rakovskii. Sub-editor: Yu. I. Shendler

The Russians describe their publication as a ' scientific, technical and production ' journal. It covers industrial instruments and instrumentation, automatic control, and production engineering for precision work. The articles which it presents not only introduce new instruments and techniques, they also afford a valuable insight into current Russian practice.

Subscription £6 yearly post free ($17.10 U.S.A. and Canada). A special rate of £3 yearly post free ($8.55 U.S.A. and Canada) is available to University and Technical College libraries.

Single copies 15*s*. each ($2.15 U.S.A. and Canada) plus postage

Orders should be sent to the Subscription Department, Taylor & Francis Ltd

Produced for the Department of Scientific and Industrial Research by the British Scientific Instrument Research Association, ' Sira ', South Hill, Chislehurst, Kent

Printed and Published for B.S.I.R.A. by

TAYLOR & FRANCIS LTD

RED LION COURT, FLEET STREET, LONDON, E.C.4